# THE MINERALOGY, PETROLOGY, AND GEOCHEMISTRY OF THE HALFWAY COVE-QUEENSPORT PLUTON, NOVA SCOTIA, CANADA

by

Linda J. Ham

Submitted in partial fulfillment of the requirements
for the degree of Master of Science

at

Dalhousie University
Halifax, Nova Scotia

September, 1988

**DALHOUSIE UNIVERSITY**

**DEPARTMENT OF GEOLOGY**

The undersigned hereby certify that they have read and recommended to the Faculty of Graduate Studies for acceptance a thesis entitled " The Mineralogy, Petrology, and Geochemistry of the Halfway Cove-Queensport Pluton, Nova Scotia, Canada "

by Linda J. Ham

in partial fulfillment of the requirements for the degree of Master of Science.

Dated September, 1988

External Examiner ___ _____

Research Supervisor _____ _____

Examining Committee _____ _____

___ _____

___ _____

D A L H O U S I E  U N I V E R S I T Y

DATE September 16, 1988

AUTHOR Linda J. Ham

TITLE The Mineralogy, Petrology and Geochemistry of the Halfway Cove-Queensport Pluton, Nova Scotia, Canada

Department or School Science

Degree Master of Science Convocation Fall Year 1988

TABLE OF CONTENTS

TABLE OF CONTENTS.....iv

LIST OF FIGURES.....ix

LIST OF TABLES.....xii

LIST OF PLATES.....xiii

ABSTRACT.....xv

ACKNOWLEDGEMENTS.....xvii

CHAPTER 1 - INTRODUCTION

1.1 Introduction..... 1

1.2 Location of the Study Area..... 2

1.3 Geology of the Surrounding Country Rocks..... 3

1.4 Previous Studies of Granitic Rocks in Southern Nova Scotia..... 6

1.5 Previous work in the Halfway Cove and Queensport areas..... 6

1.6 Purpose of Study..... 9

CHAPTER 2 - FIELD RELATIONS AND PETROLOGY

2.1 Introduction.....17

2.2 Exocontact - Meguma Group Rocks

2.2.1 Lithologies.....17

2.2.2 Structure.....18

2.2.3 Metamorphism.....20

2.3 Granite/Meguma Group Contact

2.3.1 Nature of the contact.....22

2.3.2 Relative age of the HCQP.....25

2.3.3 Isotopic age of the HCQP.....25

2.4 Endocontact

2.4.1 Phases of the HCQP

2.4.1.1 Introduction.....26

2.4.1.2 HCQP1.....32

2.4.1.3 HCQP1A.....36

2.4.1.4 HCQP2 and HCQP3.....36

2.4.1.5 HCQP4.....40

2.4.2 Enclaves.....42

2.4.3 Structure

2.4.3.1 Aerial Photograph and Satellite Imagery Interpretation.....45

2.4.3.2 Jointing.....47

2.4.3.3 Dykes and Veins.....49

2.4.3.4 Deformational and Structural features

2.4.3.4.1 Cooling features.....53

2.4.3.4.2 Post-crystallization features...55

2.5 Regional Geophysical Surveys

2.5.1 Introduction.....60

2.5.2 Aeromagnetic expression.....61

2.5.3 Airborne gamma-ray spectrometric surveys

2.5.3.1 Introduction.....63

2.5.3.2 Equivalent Uranium.....63

2.5.3.3 Equivalent Thorium.....65

2.5.3.4 Other surveys.....65

2.5.3.5 Discussion.....67

2.6 Summary.....67

CHAPTER 3 - MINERAL CHEMISTRY

3.1 Introduction.....69

3.2 Biotite

3.2.1 Introduction.....70

3.2.2 Biotite within the study area.....72

3.2.3 Discussion.....75

3.3 Muscovite

3.3.1 Introduction.....80

3.3.2 Muscovite within the study area.....81

3.3.3 Discussion.....81

3.4 Feldspar

3.4.1 Introduction.....89

3.4.2 Feldspar within the study area.....90

3.4.3 Discussion.....95

3.5 Garnet

3.5.1 Introduction.....96

3.5.2 Garnet within the study area.....98

3.6 Summary.....101

CHAPTER 4 - WHOLE ROCK CHEMISTRY

4.1 Introduction.....103

4.2 Nova Scotia Database.....103

4.3 Spearman Rank Correlation.....107

4.4 Major Element Chemistry.....107

4.5 Trace Element Chemistry

4.5.1 Introduction.....123

4.5.2 Trace Element Behaviour in HCQP.....128

4.6 Rare Earth Elements

4.6.1 Introduction.....143

4.6.2 Rare earth element patterns within the HCQP.....145

4.7 Summary.....149

CHAPTER 5 - ECONOMIC GEOLOGY

5.1 Introduction.....152

5.2 Economic Potential of the HCQP

5.2.1 Introduction.....153

5.2.2 Geochemical characteristics of mineralized granites.....154

5.2.3 Characteristics of the HCQP.....155

5.3 Additional Economic Considerations.....158

5.4 Summary.....159

CHAPTER 6 - PETROGENESIS, CONCLUSIONS AND RECOMMENDATIONS FOR FUTURE WORK

6.1 Introduction.....160

6.2 Mode of Emplacement.....160

6.3 Depth of Emplacement.....161

6.4 Petrogenesis of the HCQP

6.4.1 Introduction.....165

6.4.2 Fractional Crystallization.....166

6.4.3 Restite Unmixing.....167

6.4.4 Batch Melting.....169

6.4.5 Assimilation of country rock.....169

6.4.6 Separate sources.....171

6.4.7 Summary.....171

6.5 Source of Magma.....172

6.6 Conclusions.....176

6.7 Recommendations for Future Work.....182

APPENDIX

I Rock Collecton and Staining Technique.....184

II Geochemical Analytical Techniques.....185

III Rock Descriptions.....193

IV Electron Microprobe Analysis

IV-1 Energy Dispersive System.....205

IV-2 Biotite Analyses.....207

IV-3 Muscovite Analyses.....225

IV-4 Plagioclase Analyses.....238

IV-5 Potassium feldspar Analyses.....250

IV-6 Garnet Analyses.....259

REFERENCES 263

## List of Figures


1.1 Location map of the study area, with other granitic bodies of Nova Scotia outlined..... 3

2.1 Lithofacies and outcrop location map of the HCQP.....28

2.2a Ternary QAP diagram for modal analyses from Table 2.1.....30

2.2b Compositional fields of units.....30

2.2c Modal averages of individual units.....30

2.3 Biotite modal percentages versus muscovite modal percentages for units of the HCQP.....33

2.4 Plot of poles to joint planes in the HCQP.....50

2.5 Plot of poles of aplite and pegmatite dykes in the HCQP.....52

2.6a Plot of poles of foliation in the HCQP.....58

2.6b Representation of foliation within the rocks of the HCQP.....58

2.7 Aeromagnetic pattern over the study area.....62

2.8 Equivalent uranium radioelement pattern over the HCQP.....64

2.9 Equivalent thorium radioelement pattern over the HCQP.....64

2.10 Equivalent uranium/equivalent thorium radioelement pattern over the HCQP.....66

2.11 Equivalent potassium radioelement pattern over the HCQP.....66

3.1 Ternary phlogopite-annite-manganese end-member plot for biotite from the HCQP.....76

3.2 Plot of tetrahedral alumina versus $Fe_t/(Fe_t + Mg)$ for biotite from the HCQP.....77

3.3 Plot of octahedral alumina versus Ti for biotite from the HCQP.....79

3.4 Ternary Si-Al-(Fe + Mn + Mg + Ti) plot for muscovite from the HCQP.....85

3.5 Plot of Fe + Mg/(Fe + Mg + Mn + Ti + $Al^{vi}$) versus Na/(Na + K + Ca) for muscovite from the HCQP.....87

3.6 Ternary Ti-Na-Mg plot for muscovite from the HCQP.....88

3.7 Ternary Or-Ab-An for potassium and plagioclase feldspar from the HCQP.....91

4.1 Histogram of granitoid plutons of Nova Scotia, divided into 'northern' and 'southern' plutons.....106

4.2 Major element chemistry versus Thornton-Tuttle Differentiation Index (TTDI) for the HCQP, with fields of other granitoid plutons.....112-116

4.3a $P_2O_5$ versus $TiO_2$ for rocks of the HCQP.....118

4.3b Normative corundum versus TTDI for rocks of the HCQP.....118

4.4 Ternary Qtz-Ab-Or plot for rocks of the HCQP.....121

4.5 Ternary Or-Ab-An and $K_2O$-$Na_2O$-CaO diagram for rocks of the HCQP.....122

4.6 $SiO_2$ versus $Na_2O/K_2O$ for rocks of the HCQP.....124

4.7a Rb versus TTDI for rocks of the HCQP.....133

4.7b Sr versus TTDI for rocks of the HCQP.....133

4.8 Rb versus $K_2O$ for rocks of the HCQP.....134

4.9 U versus Th for rocks of the HCQP and rocks of the SMB.....136

4.10a Th/U versus F.....138

4.10b Th/U versus Th.....138

4.10c Th/U versus U.....138

4.11 Equivalent thorium pattern for the HCQP, with rocks units outlined.....139

4.12 Barium versus Th/U.....141

4.13a Zr versus Th.....142

4.13b Zr vs $TiO_2$.....142

4.14 Chondrite-normalized REE patterns in the HCQP, compared to rocks of the SMB.....146

6.1 P-T diagram for various AFM liquidus topologies.....164

## List of Tables


1.1 Characteristics of plutonic bodies within the Meguma Terrane.....10-12

2.1 Modal percentages of minerals of the HCQP.....31

3.1a Textural criteria used to recognize primary and secondary white mica.....82

3.1b Chemical characteristics of primary and secondary white mica.....82

4.1 Discriminating northern and southern plutons on the basis of whole-rock chemistry.....105

4.2 Spearman Rank Correlation matrix.....108

4.3 Major element chemistry of rocks of the HCQP.....109-111

4.4 Characteristics of selected trace elements.....125-127

4.5 Trace element abundances of rocks of the HCQP.....129-132

4.6 Rare Earth Element abundances of rocks of the HCQP.....147

5.1 Characteritics of granites hosing rare element mineralization, compared to rocks of the HCQP.....154-155

5.2 Representative chemical analyses of selected felsic rocks within southern Nova Scotia.....157

6.1 Characteristics of granites using different classification schemes.....174

## List of Plates


1.1a Good exposure of the barrenlands of the Queensport lobe of the HCQP..... 6

1.1b Characteristic outcrop exposure of the Halfway Cove lobe of the HCQP..... 6

2.1 Contact between monzogranitic rocks and a small roof pendant of Halifax Formation metasedimentary rocks.....23

2.2 Representative slabs of Unit HCQP1.....34

2.3 Representative slabs of Unit HCQP1.....35

2.4 "Intensely porphyritic" monzogranite of Unit HCQP1A.....37

2.5 Representative slabs of Unit HCQP2.....38

2.6 Representative slabs of Unit HCQP3.....39

2.7 Representative slabs of Unit HCQP4.....41

2.8 Enclaves within the HC lobe.....43

2.9 Enclave abundance in the HC lobe near the Lundy Fire Tower.....43

2.10 Unusual enclave in Unit HCQP1A.....46

2.11a Typical outcrop outside the barrenlands of the HC lobe.....48

2.11b Pavement outcrop typical of the barrenlands of the QP lobe.....48

2.12 Aplite veins within the HC lobe near the Lundy Fire Tower.....51

2.13 Foliation developed within the granitic rocks of the HCQP.....56

2.14 Extensive alteration and deformation from the rocks of the HC lobe.....57

3.1a Photomicrograph of representative biotite within the HCQP.....74

3.1b Photomicrograph of biotite with alteration to chlorite within the HCQP.....74

3.1c Photomicrograph of biotite with alteration to muscovite within the HCQP.....74

3.1d Photomicrograph of biotite with alteration to muscovite and feldspar.....74

3.2a Photomicrograph of primary muscovite within the HCQP.....84

3.2b Photomicrograph of primary muscovite intergrown with biotite within the HCQP.....84

3.2c Photomicrograph of muscovite altering from biotite and altering from plagioclase within the HCQP.....84

3.3a Photomicrograph of well-developed plagioclase zoning within the HCQP.....93

3.3b Photomicrograph of potassium feldspar within the HCQP.....93

3.3c Photomicrograph of well-developed rapakivi texture of Unit HCQP4.....93

3.4a Photomicrograph of garnet (plane light) within the HCQP.....100

3.4b Photomicrograph of garnet (crossed nicols) within the HCQP.....100

3.4c Almandine-spessartine-pyrope diagram for garnet analyses within the HCQP.....100

## ABSTRACT

The Halfway Cove-Queensport pluton (HCQP) of eastern Nova Scotia is a moderately deformed, post-Acadian granitoid intrusion that was emplaced into regionally deformed and metamorphosed Meguma Group metasedimentary rocks by passive stoping, with some degree of forceful emplacement. Deformation features (C-S fabrics) occur in the northern part of the body, closest to the Cobequid-Chedabucto fault zone, and within the southern part, closest to a postulated shear zone. The pluton is composed primarily of medium- to coarse-grained monzogranite, with minor granodiorite. Five rock units are recognized by textural and mineralogical characteristics (HCQP1, HCQP1A, HCQP2, HCQP3, HCQP4). There are minor late-stage intrusions of aplite, pegmatite and leuco-granite.

All rocks, except the late-stage intrusions, contain quartz, alkali feldspar, plagioclase, muscovite and biotite. Garnet is present as xenocrystic grains in monzogranite of some units, and as magmatic grains in late-stage aplites. Apatite occurs in trace amounts, and cordierite is not present. This absence contrasts with other granitoid bodies of southwestern and south-central Nova Scotia (e.g. South Mountain Batholith and the Musquodoboit Batholith) where cordierite is common. The presence of garnet and muscovite, both of presumed magmatic origin, constrains the pressure of crystallization to between 3 and 4 kbars (10.5-14 km).

Major element chemical analyses indicate that the rocks are peraluminous (i.e. $Al_2O_3/(CaO + Na_2O + K_2O) > 1$). Compositions

resemble those of the Halifax Pluton, the Musquodoboit Batholith, and the granitoid plutons of central and eastern Nova Scotia (excluding the Liscomb Complex), with lower $FeO_t$, $TiO_2$ and higher $Al_2O_3$, $P_2O_5$ and normative corundum than the South Mountain Batholith. The least evolved units of the HCQP, however, are chemically more similar to rocks of the South Mountain Batholith. A well-defined chemical break between the two least evolved units (HCQP1 and HCQP1A), and the three more evolved units (HCQP2, HCQP3 and HCQP4), suggests that, although some of the five units may be related by fractional crystallization, other processes such as assimilation and melting of heterogeneous sources may have contributed to the overall chemical variation in the HCQP. Major and trace element characteristics of the three more evolved units suggest that at least two of the units are co-magmatic. Rare earth element patterns of unit HCQP1 resemble the granodiorite patterns of the SMB, but patterns of units HCQP2 and HCQP4 are different from both HCQP1 and the SMB.

Field, petrographic and geochemical characteristics suggest that the economic potential of the HCQP is limited.

ACKNOWLEDGEMENTS

I am very grateful to my supervisor, Dr. Barrie Clarke, for his help, advice, criticisms and suggestions, all of which have contributed greatly to my work and to me, and for his patience and support for the duration of the writing. I would also like to thank both Dr. G. Muecke of my committee, for being so readily available to read the final product, and Dr. John Hill, my external examiner, for a thorough reading of this work. Financial support for this thesis was provided by Dalhousie University Graduate Fellowships for 1982-1983 and 1983-1984. Logistical support during the 1983 summer thesis field mapping was provided by the Meguma Gold project of the Nova Scotia Department of Mines and Energy.

I would like to thank all my colleagues at the Nova Scotia Department of Mines and Energy, for their interest and numerous discussions. In particular, I am grateful to Mike MacDonald, A. K. Chatterjee and George O'Reilly for their ideas and support. Special thanks to Paul Smith for his constant help and encouragement.

Mr. S. Parikh and Mr. R. MacKay provided expert assistance with the chemical and the electron microprobe analyses, respectively. I am indebted to the drafting department of the Nova Scotia Department of Mines and Energy, for their efforts with my figures. I also thank my fellow graduate students for their help, in particular, Linda Richard, Stephanie Douma and Kathy Gillis.

Lastly, a very special thank-you to my husband, Paul, for his continued support and encouragement during the entire process, and for

his many hours of collecting rocks, colouring diagrams, reading, and editing.

# CHAPTER 1 - INTRODUCTION

## 1.1 Introduction

The Meguma Terrane comprises the mainland area of Nova Scotia south of the east-west trending Cobequid-Chedabucto fault zone (Fig. 1.1), and is geologically unique within the Appalachians (e.g. Keppie, 1982; Mawer and Williams, 1986). Cambro-Ordovician metasedimentary rocks of the Meguma Group (Goldenville and Halifax Formations) underlie 30% of this area (Taylor, 1967). Overlying these formations are Ordovician, Silurian and Devonian metasedimentary and metavolcanic rocks of the White Rock, Kentville, New Cannan and Torbrook Formations. Intruded into these supracrustal rocks are numerous granitoid plutons of Devono-Carboniferous age, and there is a need for detailed studies to be undertaken on these bodies to add to our knowledge and understanding of the geology of Nova Scotia.

Previous workers (Faribault, 1908a, 1908b, 1908c, 1916, 1931; Smitheringale, 1960, 1973; Allen, 1963; Taylor, 1967, 1969; T. E. Smith, 1974) mapped the contacts of the granitic masses. Detailed studies involving the chemistry, petrology, mineralogy and economic potential of individual plutons have only recently been undertaken. These plutons are shown on Figure 1.1. South Mountain batholith studies include those of McKenzie, 1974; McKenzie and Clarke, 1975; T. E. Smith, 1974, 1979; Clarke et al., 1976; Charest, 1976; Farley, 1979; Longstaffe et al., 1980; Allan and Clarke, 1981; Muecke and Clarke, 1981; O'Reilly et al., 1982; Maillet, 1984; Logothetis, 1985; Maillet and Clarke, 1985; MacDonald et al., 1986, 1987; Musquodoboit

FIGURE 1.1. Location map of the study area. Other granitic bodies of Nova Scotia are also outlined.

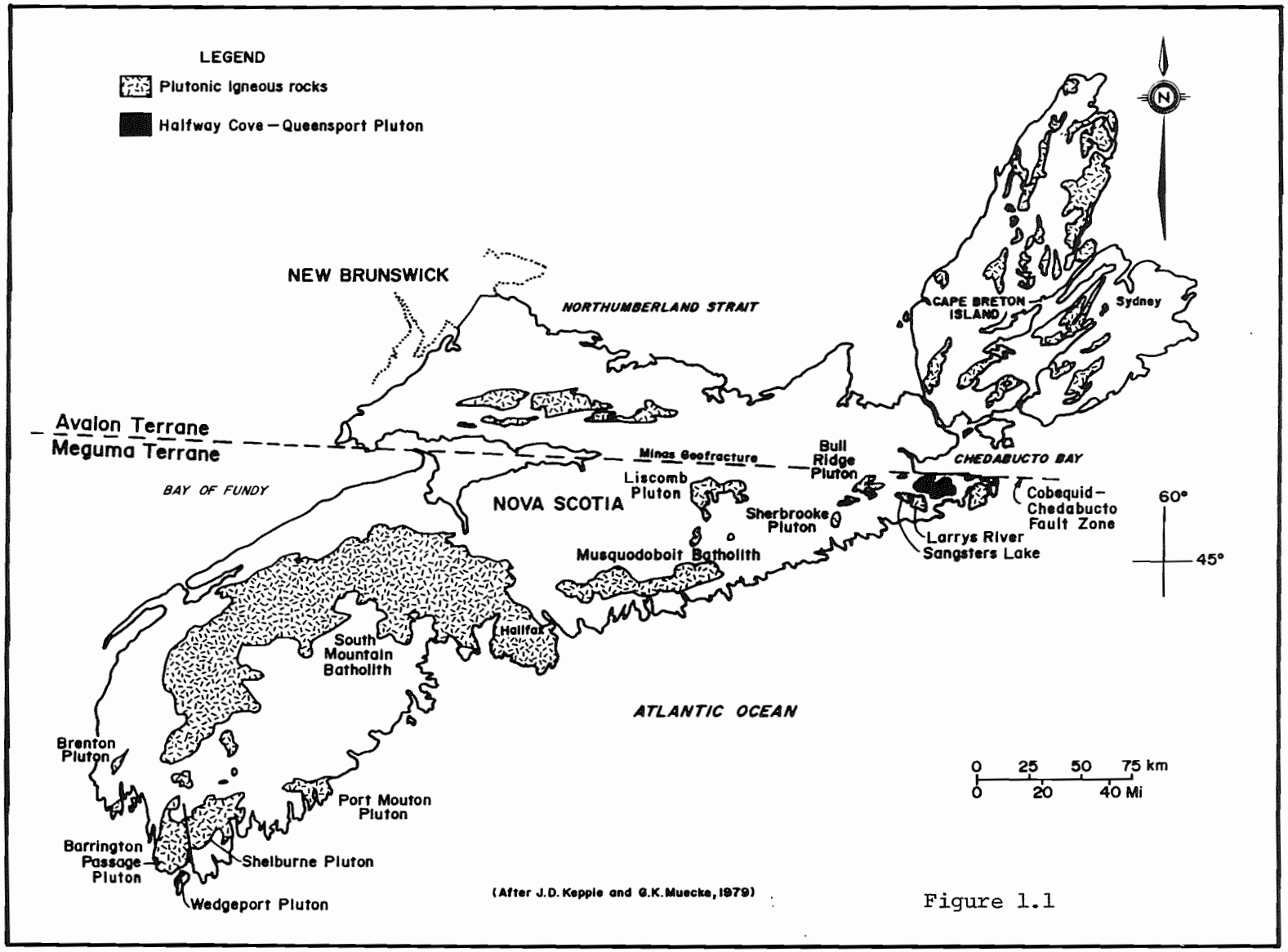
LEGEND
Plutonic igneous rocks
Halfway Cove – Queensport Pluton
NEW BRUNSWICK
NORTHUMBERLAND STRAIT
CAPE BRETON ISLAND
Sydney
Avalon Terrane
Meguma Terrane
Minas Geofracture
Bull Ridge Pluton
CHEDABUCTO BAY
BAY OF FUNDY
Liscomb Pluton
NOVA SCOTIA
Sherbrooke Pluton
Cobequid – Chedabucto Fault Zone
Larrys River
Sangsters Lake
Musquodoboit Batholith
60°
45°
South Mountain Batholith
Halifax
ATLANTIC OCEAN
Brenton Pluton
Port Mouton Pluton
Barrington Passage Pluton
Shelburne Pluton
Wedgeport Pluton
0 25 50 75 km
0 20 40 Mi
(After J.D. Keppie and G.K. Muecke, 1979)

Figure 1.1

1981; MacDonald and Clarke, 1985; and work on other smaller plutons includes that of McKenzie and MacGillivray, 1974; de Albuquerque, 1977; Alizay, 1981; Thomas, 1982; Smith, 1981; Allen and Barr, 1983; Chevalier, 1983; O'Reilly, 1984, 1985; Rogers, 1985; Hill, 1986; Giles and Chatterjee, 1987; (Woodend) Douma, 1988.

The previous studies were done mostly on plutons in the western and central portions of the Meguma Terrane, but little detailed work has been done on the granites of the eastern Meguma Terrane. The Sherbrooke pluton was the subject of both a graduate thesis (Alizay, 1981) and minor subsequent work by Nova Scotia Department of Mines and Energy (Smith, 1981). Work recently done by the Geological Survey of Canada examined the easternmost granites of the Chedabucto Bay area (Hill, 1986). A detailed study on two other granitic plutons of eastern Nova Scotia (Sangster Lake and Larrys River) is currently being undertaken by O'Reilly (1984, 1985). Giles and Chatterjee (1987) examined the Liscomb pluton, a peraluminous granitoid-gneissic-gabbroic complex in central Nova Scotia. This thesis involves a comprehensive study of an additional granitic body in the Chedabucto Bay area, the Halfway Cove-Queensport pluton.

## 1.2 Location of the Study Area

The Halfway Cove-Queensport pluton (HCQP) is situated in Guysborough County (latitude 45°16′ to 45°21′N, longitude 61°14′ to 61°30′W, N.T.S. sheet 11F/06C), is a two-lobed pluton, and covers a total area of approximately 160 $km^2$ (Fig. 1.1). The western Halfway Cove lobe is a circular mass approximately 70 $km^2$ (Fig. 1.1 and Map 1). Its northern margin lies south of the Cobequid-Chedabucto fault zone,

with outcrop in the northeastern portion reaching the shores of Chedabucto Bay, but generally separated from it by a narrow margin of metasedimentary rocks of both the Goldenville and Halifax Formations. The eastern lobe of the pluton, the Queensport lobe, is also circular, covering approximately 90 $km^2$. The Queensport lobe is separated from Chedabucto Bay both by Goldenville and Halifax Formation rocks.

Highways 16 and 316 border the body and provide reasonable access to the margins. Access to the interior is generally difficult because of a lack of road and water systems.

Outcrop exposure of both lobes is generally good to excellent in some places. Much of the eastern portion, the Queensport lobe, is comprised of barrens with exposure in places up to 50% (Plate 1A). The Halfway Cove lobe generally has a greater till cover. The western portion of this lobe is well exposed, with poor to fair exposure in the remainder (Plate 1B). Granitic boulders and blocks in varying shapes and sizes are common in both lobes. Sampling was difficult as the majority of the outcrops were flat with widely-spaced vertical or nearly vertical jointing. This massive nature of the rocks made the collection of fresh, unaltered samples by conventional methods nearly impossible, and necessitated the use of a small Pionjar drill and dynamite to blast samples large and fresh enough for geochemical analysis.

## 1.3 Geology of the Surrounding Country Rocks

The Meguma Group metasedimentary rocks in the Meguma Terrane, the Goldenville and Halifax Formations, form the country rocks into which


PLATE 1a. Good exposure of the barrens of the Queensport lobe of the HCQP.


PLATE 1b. Characteristic outcrop exposure and granite boulder cover of the Halfway Cove lobe of the HCQP.

the body has intruded, and this terrane is generally interpreted as a continental margin deposit (Schenk, 1970, 1982).

The Goldenville Formation is a sequence of thickly stratified, poorly sorted metagreywackes and metaquartzites (Taylor, 1967; Schenk, 1982), comparable to a mid-fan to deep-water fan system of a modern channel deposit. The overlying Halifax Formation consists of dark silty to sandy slates and quartz metawackes (Taylor, 1967; Schenk, 1982), and is interpreted as a turbidite sequence grading upwards to a slope and outer shelf environment.

The Meguma Group is generally considered to be Cambro-Ordovician, based on poorly preserved fossil evidence indicating Tremadocian age (Crosby, 1962; Smitheringale, 1973: Schenk, 1970; Schenk, 1982). Recent isotopic work (Clarke and Halliday, 1985) indicates the average crustal residence time for the Meguma Group source to be approximately 1750 Ma. Zircons from the Goldenville Formation (Krogh and Keppie, 1988) suggest a mixed source (ages ca. 600 and ca. 2050-2960 Ma).

The Meguma Group strata were undeformed during the Ordovician Taconian Orogeny, but were deformed and compressed during the Devonian Acadian Orogeny (Fyson, 1966; Keppie, 1982). The main episode of folding resulted in the rocks of the Meguma Group and overlying strata being compressed into a series of anticlines and synclines. The axes of these gently plunging folds strike northeast-southwest in the southwestern portion of the province and progressively rotate to strike east-west in eastern Nova Scotia. Some folds are offset by a series of northwest-trending faults (Harris and Schenk, 1976).

In the western half of the province between Yarmouth and Wolfville, the White Rock, Kentville, New Cannan and Torbrook

Formations overlie the Meguma Group rocks. The White Rock Formation consists of metasedimentary rocks (quartzite, slate, metasiltstone) with a considerable thickness of volcanic rocks (Taylor, 1967; Smitheringale, 1973; Lane, 1976, 1980; Sarkar, 1978; Schenk, 1982). The overlying Kentville Formation consists of slate and siltstone and is limited in geographic extent to the central portion of the province in the Wolfville area. The New Cannan Formation consists of tuff with interbedded siltstone and silt, and the overlying Torbrook Formation is a richly fossiliferous sequence of metasedimentary rocks. The Lower Devonian Torbrook Formation is the youngest pre-granitic formation. The latter two formations outcrop near Wolfville and in the western-central portions of the Annapolis Valley, respectively (Keppie, 1977). None of these formations is exposed in the eastern portion of the province.

Following the period of folding during the Acadian Orogeny, these pre-granitic formations were intruded by granodioritic to monzogranitic peraluminous plutons. Contact metamorphic effects (e.g. the development of andalusite and/or cordierite in argillaceous rocks and recrystallization to hornfelses) are recognizable in aureoles up to 2.4 km wide (Taylor and Schiller, 1966; Taylor, 1969).

Smith (1983) described two additional deformations which affected both the metasedimentary and granitic rocks in the Guysborough area. Mawer and Williams (1986) and Hill and Raeside (1987) described prolonged and overlapping events of deformation and metamorphism which affected both the metasedimentary and granitic rocks of the eastern Meguma Terrane. These events suggest a complex and long history of movement along the Cobequid-Chedabucto fault System, and also suggest

that the eastern granites are syn-tectonic. Further discussion of these structural and metamorphic events is in Sections 2.2.2, 2.2.3, and 2.4.3.4.2.

## 1.4 Previous Studies of Granitic Rocks in Southern Nova Scotia

Prior to 1974, the granitic bodies of southern Nova Scotia had received only limited attention. The results of subsequent work undertaken on these granitic plutons is outlined in Table 1.1. In addition, many Nova Scotia Department of Mines and Energy (N.S.D.M.E) in-house publications have also dealt with various aspects of granitic bodies throughout southern Nova Scotia. This table is not designed to be a complete reference list of all the work that has been done in every granitic pluton within the province, but contains the major references, results and interpretations.

## 1.5 Previous work in the Halfway Cove and Queensport areas

Reconnaissance geological mapping by Fletcher and Faribault (1887) outlined the HCQP and indicated that the lobes were separate, presumably based on the lack of outcrop and the low-lying nature of the topography. Schiller (1963) studied the mineralogy and geology of predominantly the Meguma Group rocks in the Guysborough area and adopted this interpretation of the nature of the intrusion. Stevenson (1964) mapped the bodies, and interpreted them as being one continuous body. These studies involved mapping the rocks simply as granite with little differentiation noted or mapped. Since that time, reconnaissance work has been conducted in the Chedabucto Bay area,

TABLE 1.1 Characteristics of plutonic bodies within the Meguma Terrane.

| | SMB | MB | Southern plutons | Eastern Meguma Terrane |
|---|---|---|---|---|
| GEOGRAPHIC LOCATION | Southwestern Nova Scotia; Halifax to Yarmouth | South central Nova Scotia | Southwestern Nova Scotia; Shelburne, Yarmouth | Eastern Nova Scotia; east of Musquodoboit Batholith (including Liscomb complex) |
| AREA | >10,000 $km^2$ | 800 $km^2$ | generally small ( 100 $km^2$), although Barrington Passage Pluton 500 $km^2$ | generally small (<200 $km^2$), although Liscomb complex 350 $km^2$ |
| ROCK TYPES | granodiorite-monzogranite-leucomonzogranite-leucogranite aplite and pegmatite | two-mica monzogranite with with later aplitic and porphyritic phases | granodiorite, monzogranite, tonalite, trondhjemite minor norite, diorite, aplite, pegmatite, lamprophyre | biotite tonalite to granodiorite, monzogranite, minor leucomonzogranite; Liscomb complex contains gneisses |
| AGES - Isotopic | Devono-Carboniferous<br>372±2 Rb-Sr whole rock<br>364-361±1 Rb-Sr w.r.<br>mean age 366.7±4 | Devono-Carboniferous<br>368±3.2 $Ar^{40}/Ar^{39}$<br>266±17 Rb-Sr w.r.<br>370 Rb-Sr bio | Devono-Carboniferous<br>249-300-350 $Ar^{40}/Ar^{39}$<br>325±9 $Ar^{40}/Ar^{39}$ bi-mu (Brenton)<br>326-356 $Ar^{40}/Ar^{39}$ bi-mu (Port Mouton) | Devono-Carboniferous<br>369±2 Rb-Sr w.r. (Sherbrooke pluton)<br>362-386 Rb-Sr w.r.<br>372-373 monazite (Halfway Cove) |
| - Stratigraphic | -intrudes Meguma Group<br>-intrudes Torbrook in part<br>-unconformably overlain by Carboniferous Horton and Windsor Groups | intrudes Meguma Group | -intrude Meguma Group and intrude Silurian White Rock formation (Brenton) | -intrude Meguma Group<br>-granitic cobbles occur in Horton conglomerate to west |
| DEPTH OF EMPLACEMENT | -high-level epizonal (sharp discordant contacts; epizonal granite features | -high-level epizonal (truncates regional structures; sharp undeformed | 3-4 kbar (ca. 12 km) | high-level epizonal (10-13 km) |

| | | | | |
|---|---|---|---|---|
| | turbid feldspars, miarolitic cavities)<br>1-4 kbar pressure (4-10 km) | -MB and SMB connected at depth (5km)<br>-close to roof zone | | |
| MODE OF EMPLACEMENT | passive stoping, fracture | passive stoping, fracture | passive stoping; possibly some forceful | passive stoping; possibly some forceful |
| XENOLITHS | -dispersed throughout<br>-biotite-rich units (granodiorite, biotite monzogranite) contain more xenoliths than two-mica monzogranite units | -dispersed throughout; some concentration at edges and central regions | -lack of xenoliths in the Brenton pluton<br>-abundant xenoliths in Port Mouton | -dispersed throughout, but not abundant |
| STRUCTURAL FEATURES | -generally undeformed (i.e. post-tectonic)<br>-internal features include igneous flow foliations, biotite schlieren | -undeformed<br>-similar internal structures listed for SMB | -Brenton, Barrington, Shelburne deformed<br>-several stages of deformational, ductile and flow foliation in Port Mouton | -deformational features in northern portions of some plutons<br>-several stages of ductile shearing (easternmost granites) |
| CHEMICAL VARIATIONS | -peraluminous<br>-single co-magmatic suite<br>-fractional crystallization<br>-trace elements show large variations; compatible elements strongly depleted in more evolved rocks; incompatible enriched in more differentiated; REE's decrease with differentiation | -peraluminous<br>-similar trends to SMB magmatic differentiation<br>-MB and eastern SMB show differences from western SMB in $Al_2O_3$, normative corundum, $P_2O_5$<br>-similar major, trace and REE trends to SMB | -peraluminous<br>-biotite tonalite distinctive from the other rocks<br>-granodiorite, monzogranite related by differentiation<br>-trends generally similar to those observed in the SMB, but variable<br>-REE's comparable with SMB and other granites | -peraluminous<br>-single, co-magmatic suite of rocks by fractional crystalliization not applicable for different plutons<br>-high normative corundum, restricted compositional range |
| MINERALIZATION | -numerous showings in New Ross area (polymetallic)<br>-greisen-hosted Sn-Zn-Cu East Kemptville<br>-topaz (East Kemptville) | -limited showings (W, U)<br>-Dunbrack (Pb-Zn-Ag-Cu)<br>-small sulphide-bearing greisen zones | -Wedgeport (Mo)<br>-Port Mouton pluton (Be, Mo) | |

| | | | | |
|---|---|---|---|---|
| | -shear-related U mineralization Millet Brook<br>-smaller showings (W,U,Pb,Sn,Be, Fe) throughout | | | |
| SOURCE OF MAGMA | -partial melting of lower crustal material; some contribution of mantle derived magmas is possible | -similar to SMB | -partial melting of meta-greywacke and possible quartz-feldspathic gneiss<br>-same petrogenic mechanism involved in formation of magma types; parental magma similar<br>-lamprophyre mantle derived | -two or more batches of magma from heterogenous source of intermediate to felsic continental crust with some proportion of pelitic material |
| MAJOR REFERENCES | McKenzie, 1974; Smith, 1974; McKenzie and Clarke, 1975; Muecke and Clarke, 1981; Chatterjee and Muecke, 1982; O'Reilly et al., 1982; Clarke and Muecke, 1985; MacDonald et al., 1987 | MacDonald, 1981; MacDonald and Clarke, 1985 | de Albuquerque, 1973; O'Reilly, 1976; (Woodend) Douma, 1988 | Alizay, 1981; Chevalier, 1983; O'Reilly, 1984, 1985; Ford and O'Reilly, 1985; Hill, 1986; Giles and and Chatterjee, 1987; Hill, 1988. |

including airborne radiometric and magnetic work by the G.S.C. and work by private exploration companies, but extensive geological and geochemical work has only recently been undertaken (Ham and O'Reilly, 1984; O'Reilly, 1984, 1985; Ford and O'Reilly, 1985; Hill, 1986).

In 1974, McKenzie and MacGillivray conducted a preliminary investigation into the granitic plutons east of Halifax. Hand specimens were collected, of which four were obtained from the HCQP. This study, coupled with work conducted by the G.S.C. (Ford and Ballantyne, 1983) and N.S.D.M.E., indicated that the pluton consists of two-mica monzogranite with foliation evident near the fault zone.

A regional lake sediment survey conducted within the Chedabucto Bay area (Bingley and Richardson, 1978) indicated elevated U and Th within the area. Stea and Fowler (1979) released till sampling data from the Eastern Shore, including results from the Chedabucto Bay areas. No samples were collected directly over the HCQP granitic rocks, but two collected down-ice from the body have slightly elevated levels (in the A horizon) of Cu and Mg. One sample collected east of Halfway Cove is anomalous in Ag and Pb in the A horizon and Pb, Zn and Mn in the B horizon.

Reconnaissance and detailed mapping, soil sampling and geophysical surveys were undertaken by St. Joe Minerals in 1981 and 1982 in the area of Larrys River slightly to the south of the pluton (N.S.D.M.E. Assessment Reports). Other companies have been involved in uranium, tin and tungsten exploration (Gulf Minerals, 1980; Esso Minerals, 1981; N.S.D.M.E. Assessment Reports) in the granitic plutons located in N.T.S. topographical sheets 11F/04C and 11F/05C. Little detailed work

has been conducted in the Chedabucto Bay area, and particularly the HCQP.

A reconnaissance airborne gamma-ray spectrometric survey was flown in 1978 by the G.S.C. over the eastern portion of Nova Scotia with line spacings of 5 km (Geological Survey of Canada, 1978). Follow-up regional surveys were conducted in 1979 and 1980 with north-south lines with spacings of 1 km. The more detailed surveys produced maps with increased resolution of the reconnaissance survey results (Ford and Ballantyne, 1983).

The G.S.C. released its compilation of results from these airborne surveys (1982) as maps with equivalent uranium (eU), equivalent thorium (eTh), equivalent uranium/equivalent thorium (eU/eTh) and equivalent uranium/potassium $10^4$ (eU/K $10^4$) (Geological Survey of Canada, 1982). These surveys outlined a prominent "Y"-shaped eTh pattern in the Queensport lobe. These results will be discussed in more detail in Chapter 4.

As a result of these surveys, Ford and Ballantyne (1983) of the G.S.C. conducted a regional geological survey to check the elevated values in the Chedabucto Bay area. They concentrated on the more westerly plutons (i.e. Sangster Lake where there was a high U response), but collected six lithogeochemical samples from traverses across the HCQP and these samples were subsequently analyzed for major, minor and trace elements. Some of the granites (i.e. Sangster Lake) classify as "specialized" granites of Tischendorf (1977), exhibiting elevated levels of U, Sn, Li, Nb and Rb and depleted levels of Th, Sr and Ba compared with the global average for granites (Taylor, 1965). The HCQP samples collected also exhibit depleted levels of Ba, Sr and

Th compared with the global averages, but these levels are not as depleted as in the Sangster Lake body. Rb, Sn and Li are slightly enriched within the HCQP over the global averages but are less enriched than in the Sangster Lake pluton. These results indicated that the HCQP rocks may exhibit some differentiation but are not as "specialized" as the Sangster Lake body.

## 1.6 Purpose of Study

In general, the purpose of this thesis is to improve on the existing geological knowledge of the HCQP by systematic geological mapping (1:50,000) and geochemical analysis. In addition, specific objectives are:

1) to determine the classification and categorization of the plutonic rocks of the HCQP and to relate these findings to other granitic rocks in the Meguma Terrane;

2) to map the contacts and boundaries of the pluton and any different units within the body;

3) to determine the mineralogical and geochemical characteristics of the pluton, and to determine if the pluton represents an intrusive complex similar to the South Mountain Batholith;

4) to establish the age relationships of the possible different units within the body, the mode and depth of emplacement and the petrogenesis of the pluton;

5) to evaluate structural features of the body for determination of the timing of events during and subsequent to intrusion;

6) to evaluate the economic potential of the pluton, in view of economically important mineral occurrences within similar granites in Nova Scotia and other parts of the world; and

7) to propose an explanation for the unusual equivalent Th (eTh) radiometric pattern apparent in the Queensport lobe.

# CHAPTER 2 - FIELD RELATIONS AND PETROLOGY

## 2.1 Introduction

Field mapping of the HCQP and surrounding Meguma Group metasedimentary rocks was conducted in parts of the summers of 1983 and 1984. Field relations, structural characteristics, and internal features were studied, and the granitic rocks divided into units initially on the basis of texture and mineralogy, followed by geochemical characteristics. Nomenclature of the rocks follows the classification of Streckeisen (1976).

## 2.2 Exocontact - Meguma Group Rocks

### 2.2.1 Lithologies

The Goldenville Formation consists of thinly to thickly bedded alternating lithic metagreywacke and feldspathic quartzite (Taylor, 1967; Schenk, 1982). Within these psammatic units are minor amounts of interbedded argillite, metasiltstone and slate. The overlying Halifax Formation consists of thinly bedded metapelite (slate and metasiltstone) (Taylor, 1967; Schenk, 1982). A gradational contact of variable thickness (500 m minimum to 1-2 km maximum) has been documented as separating the Goldenville rocks from the overlying Halifax Formation in southwestern Nova Scotia (Harris and Schenk, 1976; Taylor, 1967; O'Brien, 1986). Recent work has determined that in some areas of southern Nova Scotia (LaHave River, Mahone Bay), a new unit 1-2 km thick termed the Green Bay Formation (comprised of three members) is recognizable between the two formations (O'Brien, 1986). The ident-

ification of this unit indicates that the contact between the Halifax and Goldenville Formations is complex. With additional detailed work, this complexity may be recognized elsewhere in the Meguma Terrane.

The source of the Meguma Group rocks is thought to be an area to the present southeast, as determined by paleocurrent direction studies (Schenk and Lane, 1982; Schenk, 1982). Petrographic work yields information that the source is most likely a quartz-rich terrain that consists of gneiss, granodiorite and metasedimentary rocks (Schenk, 1982; Schenk and Lane, 1982).

### 2.2.2 Structure

Recent detailed structural studies undertaken specifically in the Guysborough and Chedabucto Bay area (Nichols, 1976; Smith, 1983; Keppie, 1983; O'Brien, 1983; Eddy, 1987) have provided information about the tectonic events in this area affecting both the metasedimentary and granitoid rocks. Three episodes of Acadian (?) deformation are recognized in minor structures (superimposed folds, cleavages and lineations) on the south side of the HCQP, while the major, regional structure consists of large scale folds and faults. The minor structures record the Sherbrooke deformation (Ds), the Guysborough deformation (Dg), and the Country Harbour deformation (Dc) (Keppie, 1983; O'Brien, 1983), so named for the location where they are best exposed, and also referred to as F1, F2, and F3, respectively (Smith, 1983).

The first phase of deformation, the Sherbrooke deformation (Ds or F1), involves penetrative cleavage, localized faults and some vein-filled fractures (O'Brien, 1983). The second phase of deformation, the Guysborough deformation (Dg or F2) and the main phase of deformation

(Keppie, 1983), produced major folds, cleavages, lineations and vein-filled fractures (O'Brien, 1983). Cleavage, lineation and, rarely, folding (O'Brien, 1983) outline the third phase of deformation, the Country Harbour deformation (Dc or F3).

In the eastern end of the Meguma Terrane, Hill (1986), Mawer and Williams (1986), and Hill and Raeside (1987) suggest that there has been multi-stage deformational history involving the Meguma Group and granitoid rocks. Hill (1986) and Hill and Raeside (1987) have divided the events into two main stages: $D_1$, the dominant event throughout most of the Meguma Terrane, includes large-scale folding and upper greenschist metamorphism; and $D_2$ involves complex, overlapping, polyphase deformation (e.g. transposition foliation, Z-shaped folds, crenulation cleavage, brittle-ductile shear zones) associated with dextral transcurrent movements along the Cobequid-Chedabucto fault zone (Mawer and White, 1987). Pluton emplacement occurred after an initial stage of regional deformation, which was at least partly synchronous with intense, but localized, dextral shearing. Metamorphic mineral growth occurred and overlapped with granite emplacement (Raeside et al., 1988).

Within the thesis area, the northern Meguma Group rocks closest to the Cobequid-Chedabucto fault zone (on the shores on Chedabucto Bay and Highway 316) are intensely deformed, with tight folding of beds, boudinaged quartz veining, steep cleavage development, fracturing, shearing and slickensides. The metasedimentary rocks surrounding the pluton away from the fault zone exhibit localized faulting, small-scale gentle folding and kinking, and minor quartz veining. Andalusite- and chiastolite-sericite schist in the southern portion of the QP lobe are

tightly folded with minor shearing. Keppie (1985) and Raeside et al. (1988) speculate that this latter area may represent part of a major shear zone.

### 2.2.3 Metamorphism

Regional metamorphism within the Meguma Group grades from chlorite, biotite and garnet zones of greenschist facies within the central portion of the Meguma Terrane to garnet, andalusite, staurolite, cordierite and sillimanite zones of amphibolite facies in the southwestern portion and to middle amphibolite in the eastern portion of the Terrane and the Chedabucto Bay area (Schiller, 1963; Taylor and Schiller, 1966; Keppie and Muecke, 1979). This regional metamorphism has been dated by the $^{40}Ar/^{39}Ar$ method (Reynolds and Muecke, 1978) and an age of 415-400 Ma, recently revised to 400-390 Ma (Elias, 1986) and 405-390 Ma (Muecke et al., 1988), has been determined, believed to represent the cooling age of the Acadian metamorphic events in Nova Scotia.

Contact metamorphic effects in the metasedimentary rocks exposed on the roads around the HCQP were difficult to determine for two reasons: 1) there are several other granitic plutons (Whitehaven, Dover, Sangster Lake and Larrys River) in the area of the HCQP, the combined effects of which could overlap in the contact aureole, and 2) the effects of the deformation possibly related to the Cobequid-Chedabucto fault zone. Cordierite poikiloblasts are recognizable in a zone approximately 400 metres wide around the HCQP in the southeastern portions of the body. These poikiloblasts, full of inclusions and commonly intensely pinitized, occur within the metasedimentary strata

south of Donahue Lake up to a distance of 500 metres from the granite/metasediment contact. Schiller (1963) attributes the development of cordierite porphyroblasts within 1.5 km of granite at Whitehead to contact metamorphism. Anhedral to subhedral, generally sericitized, andalusite grains (2-5 mm) also occur within this cordierite-bearing contact aureole and are believed to be contact-related. Andalusite, euhedral, <1 cm, and full of inclusions, is also common within Halifax Formation schists to the south and east of the HCQP, restricted to stratigraphically controlled zones that can be traced for up to 40 km in length (Schiller, 1963). These zones, not necessarily related to exposed granitic bodies, are believed to represent compositionally different strata, possibly originally kaolin-rich sedimentary units (Schiller, 1963; Taylor and Schiller, 1966). Nichols (1976) studied the structure and petrology of the Port Felix area to the south of the HCQP, and documented two episodes of andalusite growth. Small (<5mm), euhedral, pleochroic, prismatic andalusite, which is generally clear although highly sericitized near the granite contacts, formed during contact metamorphism. Larger grains (up to 1.5 cm) of blocky, non-pleochroic andalusite, which is altered to sericite, muscovite and chlorite, crystallized in the initial stages of a third phase of deformation (related to the regional $F_2$). Staurolite, reported by Schiller (1963) to occur in restricted localities within the Chedabucto Bay area (Lundy area), was not observed in the contact aureole of the HCQP.

## 2.3 Granite/Meguma Group contact

### 2.3.1 Nature of the contact

Two granite/metasedimentary rock contacts were observed, one in each lobe of the HCQP. The observed contact in the Halfway Cove lobe, located in the northeastern portion of the mass (point A on Map 1), is sharp, steep (020°/72°S) and exposed for ten metres. Although the metasedimentary rocks could represent a xenolith, no rotated or distorted bedding occurs in the metasedimentary rocks, suggesting that they are still attached to the surrounding strata. The granite is finer grained than the interior, with this grain size reduction possibly related to contact effects. There is a small (3-4 cm) chilled margin, with an increase in muscovite within the granitic rocks, but this is discontinuous along the length of the exposed contact.

An exposed contact in the Queensport lobe occurs in the southern portion of Jamieson Brook (Point B on Map 1), between the coarse-grained monzogranitic rocks (of HCQP1) and a small roof pendant (approximately 100 m x 50 m) of Halifax metasedimentary rocks close to the southern contact. The bedding attitudes in this inlier are similar to attitudes in the surrounding country rock, suggesting that the inlier is a roof pendant, rather than a xenolith. The contact is sharp, and the granitic rocks have not disturbed the metasedimentary bedding or cleavage (Plate 2.1). A small chilled margin 1 cm wide, noted within the granitic rocks, grades over 6 cm to a coarse grain size. Minor small (2 cm wide x 5 cm long) granitic veins within the Halifax Formation rocks extend from the contact. These veins could represent extensions of the pluton or partial melts within the metased-

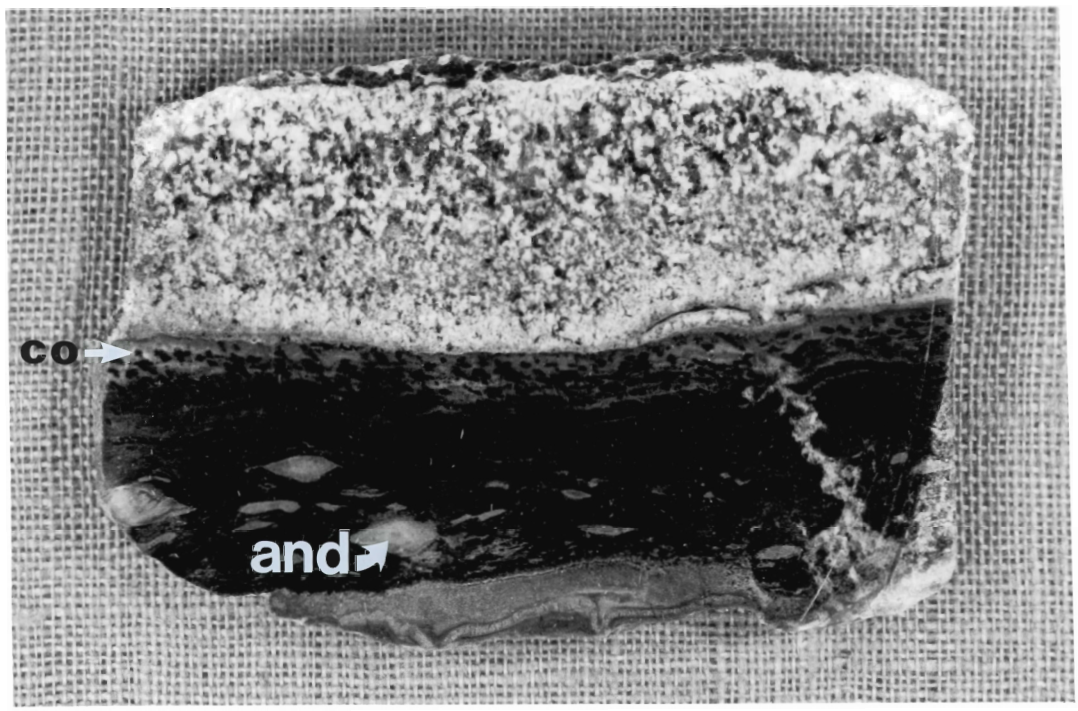


PLATE 2.1 Contact between monzogranitic rocks and a small roof pendant of Halifax Formation metasedimentary rocks. The granitic rocks exhibit a chilled margin of approximately 1 cm, with a gradation to coarse-grained rocks over 6 cm. Cordierite (co) is well-developed within the metasedimentary rocks next to the contact. Andalusites (and) present as augen are similar to those developed in andalusite zones within the Halifax Formation rocks, and their presence is not necessarily related to exposed granitic rocks. Minor granitic veins occur in the metasedimentary rocks.

imentary strata, but additional petrographic and geochemical work is necessary to resolve their origin. Cordierite, well developed within a 2 cm band within the metasedimentary rocks, occurs adjacent to the contact. The andalusite (chiastolite), well developed as augen in Plate 2.1, resemble those in the andalusite-rich zone described in an earlier section.

Other areas of the pluton do not have visible exposed contacts, but they were traced to within 5 metres in one area (south portion of Jamieson Brook), and generally to within 50-100 metres in other areas (Third Lake, Peas Brook).

Forceful intrusion and/or passive stoping are considered the main mechanisms for high-level emplacement of granites (Pitcher, 1979; Marsh, 1982). Work undertaken on other granitic plutons (the Sierra Nevada Batholith and the Massif Central) question the importance of stoping as the principal method of intrusion, particularly because of the absence of large metasedimentary xenoliths (Didier, 1973). Passive stoping mechanisms are postulated for emplacement of both the SMB and MB (McKenzie, 1974; MacDonald, 1981). O'Brien (1986), however, noted that metasedimentary rocks in areas 50 metres from the contact of the SMB, in the Mahone Bay area, have been folded and reoriented. This observation possibly suggests some degree of dynamic emplacement. Hill (1986) observed "forceful deflection" of the Meguma Group strata surrounding the Whitehaven pluton and suggests that, although passive stoping is presumably the predominant mechanism for emplacement for this pluton, dynamic emplacement may also have occurred.

In the thesis area, there is evidence to suggest that the granitic pluton was forcefully intruded. The Meguma Group rocks on the eastern

side of the pluton appear to wrap around the granite and to have been pushed aside. This deflection is noticeable in the aeromagnetic patterns (Fig. 2.7). The re-orientation of the metasedimentary rocks suggests that forceful intrusion may be, at least in part, a mechanism for intrusion of the HCQP. There are problems with the passive stoping method (i.e. the lack of abundant metasedimentary xenoliths close to the contact) to completely explain the mode of emplacement for the HCQP, but this method would have been partially responsible for intrusion of the HCQP, on the basis of the nature of the xenoliths (being Meguma Group, generally Halifax Formation, rocks) and their abundance in local areas. Therefore, a passive stoping mode of emplacement, with some degree of forceful intrusion, for the intrusion is proposed.

### 2.3.2 Relative age of the HCQP

The HCQP intrudes the Meguma Group, placing the age of the body younger than Cambro-Ordovician. Younger rocks do not overlie the pluton, and it cannot, therefore, be definitively bracketed between specific ages. However, a younger age limit is set by the presence of granitic cobbles found in early Carboniferous Horton conglomerates to the west (Benson, 1967). These cobbles are medium-grained, muscovite-biotite granites which probably are representative of the granites of the Meguma Terrane, although not definitely from the HCQP.

### 2.3.2 Isotopic age of the HCQP

A U-Pb determination from igneous monazite yielded an age of 372-373 Ma for the HCQP (Krogh and Keppie, 1988), and it probably repre-

sents the best radiometric estimate of the age of intrusion of the HCQP. Bulk fractions of euhedral zircon grains selected from granite samples of the HCQP gave an age of approximately 2000 Ma (2320 Ma and 1870 Ma for rounded and euhedral grains, respectively) for the granitic source (Krogh and Keppie, 1985, 1988).

Age dating previously undertaken (Fairbairn et al., 1960, 1964; Leech et al., 1963) on the HCQP yielded ages of 362-386 Ma (Rb-Sr whole rock) and 367-391 Ma (K-Ar biotite-muscovite), respectively. Additional dating ($^{40}Ar/^{39}Ar$) of biotite and muscovite from different rock types of the pluton (e.g. unaltered rocks, altered rocks, rocks from the fault zone area) all yielded ages between 365 and 373 $\pm$ 7 Ma (Dallmeyer and Keppie, 1985). They suggest, on the basis of the similar ages, that ductile deformation zones developed immediately after granite emplacement and prior to regional cooling below argon retention temperatures.

## 2.4 Endocontact

### 2.4.1 Phases of the HCQP

#### 2.4.1.1 Introduction

Visual estimates of modal percentages of minerals (biotite, muscovite) were undertaken initially in the field for the basis of mapping. The proportions of all minerals were subsequently determined through point counting. A total of 28 rock samples were slabbed and stained. These slabs were subsequently point counted using an average of 400 points, and the rocks classified according to the classification for granitic rocks (Streckeisen, 1976).

The HCQP (Fig. 2.1) is composed predominantly of two-mica (biotite-muscovite) monzogranite, and contains a total of five units, based on mineralogy and texture, with two in the western lobe and three underlying the eastern area. Coarse-grained biotite monzogranite (with minor muscovite) grading to granodiorite characterizes Unit 1 (HCQP1). This unit constitutes all margins of the Queensport lobe, except the northern one. Included within HCQP1, and very similar to it mineralogically, is a separate unit (HCQP1A). This unit, mapped as an "intensely porphyritic unit", contains abundant megacrysts of potassium feldspar. Units 2 and 3 (HCQP2 and HCQP3) are coarse-grained muscovite-biotite monzogranite and medium- to coarse-grained muscovite-biotite monzogranite, respectively. These two units compose the Halfway Cove lobe, with HCQP2 the dominant unit in the northern portion of the mass and HCQP3 included in the southern portion. Unit 4 (HCQP4), a fine- to medium-grained, equigranular muscovite-biotite monzogranite, underlies the interior and northern margin of the Queensport lobe. Minor late-stage intrusions (aplites and pegmatites) occur within the pluton. Several small pods of leucogranite have developed in the Queensport lobe.

The results of point counting are displayed on Figure 2.2 and tabulated in Table 2.1. Rocks from HCQP1 and HCQP1A plot closest to, and marginally in, the granodiorite field on the Q-A-P diagram. HCQP1A plots within the HCQP1 field, consistent with HCQP1A representing a textural variation of HCQP1. The averages of these two units (Fig. 2.2B and 2.2C) plot very close to the monzogranite-granodiorite division. The other phases (HCQP2, HCQP3 and HCQP4) plot in the monzogranite field, with HCQP4 containing the highest proportion of K-

FIGURE 2.1. Lithofacies and outcrop location map of the HCQP. Legend is as follows:

| | |
|---|---|
| HCQP1 | coarse-grained, megacrystic (5-10% megacrysts) biotite monzogranite (with minor muscovite), grading to granodiorite |
| HCQP1A | coarse-grained, very megacrystic ("intensely porphyritic" with up to 40% megacrysts) biotite monzogranite (with minor muscovite) |
| HCQP2 | coarse-grained (with minor medium), moderately equigranular to megacrystic muscovite-biotite (+/- garnet and apatite) monzogranite |
| HCQP3 | medium-grained (with minor coarse), moderately equigranular to megacrystic muscovite-biotite monzogranite |
| HCQP4 | fine- to medium-grained, equigranular muscovite-biotite monzogranite |
| $CO_H$ | Meguma Group Halifax Formation slates and shales, with minor siltstones |
| $CO_G$ | Meguma Group Goldenville Formation greywackes and quartzites, with minor amounts of siltstone, slate and argillite |

Symbols:

| | |
|---|---|
| x | outcrop |
| ⊗ | boulder |
| A | location of first exposed contact |
| B | location of second exposed contact |
| ——— | geological contact (defined, approximate, assumed) |

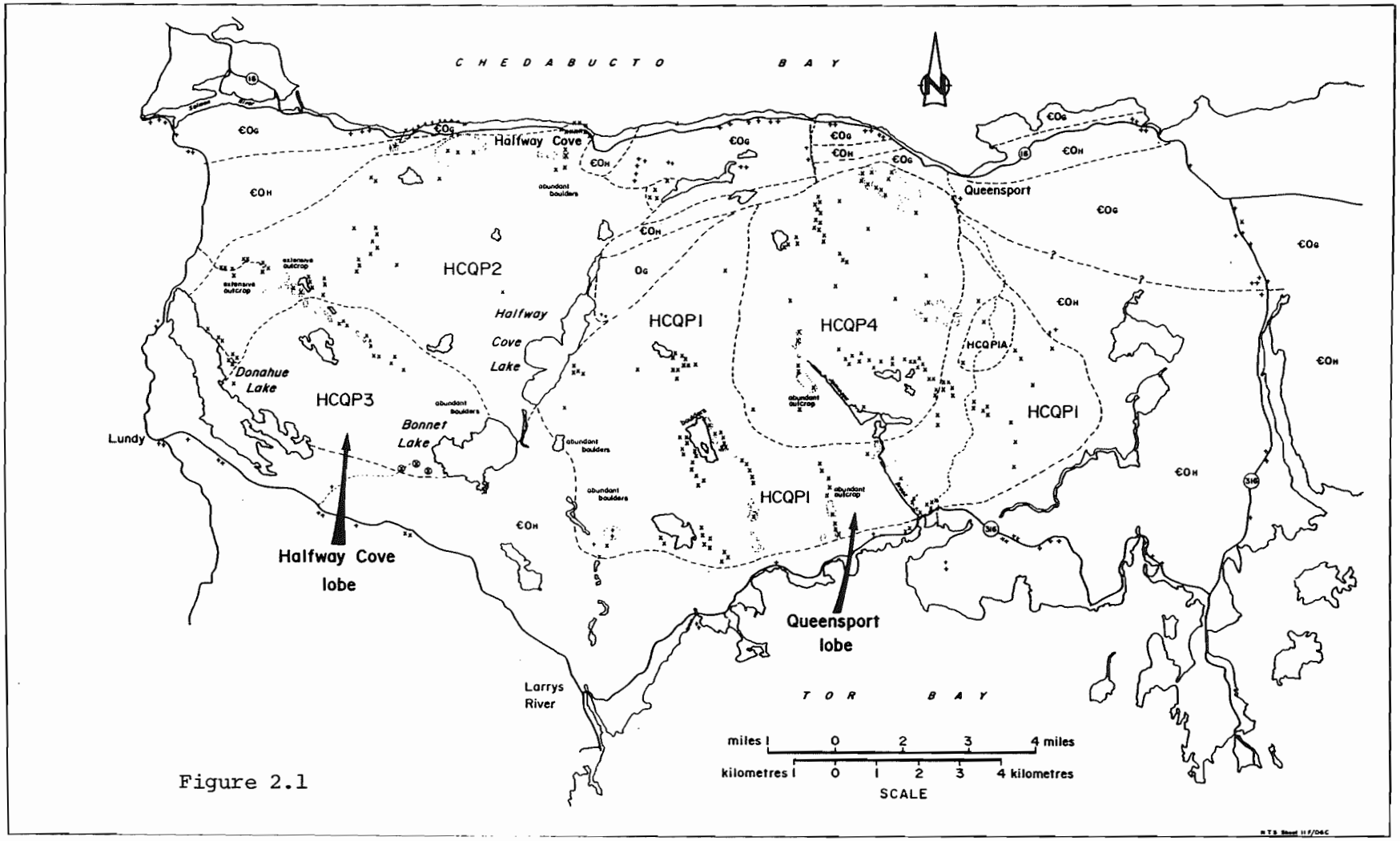
CHEDABUCTO BAY
Halfway Cove
Queensport
HCQP2
HCQP1
HCQP4
HCQP1A
HCQP3
HCQP1
HCQP1
Halfway
Cove
Lake
Donahue
Lake
Bonnet
Lake
Lundy
Halfway Cove
lobe
Queensport
lobe
Larrys
River
TOR BAY
abundant boulders
extensive outcrop
abundant outcrop
miles 0 2 3 4 miles
kilometres 0 1 2 3 4 kilometres
SCALE

Figure 2.1

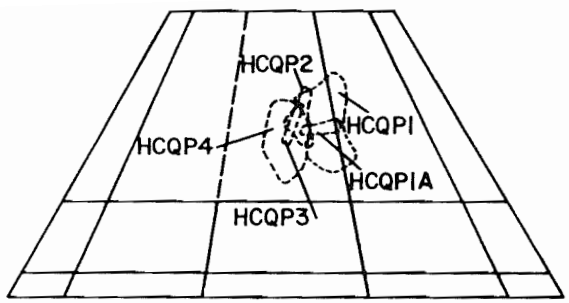


2.2b. Compositional fields of units

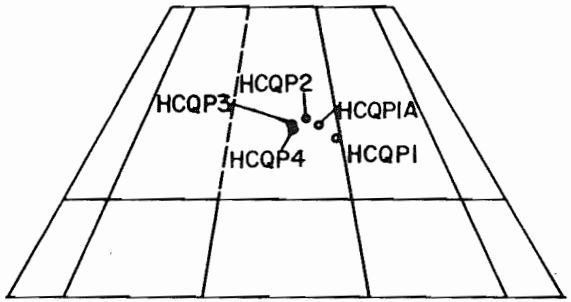


2.2c. Modal averages of units




FIGURE 2.2a. Plot of modal analyses of 28 granitic rocks of the HCQP in terms of quartz-alkali feldspar-plagioclase (QAP). Compositional fields are after Streckeisen (1976).

TABLE 2.1 Representative rocks of each unit of the HCQP. Modal percentages of minerals are based on point counting results (average 400 points).

| PHASE HCQP1 | | | | | | | | | PHASE HCQP1A | |
|---|---|---|---|---|---|---|---|---|---|---|
| | QP3 | QP6 | QP7 | QP8 | QP11 | QP12 | QP22 | L038 | QP1 | QP2 |
| quartz | 27 | 29 | 24 | 32 | 30 | 26 | 40 | 36 | 31 | 32 |
| K-feldspar | 28 | 25 | 25 | 23 | 21 | 20 | 15 | 24 | 20 | 27 |
| plagioclase | 35 | 35 | 40 | 32 | 39 | 42 | 33 | 28 | 37 | 33 |
| biotite | 7 | 8 | 9 | 8 | 7 | 11 | 10 | 11 | 10 | 6 |
| muscovite | 3 | 3 | 2 | 5 | 3 | 1 | 2 | 1 | 2 | 2 |

| PHASE HCQP2 | | | | | PHASE HCQP3 | | PHASE HCQP4 | | | |
|---|---|---|---|---|---|---|---|---|---|---|
| | HC1 | HC2 | HC7 | L034 | HC3 | HC4 | QP4 | QP5 | QP9 | QP13 |
| quartz | 39 | 31 | 28 | 33 | 29 | 34 | 30 | 30 | 23 | 27 |
| K-feldspar | 21 | 23 | 26 | 28 | 30 | 26 | 27 | 27 | 33 | 28 |
| plagioclase | 29 | 33 | 33 | 28 | 31 | 30 | 32 | 30 | 35 | 34 |
| biotite | 6 | 7 | 6 | 5 | 5 | 5 | 6 | 7 | 6 | 6 |
| muscovite | 5 | 6 | 7 | 6 | 5 | 5 | 5 | 6 | 3 | 5 |

| PHASE HCQP4 (continued) | | | | | | | | |
|---|---|---|---|---|---|---|---|---|
| | QP14 | QP15 | QP16 | QP17 | QP18 | QP19 | QP21 | L014 |
| quartz | 35 | 30 | 35 | 31 | 35 | 32 | 29 | 28 |
| K-feldspar | 23 | 30 | 25 | 29 | 27 | 26 | 25 | 34 |
| plagioclase | 32 | 30 | 31 | 29 | 26 | 31 | 32 | 27 |
| biotite | 6 | 5 | 5 | 5 | 6 | 7 | 8 | 7 |
| muscovite | 4 | 5 | 4 | 6 | 6 | 4 | 6 | 4 |

feldspar. Biotite and muscovite modal contents are plotted in Figure 2.3 and display similar trends of the units to trends on the Q-A-P diagram. The highest biotite contents (7-11%) and lowest muscovite contents (trace to 3%) occur in HCQP1, and Units 2-4 exhibit some overlap with each other. This suggests that HCQP1 and HCQP1A represent the least evolved units of the pluton.

#### 2.4.1.2 HCQP1

This unit is a medium- to coarse-grained, megacrystic biotite monzogranite (with minor muscovite) which grades to granodiorite (Plate 2.2 and 2.3). A few samples closest to the west and southeastern margins of the QP lobe plot within the granodiorite field on the Q-A-P diagram.

Quartz is grey in colour and usually strained. Plagioclase occurs as both a groundmass constituent and as megacrysts, with the average modal average percentage (40%) representing the highest value for all the units. Potassium feldspar occurs both as a minor groundmass constituent and as megacrysts, which are commonly perthitic. These megacrysts attain sizes up to 1.5 cm wide and 2-3 cm long and generally comprise 5-10% of the rock volume. Kaolinization, hematization and saussurization of the feldspars, particularly the plagioclases, are evident.

Two sizes of biotite were observed during the field mapping, one being 3-5 mm and the other being 1 mm and less, with the smaller sized group predominant. Biotite can occur in local concentrations (1-2 cm), which are commonly rounded, but also can be irregularly shaped (e.g.

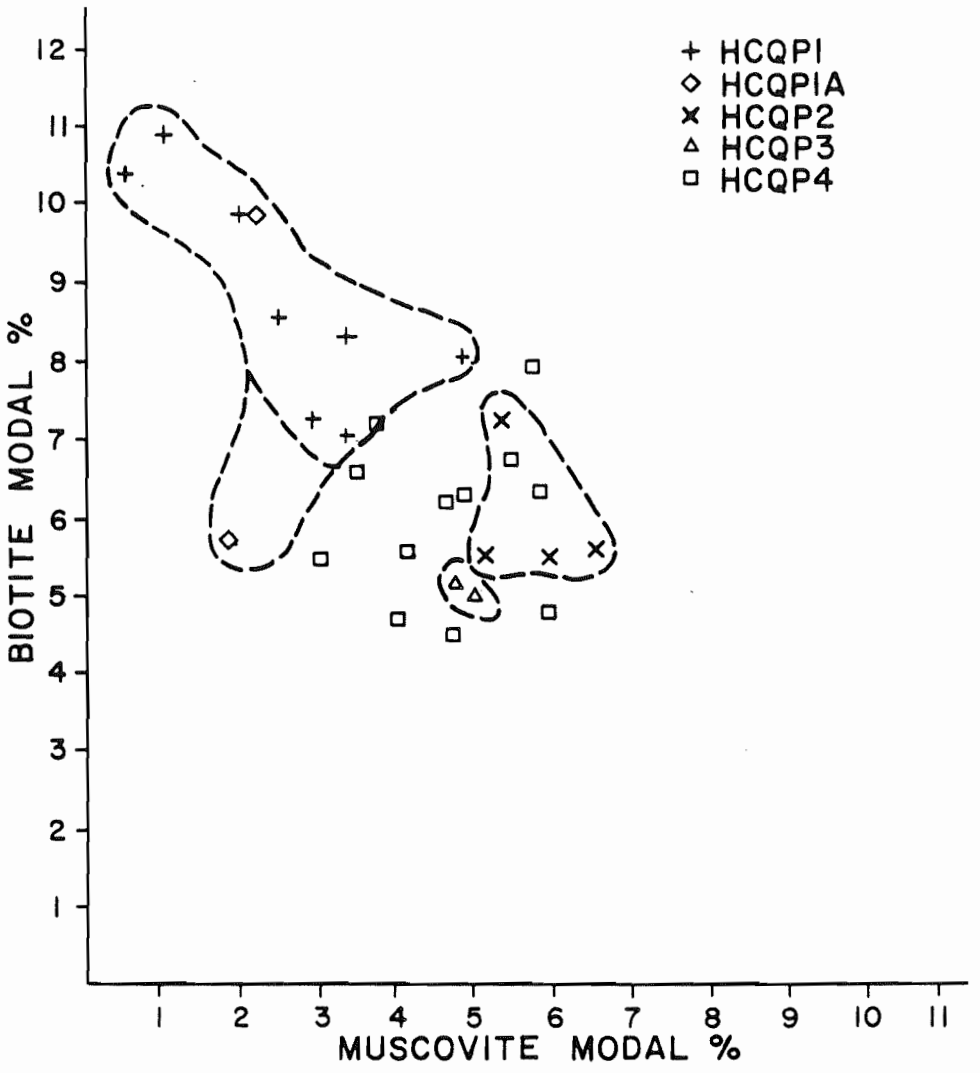


FIGURE 2.3. Biotite modal percentages vs muscovite modal percentages of 28 granitic rocks of the HCQP. Fields of individual rock units are outlined.


PLATE 2.2. Unit HCQP1. This unit is a coarse-grained biotite monzogranite (2.2a), which grades to granodiorite in composition as seen in the bottom slabs (2.2b). Biotite content is highest in this unit (approximately 9%) and muscovite contents are the lowest (trace-2%). Sodium colbaltinitrite stains potassium feldspar yellow, plagioclase feldspar white and quartz grey.


PLATE 2.3. Representative slabs of rocks from Unit HCQP1. Composition is more monzogranitic than Plate 2.2a and b. Notice the alignment of biotite (outlined by the black line) representing a weak mineral foliation discussed in the text.

elongated, oval). Selective alteration (hematization, chloritization and development of secondary muscovite) of biotite is apparent.

Muscovite most commonly occurs as alteration products of other minerals (biotite, feldspar), with only minor amounts occurring as discrete grains within the groundmass.

Accessory minerals include zircon, apatite, ilmenite, rutile and hematite.

#### 2.4.1.3 HCQP1A

This unit is completely enclosed within HCQP1, comprises <4 $km^2$, and probably represents a textural variation of HCQP1. This "porphyritic" biotite monzogranite, with minor muscovite, contains quartz, plagioclase, alkali feldspar, biotite and muscovite, with accessory zircon, apatite, ilmenite and minor rutile. It is texturally coarser-grained than HCQP1 and richer in alkali feldspar megacrysts. The feldspar megacrysts average 10-20% of the matrix, but local concentrations can constitute 30-40% of the rock volume (Plate 2.4).

#### 2.4.1.4 HCQP2 and HCQP3

The northern portion of the Halfway Cove lobe is underlain by coarse-grained (with some medium-grained), moderately equigranular, muscovite-biotite monzogranite (HCQP2) (Plate 2.5). These hypidiomorphic granular rocks are light grey to pink in colour. The southern portion of the lobe is underlain by light buff to pink, medium-grained (with minor coarse-grained), moderately equigranular, muscovite-biotite monzogranites (HCQP3) (Plate 2.6). The main difference between the units is the slight reduction in grain size. No contact is exposed

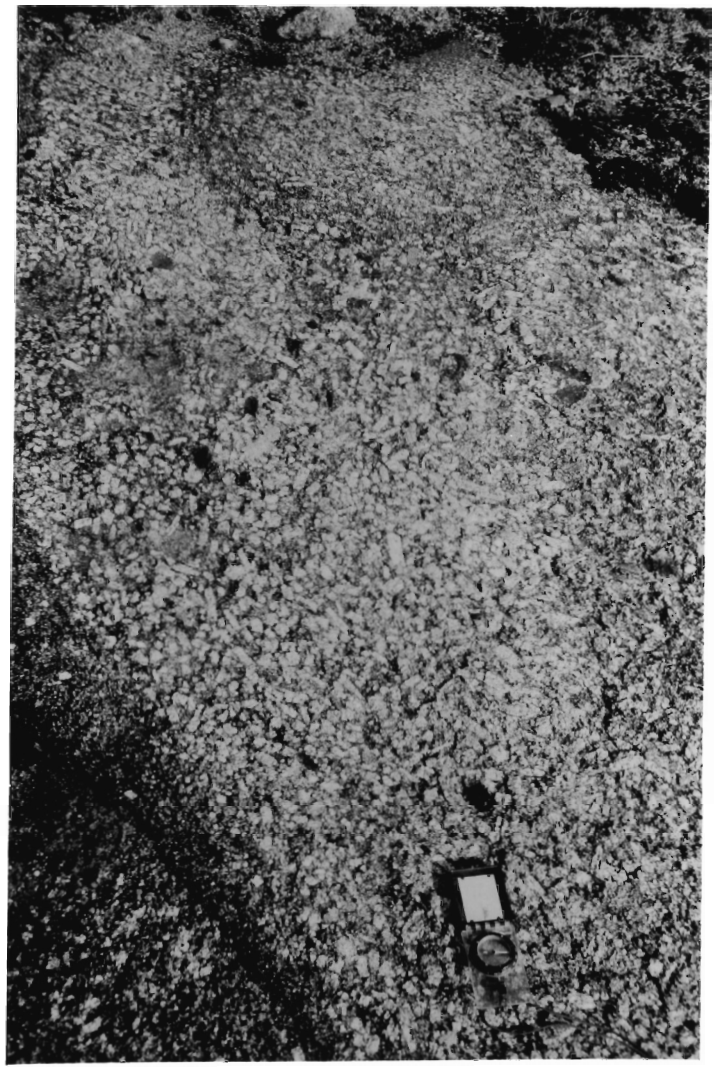

PLATE 2.4. "Intensely porphyritic" monzogranitic unit (HCQP1A) of the HCQP. Locally, the potassium feldspar megacrysts comprise 40-50% of the rock volume.


PLATE 2.5. Representative stained and unstained slabs of Unit HCQP2. This unit is coarse-grained (with minor medium-grained) muscovite-biotite monzogranite.


PLATE 2.6. Representative slab of medium-grained (with minor coarse-grained) muscovite-biotite monzogranite of Unit HCQP3.

between the two units, but grain size difference is noticeable within 10 metres in the south-central portion of the lobe. A contact is inferred in the eastern portion of the lobe near Bonnet Lake where the outcrop exposure is poor.

Mineralogically, there is little difference between the two units, with the mineral assemblage of both consisting of quartz, alkali feldspar, plagioclase, biotite and muscovite, with minor accessory minerals of garnet, apatite, zircon, ilmenite and rutile.

Modes of occurrence of the major minerals are similar to those of HCQP1 and HCQP1A, with the exception that muscovite occurs as separate and discrete rectangular grains (up to 3 mm) throughout the matrix, as well as an obvious alteration product of both biotite (as rims and intimate growth) and feldspar (included within the minerals).

Very small, reddish-pink garnets (0.1 mm to 1 mm) occur locally in trace amounts in the groundmass and as inclusions within plagioclase and minor potassium feldspar, where they are most easily seen.

A characteristic feature of the HC lobe is the presence of small (1 mm), rounded, light blue-green apatite grains within the groundmass, comprising <1% of the modal mineralogy. Local areas within this unit may not contain the apatite.

#### 2.4.1.5 HCQP4

Fine- to medium-grained, generally equigranular, muscovite-biotite monzogranite (Plate 2.7) forms the core and northern margin of the Queensport lobe (Fig. 2.1). Within this unit, pods of leucogranite are locally developed. These rocks are moderately to strongly altered on the weathered surface and are light grey to pinkish grey in colour.

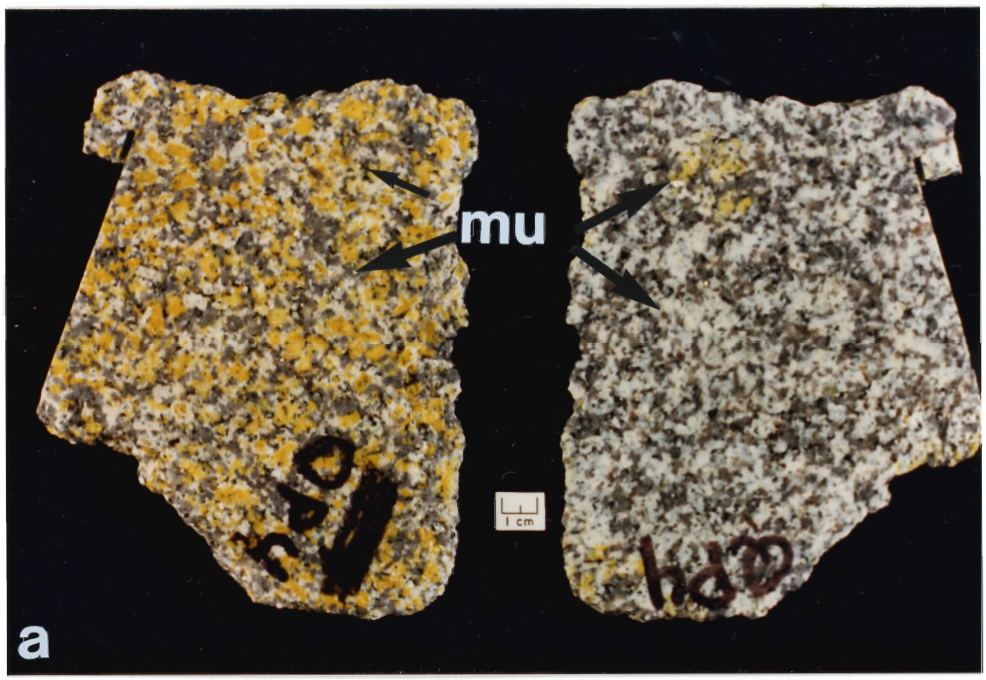


PLATE 2.7. Representative slabs of Unit HCQP4. This unit is fine- to medium-grained, equigranular muscovite-biotite monzogranite. Note in the rocks the easily visible muscovite grains within the matrix (outlined as mu).

The main mineralogy is similar, with differing amounts, to the other units. Small garnets occur along fractures and within the pods of leucogranite. Accessory minerals include apatite, zircon, ilmenite, rutile and minor hematite.

Plagioclase and potassium feldspar occur in approximately equal proportions. They often occur as slightly larger (up to 1 cm) megacrysts within the otherwise equigranular matrix. Rapakivi texture (plagioclase rims on alkali feldspar cores) is well developed in some areas within this unit. This texture is similar, but compositionally different, to the classic (i.e. magmatic) texture of granites from Finland (e.g. Backland, 1938; Vorma, 1971), where the texture refers to potassium feldspar mantled by oligoclase.

### 2.4.2 Enclaves

Enclaves occur in various shapes and sizes (angular to rounded, often elongate, average size of less than 0.5m) and exhibit varying degrees of preservation within the granitic host. Some of these are whitish, rounded inclusions composed predominantly of quartz and feldspar (Plate 2.8). The majority of the enclaves, however, are dark coloured (grey to black), fine-grained and more mafic than the surrounding host rock. Their size is variable (2 cm to 1 metre long), although most are small. Relict bedding features, often visible, suggest that the enclaves are predominantly metasedimentary in origin and are, therefore, xenolithic.

Enclaves occur most abundantly near the western edge of the body, although scattered enclaves in other parts of both lobes indicate that their distribution is not entirely related to proximity to the observed

PLATE 2.8. Enclaves within the HC lobe. The white enclave (autolith?) is composed predominantly of quartz and feldspar, with minor biotite. This enclave could represent a fragment of leucomonzogranite, an aplite, or a chilled portion of the granite. The mafic clots are composed predominantly of biotite, and could represent remnant xenoliths, biotite aggregations, or "restite" material.

PLATE 2.9. Enclave abundance in the HC lobe near the Lundy Fire Tower. These enclaves resemble metasedimentary rocks with relict bedding. Note alignment of the xenoliths trending northeast.

Meguma-granite contacts. Previous work in granitoid bodies has determined that enclaves are common near the roof and wall zones (Pitcher, 1979), but that they can occur any distance from contacts (Pabst, 1928). In other granitic bodies of Nova Scotia (SMB and MB), enclaves were also observed in localities that are not directly related to the proximity of the nearest contacts (McKenzie, 1974; MacDonald, 1981).

The largest concentration of enclaves occurs at the Lundy Fire Tower, approximately 2.5 km from the nearest contact. Most of the enclaves at this locality are grey to black, fine grained, angular, well preserved and elongate (Plate 2.9). The sizes range in length from 10 cm to 1 m. In appearance, most of the enclaves resemble the Halifax and Goldenville Formations as relict bedding is apparent, some are spotted hornfels and some contain recognizable cordierite. Others have bands of andalusite, resembling andalusite-bearing zones within Meguma Group metasedimentary rocks.

A general direction of elongation of xenoliths in the fire tower area is 030$^{o}$ (Plate 2.9). Several authors have suggested that such a concentration could represent the end product of "particle accumulation which occurs where suspensions flow over surfaces" (Komar, 1972; Pabst, 1928). Alternatively, this may be an example of flowage differentiation (Bhattacharji and Smith, 1964; Taylor, 1976; Clarke and Chatterjee, 1985).

Towards the interior of the HCQP, the enclave concentration is not as great as that in the fire tower area, consistent with findings in other granitic plutons (Pitcher, 1979; McKenzie, 1974; MacDonald, 1981). One unusual, large enclave (1 m x 0.7 m), found in the eastern

portion of the Queensport lobe, exhibits rounded and swirling gneissosity which has been truncated on one side, resulting in a semi-circular shape (Plate 2.10). Vernon (1983) suggests that distorted enclaves may have been magma globules when being deformed. Flow within the magma while the enclave was in a semi-plastic condition could account for its present appearance. Effects of such flowage are also seen within the granitic rocks in the same area, as concentrations and alignment of potassium megacrysts.

Small dark clots composed mostly of biotite are also commonly found within many granitic rocks (Berger and Pitcher, 1970; Pitcher, 1979; Marsh, 1982; Vernon, 1983) and within the HCQP (Plate 2.8). It has been suggested by some workers that these "mafic" enclaves may represent "restite" clots (Bateman et al., 1963; Didier, 1973; White and Chappell, 1977; Chappell, 1978) or modified "restite" (McBirney, 1980). Others suggest that these may simply be the remains of xenoliths in various stages of assimilation (De Albuquerque, 1973; Clarke and Chatterjee, 1985) or droplets of mafic magma that crystallized rapidly (Vernon, 1983).

### 2.4.3 Structure

#### 2.4.3.1 Aerial Photograph and Satellite Imagery Interpretation

Lineaments determined from air photo interpretation and outlined on the ground as lake shores, streams and brooks often parallel jointing patterns within the granitic rocks in proximity to these lineaments. Previous mapping by Stevenson (1964) outlined strong N-NW lineaments, particularly defined by Jamieson Brook in the QP lobe and

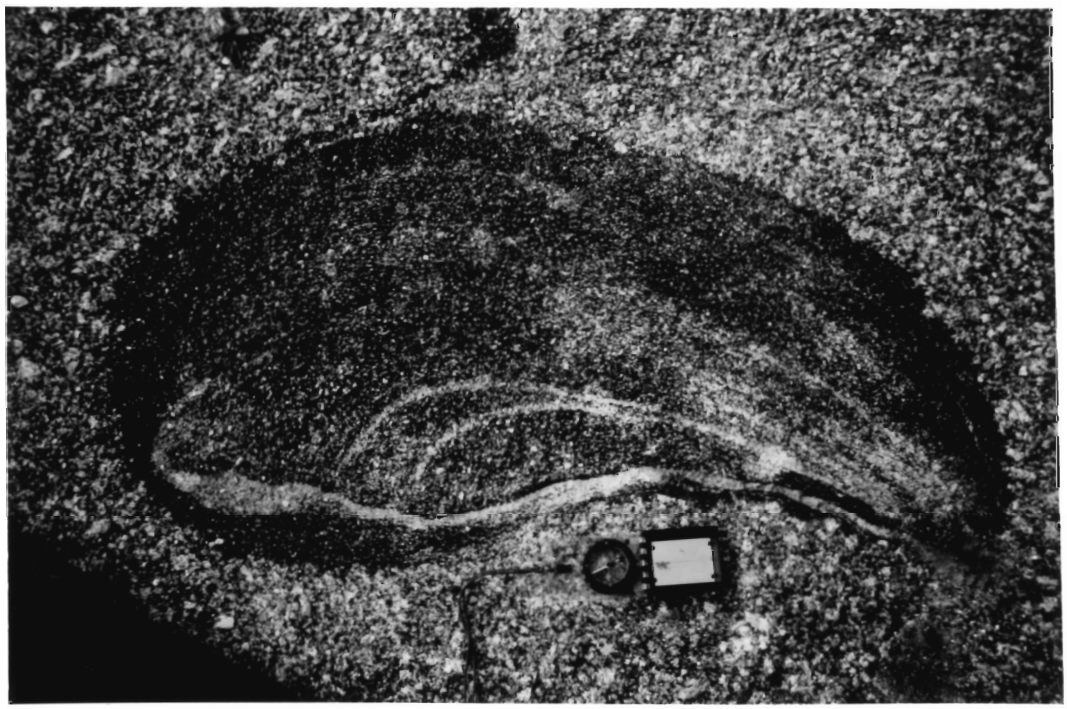

PLATE 2.10. Unusual enclave in Unit HCQP1A, a unit with abundant potassium feldspar megacrysts. Swirling effects within the enclave appear truncated on the "bottom".

other lakes and streams to the northeast. The development of such lineaments may represent jointing and fracturing patterns developed during cooling of the bodies (Price, 1978).

The Nova Scotia College of Geographic Sciences (formerly the Nova Scotia Land Survey Institute) initiated a Landsat remote sensing multispectral scanner and Thematic Mapper imagery survey of the HCQP in 1983 (Akhavi, 1985). Major north-northwest lineaments were observed, some of which are similar to those outlined during mapping by Stevenson (1964), and also several east-west structures were detected. Several small "circular" structures (< 5 $km^2$) were also observed within the north-central portion of the Halfway Cove lobe and interpreted as different units (Akhavi, 1985). Subsequent field checking did not support this interpretation.

#### 2.4.3.2 Jointing

During the intrusion and cooling of any batholith, thermal contraction will take place and new space will inevitably result. Some space will remain open after the cooling and settling of the rocks (Balk, 1937; Price, 1978; Pitcher, 1979; Clarke and Chatterjee, 1985). These open spaces will form joints and fractures which can later be intruded by aplite, pegmatite or quartz veins, and can also act as conduits for late-stage fluids (Price, 1978; Hibbard, 1980; Clarke and Chatterjee, 1985). Jointing can also form as a result of stress release during unloading or unroofing of a granitoid body (Balk, 1937; Price, 1978).

The majority of the outcrop of the HCQP is only moderately jointed (Plate 2.11), with wide spacings (average 1-2 metres) between joints.


PLATE 2.11a. Typical outcrop outside the barrenlands of the HC lobe, with rounded sides and vertical to near-vertical joints (outlined by the black arrows).

PLATE 2.11b. Pavement outcrop typical of the barrenlands of the QP lobe. Note jointing at right angles with vertical to near vertical dips.

A plot of poles to joint directions (Fig. 2.4) shows that the joints generally exhibit random orientations. The strongest joint set is developed at a strike direction of approximately north-south (350°-006°/subvertical to vertical), with two lesser-developed joint directions, 065°/subvertical and 120°/subvertical. Jointing is found parallel to some strong N-NW lineaments outlined by brooks, streams and lakes within the interior of the body (particularly the QP lobe).

#### 2.4.3.3 Dykes and Veins

Minor aplite and pegmatite occur as dykes and small irregular bodies within the monzogranites. They commonly occur in groups, are generally parallel, thin (3-5 cm), and very straight (Plate 2.12). Aplites are most common, although very minor aplite-pegmatite associations occur. In the HC lobe, aplite dykes are more abundant than pegmatite dykes. Pegmatites are relatively more common in the Queensport lobe, suggesting the presence of more late-stage volatiles.

The aplitic rocks are generally whitish, fine grained, equigranular and contain minor (1-2%), anhedral to euhedral, reddish-pink garnet, and rarely contain late-stage accessory minerals. Miarolitic cavities are present, but not common, within the aplitic dykes. Minor blue fluorite occurs in an aplite-pegmatite dyke in the southern portion of the Queensport lobe near Jamieson Brook. The pegmatite dykes contain quartz, alkali feldspar, muscovite, biotite and some garnet.

A plot of poles to aplite and pegmatite veins within the HCQP (Fig. 2.5) illustrates generally random and non-uniform orientation. The strongest strike orientations are 094° and 135°, both subvertical,

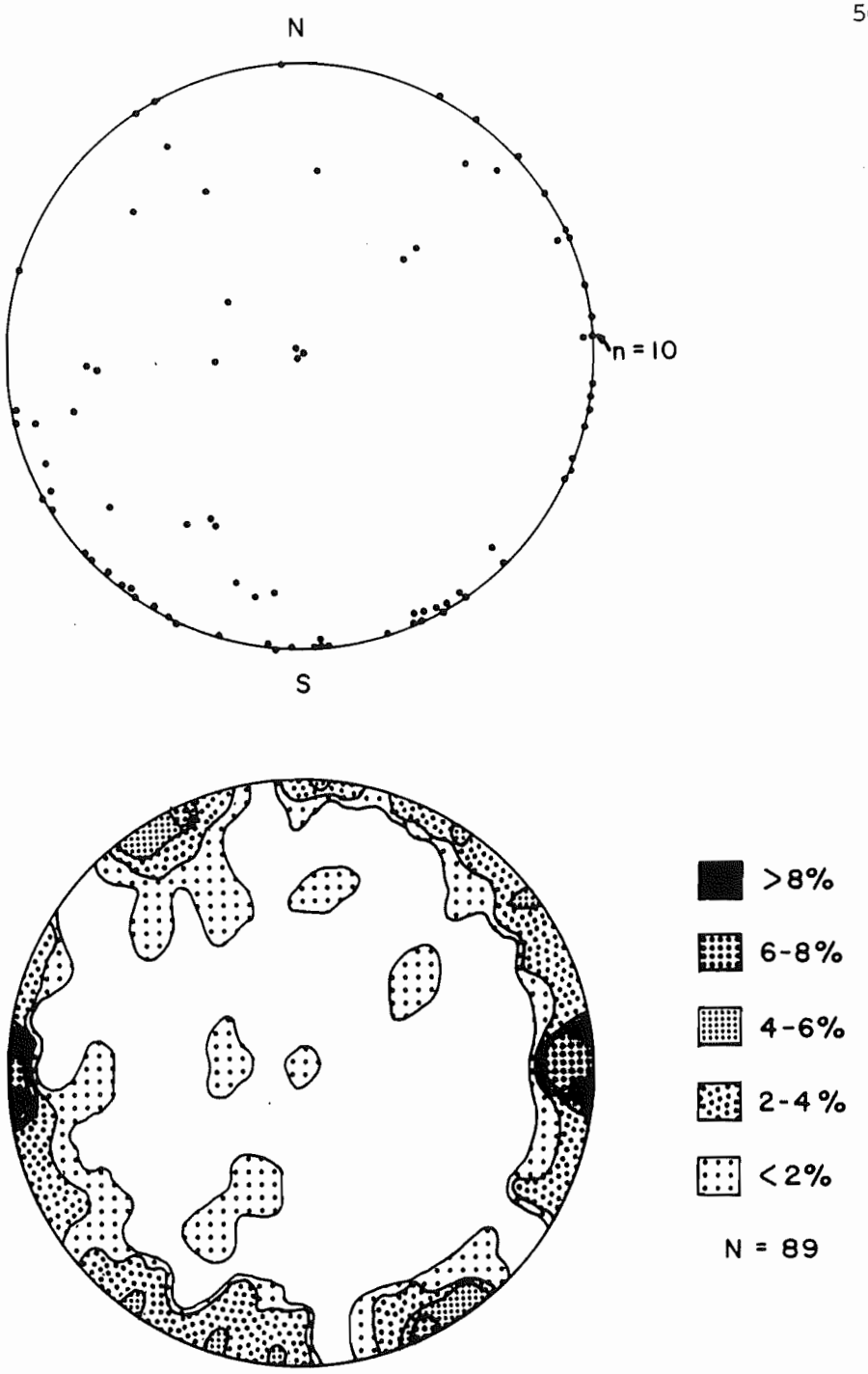


FIGURE 2.4. Jointing within the HCQP, represented by lower hemisphere equal area projection of poles to joint planes in HCQP. Points are contoured within 1% of a Schmidt equal area stereonet and contoured using a Kalsbeek counting net.

PLATE 2.12. Parallel, straight, and thin aplite veins within the HC lobe near the Lundy Fire Tower. The contacts with the host rock (Unit HCQP2) are generally sharp, indicating magmatic origin, although some have indistinct boundaries (such as the ones displayed above), and could be considered metasomatic.

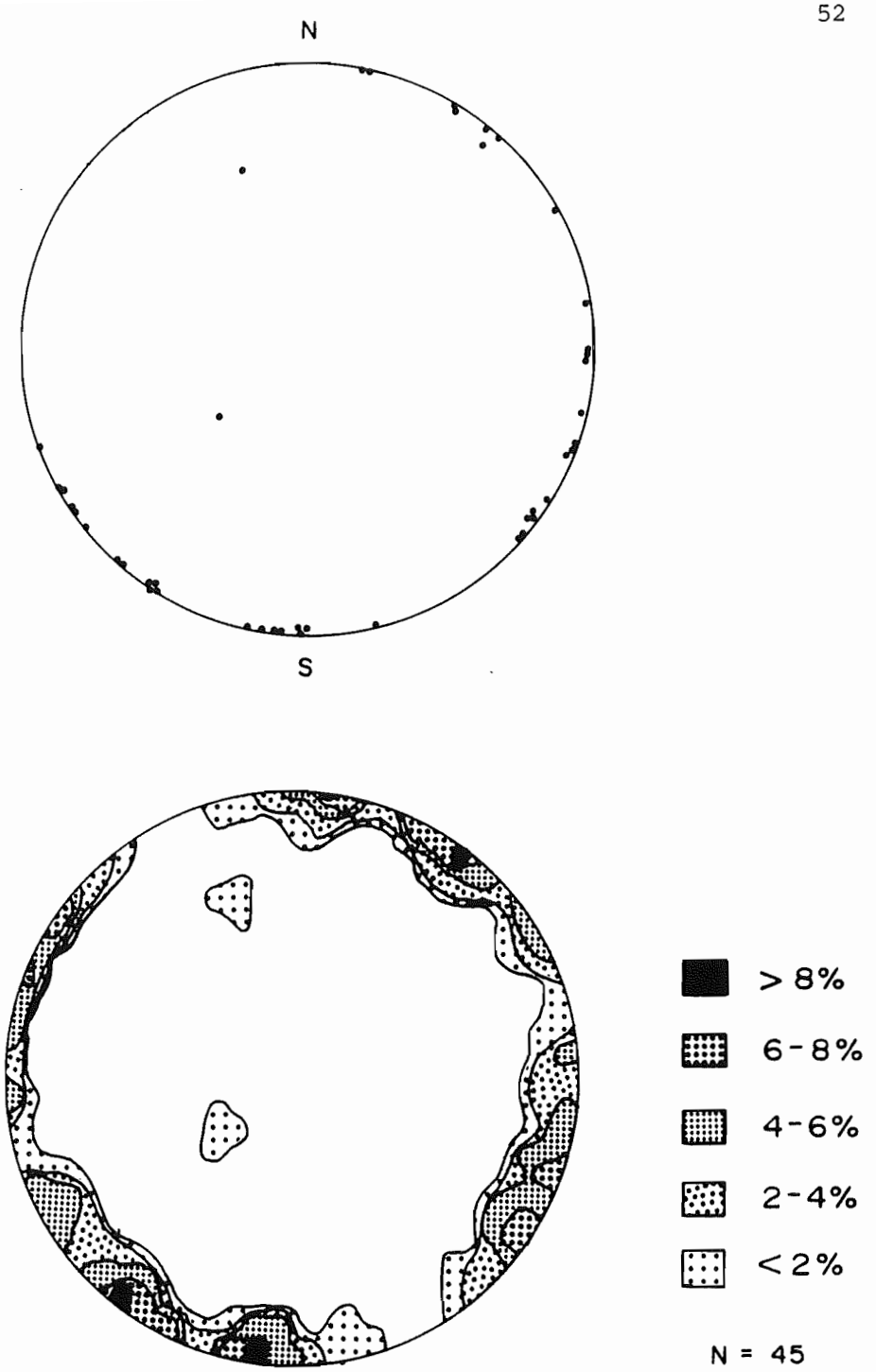


FIGURE 2.5. Aplite and pegmatite dykes within the HCQP, represented by lower hemisphere equal area projection of poles to aplite and pegmatite planes in HCQP. Points are contoured within 1% of a Schmidt equal area stereonet and contoured using a Kalsbeek counting net.

with a lesser-developed orientation corresponding to 020-030°/ subvertical.

Quartz veins are not plentiful within the HCQP. They occur as generally straight, thin (3-5 cm) veins. Minor rounded concentrations of quartz (10 x 15 cm) were noted in several areas. These could represent remains of quartz veins (Clarke, pers. comm.); remains of a xenolith or quartz vein from a xenolith (White and Chappell, 1977); remains of pegmatitic quartz (Vernon and Flood, 1982), be an example of restite quartz (Chappell, 1978), or be late-stage hydrothermal precipitation of quartz in irregular contraction cavities (Hill, pers. comm.). Based on the observations that most are small (<5 cm), are not associated with xenoliths, remnant xenoliths, or pegmatitic segregations, the author proposes that they may represent late-stage precipitation of quartz, as opposed to other sources presented above.

#### 2.4.3.4 Deformational and structural features

##### 2.4.3.4.1 Cooling features

Local concentrations of potassium feldspar megacrysts occur throughout the HCQP. A separate unit (HCQP1A) of "intensely porphyritic" monzogranite was mapped (Plate 2.4) in the Queensport lobe where there was a high concentration of these megacrysts. Arcuate patterns, over outcrop distances of 2-5 m, of aligned potassium feldspars are clearly evident.

Several authors agree that such concentrations could be developed through igneous mechanisms. Pitcher (1979) suggests that extensive overturn is not evident in granitic plutons, and attributes the concentrations to flow within the magma under natural conditions.

Clarke and Chatterjee (1985) alternatively suggest vigorous convective overturn in the early stages of a cooling magma could produce concentrations on a regional scale. Such concentrations are found within the SMB (McKenzie, 1974). Igneous layering (defined by biotite and feldspar megacrysts) seen at Chebucto Head in the SMB is postulated to represent either a process of cooling, cracking and subsequent flowage (Clarke and Muecke, 1980), or flow sorting during episodic shearing (Smith, 1975). The megacryst concentration and swirling within the QP lobe is very similar in appearance to local areas within the SMB and Chebucto Head, and the explanation that this phenomenon represents flowage differentiation is reasonable.

Biotite schlieren are seen within the HCQP as concentrations of biotite that form clumps or bands that are commonly elongate and sinuous. Balk (1937) described schlieren as "tabular, disk-like rock bodies, composed essentially of those minerals that build up the surrounding rocks, but in different proportions". They have been suggested to result from convection-stimulated magma currents which caused flowage (Didier, 1973), to represent plastic deformation during crystallization (Pitcher, 1979), or to be remnants of assimilated country rocks (Clarke, 1981). Previous authors of university theses undertaken in Nova Scotia have described schlieren and suggest that they represent remnant xenoliths (McKenzie, 1974; MacDonald, 1981).

Schlieren found within the HCQP generally occur in localities where enclaves in various stages of assimilation are also common. It is, therefore, postulated that most of the schlieren are derived from partial assimilation of country rocks.

2.4.3.4.2 Post-crystallization features

The pluton exhibits deformational and shear fabrics in varying degrees. The northern edge of the HC lobe is most deformed along Highway 16, by the hamlet of Halfway Cove, and along a power line to the west of Halfway Cove (Fig. 2.1 and Map 1). Deformation represented by S-plane foliation is defined by aligned biotite, elongate quartz grains (maximum ratio long axis:short axis 5:1) and minor elongation of feldspars (maximum ratio long axis:short axis 2:1). Shear planes (C-planes) are also apparent within the rocks closest to the Cobequid-Chedabucto fault zone. Both C- and S-planes are developed where the deformation is strong (Plate 2.13). Secondary white mica and chlorite are developed along shear plane surfaces, and also completely replace biotite within the deformed rocks. Kinked and strained mica grains, recrystallization of quartz, extensive brecciation and silicification (Plate 2.14) also occur where deformation is strong. Slickensides are apparent on horizontal to shallowly dipping surfaces. This deformation becomes progressively weaker to non-existent as a function of distance south of the fault, with only S-plane deformation (outlined by biotite foliation) exhibited in local areas in the southern portion of the HCQP.

A plot of poles to foliation in HCQP (Fig. 2.6) exhibits a strong orientation with a strike orientation of approximately 058° (054°-064°)/subvertical (078°S-090°). As seen in 2.6b, the foliation illustrated in this plot mainly represents the S-plane mineral foliation. Shear plane orientation measurements (C-planes), taken where deformation is strongest in the northern portions of the pluton, and particularly the HC lobe, are more east-west (080° to 120° with

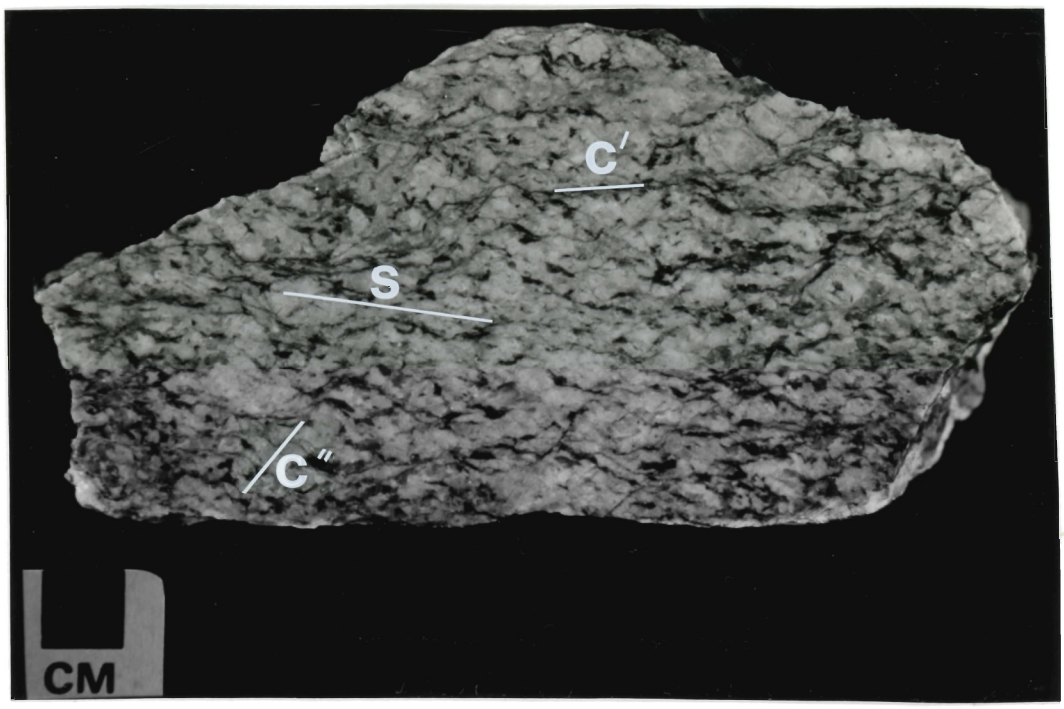


PLATE 2.13. Foliation developed within the granitic rocks of the HCQP. This foliation is better developed in the HC lobe. S fabric (S) is defined by flattening and alignment of minerals (biotite, muscovite, feldspar and quartz). Two C (shearing) fabrics are developed in the rocks. C′ is represented by mineral foliation and C" represents shearing and mineral recrystallization. These foliations are best developed adjacent to the Cobequid-Chedabucto fault zone, and decrease with distance south of the fault zone.

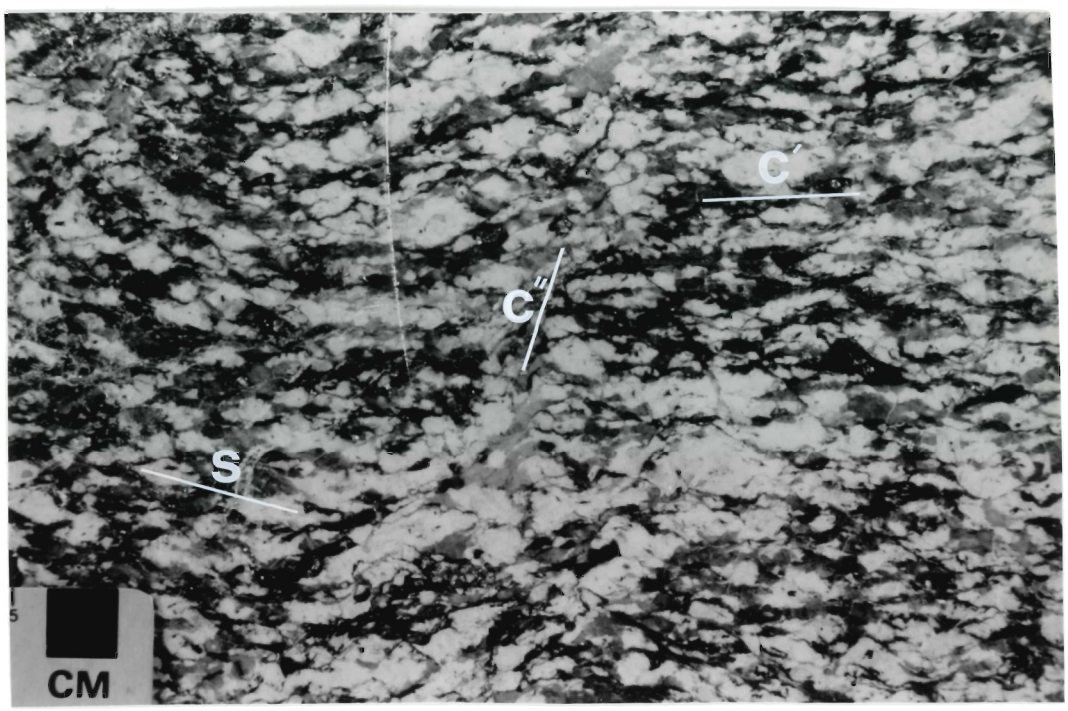

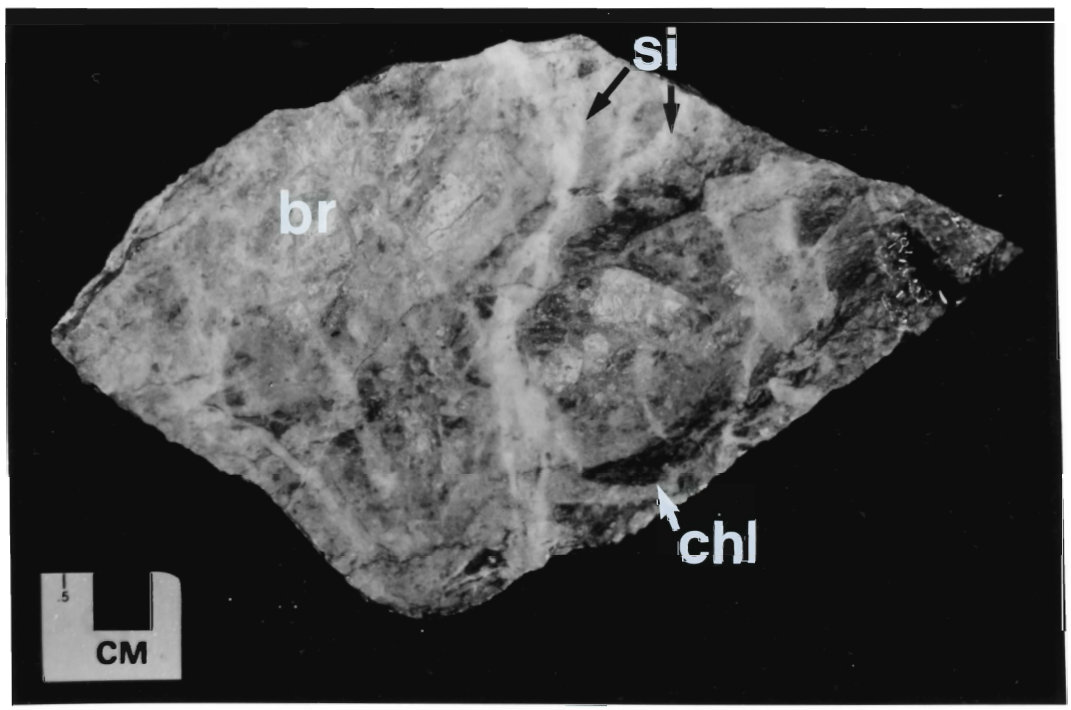


PLATE 2.14. Extensive alteration and deformation from the rocks of the HC lobe on highway 16. This alteration and deformation occurs in local areas along the Cobequid-Chedabucto fault zone. Silicification (si), brecciation (br), and chloritization (chl) are seen within the rocks.

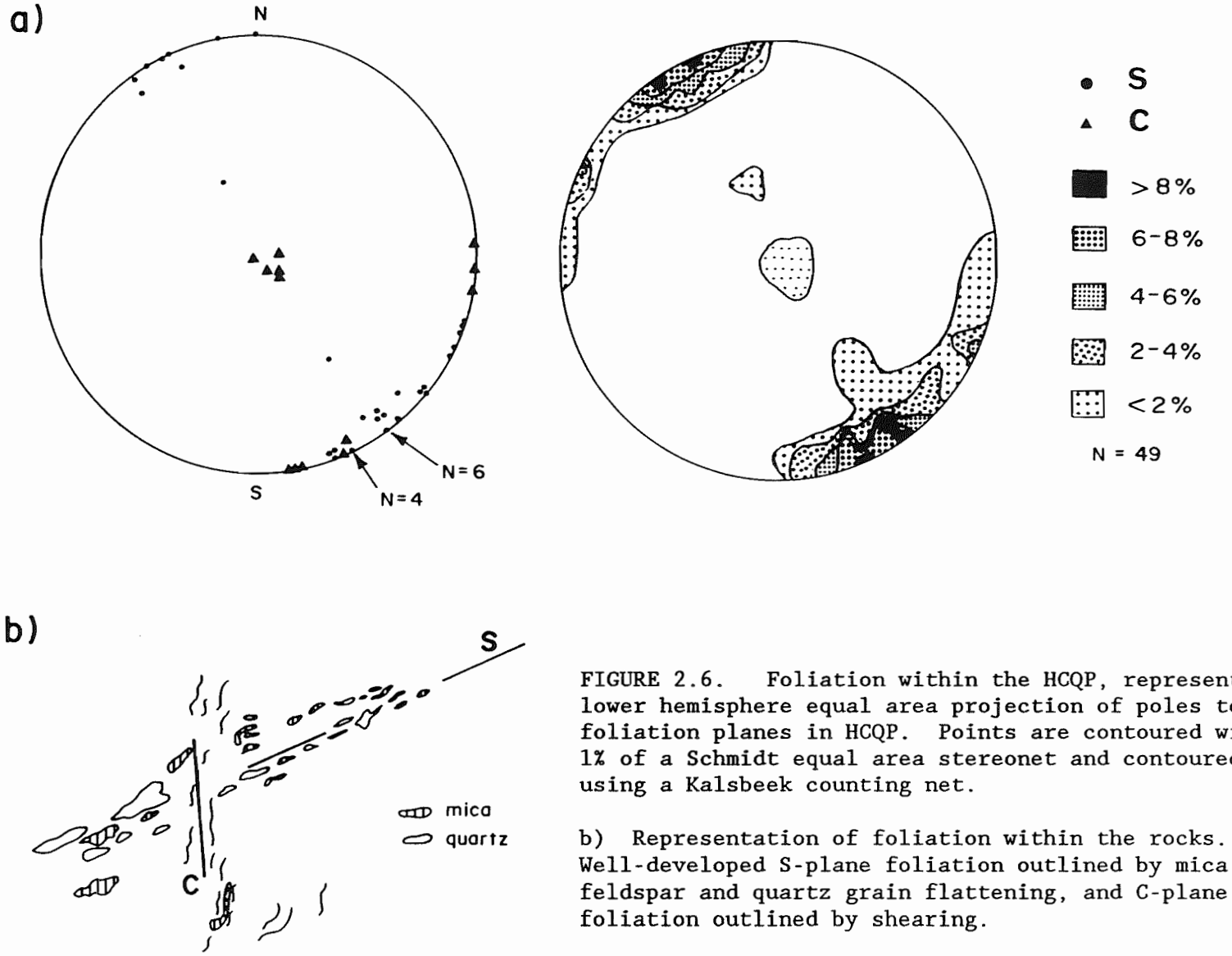


FIGURE 2.6. Foliation within the HCQP, represented by lower hemisphere equal area projection of poles to foliation planes in HCQP. Points are contoured within 1% of a Schmidt equal area stereonet and contoured using a Kalsbeek counting net.

b) Representation of foliation within the rocks. Well-developed S-plane foliation outlined by mica, feldspar and quartz grain flattening, and C-plane foliation outlined by shearing.

horizontal to shallowly dipping surfaces). The east-west foliation is approximately parallel with the fault zone. This C-S deformation is attributed to $D_2$ deformation of Hill (1986) and Hill and Raeside (1987), a deformation associated with movement along the Cobequid-Chedabucto fault zone. The 058° orientation of most of the mineral foliation (S-plane) is inclined to the fault zone and more parallel with the margins of the pluton. These findings are in agreement with results of the other studies that have documented the development of S- and C-plane in granitic rocks (Berthe et al., 1979; Ponce de Leon and Chorkroune, 1980; Mawer and White, 1987; Eddy, 1987).

The relationship between C and S planes allow definition of the sense of shear (Simpson and Schmid, 1983). The S-surfaces curve into the C-surfaces, and the curve, being S-shaped or Z-shaped, will define dextral or sinistral movement, respectively. The relationship between C-S fabric in the HCQP (Fig. 2.13) is generally S-shaped, representing dextral shear. This sense of movement corresponds to the type of movement postulated along the Cobequid-Chedabucto fault zone (Mawer and White, 1987).

Shear-related deformational features are not as well developed in the Queensport lobe and occur almost exclusively in the northern portion. This foliation diminishes with distance south of the fault zone. An exception to this is seen as well-developed east-west foliation in the southern portion of the lobe. Hill (1986) documents deformation within granitic rocks to the east (Whitehaven, Dover), that is approximately on strike with this east-west foliation. Keppie (1985) and Hill and Raeside (1987) suggest that this deformation may

indicate a shear zone in the southern portion of the HCQP and the Whitehaven and Dover plutons.

## 2.5 Regional Geophysical Surveys

### 2.5.1 Introduction

At the onset of mapping, it was unclear if the HCQP was actually two plutons, or just one irregularly-shaped pluton with two joined lobes. The area that has been mapped as both granitic and metasedimentary rocks is low-lying, flat and swampy, and forms the Halfway Cove and Bonnet Lakes (Fig. 2.1 and Map 1). The only exposed outcrops are metasedimentary rocks of the Halifax Formation which occur on the southern and southeastern shores of Bonnet Lake. Abundant monzogranitic boulders are apparent on the shores and similar to outcrop on both sides of the lakes.

The results of airborne magnetic and gamma-ray spectrometric surveys are presented in the next few pages. Surveys such as these are often conducted as an aid to mapping and mineral exploration, and for more complete knowledge of an area. Different rock types (e.g. igneous, sedimentary, altered, unaltered, etc.) have distinguishable magnetic susceptibilities (Telford et al., 1976) and will display diagnostic magnetic responses. Different rocks also contain variable abundances of elements (e.g. uranium, thorium, potassium), either as a result of magmatic proportions or enrichment or depletion as a result of alteration processes, and airborne measurements reflect the radioelement content on the ground (Killeen, 1979). The relative proportions of the elements, corrected for factors such as topography,

vegetation cover, soil thickness and elevation changes, will yield patterns and responses which can then be interpreted.

### 2.5.2 Aeromagnetic expression

The southern, eastern and western portions of the study area, underlain by Halifax Formation rocks, have a strong aeromagnetic expression (Fig. 2.7 and Fig. 2.1 for comparison of rock units) typical of those rocks elsewhere in the Meguma Terrane. The northern portion, underlain by the Goldenville Formation, is typified by a less variable pattern, with strong response patterns additionally outlining areas underlain by Halifax Formation. This pattern of low aeromagnetic relief can be traced several kilometres to the south. At this point, the contours become flat and continuous with contours extending from the granitic rocks on either side of the lakes. Three alternatives are proposed for this pattern: 1) the area of the lakes is indeed underlain by granite, thus accounting for the consistent and uninterrupted contours; 2) the area is underlain by rocks characterised by a pattern of low aeromagnetic relief which could be indistinguishable from the granite pattern (i.e. Goldenville Formation), as seen in other areas within the study area; or 3) the subtle differences are not discernible on the scale of the survey. The results are not definitive, but on the basis of the continuous pattern, the boulders on the shoreline and the only slight difference in topography from the HCQP, it is concluded that the area is underlain by granitic rocks.

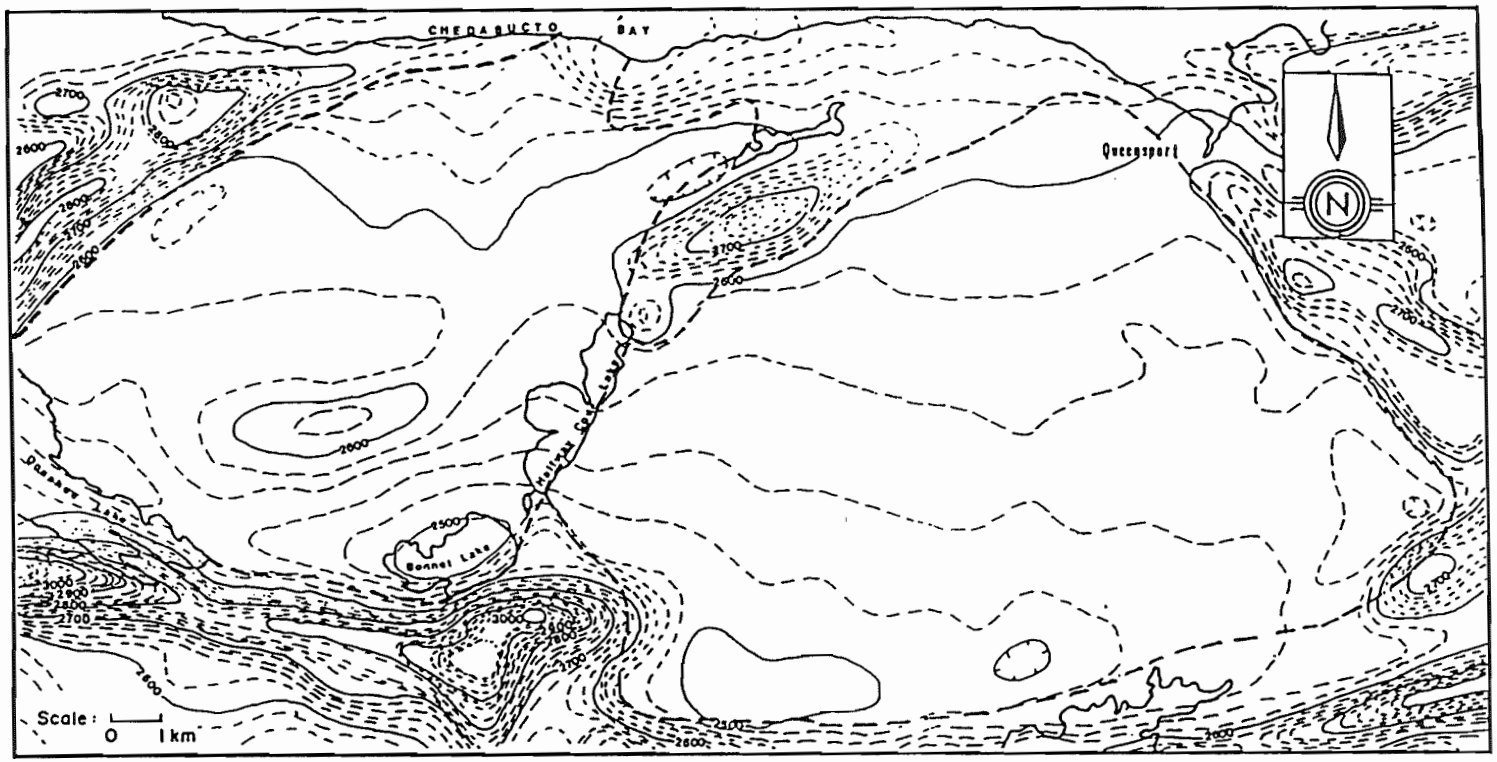


Contour Interval: 200 mgals

— — — contact between granite and metasedimentary rocks

FIGURE 2.7. Aeromagnetic pattern over the study area. The contacts separate the envelope of metasedimentary rocks from the granitic rocks which comprise the interior. Note the gentle continuous patterns through the area underlain by Bonnet and Halfway Cove Lakes. This pattern contrasts with the closely spaced lines of patterns from areas underlain by the metasedimentary rocks.

### 2.5.3 Airborne gamma-ray spectrometric surveys

#### 2.5.3.1 Introduction

Airborne gamma-ray spectrometric surveys undertaken over the study area are presented in Figures 2.8 to 2.11. These "equivalent" element maps have airborne measurements converted to element concentration (Grasty and Charboneau, 1973). Chatterjee and Muecke (1982) have indicated that radioelement diversities are related to varying degrees of differentiation within granitoid rocks, and have outlined distinctive responses of the granitic rocks within Nova Scotia. They have correlated some of these patterns with rocks enriched in Sn, Rb, Li, Be, F, and Cs and with rocks hosting economic mineralization (uranium, tin, tungsten). Further discussion about the radioelement patterns of the HCQP, and their relation to the individual units, is presented in Chapter 4.

#### 2.5.3.2 Equivalent Uranium

Figure 2.8 (equivalent uranium (eU)) shows that the contours become closely spaced at the eastern edge of Halfway Cove Lake. This is similar to other areas where a change occurs (e.g. at the contact between the granitic and metasedimentary rocks at the eastern edge of Queensport lobe near Third Lake, and the northern edge of the Halfway Cove lobe), and can be interpreted as a change in rock type (granite-metasedimentary or granite-granite).

The HCQP has several areas of slightly elevated equivalent uranium (eU) (avg. 3 ppm eU, compared with an average reading of 2 ppm within the body). This value, however, is lower than the average values for

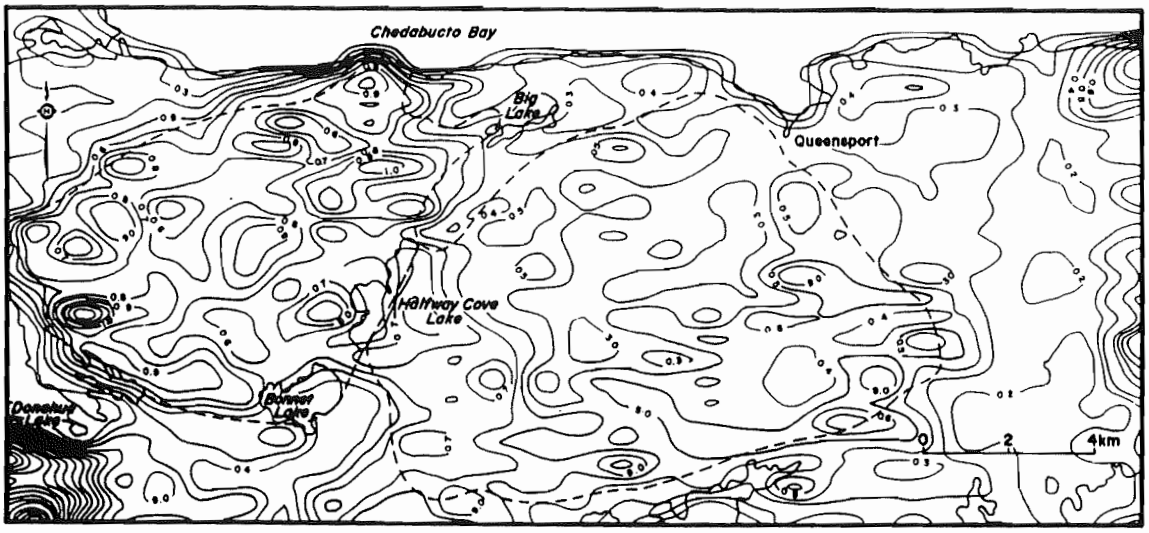


FIGURE 2.8. Equivalent uranium: Pattern of contours in the area underlain by the lakes resembles the patterns in other areas of the pluton. The contours become slightly more closely spaced in this area. Values in the southwestern corner of the HC lobe are slightly elevated (3.5-4.0 ppm) over the rest of the pluton. Contour interval: 0.5 ppm.

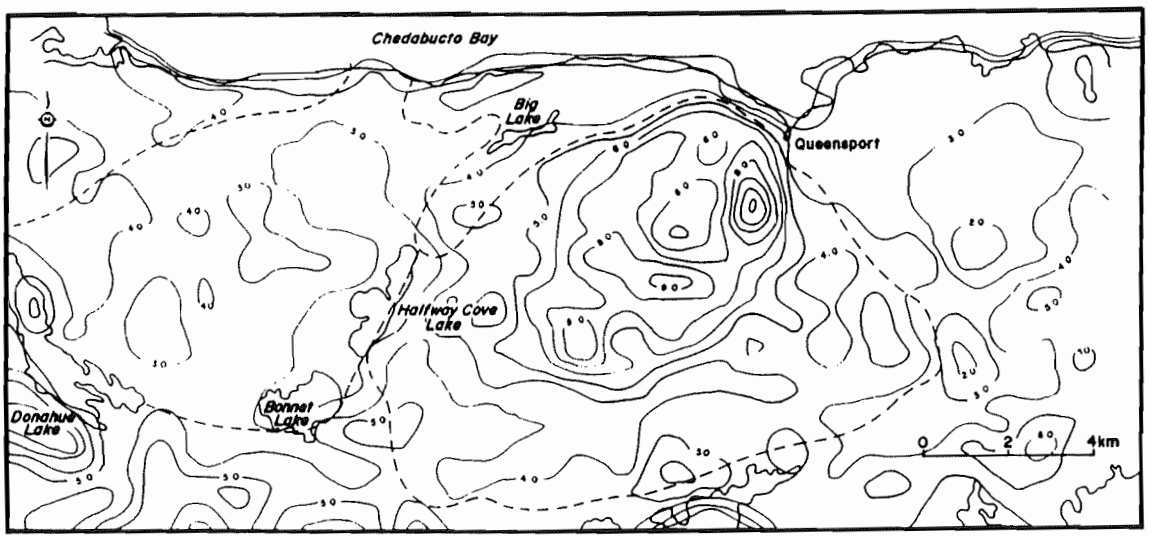


FIGURE 2.9. Equivalent thorium: Note that the area underlain by the lakes exhibits no substantial change in pattern. Note also the pattern in the QP with elevated values of 5-11 ppm over background values elsewhere in the pluton of 3-4 ppm. This elevated thorium response and pattern is unusual when compared with responses over other granites within Nova Scotia. Contour interval: 1.0 ppm.

other granitic bodies in the Eastern Meguma Terrane (6 ppm eU) and the Davis Lake leucogranite (22 ppm eU) in the western end of the SMB. Ratios of eU/eTh of Meguma Terrane granitoids are abnormally high (reaching values of >2), compared with normal crustal ratios of 0.25 (Ford and O'Reilly, 1985).

#### 2.5.3.3 Equivalent Thorium

The most striking characteristic of the HCQP is the unusual shape outlined for the equivalent thorium (eTh) radiometric values (Fig. 2.9). This pattern over the eastern and central portions of the Queensport lobe have an average eTh ranging from 2-4 ppm in the margins of the pluton to levels of 7-11 ppm in the interior. This pattern is the most pronounced response of elevated thorium of the Eastern Meguma Terrane granitoids. The response is considered valid as i) elevation differences have been corrected and ii) the Queensport lobe in the area of the elevated pattern is essentially a barren with abundant bedrock exposure. The increased thorium levels correspond with one area of slightly increased eU, but generally a correlation between eU and eTh is not developed.

#### 2.5.3.4 Other surveys

Equivalent thorium (eTh), equivalent uranium/ equivalent thorium (eU/eTh) and equivalent potassium (K x $10^4$) (Figs. 2.9 to 2.11, respectively) do not yield definitive results as to the nature of the bedrock, as even those areas that are known to be underlain by Meguma Group strata (e.g. Larrys River, Salmon River) and different phases of granitic rocks do not have readily discernible patterns. A recent

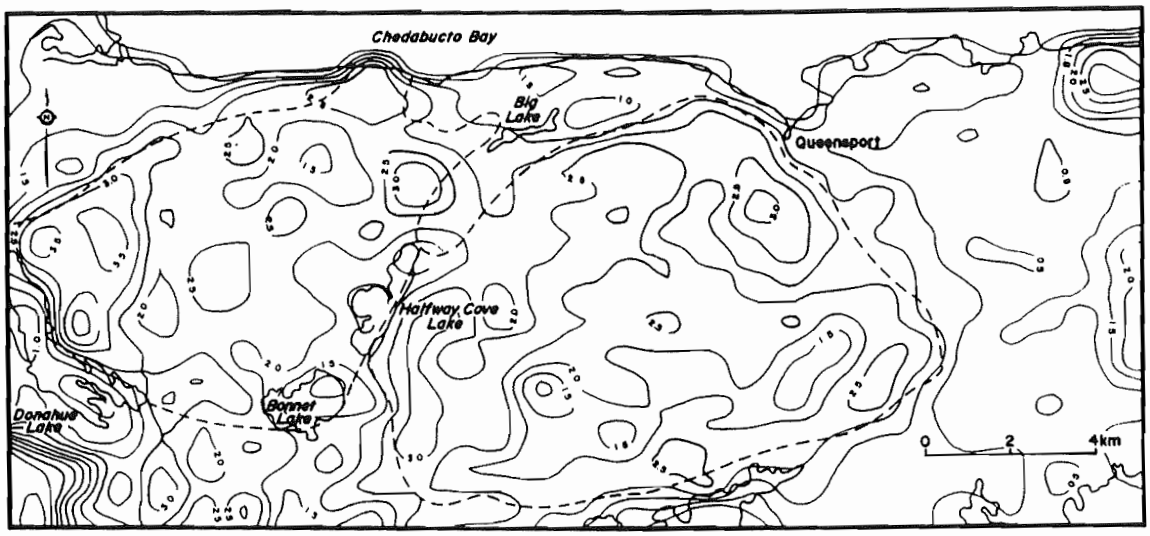


FIGURE 2.10. Equivalent uranium/equivalent thorium: The response in the area of Bonnet and Halfway Cove Lakes is very similar to the patterns over the rest of the body. The elevated areas in the southwestern part of the HC lobe reflect the similar response of elevated uranium values noted in Figure 2.8. Contour interval: 0.1.

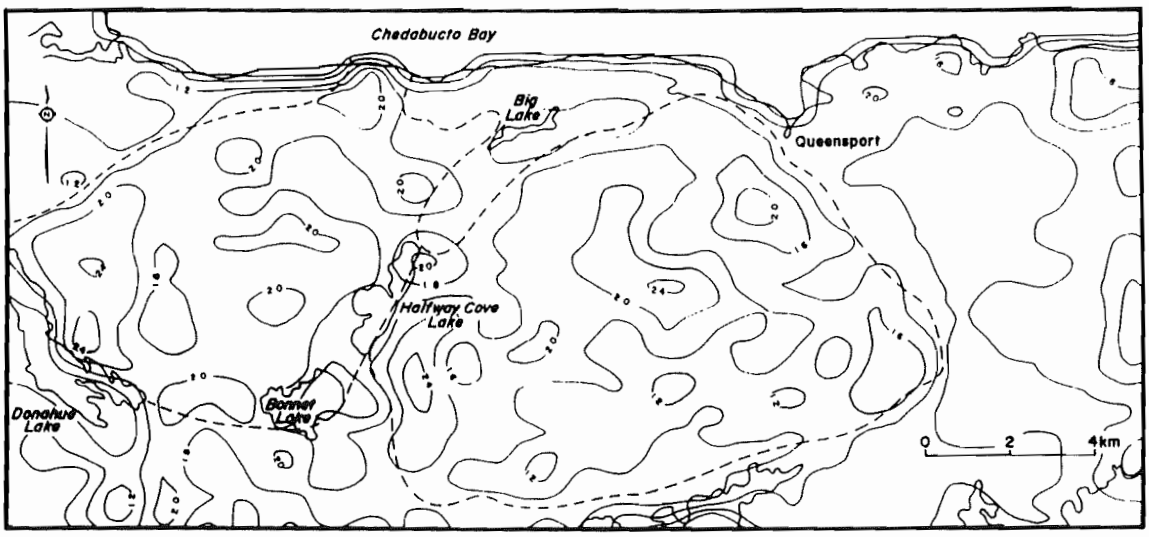


FIGURE 2.11. Equivalent potassium: Note the gentle patterns over the granitic areas and the very low response generally over areas underlain by metasedimentary rocks. Contour interval: 0.4 %.

gravity survey (Thomas, pers. comm.) over the HCQP indicates that the granite is continuous at depth. Computer-enhanced airborne radiometric images suggest that the Halfway Cove lobe and the Queensport lobe are fundamentally different in composition (Hill, pers. comm). Additionally, two different patterns are suggested in the Queensport lobe.

#### 2.5.3.5 Discussion

A contact was assumed, therefore, to lie in the area of the lakes between the coarse-grained biotite (minor muscovite) monzogranite to granodiorite phase of the Queensport lobe (HCQP1) and medium- to coarse-grained muscovite-biotite monzogranite unit of the Halfway Cove lobe (HCQP3). This was decided on the basis of the field evidence (textural characteristics, mineral proportions) and supported by the eU pattern.

## 2.6 Summary

The HCQP is composed predominantly of muscovite-biotite monzogranite, containing a total of five rock units. HCQP1 and HCQP1A mineralogically are the least evolved units, with the highest biotite and lowest muscovite contents. These two units also contain areas that are predominantly granodiorite composition. Aplite and pegmatite dykes are not abundant. Granite/metasedimentary rock contacts, where observed, are sharp and intrusive. Enclaves, the majority of which are metasedimentary in appearance, are not abundant, and occur dispersed throughout the pluton, although there are local concentrations. Structural and deformational features developed both through igneous processes (e.g. biotite schlieren, megacryst concentration) and

subsequent to emplacement (e.g. mineral foliation, shearing fabrics) occur in varying degrees throughout the pluton. Mineral foliation and shearing effects are most common in the northern portion of the HCQP, closest to the Cobequid-Chedabucto fault zone, with well-developed C-S fabric. These post-crystallization features suggest that the pluton was emplaced syn-tectonically, with C-S fabrics developed during the $D_2$ stage of deformation (Hill, 1986; Hill and Raeside, 1987) related to movement along the Cobequid-Chedabucto fault zone. Geophysical studies (e.g. equivalent uranium, equivalent thorium) conducted over the HCQP delineate a pronounced equivalent thorium pattern within the eastern Queensport lobe. Additionally, computer-enhanced airborne radiometric images suggest fundamental compositional differences between the Halfway Cove lobe and the Queensport lobe (Hill, pers. comm), and two different patterns (i.e. two different compositions) are suggested in the Queensport lobe.

# CHAPTER 3 - MINERAL CHEMISTRY

## 3.1 Introduction

To date, all granitic rocks that have been mapped within southern Nova Scotia have been classified as peraluminous, following a chemical classification scheme proposed by Shand (1927). Peraluminous rocks are those with an A/CNK ratio (whole-rock molecular proportions of $Al_2O_3/(CaO + Na_2O + K_2O)$ greater than one. These granites have a characteristic suite of minerals that include, in addition to quartz and two feldspars, one or more of phases such as biotite (usually highly aluminous), muscovite, cordierite, garnet, andalusite, sillimanite, mullite, topaz, tourmaline, spinel and corundum (Clarke, 1981). The SMB contains most of these minerals in varying proportions (McKenzie, 1974; MacDonald et al., 1986). Other plutons within southern Nova Scotia also contain most of these minerals, with different proportions (particularly cordierite) reported relative to the SMB (e.g. MacDonald, 1981; Allen and Barr, 1983; O'Reilly, 1985).

The HCQP contains quartz and two feldspars, biotite, muscovite, and minor garnet, with accessory apatite, rutile, ilmenite, chlorite, zircon and tourmaline. These minerals occur in varying proportions within the different units.

No cordierite was observed within the HCQP, and no cordierite to date has been definitively identified in any of the other granitic rocks of the Eastern Meguma Terrane (McKenzie and MacGillvray, 1974; Chevalier, 1983; O'Reilly, 1984, 1985; Ford and O'Reilly, 1985; Hill, 1986). Hill (1988) reports some smectite aggregates, which are

inferred to be cordierite pseudomorphs, in granitic rocks to the east of the HCQP. However, this general lack of cordierite in the rocks of the eastern Meguma Terrane contrasts with the SMB, the MB and smaller plutons of the south-central and southwestern Meguma Terrane, where the mineral is a common constituent of some units. Blocky cordierite has been documented throughout the MB (MacDonald, 1981; MacDonald and Clarke, 1985). It has been described as occurring within the SMB in specific localities, such as close to a contact with the Meguma Group metasediments (Maillet and Clarke, 1985). Recent mapping, however, (MacDonald et al., 1986) has shown that cordierite is more widespread throughout the SMB than was previously thought.

Microprobe analyses of selected mineral phases from the different units of the HCQP are presented. All obviously deformed and metamorphosed rocks were excluded from mineral analyses. All mineral analyses were conducted using the energy dispersive system of the Cambridge "Microscan V" electron microprobe at Dalhousie University. Mineral standards were used in all analyses (Appendix IV). Oxide proportions were determined by the microprobe and molecular proportions recalculated using the "Super Recal" program at Dalhousie University.

## 3.2 Biotite

### 3.2.1 Introduction

Biotite occurs almost ubiquitously in granitic rocks (Deer et al., 1966) and is a common 'sink' for excess alumina (Clarke, 1981; Speer, 1984). The term biotite is used to denote an iron-rich mica having a Mg:Fe ratio of <2:1 (Deer et al., 1966). The compositions of most biotites fall within a field outlined by four end-members. These are

phlogopite ($K_2Mg_6[Si_6Al_2O_{20}]OH_4$), annite ($K_2Fe_6[Si_6Al_2O_{20}]OH_4$), siderophyllite ($K_2Fe_5[Si_5Al_3O_{20}]OH_4$) and eastonite ($K_2Mg_5Al[Si_5Al_3O_{20}]OH_4$). Most biotite compositions in peraluminous granitic rocks, including the SMB, are iron-rich and closer to annite-siderophyllite in composition (Clarke, 1981).

Biotite is nearly always considered to be of primary magmatic origin (Yoder and Eugster, 1954). Exceptions are grains that have been incorporated as remnants of source region (White and Chappell, 1977), assimilated from remains of country rock (Clarke, 1981) or those that have been produced as secondary alteration products (Chatterjee and Strong, 1984).

Many attempts have been made to determine systematic changes in biotite chemistry with variation of host rock composition. With increasing $SiO_2$ in the host rock (i.e. differentiation), biotite compositions generally increase in $Fe^{2+}$ and decrease in Mg content (Deer et al., 1966). Aluminum in both the octahedral and tetrahedral sites can increase as co-existing AFM minerals (e.g. muscovite, cordierite) with high A/CNK values appear (Wones and Eugster, 1965; de Albuquerque, 1973; Guidotti et al., 1975). Tonalites and granodiorites have biotite with low Fe/(Fe+Mg) ratios, with the more highly differentiated rocks containing higher ratios and biotite compositions closer to eastonite-siderophyllite (Clarke, 1981). Stallard (1975) demonstrated that iron and magnesium varied with differentiation of granitic rocks of the SMB. Conversely, another study found that the ratio $Fe^{2+}/(Fe^{2+} + Mg)$ in biotite remained constant throughout different granitic phases of certain plutons (Dodge and Moore, 1968).

Speer (1984) suggests that magmatic micas can undergo extensive changes in element chemistry (major, trace and isotopic) by post-magmatic processes. Studies have determined that compositional fields outlined by major elements (e.g. Mg, Fe, Ti, Al) of biotites from different rock types displayed considerable overlap (Foster, 1960), had restricted, but not unique, groupings for individual rock types (Heinrich, 1946), or displayed distinctive chemical characteristics (Neilson and Haynes, 1973).

### 3.2.2 Biotite within the study area

Biotite occurs in all rocks of the HCQP, with the exception of some of the later-stage aplites, which contain muscovite and garnet. Biotite grains are pleochroic green-white to more common brown-red (Plate 3.1a). They often contain inclusions of apatite (generally <1 mm, although larger grains 1 mm are present), zircon, rutile and ilmenite. Some arrangement of inclusions along cleavage traces is observed. Pleochroic halos are common within biotite (Plate 3.1a and 3.1b), presumably around zircon, although the mineral is not always microscopically visible. Small, euhedral to subhedral (<1 mm), biotite is often found included within plagioclase, alkali feldspar and perthitic grains (Plate 3.1d). It is also found intergrown with muscovite or has muscovite growing along its cleavage planes, edges and ends. Ilmenite, rutile, and opaques (hematite ?) are often visible along cleavage traces and planes.

Chlorite and muscovite are the two common alteration products of biotite (Plate 3.1b and 3.1c). Rutile alteration product is also observed, with rutile growing along cleavage planes, or as needles

PLATE 3.1. Photomicrographs of biotite within the HCQP. Mineral abbreviations used in these, and subsequent photomicrographs, are biotite (bi), muscovite (mu), chlorite (chl), plagioclase (pl), potassium feldspar (ks), and feldspar (fs). Scale used in these, and subsequent photos, is the same as the scale indicated (0.5 mm), unless marked otherwise. Plate 3.1a illustrates representative biotite within the HCQP. The mineral is pleochroic green-white to brown-red, and contains pleochroic halos. Alteration to chlorite and muscovite (Plate 3.1b and c) are common, and minor alteration to feldspar also occurs. Biotite is often found included within other minerals (Plate 3.1d), such as feldspar grains.

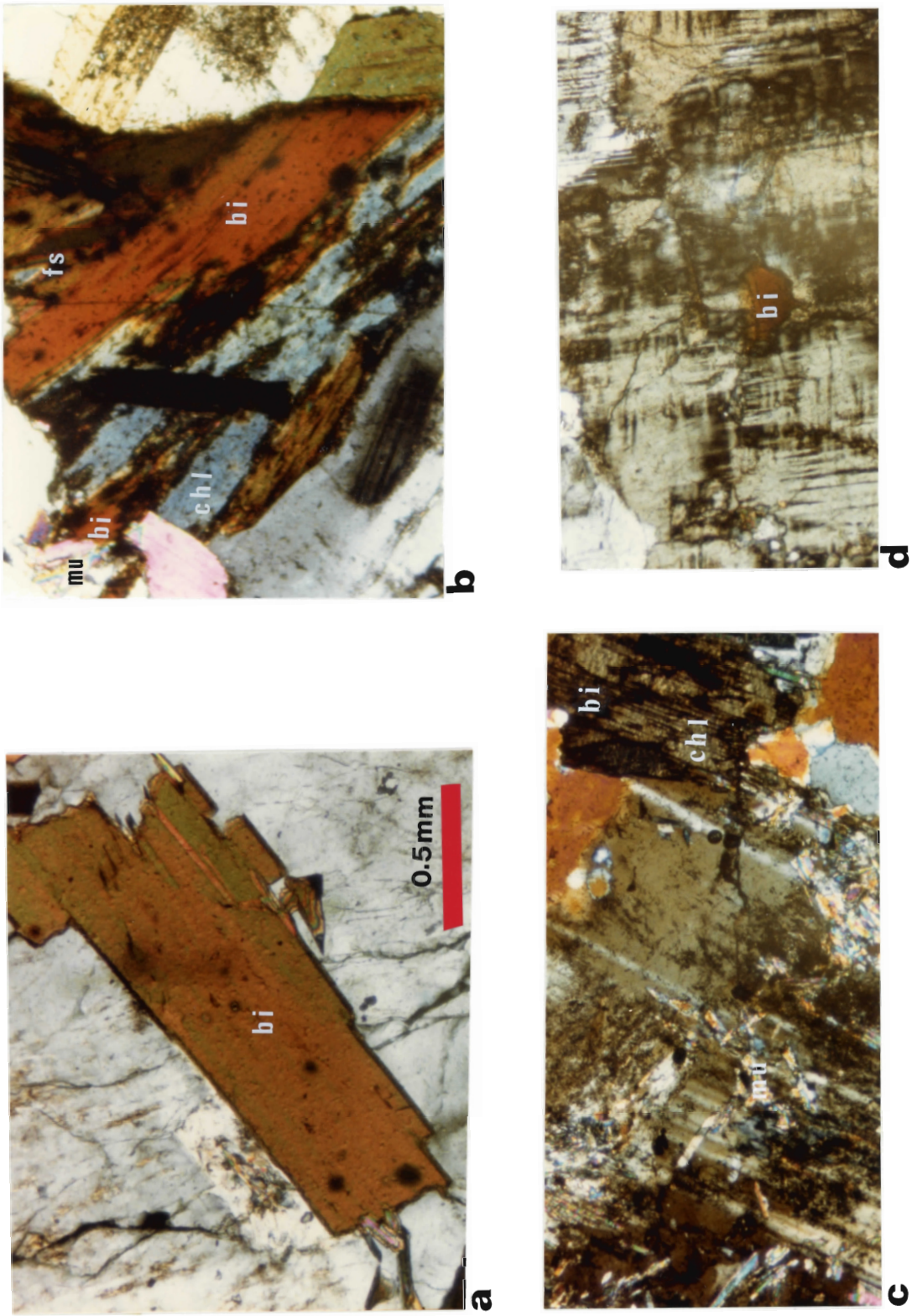


Plate 3.1

(often radiating), within the chlorite. Small alkali feldspar grains occur as alteration products within biotite.

### 3.2.3 Discussion

Analyses of biotites were obtained from selected polished sections from chemically analyzed samples of different units of the pluton. A total of 166 analyses were obtained, with 53, 21, 28, 14 and 49 obtained from intrusive phases HCQP1, HCQP1A, HCQP2, HCQP3, and HCQP4, respectively.

Biotite from HCQP generally is high in iron, averaging from 20.20 to 22.40 weight percent in the different rock units. MacDonald (1981) indicated that the biotites from the MB are also iron-rich, with contents ranging from 19.65 to 22.53 in the dominant monzogranitic rocks. HCQP2 and HCQP4 have some of the highest values (up to 24.65 weight %).

A plot of phlogopite (Phlo), annite (Ann) and a manganese end-member (Mn) (Fig. 3.1) illustrates that biotite compositions of all intrusive units are close to the Phlo-Ann join. In all rock units, the Mn content of the biotite is uniformly low. Biotites from all units overlap, and there is a spread of composition from mid-range phlogopite-annite towards the annite end-member. HCQP4 contains the most annite-rich biotite. This rock unit also has pods of leucogranite, increased development of secondary muscovite and rapakivi texture, suggesting a higher degree of differentiation and/or alteration.

Compositions of biotites from the study area are plotted using $Al^{iv}$ vs $Fe_t/(Fe_t + Mg)$ (Fig. 3.2). Biotites of the HCQP fall within

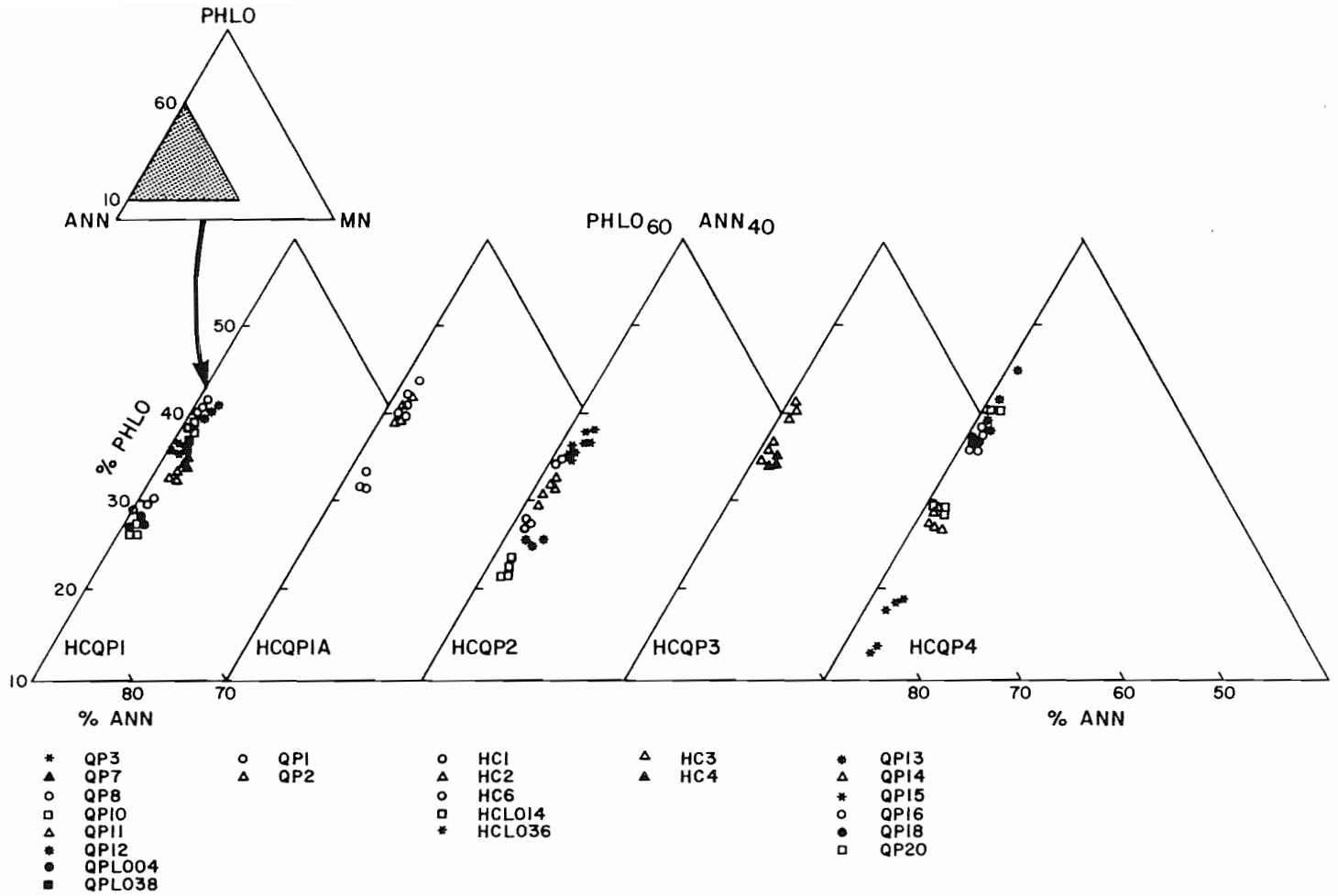


FIGURE 3.1. Biotite compositions from different rock units of the HCQP, plotted in terms of phlogophite (Phlo), annite (Ann) and a manganese end-member (Mn). Biotite compositions of all rock units are close to the Phlo-Ann join, and are uniformly low in Mn. Unit HCQP4 contains the most annite-rich biotite. Symbols represent analyses from one rock.

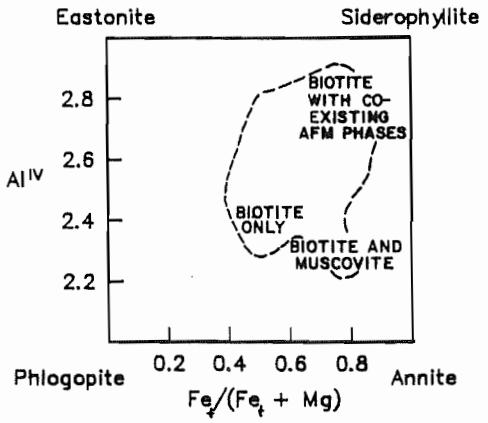


HCQP1 □ QP03
+ QP07
◇ QP08
△ QP10
× QP12
⊙ QPL004
* QPL038

HCQP1A □ QP01
+ QP02

HCQP2 □ HC01
+ HC02
◇ HC06
△ HCL014

HCQP3 □ HC03
+ HC04

HCQP4 □ QP13
+ QP14
◇ QP15
△ QP16

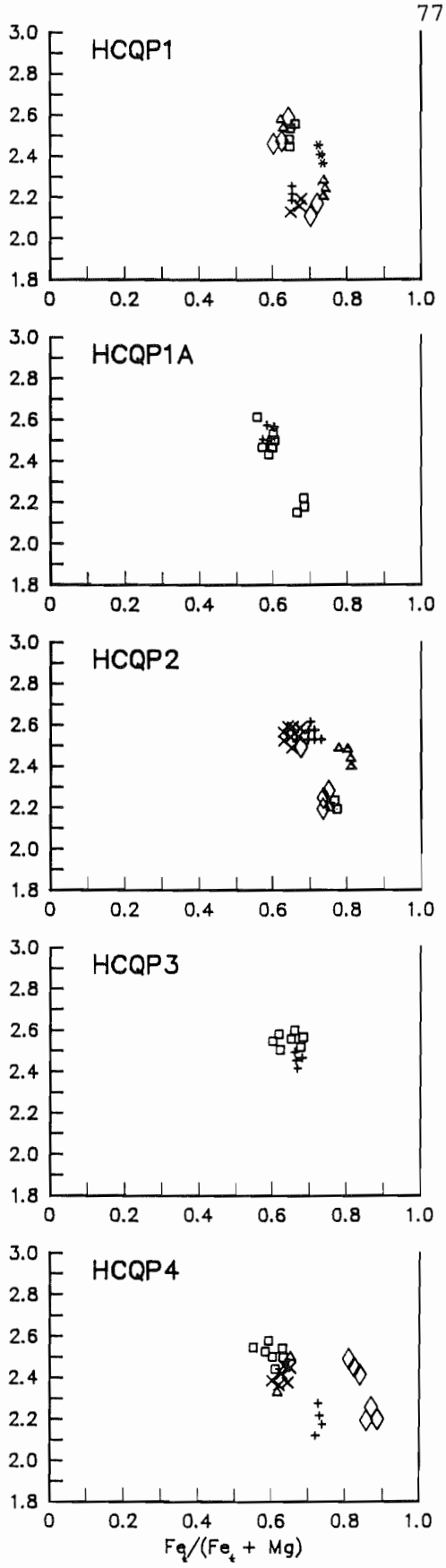


FIGURE 3.2. A plot of tetrahedral alumina versus $Fe_t/(Fe_t + Mg)$ for biotite analyses of the HCQP, with fields outlined by Clarke (1981) for biotite co-existing with other AFM mineral phases. Biotite compositions from all units of the HCQP exhibit overlap and fall within the field outlined by Clarke (1981) for rocks containing muscovite as the other AFM mineral. Symbols represent analyses from individual rocks.

the field outlined by Clarke (1981) for rocks containing muscovite as the other AFM mineral. There is a slight increase in the $Fe_t/(Fe_t + Mg)$ ratios from biotites of phases HCQP1 to HCQP4, with no significant Al increase. One sample (QP15 from HCQP4), from an outcrop that contains leucogranite pods and may reflect a higher degree of chemical evolution, curiously displays lower aluminum with higher $Fe_t/(Fe_t + Mg)$ than other rocks of the HCQP.

In a study of mineralised rocks in Peru, le Bel (1979) determined that magmatic and hydrothermal (e.g. biotite within alteration zones) biotite could be separated by their $Al^{vi}$ and Ti contents, with magmatic biotite containing low $Al^{vi}$ and high Ti. Corey (1988) and Kontak and Corey (1988) reported similar findings, using biotite from a complex of highly aluminous rocks which intrude the granodiorite of the northeastern SMB. Magmatic biotites from this complex have low $Al^{vi}$ (0.6-0.8) and high Ti (0.4 weight %). As hydrothermal activity increases within the rocks, as seen petrographically and mineralogically (e.g. metasomatic garnets, sericite development), $Al^{vi}$ contents of the biotites increase (0.9-1.3) and Ti contents decrease (0.1).

Biotites from the HCQP generally have higher $Al^{vi}$ contents (Fig. 3.3b-f) than biotite from the highly aluminous complex of the SMB. Biotites from phases HCQP1 and 1A have the lowest $Al^{vi}$ values. Ti contents of biotite from the HCQP are similar for all units, and comparable to magmatic biotite of Corey (1988). Most of the biotite of the HCQP falls within this field, although biotite from one sample from HCQP2 contains higher Al and lower Ti than the rest of the samples.

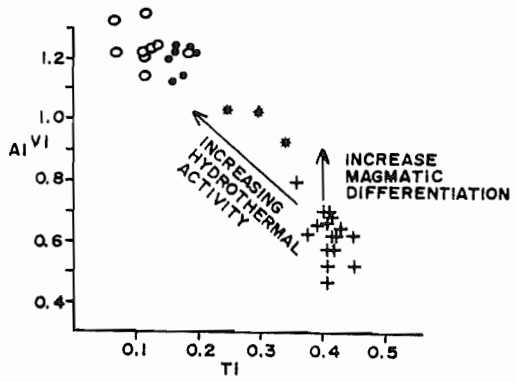


HCQPI
- □ QP03
- + QP07
- ◇ QP08
- △ QP10
- × QP12
- ⊙ QPL004
- * QPL038

HCQPIA
- □ QP01
- + QP02

HCQP2
- □ HC01
- + HC02
- ◇ HC06
- △ HCL014

HCQP3
- □ HC03
- + HC04

HCQP4
- □ QP13
- + QP14
- ◇ QP15
- △ QP16

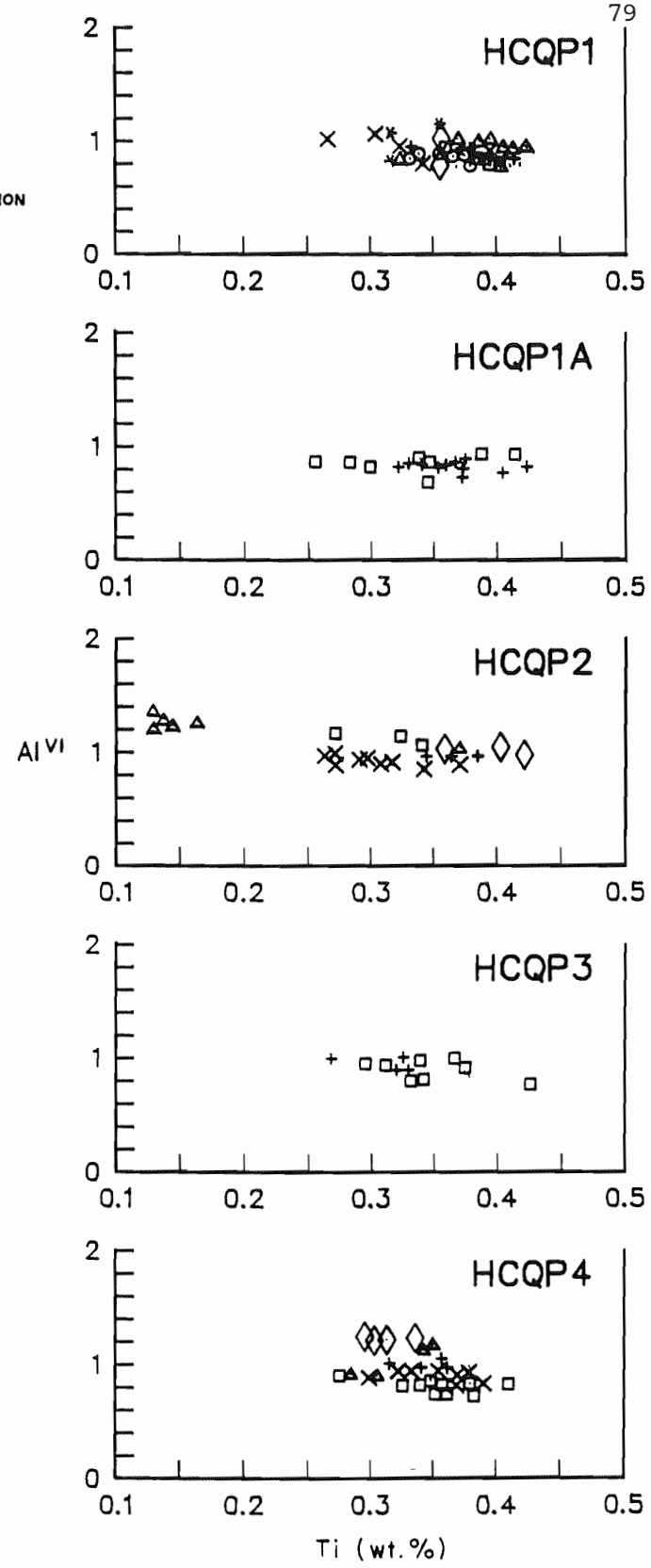


FIGURE 3.3. A plot of octahedral alumina versus Ti for analyzed biotites within the HCQP. Corey (1988) determined that magmatic-looking biotite had low $Al^{vi}$ and high Ti from rocks of a granitoid complex in the northeastern portion of the SMB. Biotite from the HCQP generally falls in the field for magmatic, and not hydrothermal, biotite.

This biotite could represent hydrothermal biotite, suggestive of minor fluid interaction.

## 3.3 Muscovite

### 3.3.1 Introduction

The presence of white mica, particularly magmatic muscovite, within granitoid rocks is generally interpreted to reflect peraluminous bulk composition (Miller et al., 1981; Clarke, 1981; Speer, 1984). Magmatic muscovite is often used for the determination of minimum pressures (i.e. depths) of crystallization of a magma. Pressures for stoichiometric muscovite have been calculated to be approximately 3 kbars (Althaus et al., 1970; Anderson and Rowley, 1981), corresponding to temperatures of 650°C and depths of 9.6-11.5 km. Secondary muscovite can also occur as a subsolidus reaction or alteration product, and the temperature and pressure constraints necessary for primary muscovite formation are removed.

The general formula for stoichiometric muscovite is $KAl_3Si_3O_{10}[OH]_2$ (Deer et al., 1966). Within the non-ideal, natural muscovite, the X group (potassium) can include substitutions of Ba, Rb, Cs, Na and Ca; the Y group (aluminum) can be replaced by Mn, Cr, Ti, Li, Mg, $Fe^3$, $Fe^2$ and V; and the Z group (silicon) can involve slight substitution of Al for Si and slight increase in the amount of Si.

A number of authors of recent works (Saavedra, 1978; Miller et al., 1981; Anderson and Rowley, 1981; Monier et al., 1984; Ham and Kontak, 1988) have classified, by texture, primary and secondary grains, and then examined the textural groupings for compositional similarities. The criteria used in different studies for recognition

of primary vs secondary muscovite are outlined in Table 3.1a. Zen (1988) additionally suggests the criteria could include the presence of euhedral contacts of muscovite against magmatic-looking biotite.

Previous studies concluded that there are indeed subtle chemical differences between primary-looking and secondary mica (Table 3.1b), with the main distinction being that the Ti concentration is higher in the primary micas.

### 3.3.2 Muscovite within the study area

Muscovite occurs in almost all rocks from the HCQP, although it is relatively more abundant in phases HCQP2, HCQP3 and HCQP4. Following criteria outlined in Table 3.1, muscovite within the HCQP is classified as both primary (magmatic) and secondary. The different textural associations of muscovite recognized, both in hand specimens and thin sections, are: 1) primary (Plate 3.2a); 2) primary intergrown with biotite (following the criteria of Saavedra (1978) and Zen (1988); Plate 3.2b); 3) secondary (muscovite that does not 'fit' textural criteria as outlined for primary muscovite); 4) alteration product of plagioclase (Plate 3.2c); 5) alteration product of potassium feldspar; and 6) alteration product of biotite (Plate 3.2c). A total of 121 analyses from the units was collected from the different associations.

### 3.3.3 Discussion

Compositions of muscovite within the HCQP are plotted in terms of Si, Al and other (Fe, Mg, Mn, Ti) octahedral cations (Fig. 3.4). Muscovite is not ideal in composition, but displays a trend towards celadonite ($K(Fe,Mg,Al)_2(Si_4O_{10}[OH]_2)$. Compositions of muscovite from

TABLE 3.1 Textural (3.1a) and chemical (3.1b) criteria used to determine primary and secondary white mica.

TEXTURAL CHARACTERISTICS

| | Miller et al. (1981) | Saavedra (1978) |
|---|---|---|
| LOCATION | North America and Europe<br>16 different peraluminous granitoid plutons<br>(41 samples) of North America and Europe | Central Spain<br>Peraluminous granites |
| CRITERIA: | 1) grain size in comparison with the other obviously primary minerals;<br>2) nature of the terminations of the grains and grain formation (clean, sharp terminations, ideally with subhedral to euhedral shapes);<br>3) grain ideally free from inclusions, and also not enclosed by minerals from which it could have been derived through alteration processes;<br>4) unaltered groundmass and igneous textures | 1) different twinning from biotite when intergrown and contact between the micas well differentiated<br>2) euhedral form;<br>3) well developed, euhedral grains within plagioclase;<br>4) absense of inclusions of accessory minerals, particularly those from which it could have been derived |

CHEMICAL CHARACTERTISTICS OF PRIMARY (P) AND SECONDARY (S) WHITE MICA

| | Miller et al., 1981 | Anderson and Rowley, 1981 | Speer (1984) | Monier et al., 1984 |
|---|---|---|---|---|
| LOCATION | Same as above | Peraluminous granites<br>Whipple Mountains, California | 59 peraluminous plutons<br>Southern Appalachians | One peraluminous pluton<br>Millevaches Massif, France |
| RESULTS | -P enriched in Ti, Na over S<br>-P depleted in Mg, Si compared with S<br>-P closer to ideal-composition than S<br>-imperfect correlation of textural types and composition<br>-P-looking micas invariably co-exist with Al-rich biotite + garnet<br>-celedonitic impurities | -Ti concentration most distinctive; higher Ti of P than S<br>-ferriceladonitic nature of muscovites; highest celadonitic component in P<br>-reported depletion in Ti, Mg, Fe, Si; enrichment in $Al^{IV}$ and $AL^{VI}$ with retrogression during mylonitization (becoming less celadonitic)<br>-other elemental variations due to Ti compensation | -Ti contents in P higher than S<br>-Fe, Mg, Na, Al, Si considerable overlap<br>-S can be more Fe-rich<br>-S occurring within plagioclase can have higher Na contents than matrix muscovite (both P and S) | -Three generations of muscovite [(1) magmatic, (2) late to post magmatic and (3) hydrothermal<br>-1 highest Ti<br>-Ti content decreased with magmatic evolution (lower in 2 and 3)<br>-Fe contents higher in 2 than 3<br>-Na/(Na + K) highest in 1<br>-variations in Fe, Si, Al, Ca, Na not systematic<br>-3 micas contain significant Ca and $H_2O$ interlayer site |

PLATE 3.2. Photomicrographs of muscovite within the HCQP. Note the euhedral shape of primary muscovite (Plate 3.2a), with ends that are generally cleanly terminated. Plate 3.2b illustrates another mode of occurrence of muscovite, that being primary muscovite intergrown with biotite. The two micas are grown at different angles to each other. Plate 3.2c illustrates two modes of occurrence, one altering from biotite, and the other (mu with white arrows), altering from plagioclase.

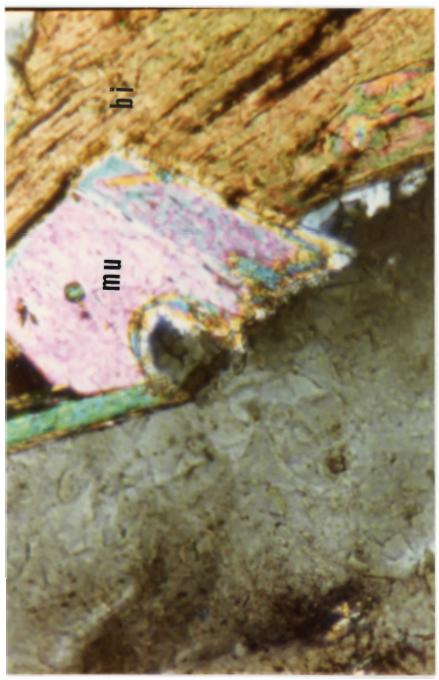


b

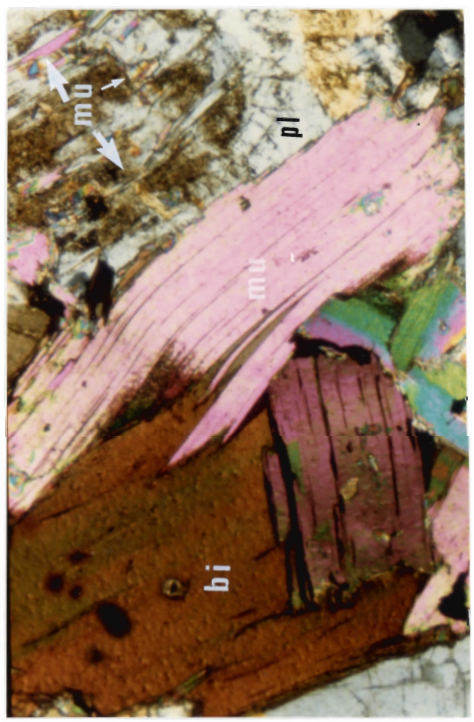


c

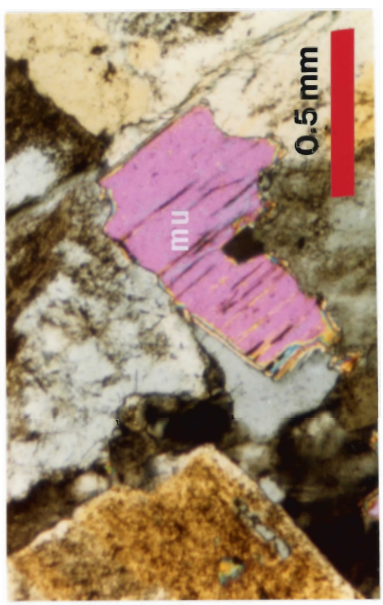


a

Plate 3.2

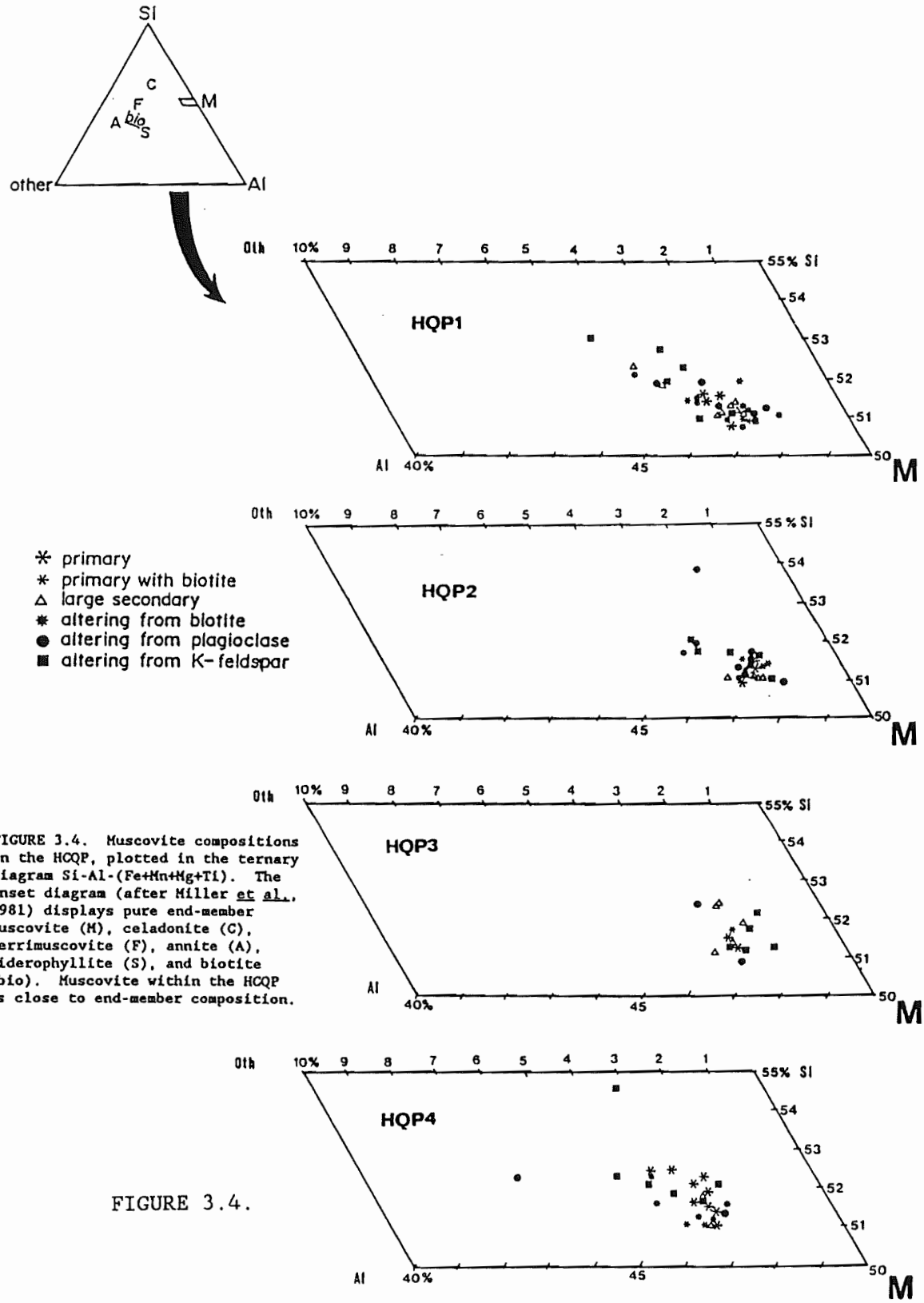


FIGURE 3.4. Muscovite compositions in the HCQP, plotted in the ternary diagram Si-Al-(Fe+Mn+Mg+Ti). The inset diagram (after Miller et al., 1981) displays pure end-member muscovite (M), celadonite (C), ferrimuscovite (F), annite (A), siderophyllite (S), and biotite (bio). Muscovite within the HCQP is close to end-member composition.

FIGURE 3.4.

all rock units overlap, with phases HCQP2 and HCQP3 showing more restricted ranges of composition. Miller et al. (1981) determined that primary muscovite is generally closer to 'ideal' composition, higher in Al and poorer in Si. Muscovite within the study area exhibits a very weak but similar trend, although secondary muscovites display considerable overlap, both with other modes of secondary occurrence and with fields outlined by primary muscovite.

Clarke (1981) displayed muscovite compositions from peraluminous granitoid rocks in terms of Y site cations (Fe + Mg/(Fe + Mg + Mn + Ti + $Al^{vi}$)) vs X site cations (Na/(Na + K + Ca) (Fig. 3.5a). This revealed that most analyses had Y site cation values of <0.2 and X site cation values of <0.1. Unique compositional fields for muscovite co-existing with different mineral assemblages could not be identified. Muscovite within the HCQP (Fig. 3.5b-e ) differs slightly from the field outlined by Clarke (1981), as the HCQP analyses are low in Na. This results in the fields expanding towards the Y axis. All analyses within the HCQP have values of Fe + Mg/(Fe + Mg + Mn + Ti + Al) <0.2 and mostly <0.1. Na/(Na + K + Ca) values are 0 - 0.1.

Muscovite analyses from the HCQP are plotted in terms of Ti-Na-Mg (Fig. 3.6), with the inset displaying the fields for primary and secondary muscovite as outlined by Miller et al. (1981). The compositions within the study area are close to the Mg apex of the triangle and extend to mid-range. Primary muscovite is generally higher in Ti, although many secondary grains (alteration products and discrete grains) also contain significant amounts of Ti. All units exhibit overlap, although HCQP1 muscovite is generally closer to the Mg apex. The other units trend towards the Na apex.

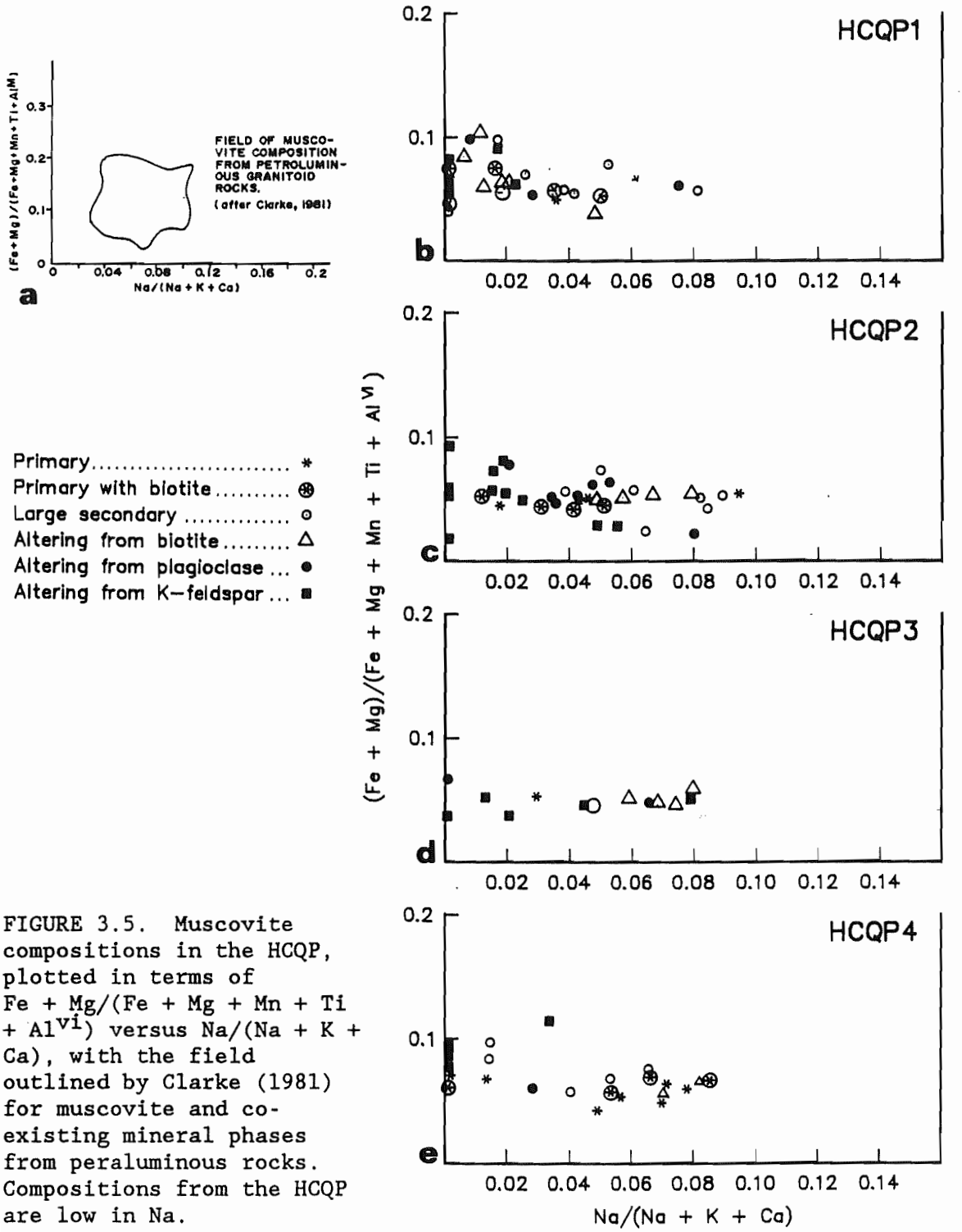


FIGURE 3.5. Muscovite compositions in the HCQP, plotted in terms of Fe + Mg/(Fe + Mg + Mn + Ti + $Al^{vi}$) versus Na/(Na + K + Ca), with the field outlined by Clarke (1981) for muscovite and co-existing mineral phases from peraluminous rocks. Compositions from the HCQP are low in Na.

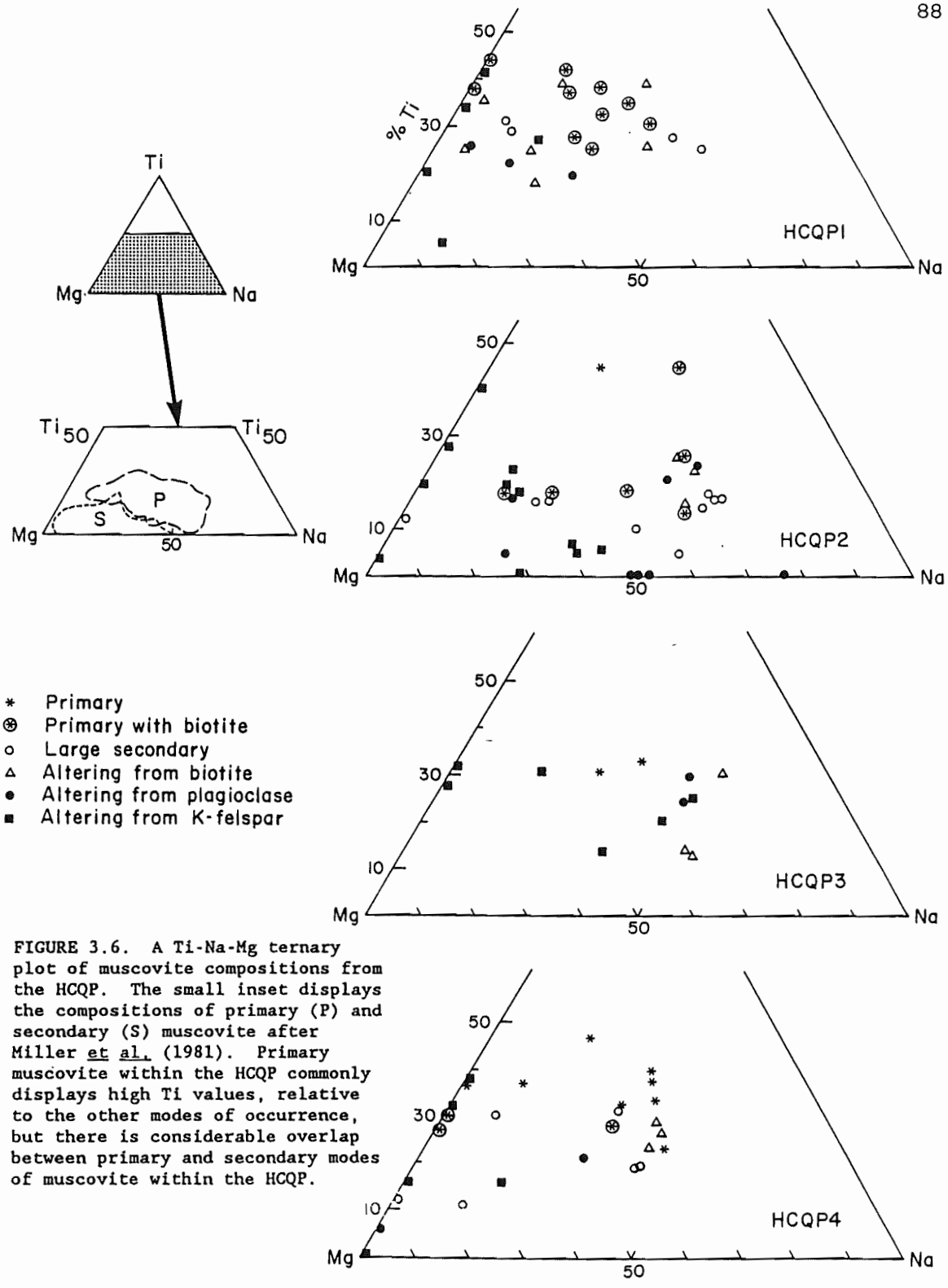


FIGURE 3.6. A Ti-Na-Mg ternary plot of muscovite compositions from the HCQP. The small inset displays the compositions of primary (P) and secondary (S) muscovite after Miller et al. (1981). Primary muscovite within the HCQP commonly displays high Ti values, relative to the other modes of occurrence, but there is considerable overlap between primary and secondary modes of muscovite within the HCQP.

FIGURE 3.6.

In conclusion, both primary and secondary muscovite, based on texture, occur within the HCQP. Primary muscovite is not ideal in composition and contains high Ti compared to most secondary modes of occurrence, although there is considerable overlap. Muscovite within HCQP1 (the least evolved unit) contains generally more Mg, while muscovite within the other units tend to be more Na-rich. These characteristics suggest a relationship between host rock and muscovite compositions, a conclusion reached by Ham and Kontak (1988) for muscovite within the SMB.

## 3.4 Feldspar

### 3.4.1 Introduction

Feldspars are abundant constituents of igneous rocks, and their major element chemistry provides the basis for classification of igneous rocks (Parsons and Brown, 1984). The majority of feldspars may be classified as members of the ternary system $NaAlSi_3O_8$-$KAlSi_3O_8$-$CaAl_2Si_2O_8$ (Deer et al., 1966; J. V. Smith, 1974; Ribbe, 1984). Feldspars in igneous rocks are the result of three stages of development, those being magmatic, hydrothermal (deuteric) and post-magmatic (subsolidus) (Parsons and Brown, 1984). Crystal growth is dominant in the magmatic stage, and relatively calcic plagioclase develops early in the crystallization sequence of most granitic magmas (Clemens and Wall, 1981; Phillips et al., 1981; Clemens et al., 1986).

Exsolution textures in alkali feldspars and compositions of feldspar phases provide information on the subsolidus history of granitoid intrusion (Parsons, 1978; Ribbe, 1983). Perthite, the

intergrowth of sodium-rich feldspar and potassium-rich feldspar, and myrmekite (plagioclase and vermicular quartz) are common in granites.

Rapakivi textures within granitic rocks are defined by large crystals of K-feldspar mantled by plagioclase (normally oligoclase for magmatic rapakivi texture; Elliston, 1985). This growth can be explained by both magmatic and alteration processes. Several explanations have been proposed in the past for rapakivi textures. These are: 1) exsolution (e.g. Gates, 1953; Elders, 1966); 2) resorption-infilling (Stull, 1978); 3) metasomatism (e.g. Hawkes, 1967); 4) magma mixing (Hibbard, 1981), and 5) rapid degassing of a liquid phase (Abbott, 1978).

### 3.4.2 Feldspar within the study area

Different compositions within the rock units are displayed on a Or-Ab-An ternary plot (Fig. 3.7). Within HCQP1 and 1A, plagioclase compositions range from $An_{10}$ to $An_{38}$ (albite to andesine), with strong and well-developed normal and discontinuous zoning (Plate 3.3a). Most rim compositions are $An_{15-20}$, with more calcic cores ($An_{32-35}$), with some plagioclase core and rim compositions averaging $An_{10}$ and $An_{2-10}$, respectively (Clarke, in prep.). Compositions from plagioclases near the western, southern and eastern edges of the plutons have the higher An compositions ($An_{22}$-$An_{35}$) in the plagioclase core.

Potassium feldspar, commonly perthitic, occurs in phases HCQP1 and HCQP1A both as a groundmass constituent and as megacrysts (Plate 3.3b). Chemical compositions are essentially $KAlSi_3O_8$ ($Or_{87}$-$Or_{92}$), with compositions of exsolution lamellae being highly albitic ($An_{1-2}$). The cores of the K-feldspars are not highly altered, and have minor

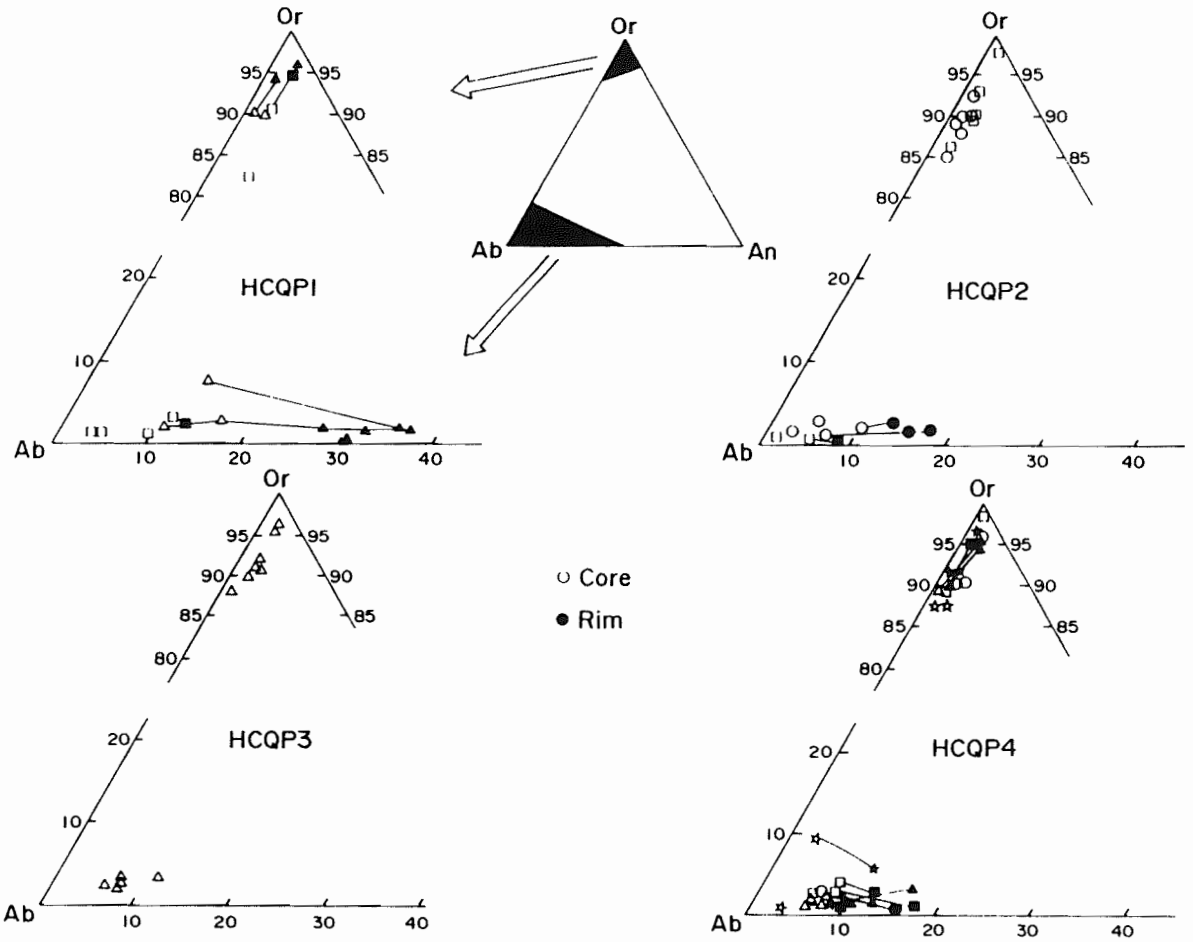


FIGURE 3.7. Plagioclase and potassium feldspar from the HCQP, plotted on a Or-Ab-An (mole %) ternary diagram. Rock units HCQP1 and 1A display the highest An compositions, and the more evolved units commonly contain plagioclase with albitic compositions. Potassium feldspar compositions are generally uniform throughout the pluton. Tie lines indicate core-rim compositions on one analyzed grain.

PLATE 3.3. Photomicrographs of feldspars within the HCQP. Plate 3.3a illustrates well-developed plagioclase zoning from HCQP1. Note the altered core. Plate 3.3b represents a potassium feldspar, with myrmekite (myr) developed at the contact between a plagioclase and the K-feldspar. Plate 3.3c illustrates well-developed rapakivi texture (albitic rim on perthitic core) of HCQP4.

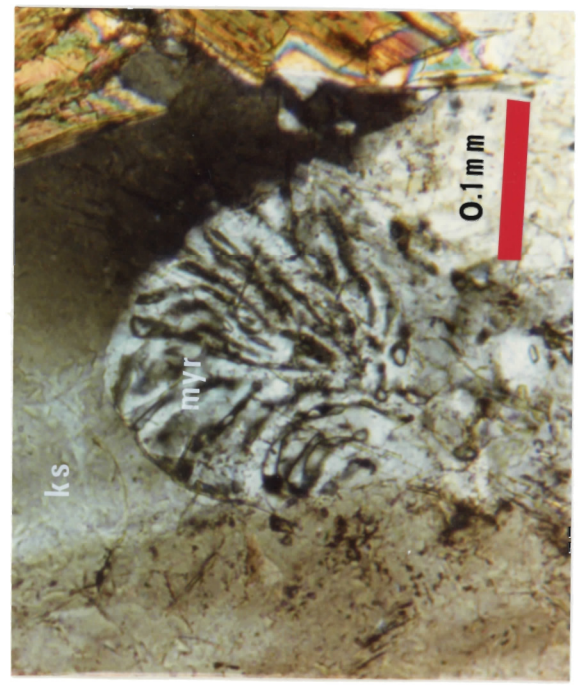


b

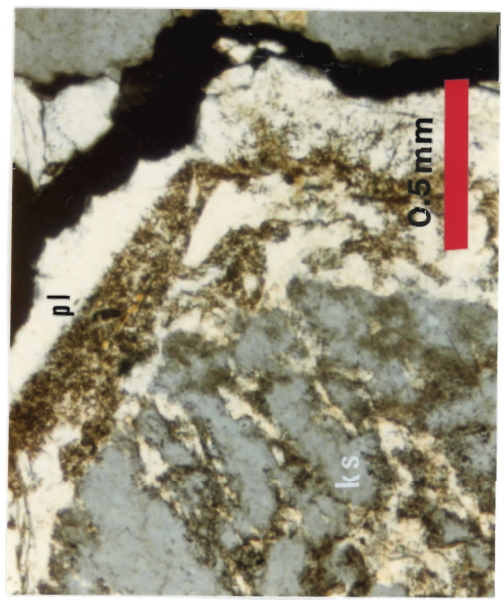


c

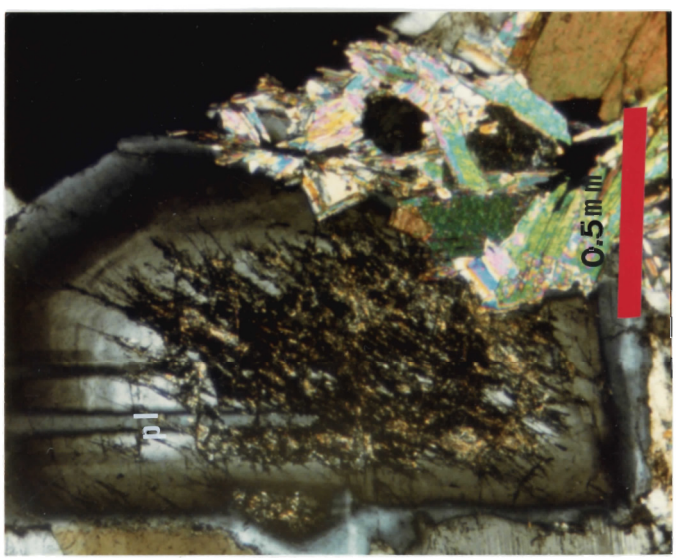


a

Plate 3.3

development of secondary muscovite. Most feldspars contain inclusions of biotite.

Within HCQP2 and 3, plagioclase feldspar has compositions $An_6$ to $An_{17}$ (albite to oligoclase), with cores which are generally calcium-rich. Normal and discontinuous zoning are common, although the zoning is not as well developed as that seen in HCQP1 and HCQP1A. Potassium feldspar occurs with compositions $Or_{88}$ - $Or_{94}$. Perthite is common, and minor microcline also occurs. Exsolution lamellae (rods, beads and strings) are abundant within alkali feldspar hosts and are albitic ($An_{2-5}$). Minor myrmekite is also developed (Plate 3.3b). Alteration of cores and rims of feldspars, particularly plagioclase feldspar (kaolinization, hematization and saussurization) is well developed.

Plagioclase feldspar compositions within HCQP4 are generally more sodic than in the other rock units. Core compositions range from $An_{7-13}$, and rim analyses range from $An_{2-10}$. Rapakivi texture is well developed in this unit (Plate 3.3c), and contacts between the sodium plagioclase rim ($An_{2-5}$) and the perthitic core are diffuse and poorly developed.

In units HCQP2, HCQP3 and HCQP4, minor amounts of plagioclase and potassium grains have a red coloration in hand specimen and clouded, pinkish appearance in thin section. Such coloration has been termed "turbid feldspars" (e.g. Poldervaart and Gilkey, 1954; Boone, 1969), and is attributed to inclusions of hematite flakes, from iron either preceipitated by hydrothermal fluids or released during chloritization of biotite (Boone, 1969; J. V. Smith, 1974; Hofmeister and Rossman, 1983).

3.4.3 Discussion

Compositions of plagioclase feldspar within the phases HCQP1 and HCQP1A contain the highest anorthite component (generally $An_{20}$-$An_{38}$). These compositions are in agreement with these units representing the least evolved of the pluton, as proposed for other plutons (Clemens et al., 1986). Additionally, the most calcic compositions ($An_{35}$-$An_{38}$) occur in the feldspars from the margins of the pluton, where granodiorite rock compositions are common. Rim values of plagioclase range from $An_5$ to $An_{22}$. Zoning, well developed within plagioclase from these units, is best developed in these two rock units, relative to the rest of the pluton.

Phases HCQP2 and 3 contain plagioclase with intermediate An values. Albitic values for most of the plagioclase feldspars ($An_{2-10}$) within HCQP4 could suggest the effects of post-magmatic processes (e.g. alteration, metasomatism) (Kontak and Corey, 1988; Parsons and Brown, 1984). Compositions of the potassium feldspar are restricted ($Or_{87}$-$Or_{94}$) in all rock units.

In conclusion, feldspars within the HCQP are products of both magmatic and alteration processes. Albitic plagioclase in all units, particularly HCQP4, could represent metasomatism or alteration effects (e.g. Kontak and Corey, 1988). Rapakivi texture (albitic rims on potassium feldspar cores) well developed in HCQP4 could additionally suggest the presence of a fluid phase, as classic (i.e. magmatic) rapakivi texture is characterized by oligoclase, and not albite, rims on potassium feldspar (Backlund, 1938; Vorma, 1971). Another alternative for the development of the texture would be rapid de-gassing of the magma, as suggested by Abbott (1978). Miarolitic

cavities occur within some of the late-stage dykes within the HCQP4, suggesting rapid de-gassing, but they are not common.

## 3.5 Garnet

### 3.5.1 Introduction

Garnet is a common accessory mineral within the groundmass of granitic rocks and is most abundant in the later stage and more felsic muscovite-bearing granites, aplites, and pegmatites (Miller and Stoddard, 1981; Abbott, 1985). Garnet in peraluminous granites can have a variety of origins, including xenocrystic, phenocrystic/ magmatic and metasomatic (e.g. Allan and Clarke, 1981; Miller and Stoddard, 1981; Vennum and Meyer, 1979; Pattison et al., 1982; Kontak and Corey, 1988). Textural and chemical evidence are deemed critical for the determination of the origin of garnet in granitic rocks. Compositions of garnet in felsic plutonic rocks are highly variable (Clarke, 1981), with most variation occurring in Mn:Fe:Mg ratios. Dominantly almandine-spessartine garnets are reported in granitic rocks (Miller and Stoddard, 1981; Vennum and Meyer, 1979), with relatively manganese-rich almandine-spessartine garnets common in granitic aplite and pegmatite (Manning, 1983). This increase in manganese could relate to the $Mn/(Mn + Fe^{2+} + Mg)$ ratio, which may increase rapidly in the aplite-pegmatite systems (Clarke, 1981). According to AFM liquidus relationships determined by Abbott (1985), garnet-muscovite and garnet-biotite-muscovite granite should not exist. However, as these mineral assemblages are common, the appearance of garnet suggests that muscovite and biotite are saturated with respect to $Mn^{2+}$.

Zoning is common within garnets and is controlled by strong diffusion of ions to the garnet nucleus (Leake, 1967). This diffusion causes rapid depletion of scarce ions (i.e. Mn) in the surrounding matrix, as the garnet acts as a sink for the Mn. Garnet from late-stage granitic rocks records different types of zoning, these being: 1) normal zoning (e.g. Leake, 1967; Bizouad et al., 1970), in which cores low in Fe and Mg and high in Mn and Ca grade into rims high in Fe and Mg and low in Mn and Ca; 2) reverse zoning (e.g. Vennum and Meyer, 1979; Kistler et al., 1981), in which garnet has opposite trends to normally zoned garnet; and 3) unzoned (Hall, 1965; Miller and Stoddard, 1981). Normal zoning is believed to form during growth in a metamorphic environment during prograde conditions, although normal zoning also occurs in garnets considered to be of magmatic origin (MacDonald, 1981; Anderson and Rowley, 1981). Reverse zoning may indicate metamorphic growth during retrograde conditions (Woodsworth, 1977) or, in the case of igneous garnets, growth during magmatic conditions (e.g. falling temperature and fractional crystallization) (Allan and Clarke, 1981).

Predominantly almandine-pyrope-spessartine garnet compositions have been reported within the SMB (Allan and Clarke, 1981). Similar compositions have been documented for garnet within the MB (MacDonald, 1981). Allan and Clarke (1981) described the origin and texture of three types of garnet within the SMB (i.e. xenocrystic, magmatic, and magmatic and xenolithic), and Kontak and Corey (1988) have described a fourth type, with its origin as metasomatic.

3.5.2 Garnet within the study area

Garnet in the HCQP occurs in several locations. Garnet is common in the groundmass of HCQP2 at the Lundy fire tower, where there are abundant enclaves and xenoliths. However, garnet is also present within the groundmass where xenoliths are absent. Garnet in HCQP2 is shown in Plate 3.4a and b, and is <5 mm, commonly subhedral to euhedral and rarely contains inclusions. The spessartine content of these garnets (Plate 3.4c) is similar to garnets found within the metasedimentary rocks, but is also within the range of those considered to be magmatic (Miller and Stoddard, 1981). Garnet within the HCQP is high in MnO (spessartine component), with values averaging 16.78-18.77 weight %. Garnet HCL014 (Fig. 3.4c) is normally zoned, suggesting growth during metamorphic conditions. MacDonald (1981) described magmatic garnets which were normally zoned within the MB. The characteristics of the garnets within the HCQP correspond generally to those of Group II of Allan and Clarke (1981), and the origin for this group is suggested to be both magmatic and xenocrystic. Where these garnets are clearly associated with biotite and xenolith-rich areas within the HCQP, they are concluded to be xenocrystic, but where found within the groundmass in xenolith-poor areas with no textural association with biotite, their origin could be magmatic.

The second mode of occurrence (HCL037 on Plate 3.4c) occurs within aplitic dyke rocks that are invariably free of xenoliths. This feature suggests that an inherited origin is unlikely. The grain shape is generally euhedral, and this feature suggests that the mineral was in equilibrium during growth. The lack of a reaction relationship with

PLATE 3.4. Photomicrographs of garnet from the HCQP, in plane light and crossed nicols for a and b, respectively. Note the euhedral shape and lack of alteration. 3.4c represents garnet compositions from selected granite and country rocks, with a field superimposed from Allan and Clarke (1981) for magmatic garnet.

a

b

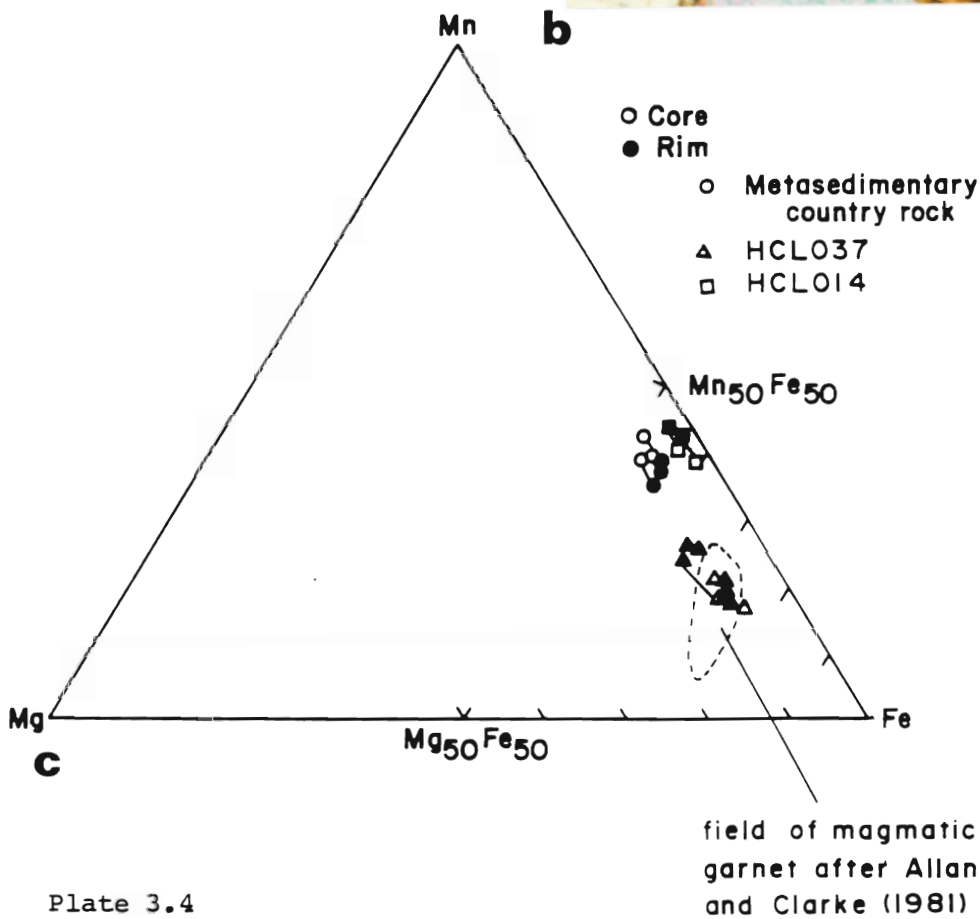
Mn
Core
Rim
Metasedimentary country rock
HCL037
HCL014
Mn50 Fe50
Mg
Mg50 Fe50
Fe
c
field of magmatic garnet after Allan and Clarke (1981)

Plate 3.4

biotite indicates that an equilibrium reaction of liquid producing garnet and biotite occurred. These observations correspond with Group III of Allan and Clarke (1981) and a magmatic origin is suggested. With reference to fields outlined by Clarke (1981) and Miller and Stoddard (1981) for plutonic garnets (Fig. 3.4c), garnets of these dyke rocks (HCL037) conform to those considered indicative of magmatic conditions. The mineral is also reversely zoned, suggesting growth in a magmatic environment.

## 3.6 Summary

Biotite (annite-siderophyllite in composition) from all rock units within the HCQP displays considerable compositional overlap. Biotite compositions are low in Mn, and compositions from HCQP4 are the most annite-rich. Using a diagram of $Al^{vi}$ vs $Fe_t/(Fe_t$ vs Mg), biotite compositions are similar to those occurring in rocks containing biotite and muscovite as the AFM minerals. Biotite from the HCQP falls within the field outlined by le Bel (1979) and Corey (1988) for magmatic, and not hydrothermal, biotite.

Muscovite within the HCQP occurs texturally in both primary and secondary modes of occurrence. Primary muscovite is marginally closer to 'ideal' composition than secondary, and primary muscovite displays a weak trend of higher Al and lower Si. Considerable chemical overlap is apparent between texturally primary and secondary modes of occurrence, although primary muscovite contains higher Ti contents on average than secondary micas. This higher Ti concentration has been determined, in several other studies, to be the main discriminator between primary and secondary crystallization.

Muscovite within the HCQP is low in Na, compared with a field for peraluminous granites from Clarke (1981). The muscovites of the study area trend towards the Mg apex of a Ti-Mg-Na triangle, a finding consistent with that of the SMB, in rocks that have undergone little post-magmatic alteration (Chatterjee and Strong, 1985; Ham, 1987).

Feldspars are considered to be products of both magmatic and alteration processes. Albitic plagioclase, the development of turbid feldspars and rapakivi textures within HCQP4 suggest alteration or metasomatic effects for some of the feldspars.

Garnet within the HCQP is considered to be of both magmatic and xenocrystic origin. Garnet occurs in several modes of occurrence, one being within aplitic dykes, where textural and chemical features suggest that the mineral is magmatic. Garnets also occur in areas within HCQP2, both in areas with abundant xenoliths and in xenolith-poor areas. Both a xenocrystic and magmatic origin are suggested for the garnets within this unit.

# CHAPTER 4 - WHOLE ROCK CHEMISTRY

## 4.1 Introduction

Thirty-five samples collected throughout the HCQP (Map 2) were analyzed for major elements and twenty-two trace elements (Ba, Rb, Sr, Y, Zr, Nb, Pb, Ga, Zn, Ni, V, Cr, Mo, Ag, Be, B, F, Li, Sn, Au, Th, and U). Six samples were analyzed additionally for rare earth elements (REE's) (Ce, Sm, Eu, Tb, Yb, and Lu).

Sample collection was constrained by the need for a geographically representative distribution, adequate coverage of different rock units and relatively unaltered samples. Samples collected were from HCQP1 (9 samples), HCQP1A (2), HCQP2 (8), HCQP3 (2), and HCQP4 (14). One sample (L037) from HCQP2 is an aplite, and another (L015A) from HCQP4 is from a small pod of leucogranite. For details of analytical procedures, see Appendix II.

## 4.2 Nova Scotia Database

Richard (1988) compiled a database (termed the Nova Scotia database) for all granitic rocks within the Meguma Terrane, using major element, trace element and REE geochemical data. Theses, published papers and personal communication provided sources of data. For a complete reference list, see Richard (1988).

Richard (1988) divided the granitic rocks into 'northern' and 'southern' plutons on the basis of geography and similar rock types. The northern plutons include the SMB, MB and plutons of the eastern Meguma Terrane, while the southern plutons include smaller bodies in

southwestern Nova Scotia (Table 4.1). The southern plutons, as a group, contain larger volumes of more mafic granitoid rocks (e.g. tonalite, granodiorite) than do the northern plutons.

Using multivariate statistical analysis, Richard (1988) separated the northern and southern plutons using certain major and trace elements: $SiO_2$, $TiO_2$, $Al_2O_3$, $Fe_2O_{3t}$, MgO, CaO, $Na_2O$, $K_2O$, $P_2O_5$, Ba, Rb and Sr (the coefficients calculated for each element are shown in Table 4.1). Using this model, 93.5% of the samples were correctly classified.

A series of histograms developed using the discriminant equation (Fig. 4.1) graphically displays the Nova Scotia database. The northern plutons generally have positive discriminant values, while the southern plutons are negative. All samples of the HCQP correctly classify as a northern pluton (similar to the SMB and the MB). The range of values of the HCQP (0.00 to 0.16) is restricted, and these values fall within the range of those of the SMB (-0.04 to 4.00). Additionally, the histograms suggest that the MB is intermediate geochemically between the SMB and the eastern Meguma Terrane granites.

This thesis uses the following selected data from the Nova Scotia database for comparison with the HCQP: SMB, Halifax Pluton (HP) of the SMB, MB, Bullridge Pluton (BR), Sherbrooke Pluton (SH), Larrys River Pluton (LRP) and Sangster Lake Pluton (SLP) (Fig. 1.1). Sources of data for individual plutons are: SMB (McKenzie (1974) and Charest (1976)), Halifax Pluton (Smith, (1981)), MB (MacDonald, (1981)), Bullridge Pluton (Chevalier, 1983), Sherbrooke Pluton (Alizay, 1981), Larrys River and Sangster Lake Plutons (O'Reilly, pers. comm). These plutons were chosen because of the relative sizes of the intrusions,

TABLE 4.1 Discriminating northern and southern plutons on the basis of whole-rock chemistry (after Richard, 1988).

| GRANITE | SAMPLES CORRECTLY CLASSIFIED | | SAMPLES MISCLASSIFED | |
|---|---|---|---|---|
| | # | % | # | % |
| NORTHERN PLUTONS | | | | |
| SMB Charest | 17 | 100 | 0 | 0 |
| McKenzie | 16 | 88.9 | 2 | 11.1 |
| Smith | 32 | 100 | 0 | 0 |
| Richardson | 8 | 100 | 0 | 0 |
| MB | 9 | 90 | 1 | 10 |
| HCQP | 36 | 100 | 0 | 0 |
| Liscomb | 9 | 90 | 1 | 10 |
| Sherbrooke | 17 | 94.4 | 1 | 5.6 |
| Bull Ridge | 9 | 75 | 3 | 25 |
| Sangster Lake and Larrys River | 29 | 96.7 | 1 | 3.3 |
| Ellison Lake | 13 | 86.7 | 2 | 13.3 |
| SOUTHERN PLUTONS | | | | |
| Barrington Passage | 30 | 100 | 0 | 0 |
| Shelburne | 22 | 81.5 | 5 | 18.5 |
| Bald Mountain | 4 | 100 | 0 | 0 |
| Port Mouton | 51 | 98.1 | 1 | 1.9 |
| Moose Point | 6 | 75 | 2 | 25 |
| Lyons Bay, Seal Island Western Granite | 6 | 60 | 4 | 40 |

DISCRIMINANT FUNCTION USING THE FOLLOWING ELEMENTS:

$SiO_2$-$TiO_2$-$Al_2O_3$-$Fe_2O_{3t}$-MgO-CaO-$Na_2O$-$K_2O$-$P_2O_5$-Ba-Rb-Sr

(data handled by log ratio transformation for major elements, and log transformation for trace elements)

Co-efficients:

| | | | |
|---|---|---|---|
| $TiO_2$ | +0.5025 | $K_2O$ | +0.3966 |
| $Fe_2O_{3t}$ | +0.3148 | $P_2O_5$ | -0.3012 |
| MgO | +0.1196 | Ba | -0.6998 |
| CaO | -0.6205 | Rb | +0.9477 |
| $Na_2O$ | +0.0335 | Sr | +0.5033 |

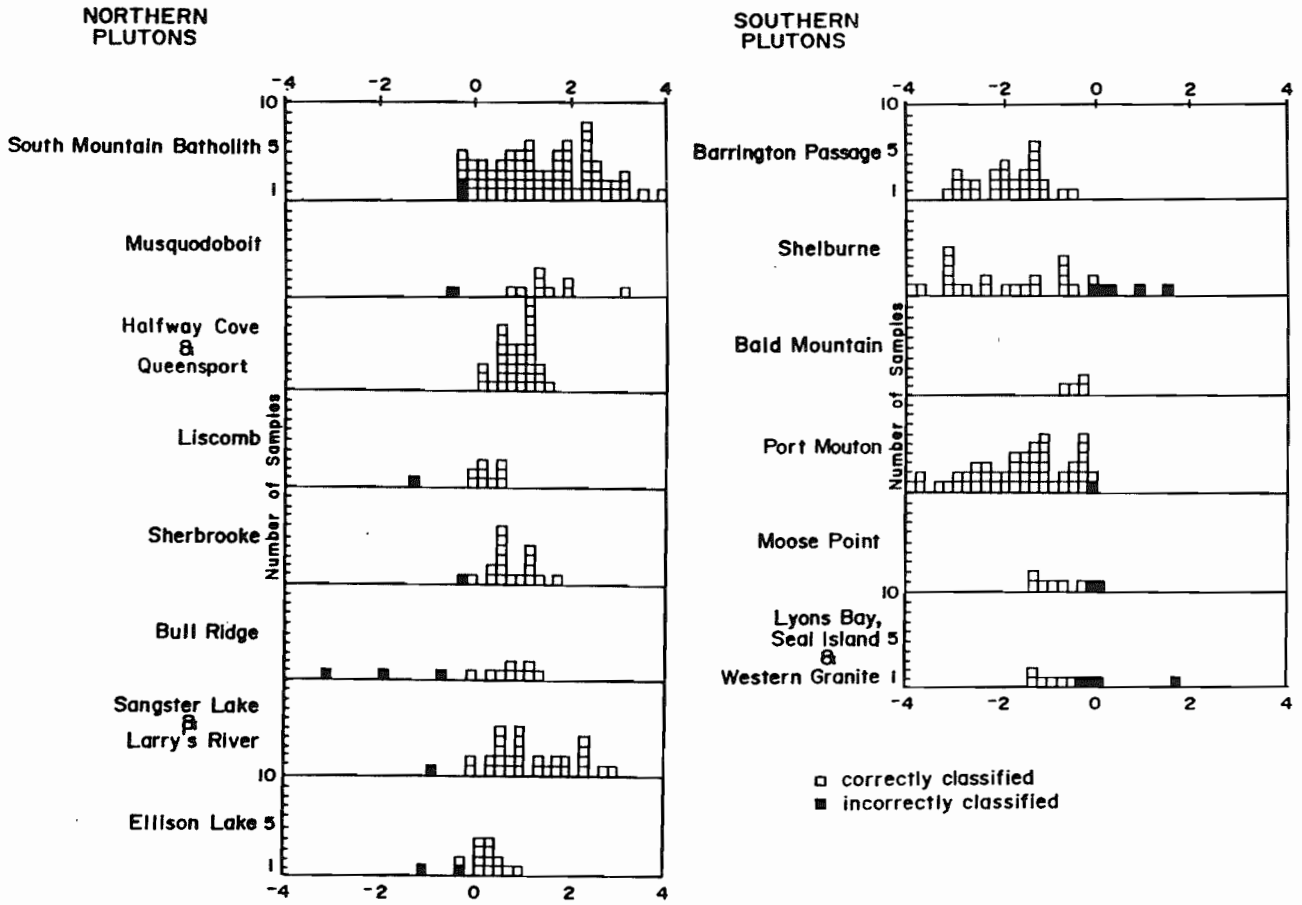


FIGURE 4.1. Granitoid plutons of southern Nova Scotia, divided into 'northern' and 'southern' plutons on the basis of geography and similar rock types. Histograms were developed using the discriminant equation listed in Table 4.1. The range of the HCQP is restricted (0.00 to 0.16) and classifies the pluton as a 'northern' pluton, similar to the SMB and MB.

close geographic location to the HCQP, and similar rock types. For the entire Nova Scotia database, refer to Richard (1988).

## 4.3 Spearman Rank Correlation

The Spearman Rank correlation procedure provides a non-parametric method of measuring the relationship between two variables (Mendenhall and Ott, 1972). This method was used to examine the HCQP major and trace element chemical data for correlations. The results are presented in Table 4.2. There are strong correlations in the data set among the major elements, particularly $TiO_2$ and $FeO_t$ with other elements (positive correlations with $FeO_t$, MnO, MgO and CaO, and negative correlations with $K_2O$ and $P_2O_5$). $P_2O_5$ displays both positive ($SiO_2$, $K_2O$) and negative ($TiO_2$, $FeO_t$, MgO, CaO) correlations. $K_2O$ has a negative correlation with most other major elements. The trace elements also have strong associations, particularly Sr, Y and Cr with elements such as $TiO_2$, $FeO_t$, MgO and CaO. Ba is positively correlated with MgO, CaO, Sr, Zr and Th/U. Zr also displays a positive correlation with Th/U. More discussion about elemental relationships is given in Sections 4.4 and 4.5.

## 4.4 Major Element Chemistry

Table 4.3 lists the major element composition, normative calculations (CIPW norms), degree of peraluminosity (A/CNK ratios) and Thornton-Tuttle Differentiation Indices (TTDI) (Thornton and Tuttle, 1960) for all samples. Selected major elements for each of the HCQP units are plotted against TTDI (Fig. 4.2a-i), with fields from other database plutons outlined in adjacent figures. The MB and the other

| | SiO2 | TiO2 | FeOt | MnO | MgO | CaO | K2O | P2O5 | Ba | Rb | Sr | Zr | Y | Cr | Th | U | Th/U |
|---|---|---|---|---|---|---|---|---|---|---|---|---|---|---|---|---|---|
| SiO2 | 1.000 | | | | | | | | | | | | | | | | |
| TiO2 | -0.602 | 1.000 | | | | | | | | | | | | | | | |
| FeOt | | 0.921 | 1.000 | | | | | | | | | | | | | | |
| MnO | -0.612 | 0.744 | 0.740 | 1.000 | | | | | | | | | | | | | |
| MgO | | 0.878 | 0.883 | 0.709 | 1.000 | | | | | | | | | | | | |
| CaO | -0.639 | 0.754 | 0.763 | | 0.892 | 1.000 | | | | | | | | | | | |
| K2O | -0.661 | -0.742 | -0.738 | -0.784 | -0.795 | -0.757 | 1.000 | | | | | | | | | | |
| P2O5 | -0.701 | -0.657 | -0.637 | | -0.785 | -0.868 | 0.755 | 1.000 | | | | | | | | | |
| Ba | | | | | 0.692 | 0.637 | | | 1.000 | | | | | | | | |
| Rb | | | | | | | | | | 1.000 | | | | | | | |
| Sr | | 0.796 | 0.798 | | 0.821 | 0.862 | | -0.770 | 0.605 | 0.682 | 1.000 | | | | | | |
| Zr | | | | | 0.630 | | | | 0.823 | | | 1.000 | | | | | |
| Y | -0.613 | 0.709 | 0.712 | 0.887 | 0.646 | | -0.757 | | | 0.625 | | | 1.000 | | | | |
| Cr | | 0.825 | 0.869 | 0.680 | 0.695 | 0.604 | -0.628 | | | | 0.629 | | 0.627 | 1.000 | | | |
| Th | | | | | | | | | | | | | | 0.728 | 1.000 | | |
| U | | | | | | | | | | | | | | | | 1.000 | |
| Th/U | | | | | | | | | 0.689 | | | 0.712 | | | 0.851 | -0.844 | 1.000 |
| F | | | | | | | | | | | | 0.645 | | | 0.703 | | 0.701 |

TABLE 4.2 Results of the Spearman Rank correlation procedure. Data used were major elements (Table 4.3) and trace elements (Table 4.4). Values listed are for correlations greater than 0.600 or less than -0.600. The closer the values are to 1 (either negative or positive), the better the correlation.

TABLE 4.3 Major element abundances of rocks of the HCQP

| SAMPLE | QP03 | QP06 | QP07 | QP08 | QP10 | QP11 | QP12 | QP22 | QPL038 | HC01 | HC02 | HC03 | HC04 | HC02 |
|---|---|---|---|---|---|---|---|---|---|---|---|---|---|---|
| PHASE | HCQP1 | HCQP1 | HCQP1 | HCQP1 | HCQP1 | HCQP1 | HCQP1 | HCQP1 | HCQP1 | HCQP1A | HCQP1A | HCQP3 | HCQP3 | HCQP3 |
| SIO2 | 70.10 | 72.25 | 69.64 | 69.63 | 71.90 | 69.00 | 69.84 | 70.51 | 69.72 | 69.07 | 69.28 | 72.65 | 72.16 | 72.17 |
| TIO2 | 0.20 | 0.26 | 0.33 | 0.39 | 0.22 | 0.41 | 0.35 | 0.38 | 0.27 | 0.39 | 0.43 | 0.25 | 0.28 | 0.30 |
| AL2O3 | 14.85 | 15.12 | 15.88 | 15.21 | 14.74 | 15.09 | 15.29 | 15.12 | 14.67 | 15.57 | 15.46 | 14.72 | 15.42 | 14.75 |
| FE2O3 | 0.03 | 0.36 | 0.00 | 0.00 | 0.15 | 0.64 | 0.16 | 0.40 | 0.00 | 0.07 | 0.55 | 0.02 | 0.30 | 0.21 |
| FEO | 1.12 | 1.27 | 1.95 | 2.36 | 1.05 | 1.69 | 1.95 | 2.15 | 1.69 | 2.02 | 1.84 | 1.38 | 1.27 | 1.64 |
| FE2O3T | 1.27 | 1.77 | 2.16 | 2.62 | 1.32 | 2.52 | 2.32 | 2.79 | 1.88 | 2.31 | 2.59 | 1.55 | 1.71 | 2.03 |
| MNO | 0.04 | 0.07 | 0.09 | 0.10 | 0.05 | 0.10 | 0.09 | 0.12 | 0.07 | 0.10 | 0.11 | 0.03 | 0.06 | 0.08 |
| MGO | 0.39 | 0.57 | 0.74 | 0.90 | 0.42 | 0.86 | 0.81 | 0.98 | 0.56 | 0.58 | 0.88 | 0.41 | 0.45 | 0.50 |
| CAO | 0.58 | 1.03 | 1.79 | 1.75 | 0.52 | 1.72 | 1.67 | 1.53 | 1.46 | 1.45 | 1.74 | 0.55 | 0.48 | 0.50 |
| NA2O | 3.54 | 3.51 | 3.65 | 3.48 | 3.56 | 3.40 | 3.44 | 3.28 | 3.47 | 3.43 | 3.52 | 3.33 | 3.39 | 3.18 |
| K2O | 5.06 | 4.44 | 4.20 | 3.86 | 5.03 | 4.03 | 4.23 | 3.96 | 4.04 | 4.14 | 3.67 | 5.20 | 4.94 | 4.63 |
| P2O5 | 0.22 | 0.18 | 0.12 | 0.13 | 0.23 | 0.14 | 0.13 | 0.15 | 0.07 | 0.16 | 0.14 | 0.32 | 0.30 | 0.37 |
| H2O+ | 0.82 | 0.85 | 0.80 | 0.83 | 1.14 | 0.74 | 0.46 | 1.03 | 1.00 | 1.00 | 1.10 | 0.85 | 0.89 | 1.08 |
| H2O- | 0.19 | 0.21 | 0.25 | 0.20 | 0.12 | 0.26 | 0.32 | 0.17 | 0.14 | 0.27 | 0.23 | 0.36 | 0.42 | 0.48 |
| SUM | 97.14 | 100.12 | 99.44 | 98.84 | 99.13 | 98.08 | 98.74 | 99.78 | 97.16 | 98.25 | 98.95 | 100.07 | 100.36 | 99.89 |
| A/CNK | 1.20 | 1.21 | 1.15 | 1.16 | 1.20 | 1.15 | 1.15 | 1.21 | 1.15 | 1.22 | 1.20 | 1.22 | 1.31 | 1.32 |
| TTDI | 88.90 | 88.38 | 82.84 | 81.22 | 91.16 | 81.69 | 82.59 | 82.64 | 83.25 | 82.85 | 79.55 | 91.51 | 90.95 | 89.70 |
| CIPW NORM | | | | | | | | | | | | | | |
| CQZ | 28.42 | 31.84 | 26.55 | 28.42 | 30.54 | 28.57 | 28.06 | 30.87 | 29.38 | 28.67 | 27.36 | 31.89 | 32.31 | 34.58 |
| COR | 30.21 | 26.52 | 25.08 | 23.05 | 30.11 | 24.06 | 25.19 | 23.68 | 24.16 | 24.78 | 21.99 | 31.10 | 29.58 | 27.79 |
| CAB | 30.27 | 30.02 | 31.21 | 29.75 | 30.51 | 29.06 | 29.34 | 28.09 | 29.71 | 29.40 | 30.20 | 28.52 | 29.06 | 27.33 |
| CAN | 1.46 | 3.98 | 8.18 | 7.91 | 1.09 | 7.70 | 7.49 | 6.69 | 6.87 | 6.23 | 7.82 | 0.65 | 0.43 | 0.07 |
| CHY | 2.77 | 3.19 | 5.10 | 6.18 | 2.61 | 4.27 | 5.09 | 5.72 | 4.23 | 4.70 | 4.67 | 3.22 | 2.89 | 3.79 |
| CMT | 0.04 | 0.53 | 0.00 | 0.00 | 0.22 | 0.94 | 0.23 | 0.59 | 0.00 | 0.10 | 0.81 | 0.03 | 0.44 | 0.31 |
| CIL | 0.38 | 0.50 | 0.63 | 0.75 | 0.42 | 0.79 | 0.67 | 0.73 | 0.52 | 0.75 | 0.83 | 0.48 | 0.54 | 0.58 |
| CAP | 0.51 | 0.42 | 0.28 | 0.30 | 0.54 | 0.33 | 0.30 | 0.35 | 0.16 | 0.38 | 0.33 | 0.75 | 0.70 | 0.87 |
| CCO | 3.05 | 3.13 | 2.38 | 2.46 | 3.08 | 2.36 | 2.34 | 3.05 | 2.12 | 3.23 | 2.90 | 3.42 | 4.39 | 4.55 |

| SAMPLE | HC02 | HC05 | HC06 | HC07 | HCL018 | HCL034 | QP04 | QP05 | QP09 | QP13 | QP14 | QP15 | QP16 | QP17 |
|---|---|---|---|---|---|---|---|---|---|---|---|---|---|---|
| PHASE | HCQP3 | HCQP3 | HCQP3 | HCQP3 | HCQP3 | HCQP3 | HCQP4 | HCQP4 | HCQP4 | HCQP4 | HCQP4 | HCQP4 | HCQP4 | HCQP4 |
| SIO2 | 71.40 | 71.56 | 72.55 | 71.20 | 72.37 | 71.88 | 70.55 | 71.11 | 72.65 | 70.90 | 70.93 | 71.29 | 70.91 | 73.67 |
| TIO2 | 0.21 | 0.25 | 0.23 | 0.18 | 0.17 | 0.16 | 0.26 | 0.26 | 0.24 | 0.27 | 0.31 | 0.24 | 0.28 | 0.24 |
| AL2O3 | 14.46 | 15.30 | 14.78 | 14.99 | 14.86 | 14.66 | 14.76 | 14.84 | 14.99 | 14.61 | 15.36 | 14.74 | 14.52 | 14.90 |
| FE2O3 | 0.12 | 0.12 | 0.00 | 0.00 | 0.09 | 0.00 | 0.00 | 0.14 | 0.03 | 0.05 | 0.28 | 0.01 | 0.03 | 0.18 |
| FEO | 1.12 | 1.24 | 1.54 | 1.18 | 1.03 | 1.12 | 1.55 | 1.28 | 1.36 | 1.44 | 1.52 | 1.38 | 1.46 | 1.25 |
| FE2O3T | 1.36 | 1.50 | 1.71 | 1.31 | 1.23 | 1.24 | 1.72 | 1.56 | 1.54 | 1.65 | 1.97 | 1.54 | 1.65 | 1.57 |
| MNO | 0.04 | 0.06 | 0.04 | 0.06 | 0.04 | 0.03 | 0.04 | 0.04 | 0.05 | 0.06 | 0.06 | 0.05 | 0.06 | 0.04 |
| MGO | 0.36 | 0.40 | 0.47 | 0.34 | 0.31 | 0.31 | 0.52 | 0.49 | 0.52 | 0.59 | 0.69 | 0.50 | 0.57 | 0.49 |
| CAO | 0.54 | 0.52 | 0.54 | 0.48 | 0.52 | 0.50 | 0.61 | 0.61 | 0.55 | 0.81 | 0.86 | 0.57 | 0.61 | 0.62 |
| NA2O | 3.41 | 3.50 | 3.23 | 3.61 | 2.73 | 3.58 | 3.62 | 3.60 | 3.65 | 3.61 | 3.55 | 3.58 | 3.55 | 3.64 |
| K2O | 4.77 | 4.92 | 5.24 | 4.75 | 5.02 | 4.73 | 4.85 | 4.77 | 4.83 | 4.66 | 4.80 | 4.62 | 4.43 | 4.68 |
| P2O5 | 0.31 | 0.35 | 0.33 | 0.34 | 0.31 | 0.34 | 0.23 | 0.23 | 0.25 | 0.20 | 0.26 | 0.24 | 0.20 | 0.24 |
| H2O+ | 1.00 | 0.88 | 0.59 | 0.79 | 0.90 | 1.07 | 0.69 | 0.78 | 0.94 | 0.65 | 0.65 | 0.78 | 0.68 | 0.94 |
| H2O- | 0.49 | 0.32 | 0.42 | 0.33 | 0.44 | 0.35 | 0.37 | 0.22 | 0.14 | 0.29 | 0.31 | 0.35 | 0.26 | 0.25 |
| SUM | 98.23 | 99.42 | 99.96 | 98.25 | 98.79 | 98.73 | 98.05 | 98.37 | 100.20 | 98.14 | 99.58 | 98.35 | 97.56 | 101.14 |
| A/CNK | 1.23 | 1.27 | 1.23 | 1.25 | 1.37 | 1.23 | 1.20 | 1.22 | 1.22 | 1.17 | 1.22 | 1.24 | 1.24 | 1.22 |
| TTDI | 90.13 | 90.58 | 90.84 | 90.18 | 89.82 | 91.09 | 88.60 | 89.22 | 90.65 | 87.90 | 88.04 | 89.09 | 87.72 | 91.91 |
| CIPW NORM | | | | | | | | | | | | | | |
| CQZ | 32.21 | 31.17 | 31.95 | 30.89 | 36.33 | 32.00 | 28.67 | 29.97 | 30.58 | 29.26 | 29.07 | 30.83 | 30.96 | 32.76 |
| COR | 28.62 | 29.43 | 31.28 | 28.39 | 30.07 | 28.36 | 28.97 | 28.48 | 28.85 | 27.80 | 28.64 | 27.62 | 26.43 | 27.98 |
| CAB | 29.30 | 29.98 | 27.61 | 30.90 | 23.42 | 30.73 | 30.96 | 30.77 | 31.22 | 30.84 | 30.33 | 30.64 | 30.33 | 31.17 |
| CAN | 0.66 | 0.30 | 0.53 | 0.16 | 0.56 | 0.26 | 1.54 | 1.54 | 1.11 | 2.74 | 2.59 | 1.27 | 1.74 | 1.53 |
| CHY | 2.62 | 2.91 | 3.73 | 2.86 | 2.41 | 2.66 | 3.83 | 3.13 | 4.26 | 3.77 | 3.91 | 3.51 | 3.76 | 3.08 |
| CMT | 0.18 | 0.18 | 0.00 | 0.00 | 0.13 | 0.00 | 0.00 | 0.21 | 0.04 | 0.07 | 0.41 | 0.01 | 0.04 | 0.26 |
| CIL | 0.40 | 0.48 | 0.44 | 0.35 | 0.33 | 0.31 | 0.50 | 0.50 | 0.46 | 0.52 | 0.59 | 0.46 | 0.54 | 0.46 |
| CAP | 0.73 | 0.82 | 0.77 | 0.80 | 0.73 | 0.80 | 0.54 | 0.54 | 0.59 | 0.47 | 0.61 | 0.56 | 0.47 | 0.56 |
| CCO | 3.49 | 4.15 | 3.63 | 3.89 | 4.79 | 3.60 | 3.02 | 3.22 | 3.39 | 2.65 | 3.41 | 3.42 | 3.28 | 3.33 |

| SAMPLE | QP18 | QP19 | QP20 | QP21 | QPL014 | QPL032 | L037 | LO15A |
|---|---|---|---|---|---|---|---|---|
| PHASE | HCQP4 | HCQP4 | HCQP4 | HCQP4 | HCQP4 | HCQP4 | APLITE | LEUCO |
| SIO2 | 70.51 | 72.61 | 71.63 | 71.78 | 70.40 | 71.84 | 74.14 | 71.05 |
| TIO2 | 0.25 | 0.26 | 0.24 | 0.26 | 0.31 | 0.33 | 0.02 | 0.19 |
| AL2O3 | 15.00 | 14.73 | 15.05 | 14.90 | 14.90 | 15.01 | 15.32 | 15.21 |
| FE2O3 | 0.08 | 0.01 | 0.00 | 0.12 | 0.02 | 0.10 | 0.00 | 0.00 |
| FEO | 1.34 | 1.43 | 1.48 | 1.38 | 1.55 | 1.62 | 0.74 | 1.65 |
| FE2O3T | 1.57 | 1.60 | 1.64 | 1.65 | 1.74 | 1.90 | 0.82 | 1.83 |
| MNO | 0.05 | 0.04 | 0.05 | 0.05 | 0.05 | 0.05 | 0.16 | 0.10 |
| MGO | 0.49 | 0.52 | 0.51 | 0.54 | 0.55 | 0.69 | 0.07 | 0.48 |
| CAO | 0.74 | 0.80 | 0.61 | 0.77 | 0.77 | 0.85 | 0.39 | 0.93 |
| NA2O | 3.66 | 3.50 | 3.62 | 3.56 | 3.54 | 3.50 | 3.35 | 3.44 |
| K2O | 4.70 | 4.87 | 4.68 | 4.78 | 4.45 | 4.51 | 5.26 | 4.68 |
| P2O5 | 0.24 | 0.23 | 0.23 | 0.24 | 0.20 | 0.20 | 0.22 | 0.22 |
| H2O+ | 1.02 | 0.76 | 0.77 | 0.89 | 1.16 | 0.71 | 0.79 | 0.70 |
| H2O- | 0.28 | 0.25 | 0.11 | 0.21 | 0.20 | 0.37 | 0.35 | 0.18 |
| SUM | 98.36 | 100.01 | 98.98 | 99.48 | 98.10 | 99.78 | 100.81 | 98.83 |
| A/CNK | 1.20 | 1.18 | 1.24 | 1.20 | 1.24 | 1.23 | 1.29 | 1.22 |
| TTDI | 88.55 | 90.04 | 89.21 | 89.40 | 87.23 | 88.04 | 93.95 | 87.25 |
| CIPW NORM | | | | | | | | |
| CQZ | 29.03 | 31.05 | 30.41 | 30.38 | 30.19 | 31.16 | 33.84 | 29.98 |
| COR | 28.14 | 29.07 | 27.90 | 28.56 | 26.67 | 26.94 | 31.44 | 27.90 |
| CAB | 31.38 | 29.92 | 30.90 | 30.46 | 30.37 | 29.94 | 28.67 | 29.37 |
| CAN | 2.13 | 2.49 | 1.54 | 2.28 | 2.55 | 2.94 | 0.50 | 3.21 |
| CHY | 3.34 | 3.59 | 3.72 | 3.48 | 3.83 | 4.20 | 1.82 | 4.13 |
| CMT | 0.12 | 0.01 | 0.00 | 0.18 | 0.03 | 0.15 | 0.00 | 0.00 |
| CIL | 0.48 | 0.50 | 0.46 | 0.50 | 0.60 | 0.63 | 0.04 | 0.36 |
| CAP | 0.56 | 0.54 | 0.54 | 0.56 | 0.47 | 0.47 | 0.52 | 0.51 |
| CCO | 3.16 | 2.82 | 3.50 | 3.07 | 3.38 | 3.33 | 3.97 | 3.35 |

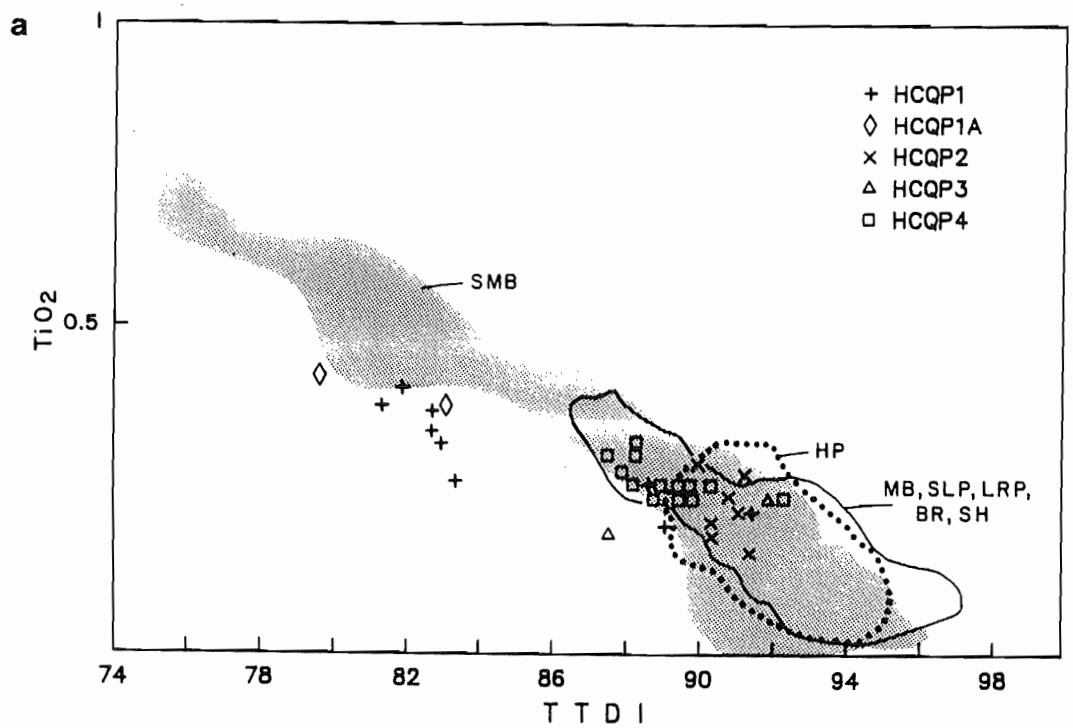


FIGURE 4.2. Major element chemistry versus Thornton-Tuttle Differentiation Index (TTDI). Fields of the South Mountain Batholith (SMB), Musquodoboit Batholith (MB), Sangster Lake pluton (SLP), Larrys River pluton (LRP), Bullridge pluton (BR), Sherbrooke pluton (SH) and Halifax pluton (HP) are superimposed on the diagrams; data are from the Nova Scotia database (Richard, 1988).

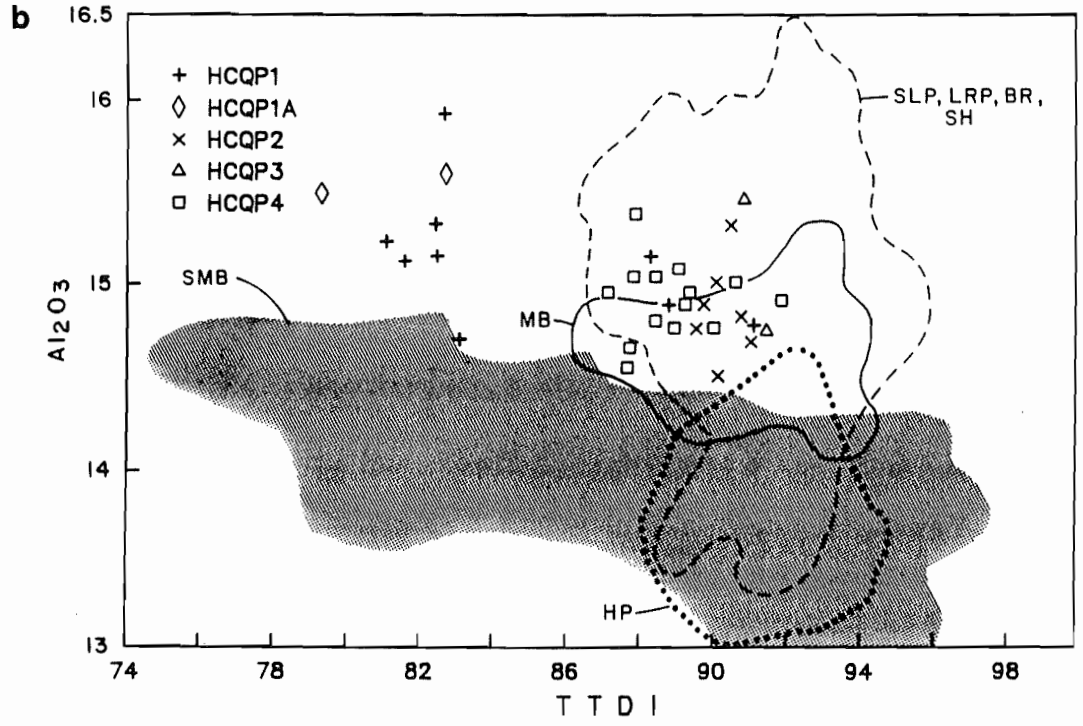

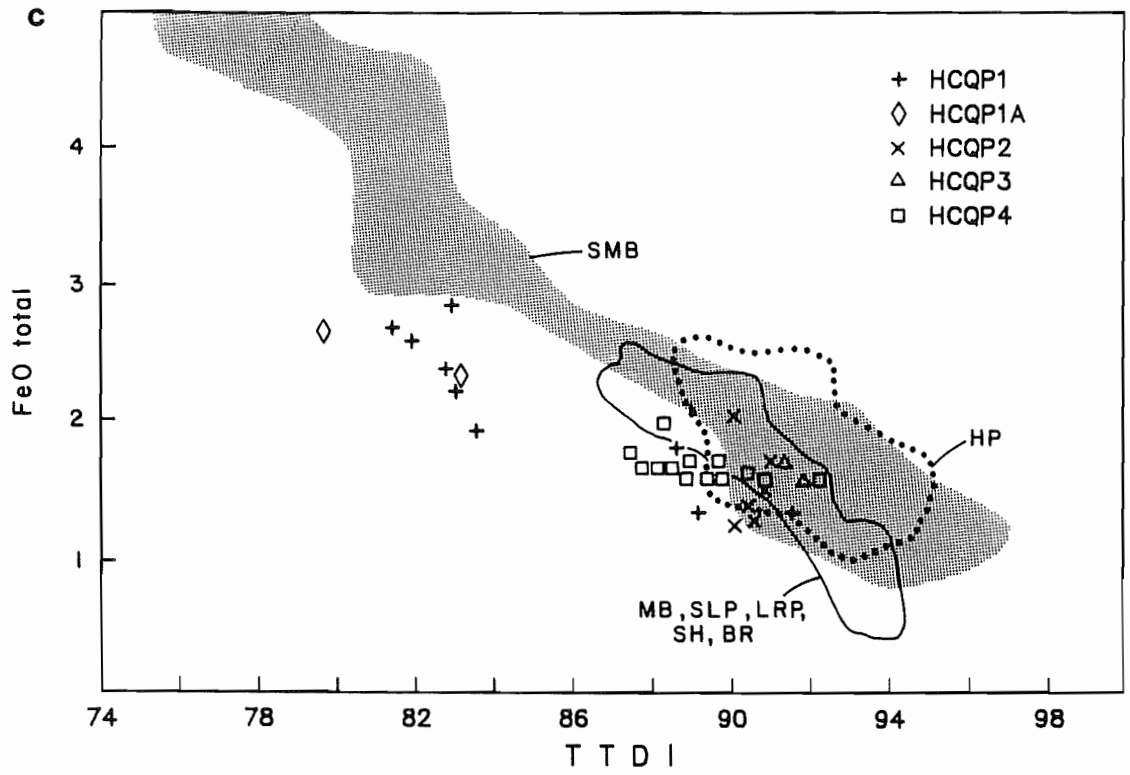
c
FeO total
4
3
2
1
74
78
82
86
90
94
98
TTDI
+ HCQP1
◊ HCQP1A
× HCQP2
△ HCQP3
□ HCQP4
SMB
HP
MB, SLP, LRP,
SH, BR

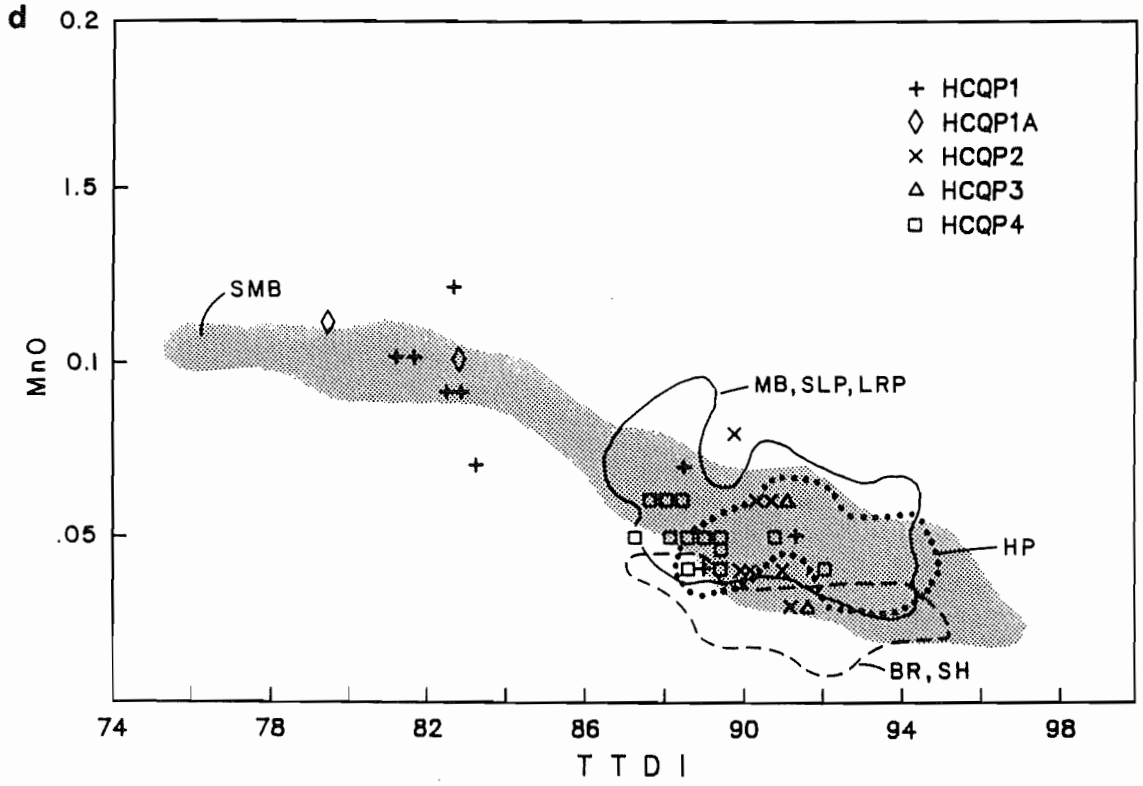
d
MnO
0.2
1.5
0.1
.05
74
78
82
86
90
94
98
TTDI
+ HCQP1
◊ HCQP1A
× HCQP2
△ HCQP3
□ HCQP4
SMB
MB, SLP, LRP
HP
BR, SH

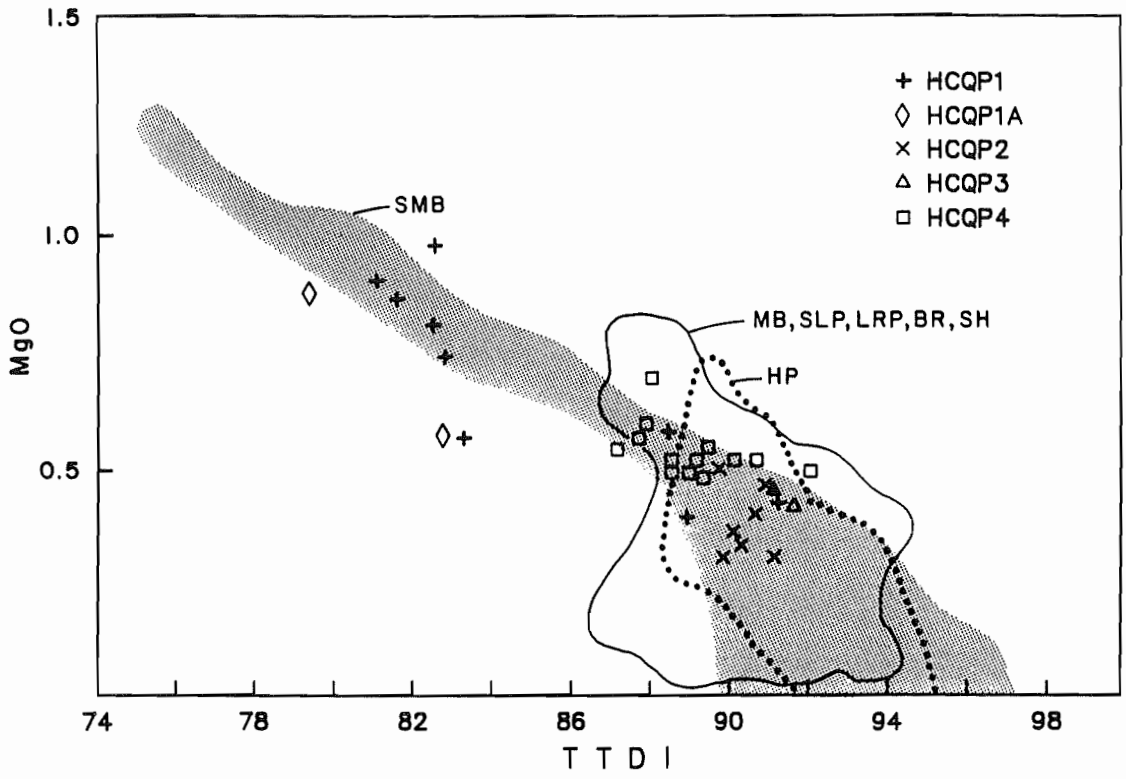
1.5
1.0
0.5
MgO
+ HCQP1
◊ HCQP1A
× HCQP2
△ HCQP3
□ HCQP4
SMB
MB, SLP, LRP, BR, SH
HP
74
78
82
86
90
94
98
T T D I

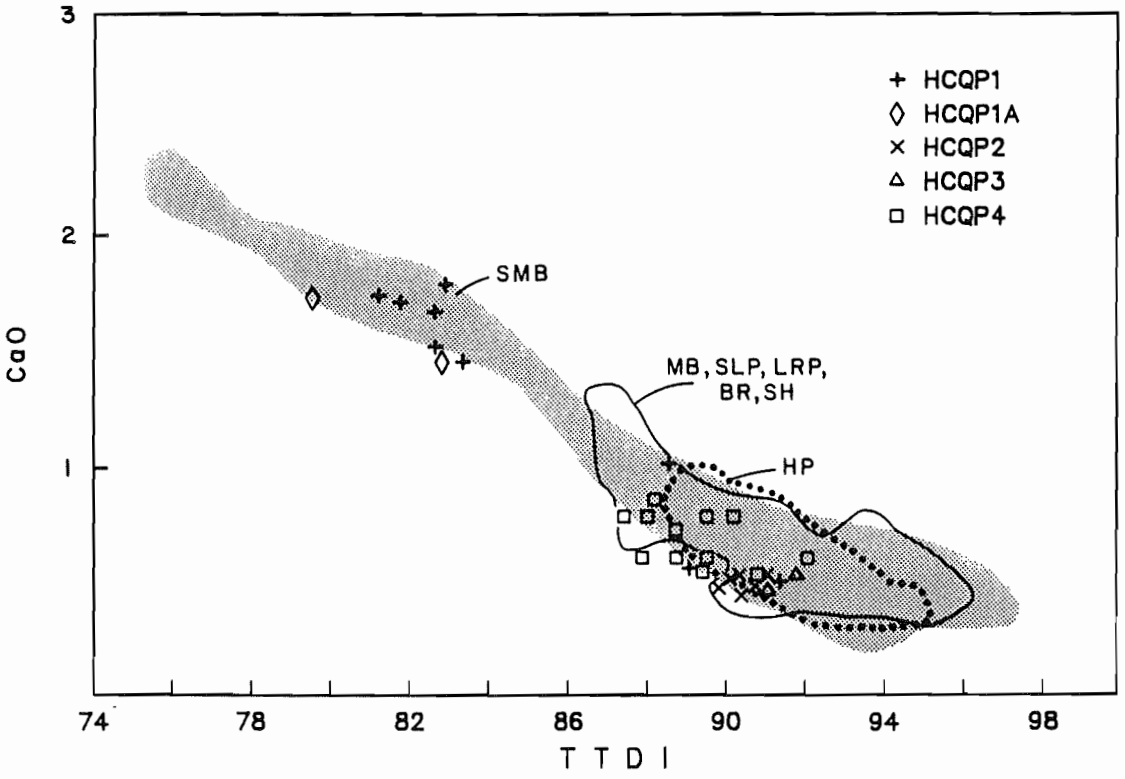
3
2
1
CaO
+ HCQP1
◊ HCQP1A
× HCQP2
△ HCQP3
□ HCQP4
SMB
MB, SLP, LRP,
BR, SH
HP
74
78
82
86
90
94
98
T T D I

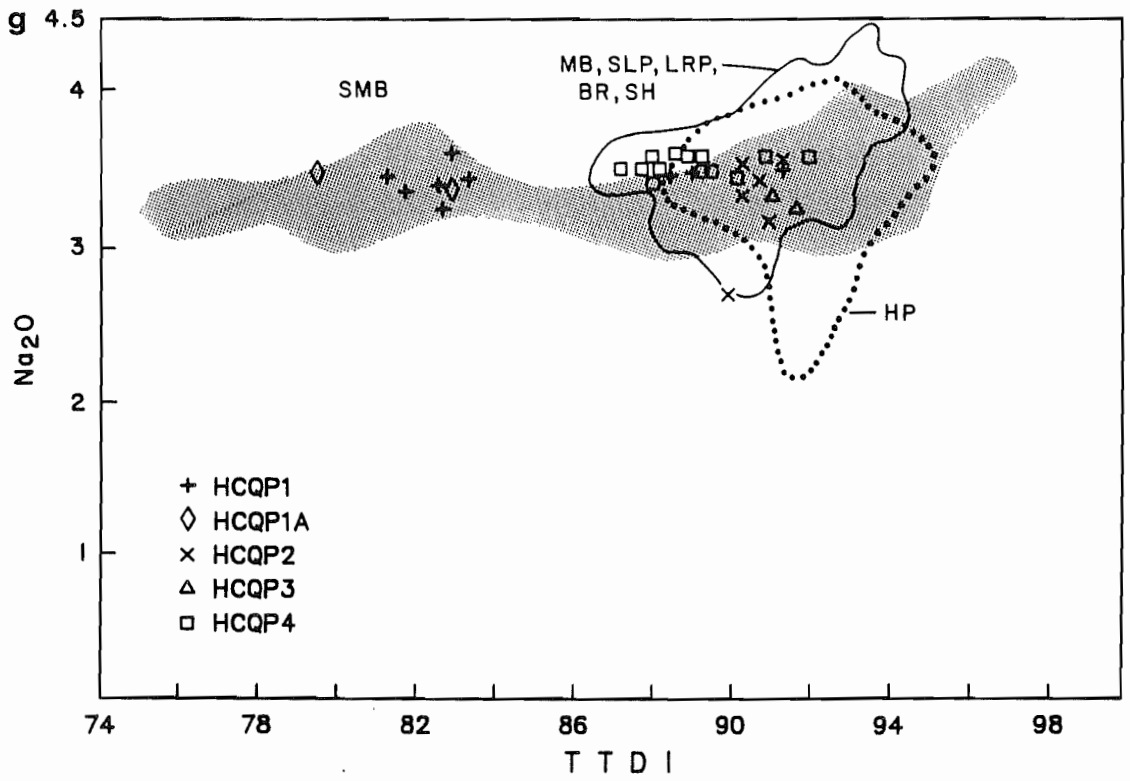
g
4.5
4
3
2
1
$Na_2O$
SMB
MB, SLP, LRP,
BR, SH
HP
+ HCQP1
◊ HCQP1A
× HCQP2
△ HCQP3
□ HCQP4
74
78
82
86
90
94
98
T T D I

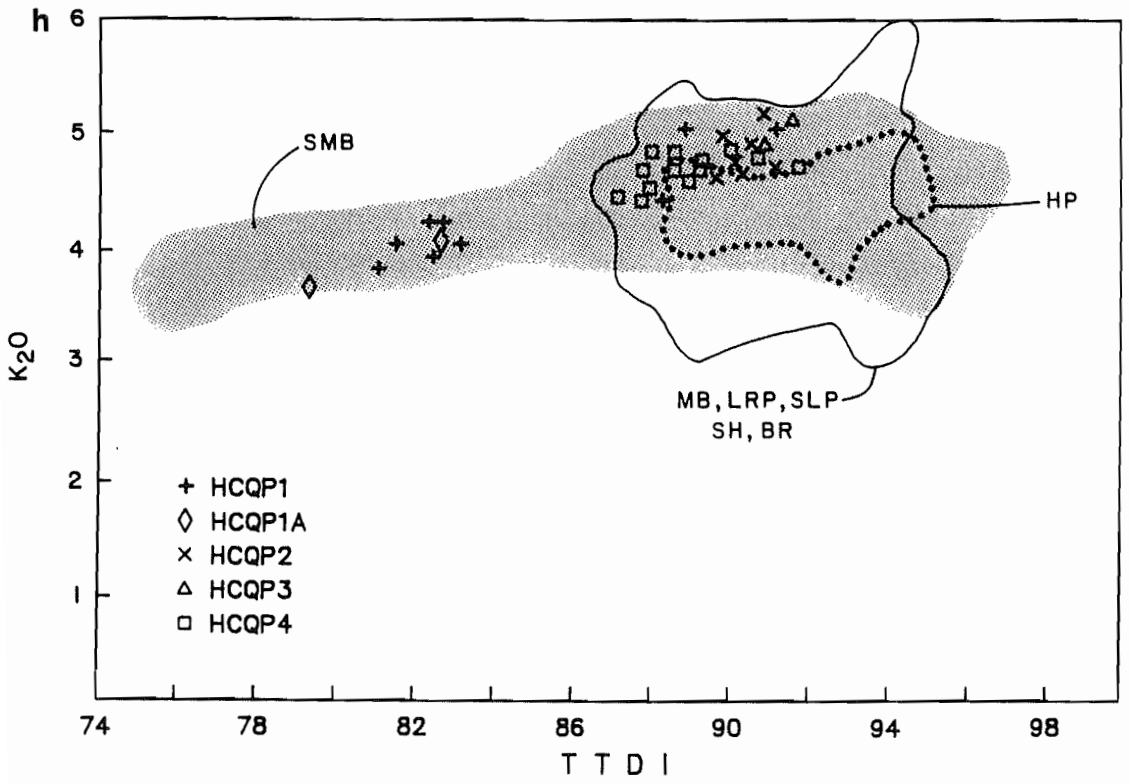
h
6
5
4
3
2
1
$K_2O$
SMB
HP
MB, LRP, SLP
SH, BR
+ HCQP1
◊ HCQP1A
× HCQP2
△ HCQP3
□ HCQP4
74
78
82
86
90
94
98
T T D I

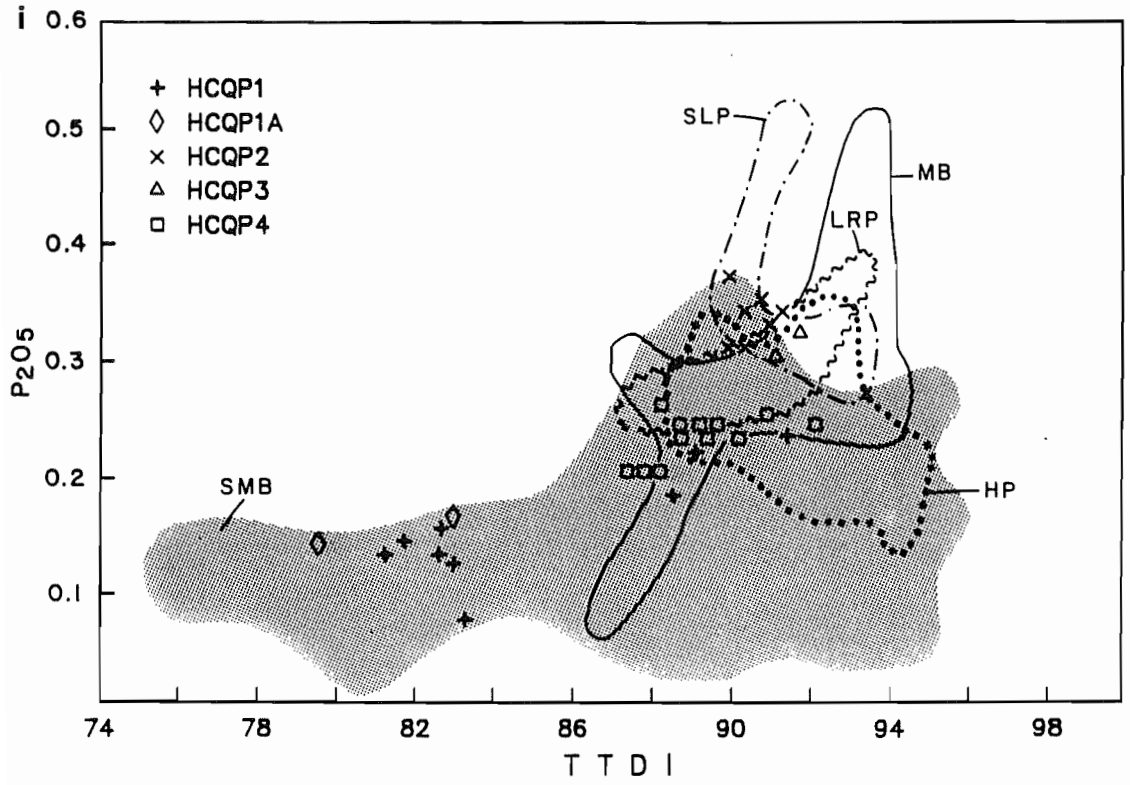
i
0.6
0.5
0.4
0.3
0.2
0.1
P2O5
HCQP1
HCQP1A
HCQP2
HCQP3
HCQP4
SLP
MB
LRP
HP
SMB
74
78
82
86
90
94
98
T T D I

eastern plutons (SLP, LRP, BR, SH) display overlapping fields for some elements, and the fields of these plutons are, therefore, considered as one in some diagrams. Where there are differences, individual fields of separate plutons are plotted.

Table 4.3 shows that all HCQP rocks have high silica, ranging from 69.00 (HCQP1) to 73.67 (HCQP4), with aplite containing slightly higher silica (74.14). Both average silica and TTDI generally increase from HCQP1 (avg. 70.29 and 83.58, respectively) and HCQP1A (avg. 69.18 and 81.20) to the other units (HCQP2 - avg. 72.41 and 91.23; HCQP3 - avg. 71.88 and 90.33; HCQP4 - avg. 71.48 and 88.97). These latter units, however, exhibit considerable overlap.

All of the rocks are peraluminous, with A/CNK ratios ranging from 1.15 to 1.37. These values are similar to other eastern plutons (e.g. MB, 1.14 - 1.27 (MacDonald, 1981); Larrys River, 1.18 -1.34 (O'Reilly, 1984); Sangster Lake, 1.14 - 1.37 (O'Reilly, 1984)), but slightly higher than the SMB (1.06 -1.20) and HP (1.08 - 1.28). This increase in degree of peraluminosity in the HCQP is manifested by the presence of Al-rich biotite, higher proportions of Al-rich muscovite and minor garnet, compared with the SMB which contains volumetrically more biotite-rich, muscovite-poor units.

In general, units HCQP1 and HCQP1A have lower $K_2O$ and $P_2O_5$ and higher MnO, CaO, $FeO_t$, MgO and $TiO_2$ than the other three units. $Na_2O$ and $Al_2O_3$ show less well-developed separations, although $Al_2O_3$ decreases with increasing silica content. HCQP2 has generally the lowest values of $TiO_2$, $FeO_t$, MgO, CaO, and highest values of $K_2O$ and $P_2O_5$ (also seen in Fig. 4.3). The level of phosphorus within the HCQP is high for felsic igneous rocks in general (Watson and Capobianco,

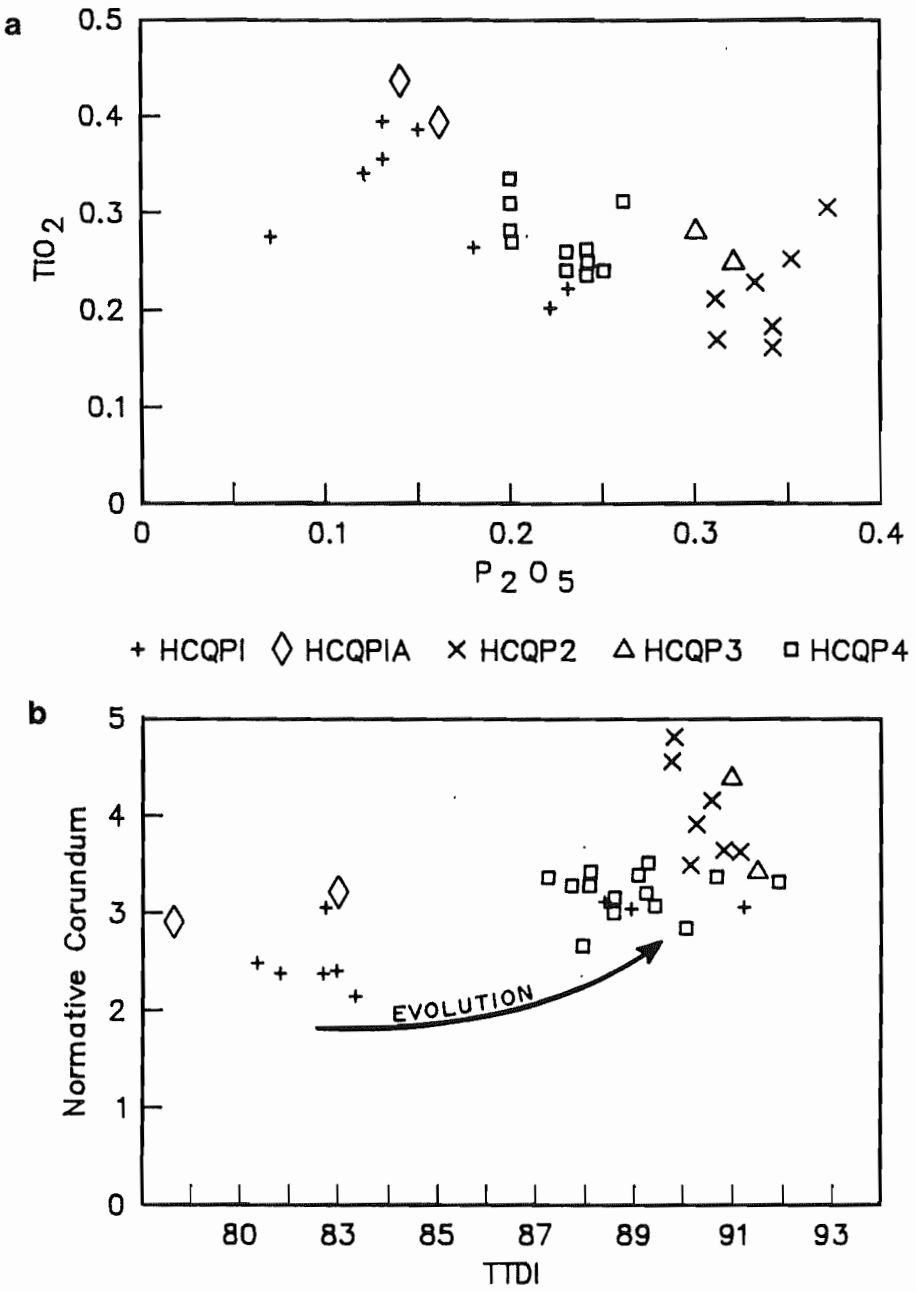


FIGURE 4.3. $P_2O_5$ vs $TiO_2$ and normative corundum vs TTDI. $P_2O_5$ is highest in HCQP2, and decreases to less evolved rock units. Normative corundum displays a similar trend and values within the HCQP are higher than the SMB and similar to the MB. An evolution trend on the diagrams follows the trend of units HCQP1 to HCQP3, and a second evolution trend follows the trend seen for unit HCQP4.

1981), although not anamalously high for levels in other granitic rocks of the Meguma Terrane, and is manifested in the HCQP by the presence of visible blue-green apatite within the groundmass. Three samples from HCQP1 are similar geochemically to the more evolved units (HCQP2, HCQP3 and HCQP4).

The SMB has a broader range of both silica and TTDI than the HCQP and the other plutons. In general, the HCQP exhibits similarities to both the SMB and the eastern plutons, including the HP and the MB. In the major oxide versus TTDI plots, HCQP1 and HCQP1A fall within the mid-range values of the SMB for CaO, MnO, $TiO_2$ and MgO, and higher than the other plutons. The SMB has lower values of $Al_2O_3$ and $P_2O_5$, with higher values of $FeO_t$ than the other bodies. Levels of CaO and MgO in the least evolved rocks (i.e. lowest values of TTDI) of the SMB are higher than the other bodies. HCQP2, HCQP3 and HCQP4 are more similar to the eastern plutons and the Halifax pluton in their lower $FeO_t$, $TiO_2$ values, and higher $Al_2O_3$ and $P_2O_5$ contents.

MacDonald (1981) suggested that the MB, the eastern portion of the SMB (i.e. the Halifax Pluton) and other plutons from the eastern Meguma Terrane display closer similarities to each other than to the middle portion of the SMB, particularly with enrichment in $P_2O_5$ and normative corundum. This observation is supported by the amount of overlap in Figures 4.2 and 4.3. Normative corundum values (Fig. 4.3b) within the HCQP range from 2.12 to 4.79 (avg. 3.29), these values being higher than the SMB (1.2 - 2.8) and similar to the MB (2.75 - 3.54).

McKenzie and Clarke (1975) interpreted the rocks of the SMB to represent a co-magmatic suite, with progressive differentiation of a single parental magma to produce granodiorite, monzogranite and late-

stage rocks. Similarities of trends in the MB led MacDonald and Clarke (1985) to also suggest that the late-stage rocks within that pluton were derived from the main monzogranite liquid through differentiation.

Lower values of $SiO_2$ and TTDI and higher values of other major element contents (e.g. $TiO_2$, CaO, $FeO_t$) indicate that HCQP1 and HCQP1A crystallized from the least evolved magma. However, the trends are less continuous than those found within the SMB and MB; that is, there commonly is an abrupt break between the rocks of Units HCQP1 and HCQP1A and the more evolved units (Fig. 4.2a-i). These more evolved units display similar, but more evolved chemistry and higher, overlapping TTDI values, suggesting that these units are co-magmatic. However, values within HCQP2 (higher $P_2O_5$, lower values of CaO, $FeO_t$, MgO) suggest that this unit is, in fact, the most evolved of the pluton.

Figure 4.4 displays the rocks of the HCQP, the compositions of the ternary minimum liquids after Tuttle and Bowen (1958) and Luth et al. (1964), and the Ab/An ratio piercing points after James and Hamilton (1969). This plot establishes a means for determining pressures of granitic magma. Although there are problems with the plot (i.e. magma must be saturated with respect to water), general inferences can be drawn. The least evolved rocks of the HCQP lie on the trend of piercing points for a pressure of approximately 4 kbars.

A ternary plot of normative Or-Ab-An for the HCQP is displayed in Figure 4.5. HCQP1 and 1A have the highest anorthite component, while HCQP2, HCQP3 and HCQP4 contain virtually no anorthite. All of these latter units are slightly enriched in albitic component over HCQP1 and HCQP1A, with HCQP2 displaying the highest degree of differentiation (i.e. lowest anorthite component). These patterns are in agreement

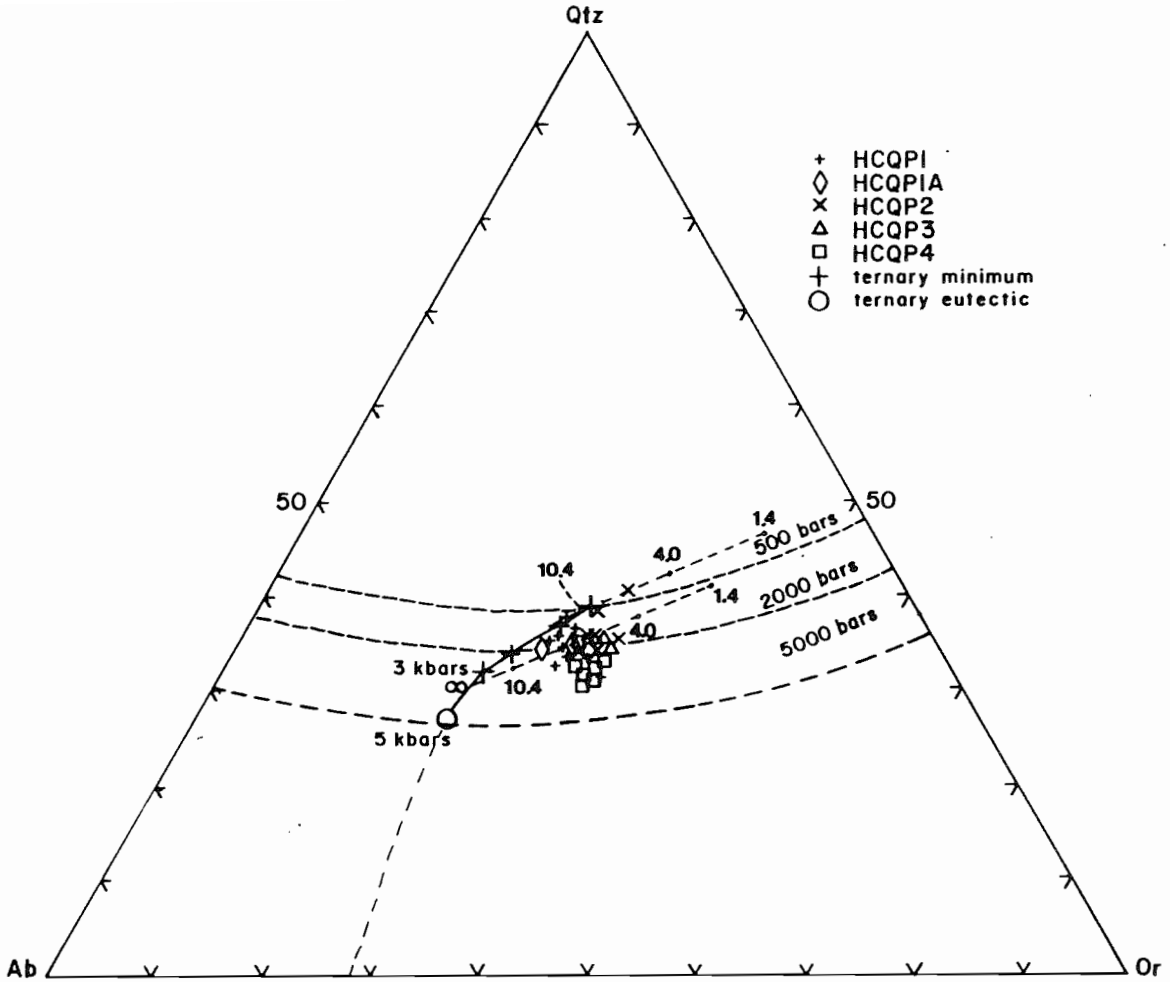


FIGURE 4.4. Ternary plot of normative Quartz-Albite-Orthoclase (Qtz-Ab-Or) for the rock units of the HCQP. Minima, eutectics and cotectics from Tuttle and Bowen (1958) and Luth et al. (1964) and Ab/An piercing points after James and Hamilton (1969). 1.4-4.0-10.4 are Ab/An ratios.

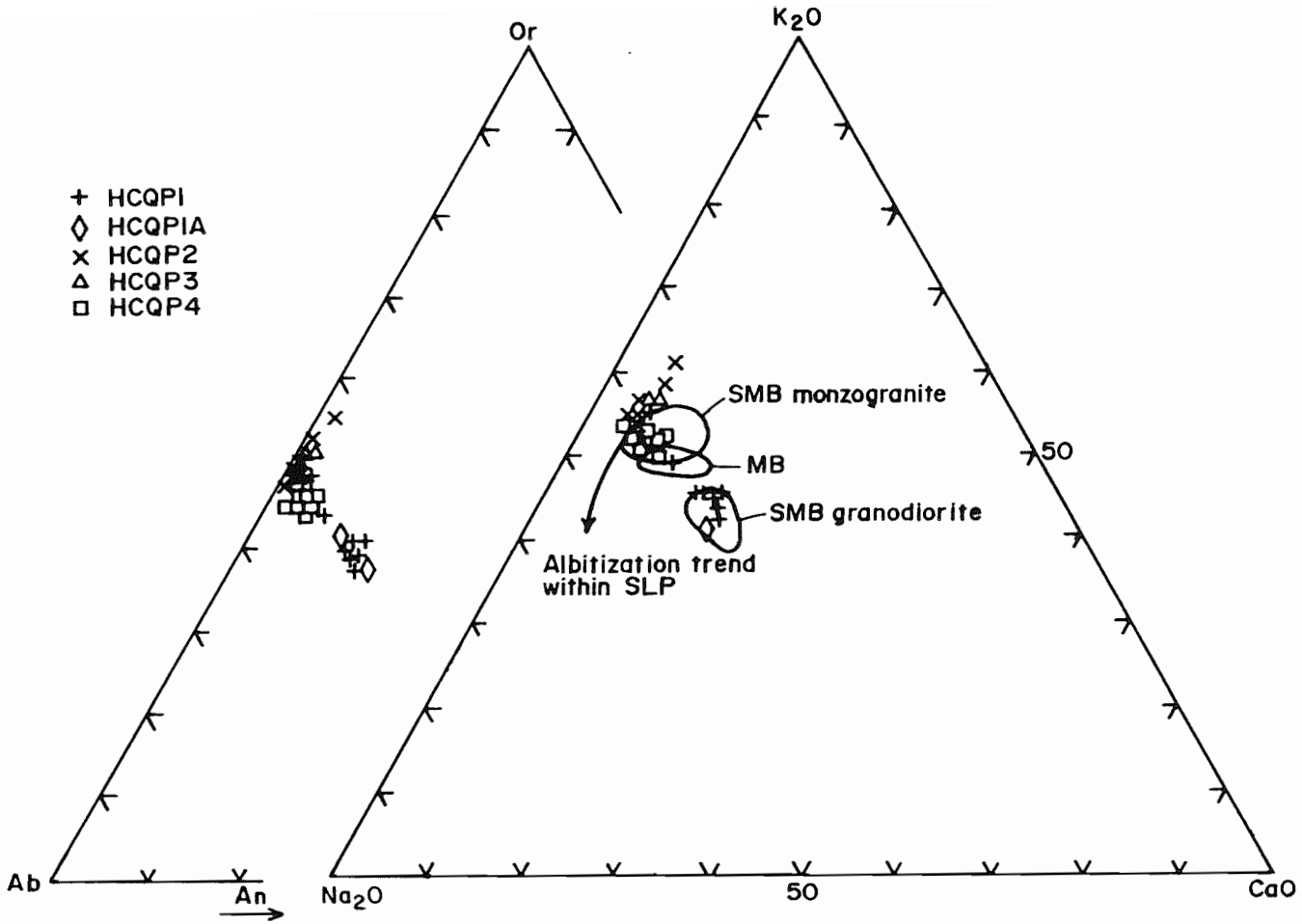


FIGURE 4.5. Orthoclase-albite-anorthite (Or-Ab-An) and $K_2O$-$Na_2O$-CaO ternary plots. Fields outlined on $K_2O$-$Na_2O$-CaO plot outline rocks of the SMB, MB and an alteration (albitization) trend within the Sangster Lake pluton (after Ford and O'Reilly, 1985). The HCQP does not display this trend, but with differentiation displays a slight increase in Or and K content.

with HCQP1 and HCQP1A representing the least evolved units of the pluton, with the other units developing through magmatic differentiation (and/or alteration). There is, again, a well-developed break between the less-evolved units and HCQP2, HCQP3 and HCQP4.

Superimposed on the Or-Ab-An plot is a plot of $K_2O$-$Na_2O$-CaO, with the outline of fields of the SMB, MB, and the trend of rocks within the Sangster Lake Pluton (Ford and O'Reilly, 1985). Within the SLP, a trend (seen both petrographically and mineralogically) of increasing albitization within the later-stage rocks occurs. This trend may represent increased metasomatism and hydrothermal alteration. Such a trend does not occur within the HCQP, suggesting that either these later-stage effects are minimal, or that different alteration processes occurred within the HCQP. Petrographically, the later units exhibit increased alteration of the feldspars and biotite and development of secondary muscovite. $Na_2O/K_2O$ ratios commonly increase with increased metasomatism (Ford and Ballantyne, 1983) and Figure 4.6 displays that, within the HCQP, this ratio decreases marginally with increased $SiO_2$ content, with the highest values (some degree of metasomatism?) apparent in HCQP2.

## 4.5 Trace Element Chemistry

### 4.5.1 Introduction

Trace elements are becoming increasingly valuable for igneous rock petrogenetic studies (Buma et al., 1971; Hanson, 1978; McCarthy and Fripp, 1979; Kay, 1984). Table 4.4 lists the behaviour of selected trace elements during magmatic crystallization, with individual trace elements grouped together when their chemical characteristics are

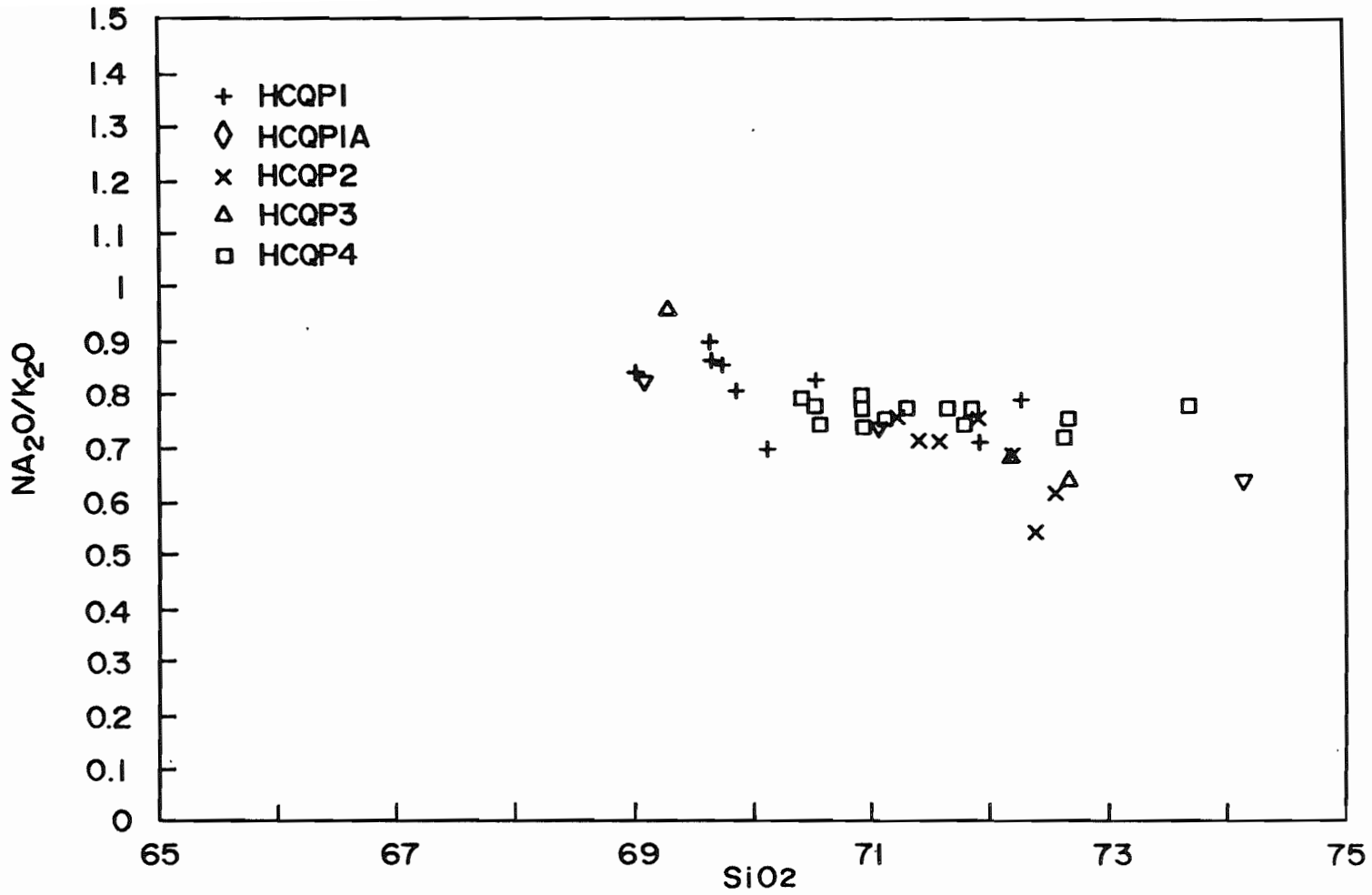


FIGURE 4.6. $SiO_2$ versus $Na_2O/K_2O$ within the HCQP. Note the marginally lower values of $Na_2O/K_2O$ with increasing $SiO_2$. Ford and Ballantyne (1983) suggest that an increasing trend of $Na_2O/K_2O$ with increasing silica indicates metasomatic effects.

TABLE 4.4 Characteristics of selected trace elements within granitic rocks.

| Element | Family and Valence State | Isotopes | Ionic Radius | Chemical Characteristics | Magmatic Characteristics | Host Minerals | References |
|---|---|---|---|---|---|---|---|
| Rubidium (Rb) | Alkali Metal 1+ | $Rb^{85}$, $Rb^{87}$ | 1.48 A | -similar to K<br>-occupy sites normally occupied by K; although larger ionic radius than K | -enriched in residual liquid<br>-differentiation produces enrichment<br>-often discussed as K/Rb ratios; ratios decrease with differentiation (160-300 common for most rocks) | -muscovite, biotite<br>-does not form own minerals | Reynolds (1972) |
| Cesium (Cs) | Alkali Metal 1+ | | 1.69 A | -can substitute for K and Rb<br>-radius difference between K, Rb and Cs preclude Cs substitution in early crystallization | -preference for concentration in late-stage differentiates (e.g. during greisenization) and pegmatites<br>-abundance in granitic rocks 1-50 ppm<br>-K/Cs decreases with with differentiation | -dispersed within feldspars and micas<br>-muscovite contains highest concentrations of the micas<br>-independent minerals can form (e.g. pollucite), if concentrations high enough | Kay (1972) |
| Strontium (Sr) | Alkaline Earth Metal 2+ | $Sr^{88}$, $Sr^{87}$, $Sr^{86}$ | 1.12 A | -can substitute for both Ca and Ba<br>-"entrapped" in minor amounts in K lattice sites | -generally depletion trend with differentiation<br>-average Sr in granites 147 in SMB; average in late-stage rocks 55 ppm pegmatites, however, can contain up to several thousand ppm | -highest amounts found in calcium-rich minerals<br>-can be incorporated into apatite; can be found in great amounts in pegmatites | Wehmiller (1972) |

| | | | | | | |
|---|---|---|---|---|---|---|
| Barium (Ba) | Alkaline Earth Metal 2+ | 1.35 A | -closely resembles Sr in behaviour<br>-substitutes for K | -substitute in early-formed phases<br>-concentration decreases with magmatic differentiation | -occurs as trace impurities in silicate crystal lattice, particularly orthoclase<br>-occurs within calcium bearing minerals, apatite or calcite<br>-can form independent minerals | Pilkey (1972) |
| Zirconium (Zr) and Hafnium (Hf) | Transition Metals 4+ | 0.79 A<br>0.78 A | -two elements very similar<br>-can replace Ti, Nb, Y, Ta, REE's | -do not concentrate in main rock-forming minerals<br>-zircon crystallizes early in magma<br>-Zr and Hf decrease with differentiation; hafnium slightly enriched relative to zirconium | zirconium forms own mineral, zircon<br>-both elements found as trace impurities in micas, feldspars, garnets | McNally (1972), Hampol (1972) |
| Tantalum (Ta) | Transition Metal 5+ | 0.68 A | -closely associated with niobium<br>-usually occurs in complex oxides, combined with Nb, Ti, Yb and lanthanides<br>-element camaflauged in other iron and iron-titanium oxides and silicates | -concentrated in late stages of magmatic differentiation<br>-typically concentrated in pegmatites<br>-average Ta levels 4.0-4.6 ppm<br>-Ta increases with $SiO^2$ content increases | -trace amounts in minerals, such as biotite, muscovite, magnetite, ilmenite, sphene, rutile, zirconium, silicates, cassiterite<br>-may form own minerals (e.g. tantalite) | Wedephol (1970) Doman (1972) Rankama and Shama (1950) |
| Uranium (U) | Actinide Series 3+,4+,5+ | $U^{238}$ $U^{235}$ $U^{234}$ | 0.97 A | -similar behaviour to Th<br>-resembles Zr, Hf, Ce and Ti<br>-can substitute for REE's, Zr and Ca | -$U^{4+}$ exists under most magmatic conditions; $U^{6+}$ under surface and oxidizing conditions<br>-U contents generally increase with increasing Si contents; may decrease | -primary uranium minerals (e.g. uraninite, pitchblende) within igneous rocks<br>-trace amounts within sphene, zircon, apatite | Rogers and Adams (1970); Haglund (1972); Kimberley (1978); Chatterjee and Muecke (1982) |

| | | | | | | |
|---|---|---|---|---|---|---|
| | | | | -SMB has two trends; increasing U with increasing Th, and increasing U with decreasing Th<br>-Th/U ratios often used; averaging 3.5-4.0 in granitic rocks | | |
| Thorium (Th) | Actinide Series 4+ | 0.99 A | -similar behaviour to U<br>-differences in Th/U ratios in minerals indicate crystal lattice can differentiate between two elements | -substitute in late stages of crystallization; also believed to enter apatite and zircon early in differentiation sequence | -thorium mainly in monazite; also in allanite, apatite, huttonite, sphene, zircon; minor amounts in epidote and feldspars | Rogers and Adams (1969); Moore and Swami (1972) |

similar. Table 4.5 tabulates the trace element abundances within the HCQP.

### 4.5.2 Trace Element Behaviour in HCQP

Figures 4.7a and b display Rb and Sr values plotted against TTDI. Rb and Sr reflect increasing and decreasing trends, respectively, with increasing TTDI, although the more evolved units of intrusion display considerable overlap. Rb values are enriched within HCQP4 (avg. 226 ppm) over HCQP1 (avg. 195 ppm), as expected in either a differentiation or alteration trend. With both Rb and Sr, there are two well-developed clusters, one characterizing HCQP1 and HCQP1A, and the other representing HCQP2, HCQP3 and HCQP4.

K/Rb ratios are often used as a tool for determination of magmatic differentiation, as the ratio decreases with increased differentiation (Butler et al., 1962; Reynolds, 1972; Hanson, 1978). Most granitic rocks range from 160-300 for K/Rb (Reynolds, 1972), although rubidium-rich granites have even lower values. K-feldspar, as a residual phase, will contribute greatly to a reduction in the K/Rb in the melt, while biotite, as a stable phase during melting, will also decrease this value (Hanson, 1978). Rb values in the HCQP increase slightly with differentiation, while $K_2O$ values range from 4.31% (HCQP1) to 4.18% (HCQP2) and 4.68% (HCQP4). This combined effect results in a slight decrease of K/Rb ratios with differentiation within the HCQP (Fig. 4.8).

Similar trends have been documented with the MB (MacDonald and Clarke, 1985) and SMB (McKenzie and Clarke, 1975; Charest, 1976) and interpreted as resulting from a decrease in modal abundance of biotite

TABLE 4.5 Trace element abundances (ppm) of rocks of the HCQP

| SAMPLE<br>PHASE | QP03<br>HCQP1 | QP06<br>HCQP1 | QP07<br>HCQP1 | QP08<br>HCQP1 | QP10<br>HCQP1 | QP11<br>HCQP1 | QP12<br>HCQP1 | QP22<br>HCQP1 | QPL038<br>HCQP1 | QP01<br>HCQP1A | QP02<br>HCQP1A |
|---|---|---|---|---|---|---|---|---|---|---|---|
| BA | 318 | 342 | 527 | 473 | 306 | 412 | 405 | 355 | 293 | 419 | 435 |
| RB | 245 | 209 | 175 | 175 | 251 | 186 | 182 | 188 | 163 | 187 | 178 |
| SR | 79 | 113 | 184 | 167 | 73 | 160 | 162 | 137 | 140 | 146 | 168 |
| Y | 10 | 14 | 14 | 16 | 11 | 19 | 15 | 21 | 18 | 17 | 18 |
| ZR | 80 | 79 | 90 | 98 | 87 | 100 | 91 | 102 | 79 | 101 | 109 |
| NB | 8 | 11 | 9 | 10 | 9 | 10 | 8 | 11 | 8 | 11 | 9 |
| TH | 11 | 9 | 11 | 11 | 10 | 10 | 8 | 10 | 7 | 10 | 8 |
| PB | 26 | 30 | 32 | 30 | 25 | 30 | 27 | 21 | 30 | 31 | 26 |
| GA | 22 | 20 | 17 | 20 | 25 | 19 | 20 | 23 | 17 | 19 | 19 |
| ZN | 61 | 54 | 46 | 54 | 74 | 54 | 47 | 63 | 42 | 58 | 55 |
| NI | 6 | 8 | 5 | 7 | 11 | 6 | 8 | 11 | 3 | 6 | 6 |
| CR | 8 | 14 | 21 | 20 | 8 | 23 | 21 | 26 | 19 | 23 | 29 |
| BE | 5 | 8 | 5 | 6 | 4 | 3 | 3 | 3 | 5 | 6 | 4 |
| B | 15 | 15 | 10 | 20 | 15 | 15 | 15 | 20 | 15 | 20 | 15 |
| F | 630 | 660 | 540 | 540 | 550 | 670 | 470 | 780 | 330 | 570 | 730 |
| U | 5.7 | 5.8 | 6.0 | 5.6 | 7.9 | 6.9 | 4.2 | 5.5 | 3.4 | 4.0 | 3.5 |
| W | 10 | 3 | 1 | 3 | n.a. | n.a. | n.a. | n.a. | 3 | 6 | n.a. |
| SN | 9 | 9 | 5 | 1 | 13 | 6 | 6 | 10 | 2 | 3 | 6 |
| MO | 1 | 1 | 1 | 1 | 2 | 2 | 2 | 3 | 1 | 1 | 2 |

| SAMPLE<br>PHASE | HC01<br>HCQP2 | HC02<br>HCQP2 | HC05<br>HCQP2 | HC06<br>HCQP2 | HC07<br>HCQP2 | HCL018<br>HCQP2 | HCL034<br>HCQP2 | HC03<br>HCQP3 | HC04<br>HCQP3 | QP04<br>HCQP4 | QP05<br>HCQP4 |
|---|---|---|---|---|---|---|---|---|---|---|---|
| BA | 215 | 274 | 310 | 378 | 276 | 248 | 240 | 384 | 322 | 386 | 379 |
| RB | 285 | 240 | 247 | 225 | 263 | 255 | 226 | 217 | 246 | 268 | 267 |
| SR | 58 | 70 | 79 | 80 | 62 | 65 | 66 | 90 | 81 | 82 | 77 |
| Y | 14 | 11 | 11 | 10 | 11 | 9 | 9 | 11 | 11 | 9 | 8 |
| ZR | 81 | 74 | 81 | 92 | 63 | 62 | 63 | 90 | 84 | 95 | 95 |
| NB | 15 | 10 | 11 | 11 | 12 | 10 | 11 | 9 | 11 | 9 | 8 |
| TH | 8 | 7 | 7 | 8 | 6 | 6 | 6 | 9 | 9 | 17 | 16 |
| PB | 22 | 27 | 25 | 29 | 27 | 23 | 65 | 28 | 28 | 26 | 25 |
| GA | 24 | 20 | 24 | 24 | 22 | 19 | 21 | 21 | 23 | 21 | 23 |
| ZN | 90 | 60 | 55 | 66 | 49 | 44 | 195 | 64 | 53 | 68 | 67 |
| NI | 10 | 4 | 3 | 10 | 10 | 6 | 4 | 4 | 4 | 7 | 3 |
| CR | 23 | 12 | 15 | 19 | 9 | 13 | 10 | 10 | 19 | 14 | 12 |
| BE | 7 | 7 | 7 | 4 | 4 | 7 | 7 | 5 | 5 | 7 | 6 |
| B | 15 | 15 | 20 | 20 | 20 | 15 | 20 | 25 | 10 | 10 | 10 |
| F | 690 | 530 | 570 | 450 | 530 | 600 | 540 | 510 | 540 | 810 | 690 |
| U | 11.5 | 7.4 | 5.5 | 6.0 | 9.6 | 7.7 | 24.6 | 6.2 | 7.2 | 2.8 | 3.6 |
| W | 2 | 5 | 4 | n.a. | n.a. | 1 | 5 | 1 | 6 | 8 | 3 |
| SN | 13 | 10 | 9 | 9 | 12 | 6 | 6 | 1 | 5 | 7 | 13 |
| MO | 1 | 1 | 1 | 2 | 2 | 1 | 1 | 1 | 1 | 1 | 1 |

| SAMPLE PHASE | QP09 HCQP4 | QP13 HCQP4 | QP14 HCQP4 | QP15 HCQP4 | QP16 HCQP4 | QP17 HCQP4 | QP18 HCQP4 | QP19 HCQP4 | QP20 HCQP4 | QP21 HCQP4 |
|---|---|---|---|---|---|---|---|---|---|---|
| BA | 392 | 504 | 567 | 415 | 443 | 370 | 382 | 441 | 408 | 420 |
| RB | 26 | 259 | 267 | 282 | 245 | 268 | 275 | 256 | 269 | 266 |
| SR | 75 | 93 | 94 | 79 | 79 | 74 | 76 | 85 | 79 | 80 |
| Y | 10 | 11 | 12 | 11 | 13 | 9 | 11 | 9 | 10 | 10 |
| ZR | 90 | 106 | 124 | 96 | 112 | 97 | 101 | 106 | 95 | 106 |
| NB | 9 | 9 | 9 | 10 | 10 | 10 | 10 | 9 | 8 | 10 |
| TH | 18 | 18 | 22 | 16 | 20 | 14 | 14 | 14 | 14 | 16 |
| PB | 24 | 25 | 26 | 36 | 25 | 23 | 25 | 27 | 23 | 27 |
| GA | 21 | 23 | 24 | 27 | 25 | 26 | 25 | 25 | 27 | 25 |
| ZN | 58 | 72 | 82 | 64 | 75 | 62 | 62 | 68 | 72 | 69 |
| NI | 6 | 11 | 12 | 12 | 8 | 11 | 11 | 10 | 9 | 7 |
| CR | 13 | 16 | 19 | 8 | 14 | 19 | 14 | 17 | 11 | 11 |
| BE | 6 | 3 | 5 | 0 | 2 | 4 | 4 | 4 | 4 | 3 |
| B | 20 | 10 | 15 | 0 | 15 | 150 | 10 | 15 | 20 | 15 |
| F | 790 | 1000 | 960 | 0 | 930 | 820 | 960 | 730 | 930 | 790 |
| U | 2.9 | 3.1 | 3.7 | 8.2 | 2.8 | 3.5 | 5.9 | 6.5 | 3.4 | 3.3 |
| W | 5 | n.a. | n.a. | n.a. | n.a. | n.a. | n.a. | n.a. | n.a. | n.a. |
| SN | 9 | 8 | 9 | 0 | 6 | 12 | 12 | 11 | 8 | 11 |
| MO | 1 | 2 | 2 | 0 | 2 | 2 | 2 | 2 | 2 | 2 |

| SAMPLE<br>PHASE | QPL014<br>HCQP4 | QPL032<br>HCQP4 | HCL037<br>APLITE | QPL015A<br>LEUCO |
|---|---|---|---|---|
| BA | 464 | 506 | 64 | 310 |
| RB | 265 | 262 | 257 | 227 |
| SR | 87 | 93 | 34 | 94 |
| Y | 11 | 11 | 8 | 13 |
| ZR | 113 | 119 | 29 | 69 |
| NB | 9 | 10 | 8 | 10 |
| TH | 23 | 26 | 2 | 6 |
| PB | 27 | 25 | 32 | 34 |
| GA | 21 | 22 | 21 | 22 |
| ZN | 57 | 62 | 13 | 54 |
| NI | 9 | 8 | 6 | 8 |
| CR | 19 | 19 | 7 | 15 |
| BE | 6 | 5 | 0 | 0 |
| B | 20 | 15 | 0 | 0 |
| F | 810 | 1075 | 0 | 0 |
| U | 6.6 | 2.9 | 7.3 | 7.3 |
| W | 8 | 4 | n.a. | n.a. |
| SN | 4 | 1 | 0 | 0 |
| MO | 1 | 1 | 0 | 0 |

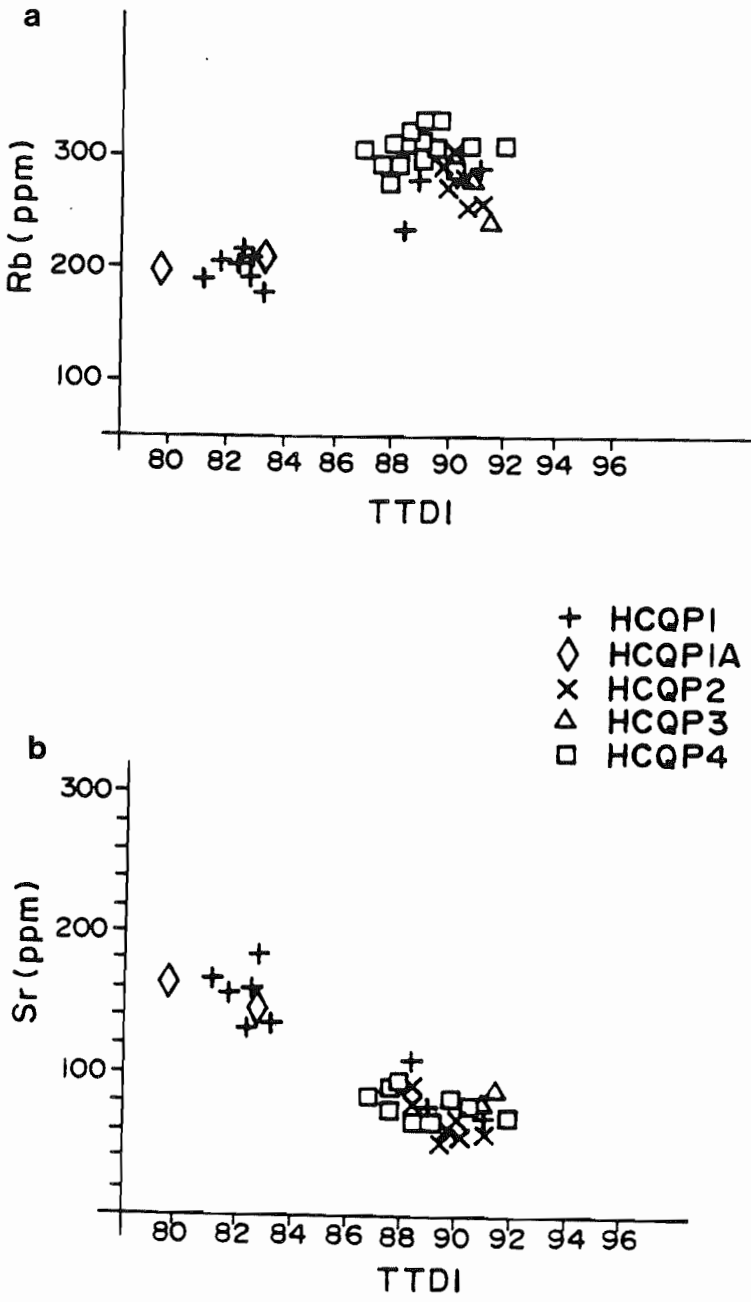


FIGURE 4.7. Rb and Sr vs TTDI for rocks of the HCQP. Rb and Sr exhibit increasing and decreasing trends, respectively, with increasing TTDI. With both Rb and Sr, two well-developed populations occur, with HCQP1 and HCQP1A representing one and HCQP2, HCQP3 and HCQP4 representing the other.

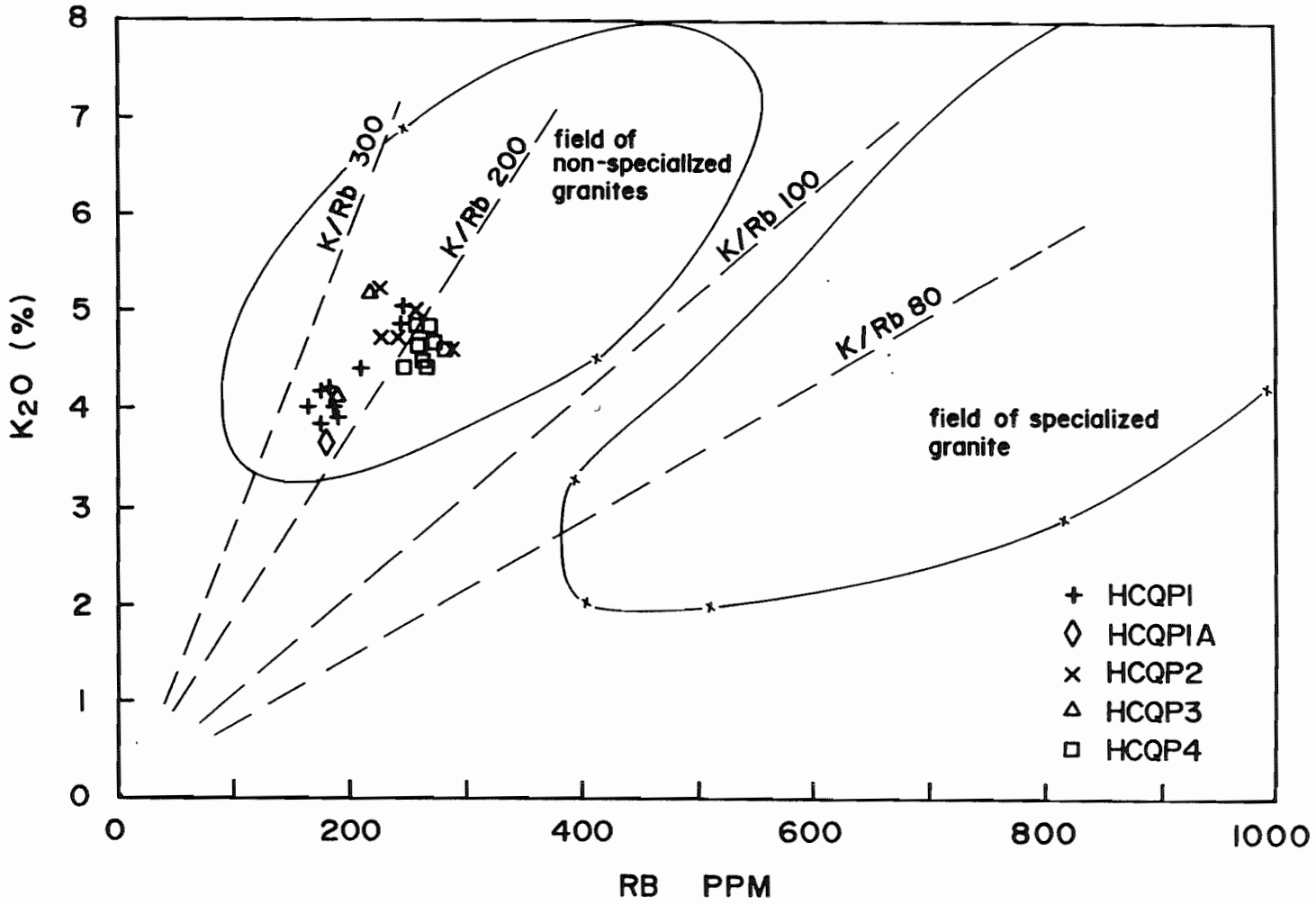


FIGURE 4.8. Rb-$K_2O$ plot with K/Rb ratio lines. The K/Rb ratios generally decrease with differentiation. Fields for specialized and non-specialized granites of the Meguma Zone are after Chatterjee and Muecke (1982). The HCQP rocks clearly fall within the non-specialized group.

and plagioclase feldspar. This K/Rb decrease is explained by the decreasing modal concentration of biotite also within the HCQP. The general increase of $K_2O$ within the units could relate to an increase in muscovite content.

Chatterjee and Muecke (1982) have defined a "paraintrusive suite" of rocks associated with significant Sn-U mineralization within the SMB. This suite is believed to be the result of fluid interaction and these rocks are specialized in Li, Be, F, Rb, Cs, U, and Sn. Rocks of the HCQP clearly fall within the non-specialized field (Fig. 4.8) of Chatterjee and Muecke (1982). The economic potential of the HCQP is discussed in further detail in Chapter 5.

As mentioned previously in Chapter 2, the HCQP displays a striking equivalent thorium response. Uranium and thorium, as determined by whole rock analyses, range from 2.8-24.6 ppm and 7-26 ppm, respectively (Table 4.5), supporting the airborne equivalent thorium results. Plutons showing a peculiar increasing thorium trend with decreasing or virtually constant uranium, such as HCQP, are virtually unknown. Many authors have documented increasing Th and U with igneous evolution (e.g. Adams et al., 1959; Rogers and Raglund, 1961). Chatterjee and Muecke (1982) determined two general trends, associated with degree of differentiation, within the SMB in areas that host mineralization to be either: 1) increasing uranium with generally decreasing thorium (New Ross, Lake George, East and West Dalhousie) and 2) increasing uranium and increasing thorium (Davis Lake, Plymouth). Farley (1979) and Logothetis (1985) also determined similar trends in the New Ross area of the SMB. Figure 4.9 displays rocks of the HCQP, compared with the SMB and the Davis Lake Pluton, after Chatterjee and Muecke (1982). The

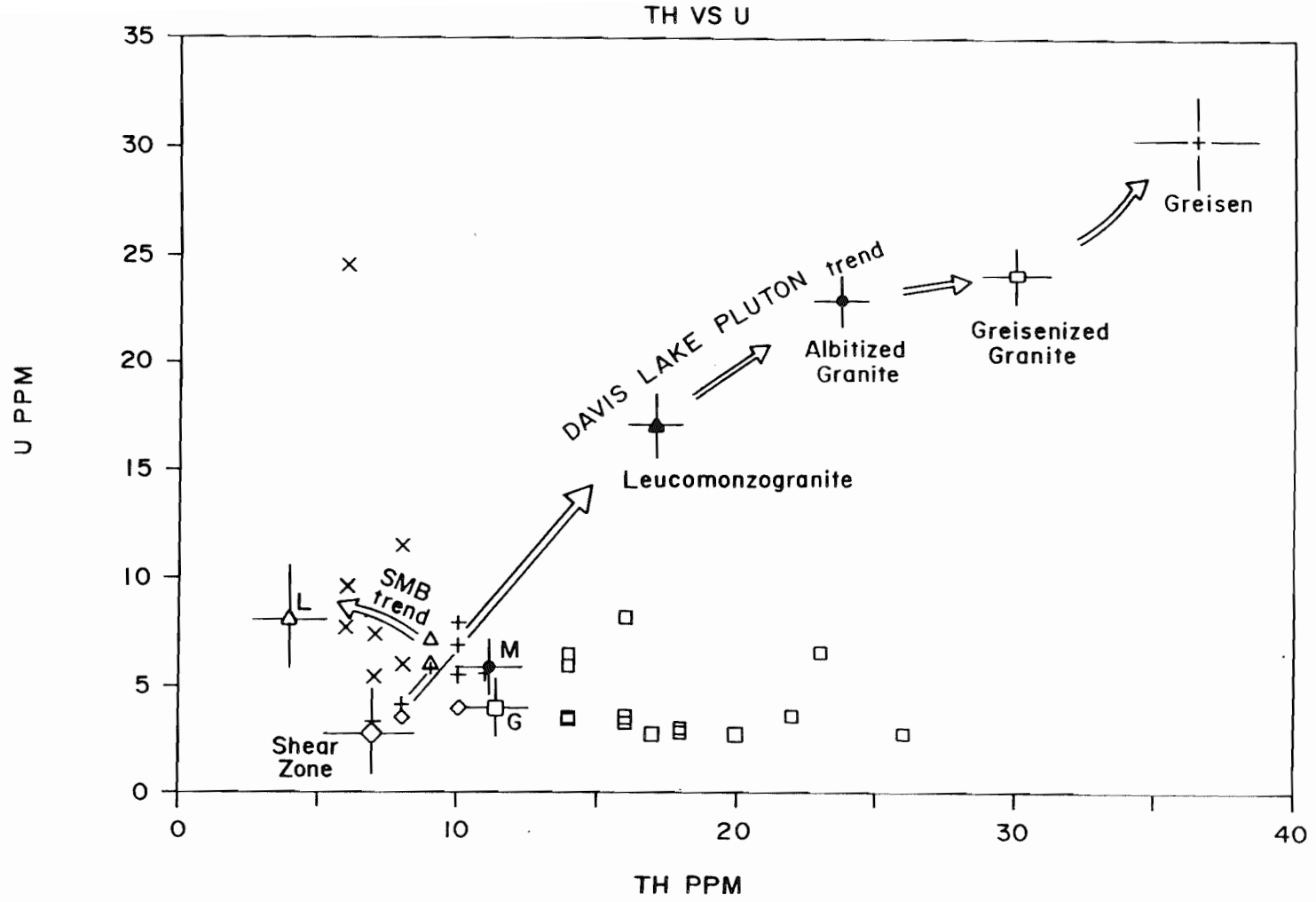


FIGURE 4.9. U vs Th for the HCQP, compared with the U-Th data for the SMB and the Davis Lake pluton, as defined by Chatterjee and Muecke (1982). Rocks of the SMB are granodiorite (G), monzogranite (M) and leucogranite (L). Note different trend within the rocks of the HCQP.

trend of increasing Th with constant or decreasing U within the HCQP contrasts with the trends outlined for the SMB. Metcalf and Blackburn (1981) speculated that anomalously high Th/U ratios in the central portion of an intrusion represents oxidation and solution of U by late-stage differentiates. A similar conclusion was reached by Whitfield et al. (1959) to explain increasing Th with irregular U. However, within the HCQP where the Th/U ratios range from 2 in the margins to 9 in the interior (illustrated in Figs. 4.10a-c), evidence for late-stage fluid interaction is minor.

Field mapping indicates that the high thorium pattern is closely associated with unit HCQP4 (Fig. 4.11). However, HCQP2 is mineralogically similar to HCQP4, often reflects chemical trends similar to, and overlapping with, this unit, but does not display a similar thorium enrichment.

In an attempt to determine an explanation for this unusual pattern, the chemical behaviour of thorium was investigated. Numerous studies (e.g. Fourcade and Allegre, 1981; Miller and Mittlefehldt, 1982; Pagel, 1982; Gromet and Silver, 1983) suggest that these elements are contained mostly in accessory minerals (monazite, allanite, xenotime, zircon, sphene). Table 4.4 outlines possible substitutions for thorium. Thorium will substitute for REE's within monazite, allanite, huttonite, Ca in apatite and sphene, and zirconium in zircon. Minor amounts may be incorporated in major rock-forming minerals.

An increase in thorium could be related to an increase in incorporation within the monazite structure (Rogers and Adams, 1969; Weber et al., 1985; Rapp and Watson, 1986). Biotite is the most common host for monazite inclusions (Mittlefehldt and Miller, 1983; Weber et

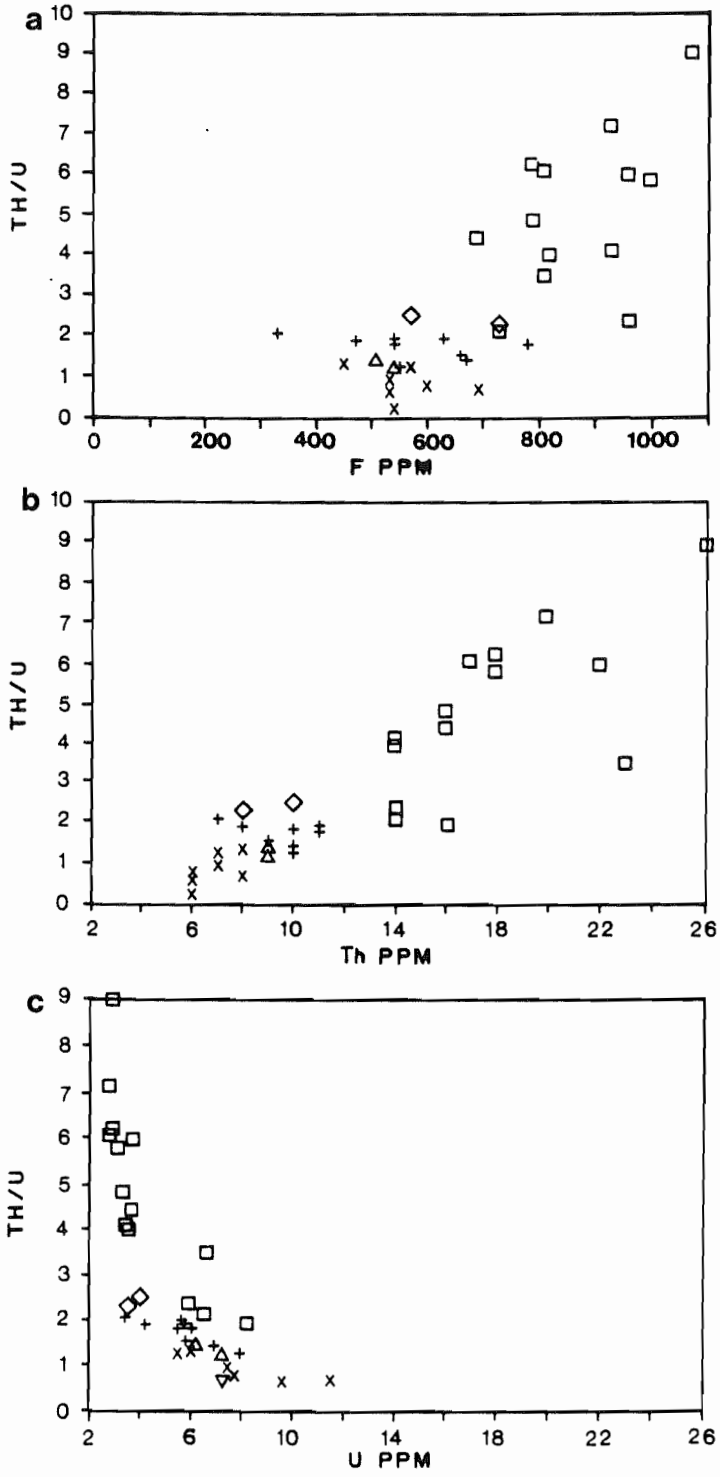


FIGURE 4.10. Th/U values plotted against F, Th and U values for rocks of the HCQP.

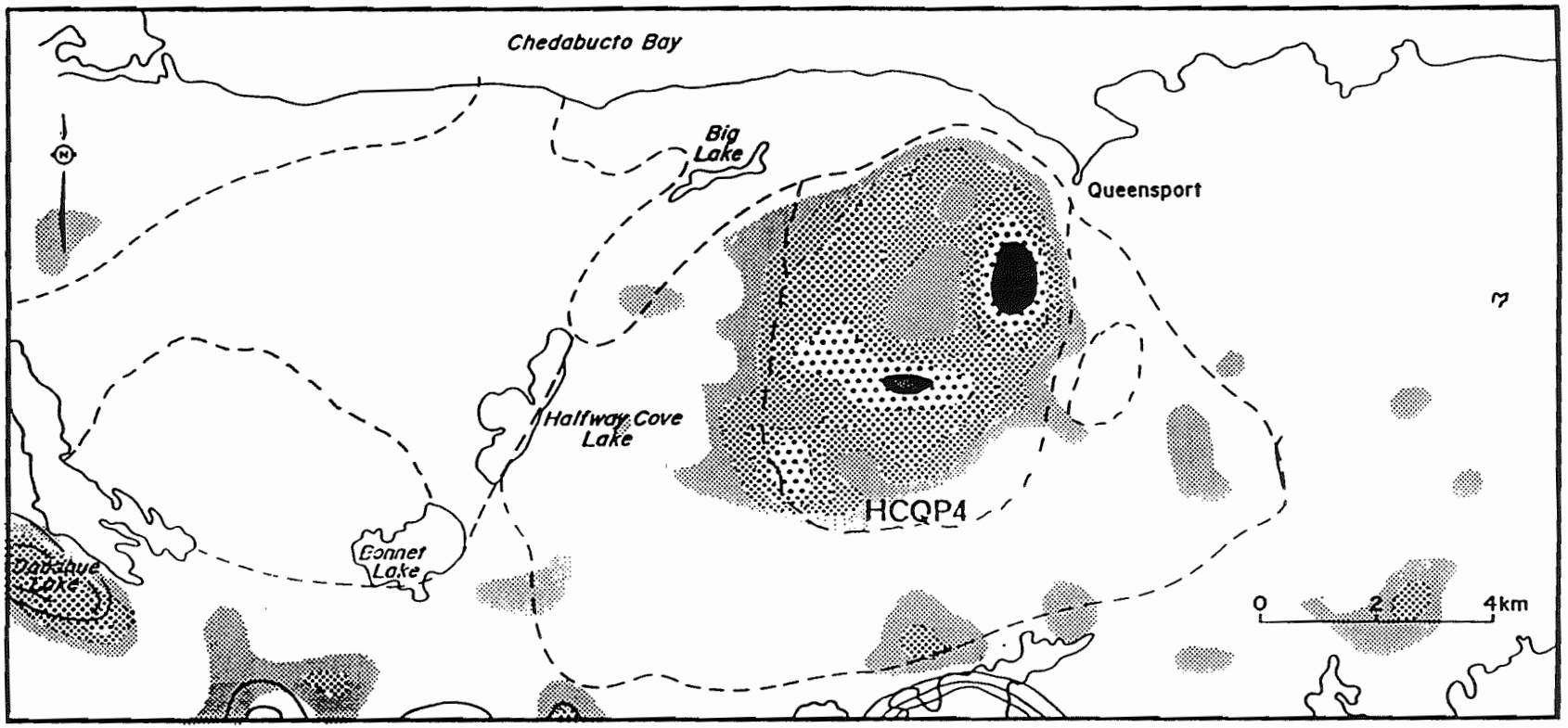


Figure 4.11 Radioelement equivalent thorium (eTh) response over the HCQP, with the unit HCQP4 outlined.

al., 1985). Rocks of HCQP4 contain biotite with larger and more abundant inclusions than the other rock units, and a higher proportion of (secondary?) biotite (i.e. biotite with no inclusions) than the other units, suggesting some degree of metasomatism (Ford and Ballantyne, 1983) or metamorphism. However, microprobe results were inconclusive as to whether any of the inclusions were monazite. The REE patterns for HCQP4 (seen in Fig. 4.14) indicate more HREE depletion compared with the other rock units, suggesting that zircon and possibly garnet, and not monazite, played a greater role in HCQP4.

The Spearman Rank correlation matrix (Table 4.2) determined, in addition to Zr, a positive correlation of Th/U with both Ba and F. Barium values are variable in the rock units of the HCQP (Fig. 4.12), and do not follow an expected differentiation trend (i.e. do not decrease with differentiation). This correlation of Th/U with Ba and the variability of Ba is unresolved. Thorium and Zr (Fig. 4.13a) display positive correlation. A plot of Zr vs $TiO_2$ (Fig. 4.13b) also displays positive correlation that splits into two trends, the one with higher values associated with HCQP4. This split suggests that zirconium values are anomalous within HCQP4.

Gulson and Krogh (1975), in a study of zircons from rocks in Greenland, concluded, from ages and characteristics of the zircons, that there were multiple intrusions, and the youngest unit contained zircons with less uranium than the older units. While the uranium and thorium levels within the zircons of the HCQP were not investigated, zircons within HCQP4 could also contain less U and more Th. If this was the case, the zircon characteristics of HCQP4 might explain the

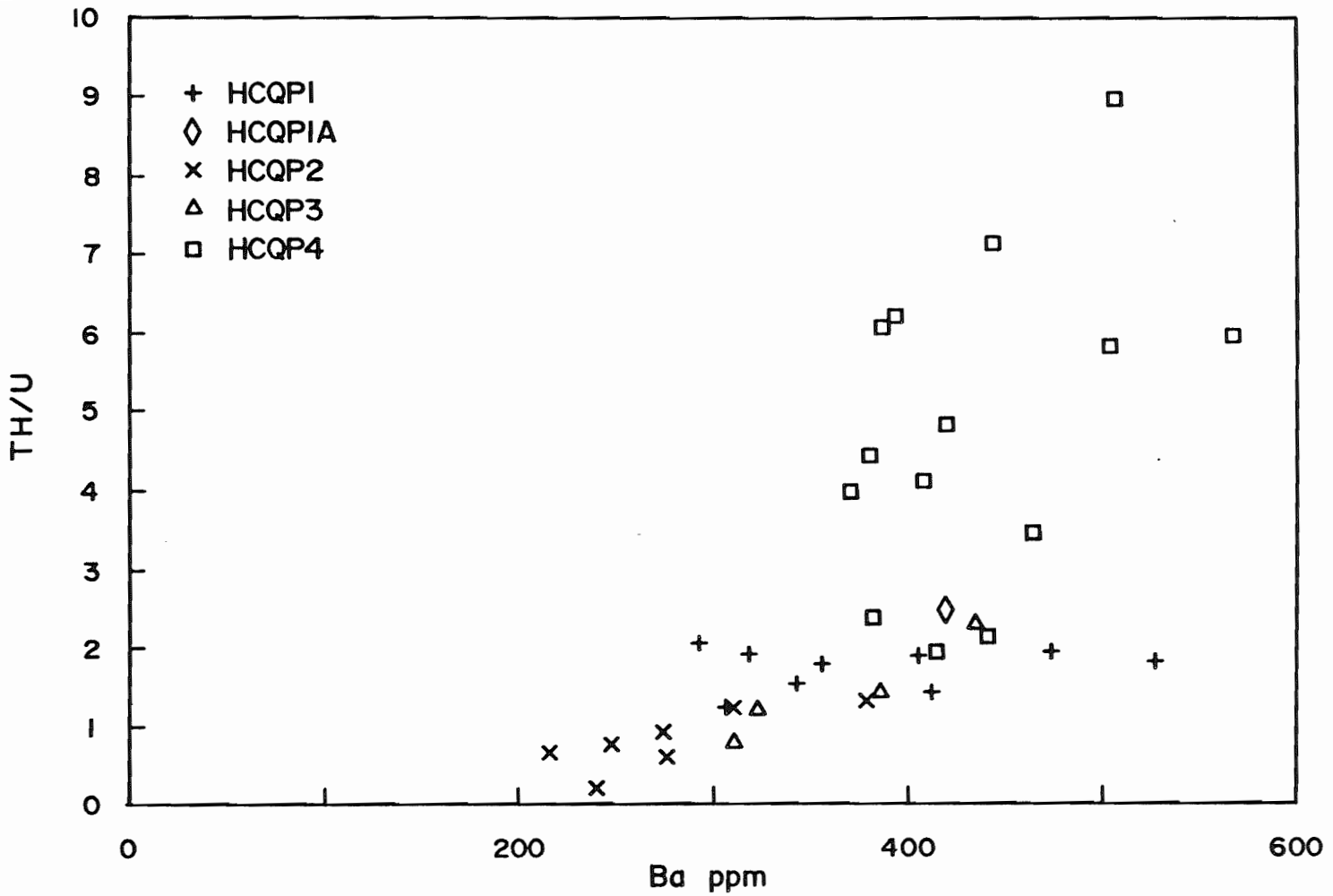


FIGURE 4.12. Barium versus Th/U values for rocks of the HCQP. Barium values are variable within the rocks, and generally display an unusual trend increasing with differentiation.

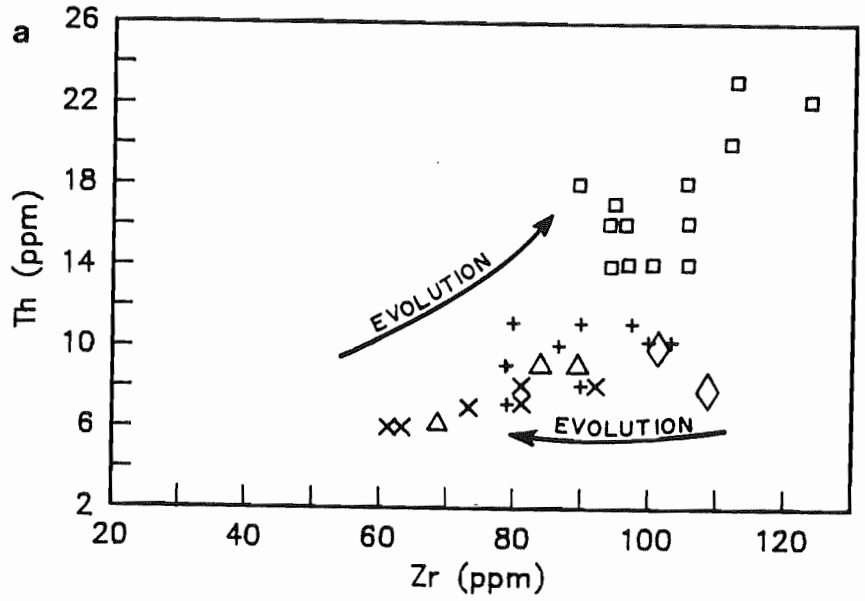


FIGURE 4.13. Zr versus Th and Zr vs $TiO_2$ plots for the HCQP. Note increase in zirconium within HCQP4, and positive correlation of Th with zirconium.

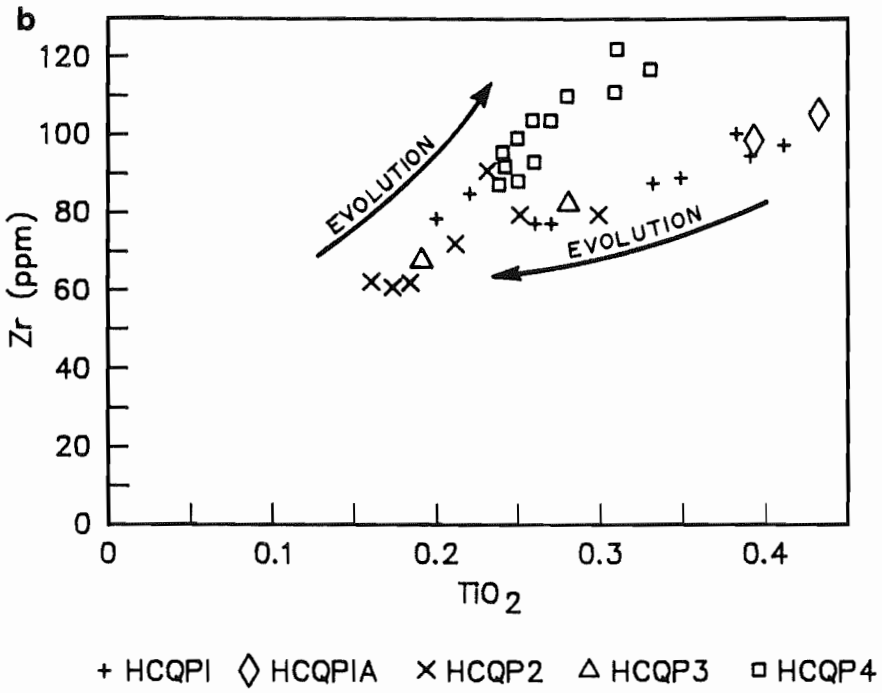

increase in Th and eTh ratios, and the Th-Zr correlation. Additional work is necessary to infer this possibility.

Pagel (1982) indicates that U and Th/U values differ between northern and southern facies of granitic rocks in the Vosges, France and suggests that these factors indicate separate magmatic sources for the granites. This may also be the case in the HCQP. The least evolved units (HCQP1, HCQP1A) and the more evolved units (HCQP2, HCQP3, HCQP4) show two distinct populations with respect to many elements (e.g. Rb, Sr, Zr, $TiO_2$), and have differing U and Th/U values.

Based on the abrupt break in composition, two alternatives are suggested: 1) all the units may not necessarily be from the same magma (i.e. the units represent different pulses of magmatism), or 2) time elapsed after the original intrusion of units HCQP1 and HCQP1A, allowing further evolution of the original magma, before a second intrusive pulse.

## 4.6 Rare Earth Elements

### 4.6.1 Introduction

The rare-earth elements (REE's) refer collectively to the fifteen elements lanthanum (La) to lutetium (Lu) (atomic numbers 57-71). Fourteen of the elements occur naturally, and they tend to occur as a group (Taylor, 1972; Hanson, 1980; Henderson, 1984). These elements display a small but consistent decrease in their ionic radius with increasing atomic number (La radius = 1.14 A, Lu radius = 0.85 A). Because of similar electronic configuration and ionic state (3+), the REE's have similar chemical and physical properties: these similarities make the elements particularly useful for petrogenetic studies. The

light rare earths (LREE's) refer to elements lanthanum to samarium (Sm), with gadolinium (Gd) to ytterbium (Yb) termed the heavy rare earths (HREE).

The REE's occur dispersed within many of the common rock-forming silicate minerals (e.g. feldspars, micas), with a general trend of decreasing abundance with increasing atomic number (Clark, 1984). These elements substitute principally for only one major cation, Ca, with less substitution for Zr, Hf, U and Th. Minerals with large co-ordination number sites (e.g. allanite, monazite) favour LREE, apatite and sphene favour the middle REE, and zircon and garnet preferentially incorporate HREE. The REE's commonly concentrate in residual liquids and pegmatites formed from these liquids can host many REE-bearing minerals (Taylor, 1972; Clark, 1984). Previous studies (Koljonen and Rosenberg, 1974; Hanson, 1980; Gromet and Silver, 1983) have documented REE immobility in the silicate rock systems in the absence of substantial volumes of a suitable fluid (e.g. $CO_2$-rich fluid, metamorphic or metasomatic fluids). Other studies suggest these elements are mobile during late-stage hydrothermal alteration (Alderton et al., 1980; Eugster, 1985; Logothetis, 1985; Strong and Chatterjee, 1985; Kamineni, 1986; Muecke and Moller, 1988).

Europium occurs in both divalent and trivalent states in igneous rocks. Feldspars, particularly plagioclase, preferentially incorporate $Eu^{2+}$ into their structure. On a chrondrite-normalized plot, the plotted Eu concentration in a sample commonly lies away from the trend defined by the other elements, and this departure is called the europium anomaly. If $Eu_{CN}$ exceeds the median value of $Sm_{CN}$ and $Gd_{CN}$, the Eu anomaly is positive, whereas the anomaly is negative if $Eu_{CN}$ is

less than the median value of $Sm_{CN}$ and $Gd_{CN}$. Eu/Eu* indicates the extent of the anomaly, where Eu* is the value obtained by straight line extrapolation between the Sm and Gd values for the sample, and Eu is the europium concentration (Henderson, 1984). Feldspars (especially plagioclase) characteristically display pronounced positive europium anomalies.

Normalizing the REE concentrations in the sample to a chosen reference material (commonly chondrites) proves a useful method of displaying this data. The shape and absolute abundance of REE patterns characterize different granitic rocks (Emmermann et al., 1975; Gromet and Silver, 1986).

Igneous rocks display a wide variety of patterns. REE concentrations often decrease with increasing differentiation in silicic compositions (probably related to fractional crystallization of accessory minerals, such as allanite and sphene, that contain high abundances of the REE's (Taylor, 1972; Cullers and Graf, 1984), with an increased depletion in the HREE (Taylor, 1972; Gromet and Silver, 1983). The SMB and MB display patterns in which the total REE's, the LREE's and the HREE's decrease with differentiation (Muecke and Clarke, 1981; MacDonald and Clarke, 1985). Other works discuss general enrichment of REE's within older to younger granites (Koljonen and Rosenberg, 1974; Haskin et al., 1975; Emmermann et al., 1975).

### 4.6.2 Rare earth elements patterns within the HCQP

Figure 4.14 and Table 4.6 display REE patterns within the HCQP, normalized to chondrites following Haskin et al. (1968), and compared with patterns within the SMB. The HCQP rocks display a 'typical'

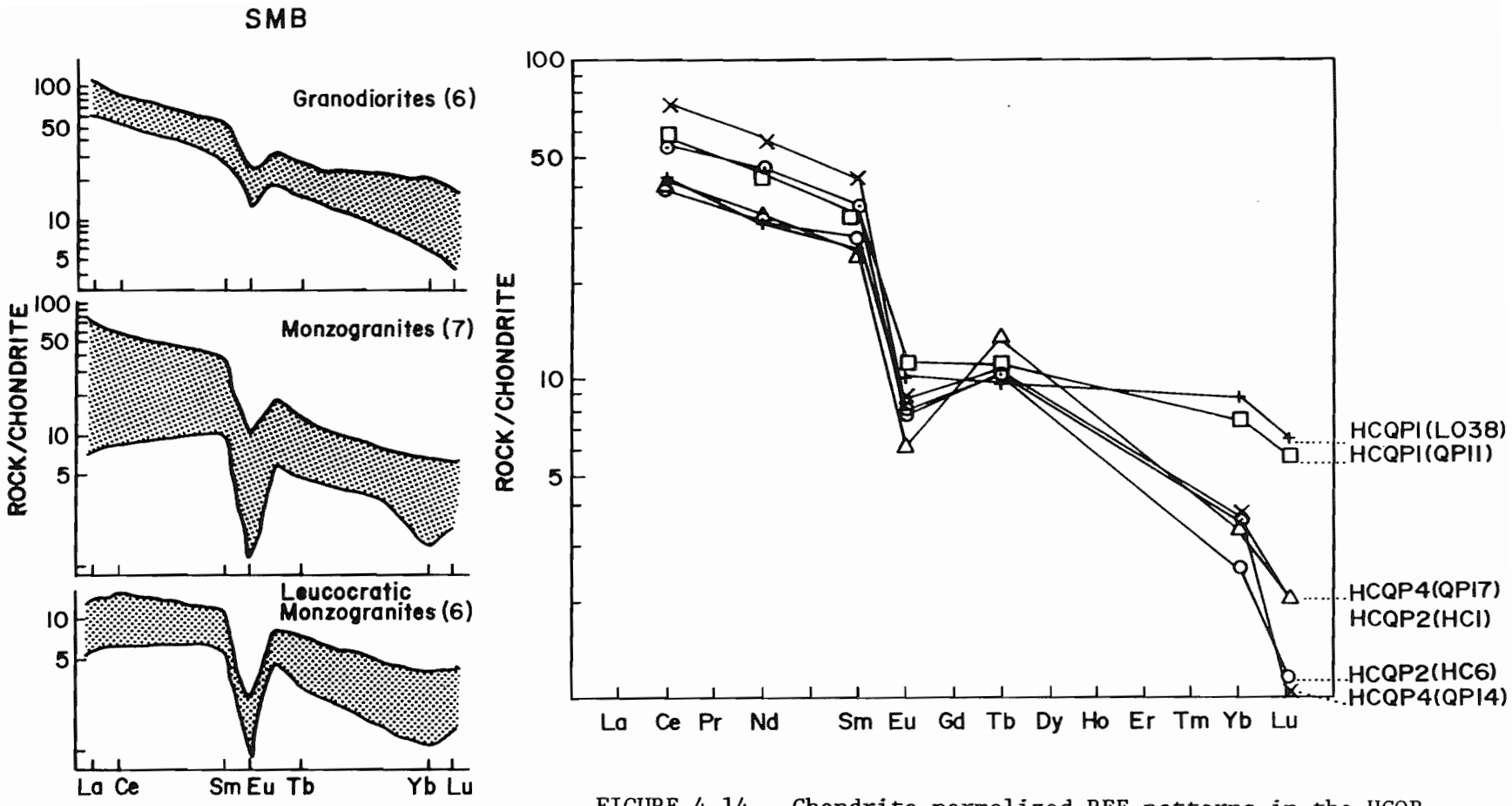


FIGURE 4.14. Chondrite-normalized REE patterns in the HCQP, compared with patterns within the SMB (after Muecke and Clarke, 1981). There is considerable overlap in the LREE's and the middle REE's with all rock units of the HCQP. The more differentiated units (HCQP2 and HCQP4) display greater HREE depletion. The Eu anomalies are much less pronounced than those seen within the SMB monzogranites, and the patterns are more similar to the SMB granodiorites.

TABLE 4.6 Rare earth element abundances of rocks of the HCQP

| | QPL038 | QP11 | QP14 |
|---|---|---|---|
| Ce | 37.84 ±0.08 | 52.72 ±0.16 | 65.27 ±0.15 |
| Nd | 18.27 ±0.18 | 25.95 ±0.15 | 34.06 ±1.06 |
| Sm | 4.76 ±0.05 | 6.01 ±0.06 | 7.71 ±0.07 |
| Eu | 0.70 ±0.00 | 0.79 ±0.00 | 0.60 ±0.00 |
| Tb | 0.46 ±0.00 | 0.52 ±0.00 | 0.56 ±0.00 |
| Yb | 1.79 ±0.01 | 1.67 ±0.02 | 0.77 ±0.30 |
| Lu | 0.23 ±0.00 | 0.20 ±0.00 | 0.03 ±0.01 |

| | HC01 | HC06 | QP17 |
|---|---|---|---|
| Ce | 36.12 ±0.21 | 34.70 ±0.04 | 48.99 ±0.14 |
| Nd | 19.80 ±0.24 | 19.04 ±0.18 | 27.77 ±0.15 |
| Sm | 4.67 ±0.04 | 5.10 ±0.08 | 6.38 ±0.36 |
| Eu | 0.42 ±0.00 | 0.55 ±0.00 | 0.54 ±0.00 |
| Tb | 0.65 ±0.00 | 0.50 ±0.01 | 0.51 ±0.00 |
| Yb | 0.69 ±0.01 | 0.51 ±0.01 | 0.71 ±0.02 |
| Lu | 0.08 ±0.01 | 0.04 ±0.00 | 0.07 ±0.00 |

granitic pattern, with LREE enrichment, small to moderate negative Eu anomalies and depletion of HREE's. The laboratory where the analyses were conducted (Waterloo University) did not analyze for La, making difficult the comparison of absolute numbers and patterns of the REE's with other granitic rocks within the province. However, the rocks of HCQP1 contain a small negative Eu anomaly (Eu/Eu*=0.32 to 0.54), with the size of the anomaly increasing with increased differentiation. Samples from HCQP1 have the largest europium anomaly (.52-.54). The concentrations of the REE's (sum of 7REE) ranges from 109 to 59.39. There is considerable overlap of the LREE and the middle REE between the different rock units. The HREE's are highest in unit HCQP1, and rock units HCQP2 and HCQP4 are HREE depleted.

The patterns of HCQP1 broadly correspond to the granodiorite patterns of the SMB. The patterns from HCQP2 and HCQP4 are different, both from the HCQP1 patterns and from patterns of both the granodiorites and the monzogranites of the SMB. The LREE levels within HCQP2 and HCQP4 generally are similar to those of both the SMB and HCQP1, but the europium anomalies from HCQP2 and HCQP4 are not as pronounced as those seen within the SMB, and the HREE values within HCQP2 and HCQP4 are considerably depleted, particularly Lu.

The differences in the patterns of the rocks of the HCQP suggest that the postulated processes involved in the SMB (i.e. fractional crystallization of granodiorite to monzogranite, followed by fluid stripping in leucomonzogranite) were not similar to processes acting in the HCQP to produce the more evolved units (HCQP2, HCQP3 and HCQP4) from the least evolved units (HCQP1 and HCQP1A). These marked

differences in the patterns from HCQP1 and the other phases suggest that the units may have been derived from different sources.

Rocks within the more evolved units of the HCQP have slightly elevated levels of F over the least evolved units, suggesting some fluid interaction. These levels are, however, extremely low compared with F-rich rocks and rocks that have undergone extensive fluid interaction (i.e. the Davis Lake leucogranite of East Kemptville, Richardson et al., 1982, Kontak, 1987). As previously discussed, although there is some evidence for alteration and/or metasomatism (e.g. turbid feldspars, albitic plagioclase, rapakivi textures), these processes did not play a major role in the HCQP, suggesting that the fluid interaction was minimal and F-rich fluids were not involved.

## 4.7 Summary of Geochemistry

The HCQP plots well within the N.S. database classification of 'northern' plutons (Richard, 1988), similar to the SMB, MB and other eastern Meguma Terrane granitoids. Rocks of the HCQP, particularly HCQP2, HCQP3, and HCQP4, display characteristics more similar to the eastern plutons, MB and HP than to the SMB. Units HCQP1 and HCQP1A, however, have characteristics more similar to the SMB (lower $P_2O_5$, lower $K_2O$, higher MnO, CaO, $FeO_t$, MgO and $TiO_2$, compared to the other units). The HCQP rocks, in general, display higher $P_2O_5$, normative corundum and A/CNK ratios than the SMB. MacDonald (1981) observed these chemical features in the MB.

A well-developed geochemical separation exists between units HCQP1 and HCQP1A and the other three units in a number of elements. Most major elements, normative corundum, TTDI, Rb, Sr, K/Rb, $P_2O_5$, and Ba

all show two distinct populations. The REE patterns also underline this difference between the less evolved units and the three more evolved units. HCQP2, HCQP3 and HCQP4 may, in fact, represent a more differentiated magma, or a separate magma pulse. Different source regions are suggested for granites from France which have different elemental values (e.g. Th and U).

HCQP2 and HCQP4 often have conflicting degrees of differentiation. HCQP2 displays higher Rb, higher $P_2O_5$, lower of CaO, $FeO_t$, MgO, and anorthite component, suggesting that it is the more evolved. However, HCQP4 has higher values of Rb, lower K/Rb ratios, and higher values of Th, Zr, F, and Th/U ratios. HCQP2 and HCQP4 are similar in other mineralogical and petrological respects (e.g. grain size, modal mineralogy) and may, in fact, be co-magmatic.

Reasons for the unique elevated Th and eTh responses in HCQP4 might be explained by HCQP4 representing a separate magma pulse, as suggested by a number of the major and trace elements. One study determined different or low levels of U within several zircon populations (Gulson and Krogh, 1975), and explained the zircon characterstics by separate intrusions and/or magma sources. A positive correlation of Zr-Th within HCQP4 might suggest different levels of U and Th within the zircon structure.

Rare earth element patterns within Unit HCQP1 patterns are generally similar to the granodiorite patterns of the SMB, but units HCQP2 and HCQP4 patterns are different, both from those of the HCQP1 from the SMB. These differences suggest that the processes postulated for granodiorite to monzogranite to leucomonzogranite development within the SMB (i.e. fractional crystallization, followed by fluid

stripping; Muecke and Clarke, 1981) were not similar to processes operating within the HCQP. Additionally, these differences may suggest a different source region or a different magma pulse for HCQP2 and HCQP4.

Using a ternary diagram of Qtz-Ab-Or, pressure during the time of cooling for the HCQP is suggested to be approximately 4 kbars, as the least evolved units lie on the trend of piercing points for this pressure. Pressure determinations in granitic rocks is never very precise because of the uncertainties (e.g. water saturation of the magma), but approximate pressures involved during crystallization can be inferred. This pressure is slighly higher than that determined for the SMB, and similar to pressures suggested for the MB.

# CHAPTER 5 - ECONOMIC GEOLOGY

## 5.1 Introduction

The granites of southern Nova Scotia have recently invoked considerable interest from both economic and exploration viewpoints, because of their geochemical and mineralogical similarities to mineral-bearing (Sn-W-U) granites world-wide (e.g. France, Portugal, Thailand, Malaysia, Czechoslovakia, Bolivia). The SMB hosts numerous poly-metallic (Sn-W-Mo-U-Zn-Cu-Mn) mineral occurrences, many of which are associated with later-stage leucocratic monzogranites. Notable among these occurrences are the East Kemptville tin mine (Richardson et al., 1982; Kontak, 1987) and the Millet Brook uranium showing (Chatterjee et al., 1982). To the east, the MB contains relatively few mineral occurrences (e.g. Dunbrack Pb-Zn-Ag deposit and several minor sulphide showings listed in MacDonald, 1981) and the Sangster Lake pluton contains no visible mineralization, but has a high U radiometric response (Ford and O'Reilly, 1985).

## 5.2 Economic Potential of the HCQP

### 5.2.1 Introduction

Compared with the SMB and the MB, the HCQP is generally similar in mineralogy, petrology, geochemistry, mode, time and depth of emplacement (McKenzie, 1974; McKenzie and Clarke, 1975; MacDonald, 1981). However, there are also profound differences (e.g. low contents of volatile and LIL trace elements (F, Cl, Li, B), and lack of differentiated units, such as leucogranite and leucomonzogranites). There

are no economic mineral showings present within the HCQP, as discussed in Chapter 1 (Section 1.4).

### 5.2.2 Geochemical characteristics of ore-bearing granites

Granites associated with Sn-W deposits are usually considered to be highly differentiated, "S-type" granitoids (Taylor, 1979; Ishihara, 1981). Tischendorf (1977) proposed a geochemical and petrological classification for granitic rocks associated with mineralization. Table 5.1 outlines the characteristics of these granites, and compares the HCQP with other granitoid bodies, both mineralized and barren, within southern Nova Scotia. The HCQP satisfies only four of nine criteria, while the SMB and East Kemptville Leucogranite (EKL) satisfy almost all the criteria, and the MB and Sangster Lake pluton (SLP) satisfy six or seven characteristics.

Several authors (e.g. Burnham and Ohmoto, 1980; Eugster, 1985) discuss the geochemical evolution and processes involved with Sn-W and associated sulphides deposits within granitic rocks. These authors divide the processes into different stages, beginning with magma generation, and culminating with incorporation and deposition of the ore minerals. High concentrations of volatile elements, particularly F and Cl, within hydrothermal fluids are postulated to be critical for ore deposit development (Tischendorf, 1977; Gunow et al., 1980; Manning and Pichavant, 1985). Eugster (1985) suggests that the crucial difference between mineralized and barren granites is the presence (or absence) of NaCl in high concentrations in the fluid phase.

TABLE 5.1 Comparison of characteristics of Tischendorf's (1977) classification for granite-hosted rare element mineralization and selected granitoid plutons of southern Nova Scotia.

| Characteristics | SMB[1] | EKL[2] | MB[3] | Sangster Lake pluton[4] | HCQP |
|---|---|---|---|---|---|
| middle to late stages of orogeny (post-tectonic) | Yes | Yes | Yes | Yes | Yes, with respect to 400 Ma deformation, but syn-tectonic with respect to 370 Ma shearing |
| pronounced sialic magmatism, true intrusive character | Yes | Yes | Yes | Yes | Yes |
| polyphase intrusive complex | Yes<br>-numerous rock types<br>-leuocogranite developed | No, but highly evolved end-member (topaz granite) | No, less variable than SMB<br>-no leucogranite developed | No, less variable than SMB<br>-leucogranite developed | No, less variable than SMB<br>-minor leuco-granite developed |
| confinement to apical portions of main batholith and having undulatory roof morphology | Yes<br>-in places | Yes | Yes<br>-near roof in places | Yes | Possibly<br>-local concentrations of xenoliths suggest proximity to roof in places |
| increase in granitophile elements (F, Li, Rb, Sn, Be, W)<br>(SEE ADDITIONAL TABLE) | Yes | Yes<br>-anomalously high Rb, Li, F, Nb, U, Y, Sn, Y, Sn, Ga, P | Yes | Yes<br>-slight | none to slight enrichment in some elements |
| association of accessory minerals (e.g. fluorite, cassiterite, topaz, tourmaline, columbite, beryl, tantalite) | Yes | Yes<br>-topaz occurs as probable magmatic phase<br>-rare-metal | minor amounts of tourmaline | minor amounts of topaz, tourmaline | trace amount of tourmaline |

| | | | | | |
|---|---|---|---|---|---|
| unusual sequence of crystallization | minor in late-stage rocks | Yes | No | No | No |
| presence of late-stage auto-metasomatic microlinization, muscovitization, albitization | Yes | Yes | No | Yes | No |
| post-magmatic greisenization | Yes<br>-well-developed in places | Yes<br>-well-developed in places | Yes<br>-minor | Yes<br>-minor | No |

1 data from McKenzie (1974)
2 data from Kontak (1987)
3 data from MacDonald (1982)
4 data from O'Reilly (1984)

5.2.3 Characteristics of the HCQP

Table 5.2 tabulates the geochemical features of mineralized granites, according to Tischendorf (1977), and compares the HCQP and other Nova Scotian granites. Although selected major element data of the HCQP ($TiO_2$, $Al_2O_3$, MnO, MgO, $Na_2O$, $K_2O$) are similar to those of specialized granites both world-wide and within Nova Scotia, the volatile and trace element contents within the HCQP are substantially lower (F values range from 330 to 1075 ppm, Li values from 68 to 114 ppm, Rb values from 163 to 285 ppm). This compares unfavourably with the anomalously enriched EKL (F: 11500 ppm; Li: 360 ppm; Rb: 965 ppm). Additionally, the Sn and W values (both 1-10 ppm) within the HCQP are low for mineralized granites (e.g. Taylor, 1979). All of the above features, particularly the low volatile element contents, suggest that the mineral-bearing potential of the HCQP is limited. The rocks of the HCQP also clearly plot within the non-specialized field (seen in Figure 4.8) for granites.

Several other factors and geochemical characteristics are indicative, or suggest the presence, of mineralization within granitic rocks. The factors include:

1) mineralogical evidence (e.g. mineral recrystallization, new mineral development) of fluid interaction (Burnham, 1979; Pollard, 1983; Taylor and Pollard, 1985). The presence of albite, albitic rims, rapakivi texture (particularly within HCQP4) and some development of secondary minerals (i.e. muscovite) could suggest a limited amount of alteration (metasomatism) within these later-stage rocks;

2) chemical evidence, such as: a) fluid 'stripping' of elements such as the REEs (Alderton et al., 1980; Muecke and Clarke, 1981; Baker,

TABLE 5.2 Representative chemical analyses of selected felsic igneous rocks within southern Nova Scotia, compared with Tischendorf's classification (1977)

| | Tischendorf | SMB | | EKL | MB | | SLP | | HCQP | |
|---|---|---|---|---|---|---|---|---|---|---|
| | | 1 | 2 | 3 | 4 | 5 | 6 | 7 | 8 | 9 |
| $SiO_2$ | 73.38 ±1.39 | 69.40 | 75.80 | 73.06 | 72.06 | 73.60 | 73.23 | 73.73 | 70.30 | 71.48 |
| $TiO_2$ | .16 ±0.10 | .61 | .13 | .02 | .28 | .17 | .20 | .05 | .31 | .26 |
| $Al_2O_3$ | 13.97 ±1.07 | 14.36 | 12.65 | 14.62 | 14.57 | 14.68 | 14.63 | 14.89 | 15.11 | 14.88 |
| $Fe_2O_3$ | .80 ±0.47 | .44 | 1.75 | 1.25 | -- | -- | .01 | .02 | 1.67 | 1.66 |
| MnO | .045±0.04 | .10 | .04 | .06 | .06 | .09 | .04 | .05 | .08 | .05 |
| MgO | .47 ±0.56 | 1.02 | .18 | .03 | .53 | .24 | .46 | .08 | .69 | .42 |
| CaO | .75 ±0.41 | 1.93 | .67 | .52 | .86 | .32 | .66 | .55 | 1.34 | .70 |
| $Na_2O$ | 3.20 ±0.61 | 3.29 | 3.41 | 3.68 | 3.52 | 4.17 | 3.52 | 4.58 | 3.48 | 3.58 |
| $K_2O$ | 4.69 ±0.68 | 3.86 | 4.08 | 3.81 | 4.60 | 4.04 | 4.60 | 3.43 | 4.32 | 4.69 |
| $P_2O_5$ | ---- | .10 | .11 | .57 | .29 | .34 | .29 | .59 | .15 | .26 |
| F | 3700 ±1500 | -- | 3318 | 11500 | -- | -- | 633 | 467 | 574 | 869 (n=1) |
| B | --- | -- | -- | <10 | -- | -- | 24 | 19 | 17 | <15 |
| Li | 400 ± 200 | -- | 146 | 360 | 182 | 97 | 156 | 69 | 83 | 93 (n=5) |
| Rb | 580 ± 200 | 147 | 700 | 965 | 294 | 503 | 231 | 404 | 197 | 283 |
| Sn | 40 ± 20 | 12 | 31 | 57 | -- | -- | 7 | 23 | 7 | 8 (n=13) |
| Ba | --- | 667 | 73 | n.d. | 253 | 15 | 219 | 17 | 381 | 434 |
| Zn | --- | -- | -- | 28 | 54 | 25 | 54 | 19 | 55 | 67 |
| U | --- | -- | 23 | 25 | 5.8 | 16.6 | 4.5 | 15.7 | 5.7 | 3.7 |
| Th | --- | -- | 25 | 5 | 5.8 | 2.8 | 7 | 1.4 | 10.8 | 17.8 |

1. granodiorite, SMB McKenzie and Clarke (1975) n=11
2. Davis Lake leucogranite Chatterjee et al. (1983) n=94
3. East Kemptville leucogranite Kontak (1987) n=13
4. monzogranite, Musquodoboit batholith MacDonald (1981) n=7
5. dyke rocks, Musquodoboit batholith MacDonald (1981) n=3
6. monzogranite, Sangster Lake pluton Ford and O'Reilly (1985) n=4
7. leucogranite, Sangster Lake pluton Ford and O'Reilly (1985) n=5
8. Unit 1, HCQP n=9
9. Unit 4, HCQP n=14

1985; Giuliani et al., 1987); or, b) unusual elemental ratios (e.g. low K/Rb, high $Na_2O/K_2O$). The REE values and patterns (Fig. 4.14) of HCQP1 are similar to granodiorite from the SMB. The patterns of HCQP2 and HCQP4, although different from HCQP1, are unlike those of the leucogranites of the SMB, suggesting that there has been little fluid stripping or remobilization of the elements, such as that postulated by Muecke and Clarke (1981) based on REE patterns within the leucogranites of the SMB. Elemental ratios within the HCQP suggest little fluid interaction, as the K/Rb ratios are high (avg. 200). The ratio $Na_2O/K_2O$, which may reflect varying degrees of metasomatism (Ford and O'Reilly, 1985), is generally constant in all phases of the HCQP (average 0.76), and compares with values of 0.78 (least evolved rocks) to 1.34 (more evolved rocks) in the SLP (Ford and O'Reilly, 1985); and, 3) textural evidence (e.g. alteration, greisenization) of fluid interaction. Within the HCQP, there is virtually no greisenization. Alteration is moderate, with minor hematization and alteration of minerals (biotite, feldspars).

## 5.3 Additional Economic Considerations

Within Nova Scotia, there is currently a building stone study underway to examine different rock types (e.g. sandstone and granite) for qualities that are acceptable for monumental and building cladding purposes (Dickie, 1986; 1987). Such qualities for granitic rocks include a pleasing appearance, a compact nature and lack of fractures and joints. The HCQP rocks have such characteristics, and a quarry was worked in the past in the Queensport lobe (Stevenson, 1964).

## 5.4 Summary

The geochemical and petrographic characteristics of the HCQP, compared with mineralized or specialized granites within Nova Scotia and world-wide, suggest that the mineral-bearing potential of the body is limited. Some of the economically significant characteristics that are lacking within the HCQP include: the presence of considerable leucomonzogranite, leucogranite, greisen or pegmatite; evidence of extensive hydrothermal alteration or fluid interaction; high volatile contents (e.g. F, Cl), and enrichment of LIL trace elements. However, the building stone potential for these rocks is good, suggested by the compactness, colour and appearance of the rocks.

# CHAPTER 6

# PETROGENESIS, CONCLUSIONS AND RECOMMENDATIONS FOR FUTURE WORK

## 6.1 Introduction

The HCQP is composed predominantly of two-mica monzogranite, with minor amounts of granodiorite and late-stage intrusions (aplites and pegmatites). The pluton is two-lobed, with two rock units (HCQP2 and HCQP3) in the western lobe (the Halfway Cove lobe), and three units (HCQP1, HCQP1A, and HCQP4) in the eastern portion (the Queensport lobe). The east-west trending Cobequid-Chedabucto fault zone to the north of the pluton has deformed and sheared both the granitic and the metasedimentary rocks closest to the fault. A small shear zone to the south of the pluton has deformed the rocks in the southern portion of the Queensport lobe.

Mineralogically, the pluton differs from the larger SMB, MB, and other smaller plutons in the southwestern portion of the province in that muscovite and biotite (+/- garnet) are the only AFM minerals. In other plutons, cordierite, aluminosilicates and garnet are common.

## 6.2 Mode of Emplacement

Where exposed, the HCQP is characterized by sharp granite/ metasedimentary contacts. Enclaves occur throughout the pluton, with local areas (e.g. Lundy fire tower) containing high concentrations. The least assimilated of the enclaves resemble Meguma Group metasedimentary strata in appearance and bedding characteristics and are, therefore, probably xenoliths of the Meguma Group formations.

Some deformation in the Meguma Group rocks may be related to the intrusion of the HCQP. The metasedimentary rocks on the eastern side of the QP lobe appear to diverge and wrap around the pluton to the north and south. The results of an airborne magnetic survey (Fig. 2.7) show a separation and bending of the metasedimentary patterns around the pluton. These features suggest some degree of dynamic, forceful emplacement. Minor granitic dykes occur along bedding planes of the metasedimentary country rocks. A thermal metamorphic aureole is superimposed over the regional metamorphism, i.e. development of cordierite and andalusite (hornblende-hornfels facies) over middle amphibolite. Therefore, from all of these observations, the HCQP was emplaced both by passive stoping, primarily as a liquid (or a 'crystal-mush' which behaved as a liquid) granitic body into previously deformed and metamorphosed Meguma Group metasedimentary rocks, and by dynamic, forceful emplacement. Hill (1986, 1988) reached similar conclusions for the emplacement of granitic plutons to the east of the HCQP.

The aplite and pegmatite dyke rocks have both sharp intrusive and gradational contacts with their monzogranite hosts. The late-stage intrusive rocks with sharp contacts probably represent emplacement along fractures in a brittle, semi-cooled host, whereas the others may represent metasomatic veins.

## 6.3 Depth of Emplacement

The depth of emplacement of the HCQP can be deduced using only a few petrological and geochemical features of the body. Some of these features and observations follow.

Both McKenzie (1974) and MacDonald (1981), following criteria outlined by Buddington (1959), concluded that features such as sharp discordant granite/metasedimentary contacts, intrusion of granite into low-grade metasedimentary rocks, granophyric texture, miarolitic cavities and turbid feldspars (the latter three features suggesting the presence of a vapour phase) represent emplacement into high crustal levels, corresponding to the epizone (i.e. 4-10 km) level of Buddington (1959). Turbid feldspars and sharp, discordant granite/metasedimentary rock contacts are observed also in the HCQP, although the metamorphic grade of the metasedimentary country rock for the HCQP is higher than the grade of the metasedimentary country rock for the SMB. Miarolitic cavities were not common, being present only in some aplite dykes, and granophyric textures were not observed, suggesting the lesser role of a vapour phase. These observations suggest that the level of emplacement for the HCQP is lower epizone to mesozone.

The presence of andalusite and sillimanite, both of which are generally the same age as the pluton, in regional metamorphism suggests a maximum pressure of 3.8 kbars (Holdaway, 1971; Holdaway and Lee, 1977).

A normative Qtz-Ab-Or ternary diagram (Fig. 4.4) provides additional evidence for depth of emplacement. Although there are problems with such a plot (e.g. water saturation of magma is required), a general approximation of pressures can be determined. The least evolved rocks of the HCQP lie on the trend of piercing points for a pressure of approximately 4 kbars.

Primary muscovite in granites constrains the minimum pressure conditions prevailing during evolution to 2.6-3.1 kbar (Anderson and

Rowley, 1981, Miller et al., 1981), with corresponding temperatures of 650-680°C. However, if the magmatic muscovite is non-ideal in composition, then the pressure constraints are lowered. If the muscovite is secondary in origin, the lower pressure and temperature constraints would be removed. Based principally on texture, primary muscovite is believed to occur within the HCQP (Chapter 3). AFM (A = $Al_2O_3$-$K_2O$-$Na_2O$-CaO, F = FeO, M = MgO) liquidus projections for muscovite granites devised by Abbott (1985) are displayed in Figure 6.1. The muscovite-biotite mineral assemblage of the HCQP corresponds to the shaded field of Figure 6.1, suggesting minimum pressure of 3.5-4 kbars and temperatures of 650-725°C. These pressures prevailing during crystallization of the HCQP were similar to those of the SMB and MB (pressures of 3-6 kbar; Abbott and Clarke, 1979; MacDonald, 1981). Ham and Kontak (1988), using trace element chemistry from muscovite mineral separates from different rock units and recently published experimental data of Monier and Robert (1986) for muscovite solid solution chemistry, suggest lower pressures (as low as 2 kbar, or 6-8 km depth of emplacement) may have prevailed for the SMB. Both Thompson (1982) and Abbott (1985) concluded that, with increasing pressure, the AFM liquidus field for muscovite expands and effectively eliminates the liquidus fields for the other AFM minerals (cordierite, aluminosilicate, garnet). These slightly higher pressure conditions prevailing during crystallization of the HCQP may explain the absence of the other AFM minerals.

Garnet occurs as a minor constituent within the groundmass of HCQP2, and in some aplite and aplite-pegmatite dykes within the HCQP. Green (1977) showed that low Ca and Mn garnet is stable in silicate

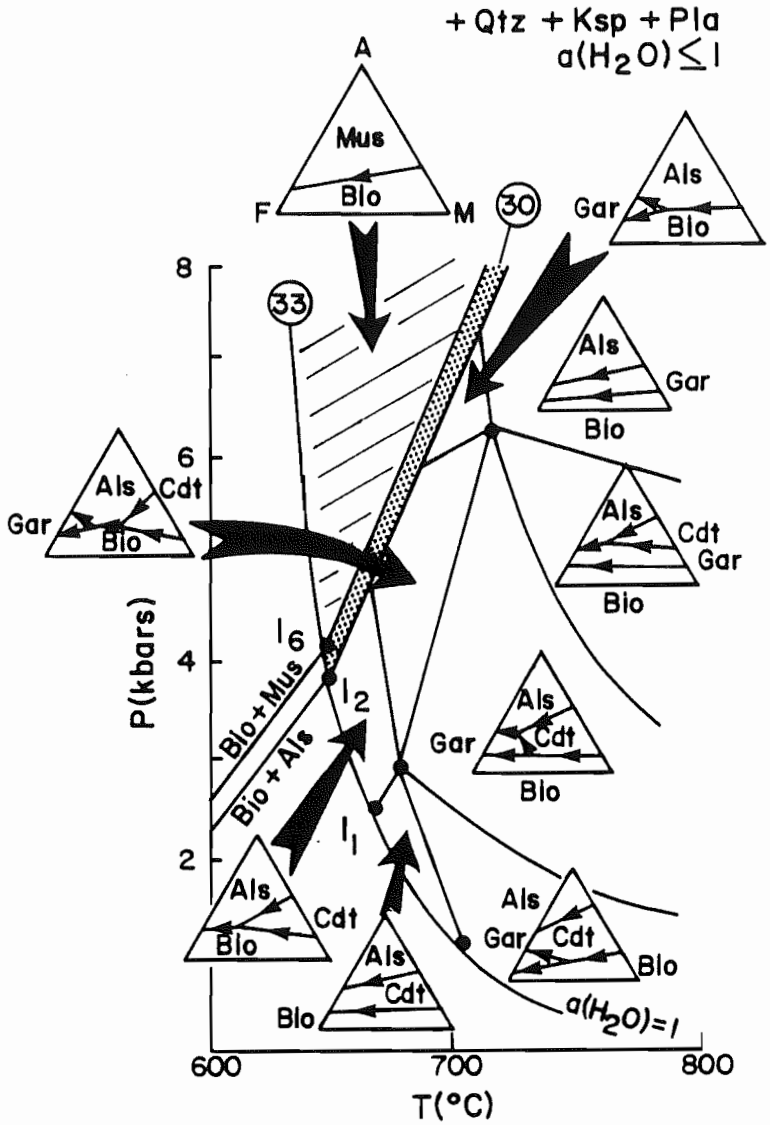


FIGURE 6.1. A P-T diagram for various AFM liquidus topologies (after Abbott, 1985), giving minimum pressures and temperatures for individual mineral assemblages. The HCQP contains muscovite and biotite (+/- garnet), and corresponds with $I_6$ and the shaded area.

liquids from 7-10 kbars. Abbott (1985) suggests that the appearance of garnet results from strong partitioning of $Mn^{2+}$ into the liquid relative to muscovite and biotite. If MnO is added to the system (e.g. by adding pelites from the surrounding country rock), Mn-rich garnet becomes stable in silicate liquids down to approximately 3 kbars (Green, 1977). Garnet within the HCQP is high in Mn, and it is suggested that the minimum pressure in the HCQP is 3 kbar.

Using standard pressure/depth relationships, the HCQP was emplaced at a depth of approximately 10.5-14 km. This value suggests deeper levels of emplacement (i.e. lower epizonal to mesozone regions of the crust; Buddington, 1959) than that suggested for the SMB (4-10 km; McKenzie and Clarke, 1975) and more similar to those levels suggested for the MB (11.5-15 km; MacDonald, 1981).

## 6.4 Petrogenesis of the HCQP

### 6.4.1 Introduction

This section will examine the possible petrogenetic relationships among the five units defined in the HCQP. Much of the major and trace element data of the HCQP show distinct fields for the least evolved units (HCQP1 and HCQP1A) and the three more evolved units (HCQP2, HCQP3 and HCQP4). This well-developed separation can be explained by several processes, including: 1) a time break, which allowed further evolution of magma; 2) a difference in source region, and 3) a sampling bias, which additional sampling may occupy. The first two processes will be discussed in following sections. The third possibility is probably negligible because representative geochemical samples were collected throughout the HCQP with good geographic, mineralogical and textural

coverage. Any model proposed must explain this well-developed separation between the two units and the three more evolved units, and must also explain the two distinct trends seen with selected trace elements ($TiO_2$, Zr, Th) among four units (HCQP1 to HCQP3) and HCQP4.

Several models and processes are suggested for the chemical evolution of granitic plutons, including: 1) fractional crystallization; 2) restite unmixing; 3) batch melting; 4) assimilation of country rock; 5) separate sources, and 6) role of fluids (described in Section 5.2.3).

### 6.4.2 Fractional crystallization

Fractional crystallization of plagioclase and biotite can account for much of the variation within the rocks of the SMB (McKenzie and Clarke, 1975). In addition, the continuous chemical trends suggest that all rocks are the product of a single magma differentiating through time. Characteristics of the HCQP which favour fractional crystallization are: 1) general decrease in both plagioclase and biotite (Fig. 2.2 and Fig. 2.3) from units HCQP1 and HCQP1a to units HCQP2, HCQP3 and HCQP4, and 2) generally similar trends, shown by major and trace element contents (Fig. 4.2a-i, Fig. 4.7) from HCQP1, 1A to units HCQP2, HCQP3 and HCQP4, to those expected in a normal differentiation trend. However, evidence against a simple fractional crystallization model are: 1) trends are not continuous (i.e. show a well-developed separation) from units HCQP1 and HCQP1A to units HCQP2, HCQP3 and HCQP4 (Fig. 4.2a-i, Fig. 4.3, Fig, 4.7); 2) trace elements (Ti, Zr, Th, Ba), although generally following normal differentiation (i.e. decreasing) trends for units HCQP1 to HCQP2 and HCQP3, show

markedly different trends for HCQP4 (Fig. 4.9, Fig. 4.10, Fig. 4.13); and 3) units HCQP2, HCQP3 and HCQP4 often exhibit overlapping trends in both major and trace elements (Fig. 4.2a-i, Fig.4.7, Fig. 4.13). These characteristics suggest that units HCQP2 and HCQP3 may, in fact, have evolved from HCQP1 and HCQP1A, and may be co-magmatic with each other, but HCQP4 does not appear to represent the product of simple fractional crystallization from the other units.

A time delay could have occurred between the intrusion of the two less evolved units and the three more evolved units. This delay could result in compositional bimodality in the presently exposed rocks; the intermediate products may be at a deeper level. Isotopic work would be necessary to resolve this interpretation.

### 6.4.3 Restite unmixing

White and Chappell (1977) proposed a model of "restite unmixing" to explain geochemical and mineralogical characteristics of granitoids and their inclusions. This model suggests that most granitoid magmas are composed of variable amounts of liquid (granitic melt) and solid (restite - melt-depleted source material) components which separate to varying degrees of produce the chemical variations observed in plutonic bodies. Granites which form by restite unmixing, according to these authors, will have: 1) linear trends of major and trace elements on Harker variation diagram; 2) inclusions (enclaves, interpreted as restite) which are more abundant in mafic members of granitoid suites; 3) 99% of xenoliths are of relict source rock material; 4) biotite, aluminosilicates, garnet, and cordierite are refractory residua after

partial melting of source rock, and 6) milky white quartz inclusions, which result from vein quartz of high-grade metamorphic terrains.

Clemens et al. (1983) and Wall et al. (1987) present numerous arguments against the restite model, based on mineralogical, textural and chemical evidence. Examples of some of these arguments include: 1) Variation in elemental concentrations with $SiO_2$ in many granitoid suites is decidedly non-linear. Wall et al. (1987) demonstrate also that other mechanisms can produce similar patterns of variation. 2) Textures of enclaves within granitic rocks commonly indicate magmatic crystallization. Enclaves within granitic bodies can have a variety of origins (e.g. wall rock, granitic) and not be representative of restite material as postulated by White and Chappell (1977). Also, the chemistry of many enclaves is not compatible with the granitoid host. 3) Enclaves commonly are not representative of high-grade, regionally metamorphosed terrains of upper amphibolite to granulite facies, and those representative of these terrains do not comprise 99% of the total enclave abundance. 4) Minerals such as garnet, cordierite, biotite and aluminosilicates, suggested to be restite, often have euhedral shapes and few inclusions and are demonstrated to be products of magmatic crystallization. 5) Milky quartz inclusions included within granitic rocks can have a variety of origins, including remains of quartz veins, remnants of xenoliths or vein from a xenolith, remains of pegmatitic quartz, or represent precipitation of quartz in a cavity.

Within the HCQP, whole-rock chemical plots generally do not exhibit well-defined linear trends. Minerals which White and Chappell (1977) suggest are restite minerals (e.g. biotite, garnet) are believed to be of magmatic origin in the HCQP. Enclaves, though not abundant,

are dispersed throughout the pluton and are not concentrated in the more mafic units. These enclaves generally resemble rocks of the Meguma Group, and are not suggestive of high-grade, regionally metamorphosed terrains. Milky quartz inclusions occur within the HCQP, but can be explained as late-stage precipitation of quartz in cavities. These features suggest that restite unmixing was not an important process in the HCQP.

### 6.4.4 Batch melting

Batch melting involves the progressive partial melting of a single source region, with repeated removal of the liquid fraction from the solid (Pitcher, 1979). The initial rock formed under these conditions will be the most evolved and contain the highest levels of volatile and LIL concentrations. Within the HCQP, field observations are not conclusive as to which unit(s) is/are older. However, aplite and pegmatite dykes cross-cut the other (older) units, suggesting that the most evolved magma (i.e. aplite and pegmatite) was not the earliest. Field relations in the Queensport lobe, also show an inward gradation from granodiorite to biotite monzogranite, with muscovite-biotite monzogranite in the core of the body, suggesting that granodiorite and biotite monzogranite are the initial rock units. Although these features are not definitive, they suggest that batch melting from the same source was not an important process in the HCQP.

### 6.4.5 Assimilation of country rock

It is unlikely that the a granite would completely incorporate large volumes of xenolithic material (Pitcher, 1979), based on physical

and chemical constraints (e.g. heat necessary to melt the material), but assimilation by Meguma Group country rocks may be partially responsible for the development of the HCQP. Xenoliths of presumed Meguma Group origin occur in various degrees of assimilation in several areas throughout the HCQP. Partial assimilation, as seen by rounded xenoliths and other features (biotite schlieren, mafic clots) which may represent remnant xenoliths, has occurred throughout the HCQP. If xenolith assimilation were an important factor in the HCQP, trends shown by major element contents (e.g. Na, Fe) should reflect this interaction with the metasedimentary rocks. The Fe content should increase with assimilation of the Fe- and sulphide-rich Meguma Group and the Na content should decrease. However, within the rocks of the HCQP, the Fe content decreases from units HCQP1 to HCQP4 and the Na content remains virtually constant. These trends are similar to those seen within other granitoid bodies (e.g. SMB, MB) where assimilation of xenoliths has been proven (e.g. isotopic work) to be negligible. Trace elements, such as $TiO_2$ and Zr, exhibit a normal decreasing differentiation trend in granitic rocks and in units HCQP1 to HCQP3, but are elevated in HCQP4. Both the Ti and Zr contents of the Meguma Group rocks are higher (approximately 0.50-0.70 wt. % Ti and 130-200 ppm Zr; Smith, 1984; pers. comm.) than the values in the HCQP. These characteristics suggest that assimilation of Meguma Group rocks may have been negligible in all units except possibly HCQP4. If true, the absence of enclaves (xenoliths) from this unit suggests that the assimilation of Meguma material may have been complete.

### 6.4.6 Separate sources

Trace element data (e.g. $TiO_2$, Zr, Th) outline two distinct trends within the HCQP (Fig. 4.13). One trend, which generally decreases with evolution, is outlined by units HCQP1 to HCQP3. A second trend, represented by the rocks of unit HCQP4, of increasing $TiO_2$, Zr, and Th, is contrary to those trends normally found within a differentiation sequence. Chemical characteristics, such as Eu/Eu*, suggest that HCQP1 and 1A cannot simply represent the host magma (plus feldspar) to units HCQP2, HCQP3 and HCQP4. If units HCQP1 and 1A did represent the host magma, the europium anomaly should become more pronounced in units HCQP2, HCQP3 and HCQP4, and this is not the case in the rocks (Fig. 4.14). Gulson and Krogh (1975) determined two populations of zircon within granitic rocks in Greenland and, based on the different uranium and thorium contents within the zircon, suggested that these characteristics reflected different source regions. Computer-enhanced airborne radiometric images (Hill, pers. comm.) display several markedly different colours over the HCQP. The HC lobe is fundamentally the same colour, but the QP lobe displays two colours, both of which are different from the HC lobe. These patterns suggest that the HC and the QP lobes are fundamentally different in composition, and that within the QP lobe, there are additional differences. These characteristics could represent separate magma sources.

### 6.4.7 Summary

The chemical separation (major, trace and rare earth elements) suggests that more than one magma was involved in the HCQP. The

intrusion of similar granites (mineralogically, texturally, chemically) in the same area (HCQP2, HCQP3) implies a co-genetic relationship. Fractional crystallization of HCQP1 and HCQP1A is not postulated to be an important process in the HCQP, based on the non-continuous trends of the elements. A time delay may explain these different trends, but isotopic work is necessary to resolve this problem. Restite unmixing and batch melting are also not believed to be important processes. Assimilation of country rock may have had a role in the development of the HCQP, although major element data such as Fe, Na do not support this interpretation. Several lines of evidence (airborne radiometric images, trace element data exhibiting different trends) suggest that the HCQP may represent intrusion of two or more batches of magma from heterogeneous source regions. Hill (1986, 1988) suggests such processes occurred in the development of the granites to the east of the HCQP.

## 6.5 Source of Magma

Several chemical classification schemes, suggested to identify source material for granites by their chemical characteristics, employ mineralogy and major and trace element characteristics of the granites. Chappell and White (1974) divide granites into "S-type" (sedimentary source) and "I-type" (igneous source). Additionally, a sub-group of the "I-type" granites involve "A-type" granites (alkaline or anorogenic: Loiselle and Wones, 1979; Whalen *et al.*, 1987). However, although some features of granitoid chemistry (trace elements, isotopes) may reflect the source chemistry, extreme caution must be used where genetic implications are based on simple criteria (Clarke,

pers. comm). Another classification scheme divides granites mineralogically into magnetite-series and ilmenite-series granites (Ishihara, 1977), and involves no genetic distinctions. Magnetite-series granitoids are "I-type", but ilmenite-series can be both "S-type" and "I-type" (Takahashi et al., 1980).

Table 6.1 outlines various criteria used in the above-mentioned classification schemes. Based on chemical characteristics, the HCQP, along with the SMB and MB, generally qualifies as an "S-type" granite, according to Chappell and White (1974) and is ilmenite-bearing.

Four models were considered for the source of the SMB (McKenzie, 1974; McKenzie and Clarke, 1975). These included: 1) melting of the subducted lithospheric plate; 2) wet melting of mantle peridotite; 3) partial melting of the crust, and 4) crustal contamination of a mantle-derived magma. Clarke (1981) suggests that peraluminous granites in general may be the result of many processes, including fractional crystallization, anatexis, contamination by crustal material and/or removal of alkalies. Using isotopic data (Sm-Nd and Rb-Sr), Clarke and Chatterjee (1988) concluded that the SMB may have been derived from mafic-felsic gneisses, similar to those of the Liscomb complex, with modification by assimilation of Meguma Group metawackes and meta-pelites. A dominantly Goldenville Formation source, compatible with a North African source, is suggested for the HCQP (Krogh and Keppie, 1988), but this single source is contrary to conclusions reached using coupled Sm and Nd isotopic data for other granitoid plutons in the Meguma Terrane (Clarke and Chatterjee, 1988; Clarke and Halliday, 1985; Clarke et al., 1988).

TABLE 6.1 Characteristics of granitoids, using different classification schemes. "S-type" and "I-type" criteria are after Chappell and White (1974), "A-type" after Whalen et al. (1987), and magnetite and ilmenite after Takahashi et al. (1980).

| | S-TYPE | I-TYPE | A-TYPE | MAGNETITE SERIES | ILMENITE SERIES | HOQP |
|---|---|---|---|---|---|---|
| MAJOR ELEMENT CHEMISTRY | $Na_2O$ <3.2%, $K_2O$ 5% <2.2%, $K_2O$ 2% $Fe_2O_3/FeO+Fe_2O_3$ low | $Na_2O$ >3.2% felsic rocks >2.2% mafic rocks $Fe_2O_3/FeO+Fe_2O_3$ higher | $Na_2O$, $K_2O$, Fe/Mg, F, Zr, Nb, Ca, Sn, Y, REE (except Eu); low CaO, Ba and Sr than other I, S-type granites | $Fe^{3+}/Fe^{3+} + Fe^{2+}$ ratios significantly different -magnetite series more oxidized | | $Na_2O$ 2.7-3.7 $K_2O$ 3.9-5.2 ferric iron low |
| CHEMICAL SIGNATURE | A/CNK >1.1 | A/CNK <1.1 | | | | A/CNK 1.15-1.32 |
| NORMATIVE MINERALOGY | >1% CIPW normative corundum | CIPW normative diopside, or <1% CIPW normative corundum | | | | >1% CIPW normative corundum |
| COMPOSITIONS | compositions relatively restricted to high $SiO_2$ | compositions range from felsic to mafic | high $SiO_2$ compared to other I, S-type; volcanic equivalents common | | | $SiO_2$ 69.0-74.14 |
| ELEMENTAL PATTERNS | irregular trends with variation diagrams | regular inter-element variation patterns within plutons; linear or near-linear patterns | | high magnetic susceptibilities | | some irregularity in variation diagram patterns |
| MINERALOGY | mu[1], bi (<35%) common; hbld absent; aluminosilicates, gr, co occur in xenoliths | mu rare, hbld common; sphene common accessory; ap inclusions in bi; | annite-rich bi +/- alkali amphiboles, sodic pyroxene; mafic minerals crystallize late; feld- | 0.1-2% volume total opaques; mag, il; hem replacing mag; py, cp, sphene, | <0.1% volume total opaques; magnetite-free; po, graphite | mu, bi common; hbld absent; minor gr, ap accessory |

| | | | | | | |
|---|---|---|---|---|---|---|
| | or in granite matrix; ap, monazite common accessories | hbld common | spar is K-spar (albite-orthoclase solid sol'n) | epidote, bi, hbld iron-poor | | |
| ISOTOPIC SIGNATURE | $Sr^{87}/Sr^{86}$ >.708 | $Sr^{87}/Sr^{86}$ .704-.706 | | similar to I-type | different ranges | |
| XENOLITHS | metasedimentary xenoliths | hornblende-bearing xenoliths | | | | most meta-sedimentary in appearance |
| ECONOMIC MINERALS | Sn, W, U | porphyry-Cu, Mo | Sn, Mo, Bi, Nb, W, Ta, Ti | Mo, W, porphyry-Cu | Sn, W | none |
| SOURCE CHAR-ACTERISTICS | sedimentary source | igneous source | recycled, dehydrated continental crust; high T, $H_2O$ undersaturated completely molten magma; high level of emplacement; final plutonic event in orogenic belts and rift-related anorgenic magmatism | deep source region upper mantle, lower crust; extensional environment, subduction zones; I-type granites | shallower region in crust; large scale magma-crust inter-action; compressional environment; I- and S-type granites<br><br>granites | sedimentary, with some mantle component |

[1]mineral abbreviations used: mu = muscovite, bi = biotite, hbld = hornblende, gr = garnet, co = cordierite, ap = apatite mon = monazite, il = ilmenite, mag = magnetite, hem = hematite, po = pyrrhotite.

With the present data of the HCQP, the author can do little more than agree with previous models for magma generation in the Meguma Terrane for a possible source of the magma for the HCQP. However, a few generalizations can be made. The large volume of highly felsic rocks within the Meguma Terrane negates a mantle source. The high Si, K, and Rb and low Mg, Ca and Sr suggest a quartzo-feldspathic source. Additional work with extensive Sr, Nd, and Pb isotopes is necessary in order to make a significantly greater contribution.

## 6.6 Conclusions

This study has provided an insight into the mineralogy, composition, origin and relationship of the HCQP to other granitoids of the Meguma Terrane of southern Nova Scotia. These conclusions include:

1) The HCQP is composed mostly of muscovite-biotite monzogranite, and can be divided into five units. The pluton is two-lobed, with two units occurring in the western lobe (a medium-grained muscovite-biotite monzogranite and a coarse-grained monzogranite) and three units (a coarse-grained biotite monzogranite grading to granodiorite, an intensely megacrystic biotite monzogranite, and a fine- to medium-grained, equigranular muscovite-biotite monzogranite) underlying the eastern lobe. All these rocks contain variable amounts of biotite, muscovite, alkali feldspar, plagioclase and quartz, with garnet and apatite (+/- chlorite, ilmenite, rutile, hematite and zircon).

2) Late-stage intrusive rocks (e.g. aplites and pegmatites) constitute a minor portion (< 1%) of the entire pluton.

3) Deformation (C-S fabric) is well developed in the northern portions of the HCQP, closest to the Cobequid-Chedabucto fault zone.

This deformation decreases in intensity with distance south of the fault. This post-crystallization shearing indicates that the HCQP was emplaced subsequent to metamorphism of the Meguma Group (after 405-390 Ma; Muecke et al., 1988), but was syn-tectonic with respect to movement along the Cobequid-Chedabucto fault zone (approximately 370 Ma).

4) Major element chemistry of the HCQP is, in general, similar to the SMB, MB and other plutons within the Meguma Terrane. All HCQP rocks have high silica (69% to 73%). The least evolved units (HCQP1 and HCQP1A) display characteristics more similar to the SMB (lower $P_2O_5$, lower $K_2O$, higher MnO, CaO, $FeO_t$, MgO and $TiO_2$), compared with the other units. The more evolved units (HCQP2, HCQP3 and HCQP4) display characteristics more similar to the eastern plutons, the MB and the Halifax Pluton.

5) Major and trace element trends indicate that HCQP1 and HCQP1A represent the least evolved magma. Trends within the other units are less continuous, but these more evolved units have similar, evolved chemistry, and higher, overlapping Thornton-Tuttle differentiation index values. A well-developed separation exists between the two least evolved units and the three more evolved units (e.g. Thornton-Tuttle Differentiation Index values, $SiO_2$ and most other major and trace element chemistry). This separation suggests that the more evolved units may represent a more differentiated magma, or a separate magma pulse, and these more evolved units may be co-magmatic.

6) The HCQP rocks display higher $P_2O_5$, normative corundum and A/CNK ratios than the SMB. These values are similar to, and marginally higher than, the MB, and similar to other eastern plutons (e.g.

Sangster Lake and Larrys River). The higher values of $P_2O_5$ are manifested by the presence of blue-green apatite within the groundmass.

7) REE's of the HCQP display a 'typical' granitic pattern (Henderson, 1984), with LREE enrichment, small to moderately negative Eu anomalies, and increased depletion of HREE. The patterns of HCQP1 display similarities to patterns of granodiorite of the SMB (Muecke and Clarke, 1981), but the patterns of HCQP2 and HCQP4 are markedly different, both from those of HCQP1 and from patterns of the SMB, with increased HREE depletion and less pronounced Eu anomalies. These differences suggest different processes acting in the HCQP, and possibly a separate magma pulse and/or source region for the less evolved units (HCQP1 and HCQP1A) and the more evolved units (HCQP2, HCQP3 and HCQP4).

8) Muscovite and biotite (+/- garnet) are the common AFM minerals within the HCQP. The HCQP does not contain any cordierite, perhaps because of different Fe or Mg values in the magma (MacDonald, pers. comm.). This mineralogy contrasts with the SMB, MB and other plutons in the southwestern portion of the province. Cordierite, garnet, and aluminosilicates are common within these other plutons.

9) Biotite occurs in all units, with the exception of the late-stage aplites and pegmatites. The modes of occurrence in all units are similar. Biotite within the HCQP is high in iron, with compositions of annite-siderophyllite.

10) Muscovite occurs in all rocks and is relatively more abundant in units HCQP2, HCQP3, and HCQP4. It is believed to occur both as a primary, magmatic phase and as secondary, alteration products of other minerals. Primary muscovite contains marginally higher values of Ti,

although many secondary muscovites contain similar concentrations. Muscovite within the HCQP is low in $Na_2O$, compared with the SMB.

11) The presence of primary ideal muscovite constrains the pressure conditions prevailing during crystallization of the magma to a minimum of 3 kbars. Abbott (1985) developed P-T diagrams for various AFM liquidus topologies, which suggest pressures of a minimum of 3.5-4 kbar are suggested for the HCQP. These pressures correspond to a depth of crystallization of 10.5-14 km. The presence of Mn-rich garnet additionally constrains the pressure to <3.5 kbars.

12) Garnet occurs both as xenocrystic grains in the granitic groundmass in one unit (HCQP2) and as magmatic grains within aplite-pegmatite dykes. These garnets are high in MnO and are normally zoned. The presence of garnet within muscovite-bearing granites suggests strong partitioning of $Mn^{2+}$ into the liquid relative to muscovite and biotite (Abbott, 1985).

13) The pluton satisfies only four of nine criteria for specialized granites, according to the classification of Tischendorf (1977). Major element chemistry indicates some degree of specialization, but the trace, volatile and LIL element concentrations are substantially lower than ore-bearing granites world-wide. The pluton contains only minor accessory minerals (tourmaline) which contain volatile elements and low levels of fluorine. All of these factors suggest that the economic potential of the HCQP is limited.

14) Other evidence which might indicate good economic mineral potential is also lacking. Such evidence includes fluid stripping of REE's, unusual elemental ratios (e.g. $Rb/K_2O$) and the presence of

leucomonzogranite or leucogranite phases. Minor leucogranite pods are developed within local areas of the HCQP, but are not extensive.

15) Late-stage effects (e.g. greisenization, metasomatism, hydrothermal alteration, pegmatitic development, miarolitic cavities) are minimal. Elemental ratios which often indicate some of these later effects (e.g. increasing $Na_2O/K_2O$ ratios) do not follow an indicated trend. These factors indicate that the separation of a vapour-phase was not important in the HCQP. In this respect, the HCQP differs from the Sangster Lake pluton to the west (Ford and O'Reilly, 1985, O'Reilly, pers. comm.), where metasomatism and hydrothermal alteration effects are common. This lack of late-stage effects within the HCQP also contrasts with the SMB (particularly the New Ross-Vaughan complex), where the effects of a vapour-phase are apparent (Charest, 1976; O'Reilly et al., 1982).

16) Rapakivi texture is well-developed in HCQP4, with the rims being albitic. This texture is believed to be related to metasomatic processes.

17) The HCQP shows an unusual pattern of increasing thorium with decreasing or constant uranium. This pattern corresponds to the area underlain by HCQP4, a fine- to medium-grained, equigranular muscovite-biotite monzogranite. There is a positive correlation of zirconium with thorium, and this observation suggests that thorium may be incorporated within the zircon structure. A study undertaken in Greenland determined several ages of zircons within different granitoid phases (Gulson and Krogh, 1975). The zircons contained differing concentrations of uranium and thorium, and their ages reflected different sources for the different granites. This correlation of

zirconium with thorium may also suggest different sources for various phases of the HCQP.

18) The HCQP generally satisfies the criteria for an "S-type" granite (Chappell and White, 1974). Although this classification implies that the source for the granite is sedimentary, caution is urged for this conclusion based on these mineralogical and chemical criteria outlined by Chappell and White (1974). Krogh and Keppie (1988) suggest a sedimentary source (dominantly Goldenville Formation), based on zircon characteristics, for the HCQP. However, conclusions based on isotopic data for the source rocks for the Meguma Group and the SMB (Clarke et al., 1988; Clarke and Chatterjee, 1988; Clarke and Halliday, 1980) suggest that the source for these granitoids is mafic-felsic gneisses, like the Liscomb complex, with assimilation of Meguma Group metasedimentary rocks, and indicate that the former conclusion for the HCQP source should be viewed with caution.

19) Several models were considered for the petrogenesis of the HCQP. The chemical separation suggests that more than one magma was involved. HCQP2 and HCQP3 may represent co-magmatic intrusions, based on similar mineralogy and chemistry. Fractional crystallization, although possibly responsible for HCQP1A from HCQP1, may not entirely account for trends to units HCQP2, HCQP3, and particularly HCQP4 from the less evolved units. Restite unmixing and batch melting are similarly dismissed as important processes in the HCQP. Assimilation of country rock may be important, as this process may explain several trace element trends. Several lines of evidence (airborne radiometrics, trace element data) suggest that the HCQP represents intrusion of two or more batches of magma from heterogeneous source regions.

## 6.7 Recommendations for Future Work

The objectives of this thesis were to describe the mineralogy, petrology and geochemistry of the Halfway Cove-Queensport pluton, and to describe its characteristics in relation to other granites, particularly those others within the Meguma Terrane (e.g. the SMB, MB, and other smaller plutons). As a result of this study, several topics warrant additional consideration. These are:

1) To determine by radiometric methods (e.g. $Sr^{87}/Sr^{86}$ dating methods) the precise ages of the different units, with particular reference to HCQP4. Previous dating undertaken on the pluton has not addressed the question of age for the different units.

2) To investigate the zircons (e.g. microprobe techniques) within the different units, with particular attention given to those within HCQP4, to determine the contents of uranium and thorium. This study would determine if excess thorium is resident within the zircon of HCQP4. Additionally, microprobe analyses could also determine the proportion of monazite (a known host for thorium) within the HCQP.

3) To investigate more fully reasons for the well-developed break seen in major, trace and rare-earth element chemistry, to determine if this does reflect source differences, or whether the later units could have evolved from the earlier units by a process of, for example, fractional crystallization. This work would involve detailed statistical work and modelling.

4) To examine the behaviour of some of the trace elements (i.e. Ti, Ba) within minerals separates (i.e. feldspar, muscovites). Ba

particularly displays an unusual trend with differentiation, and this feature is unresolved.

5) To investigate more fully differences between biotite compositions within the different units, to see if biotite with fewer or no inclusions (e.g. biotite within HCQP4) is secondary and chemically different from the magmatic biotite.

# APPENDIX I

## I-1. Modal Analysis

Modal analysis of selected rock samples (rocks collected for geochemical analyses plus additional rock samples) from individual rock units was carried out by point counting stained slabs following the method outlined by Hutchison (1974). 400-600 points were counted per slab using different grid sizes for the individual units. Thin sections were also point counted to determine the amount of the minerals occurring in trace and minor amounts (e.g. muscovite, apatite, garnet, chlorite).

## I-2. Method for Staining K-feldspar

Staining rock slabs involved the method of Lyons (1971), with minor modifications. The slabs are etched with hydrofluoric acid, then bathed in sodium cobaltinitrite which stains the alkali-feldspar grains yellow, the plagioclase grains white and the quartz grains translucent gray. The method used follows:

1) Double-cut the rock to yield a slab approximately 2-3 cm thick. Rinse well to remove any grit and oil from the saw. Allow the slab to dry.

2) Immerse one side of the slab in a bath of hydrofluoric acid (49% concentrated HF) for 45 seconds to 1.5 minutes, depending on the degree of alteration of the sample.

3) Rinse well with tap water.

4) Immerse etched surface in a saturated solution of sodium cobaltinitrite for 45 seconds to 1.5 minutes (approximately the same length of time that the slab was immersed in hydrofluoric acid).

5) Remove excess stain from the rocks slab by gently and carefully rinsing with tap water. Let sample dry completely.

## APPENDIX II

## Geochemical analytical procedures

### II-1. Sample Preparation

#### II-1-1. Sample Collection

Thirty-six rock samples were collected for whole rock chemical analysis. The outcrop in the field area was low-lying, competent and moderately jointed with vertical fractures. These factors made the collection of good geochemical samples by conventional methods (chisels and sledge hammers) difficult to impossible. This necessitated drilling representative outcrops with a Pionjar pack-sack drill, inserting dynamite into the hole and blasting sufficient sample (10-15 kg).

#### II-1-2. Sample Pulverisation

The specimens selected for geochemical analyses were broken down into smaller fragments with a 4 lb. hammer (where necessary), and further reduced in size (2-3 cm cubes) using a cutrock. Weathered surfaces and xenoliths were removed. The rock cubes were then fed through a ceramic jaw crusher (Dayton Jaw Crusher, model 4K 371) to produce chips averaging <5mm in size. The ceramic plates were replaced by the author prior to the crushing process and were frequently cleaned during crushing.

The crushed samples were split using a Soiltest splitter. A portion weighing approximately 300-400 g was pulverised in either a ceramic ring mill (for samples to be analyzed for tungsten) or in a tungsten ring mill (for samples not being analyzed for tungsten). A small amount of sample (50 g) was ground in the ring mills prior to the main grinding for self-contamination and discarded.

All rock powders were stored in new sealed plastic containers. The unpulverised rock chip splits were stored in sealed plastic bags.

## II-2. Sample Decomposition

### II-2-1. Decomposition Procedures for Fe3+, Ti, Al, Mn, Mg, Ca, Na, K and P

Weigh accurately 0.5000g of rock powder (sample and rock standards) on to weighing paper, and transfer into a teflon cup. Make a blank at this stage also. Add 0.5 ml distilled water to the sample using a pipette to make a slurry. To this mixture, add 2.5 ml $HNO_3$ and 20 ml of 1:4 mixture of perchloric acid and HF. Cover the cups and put on the steam bath set on low setting. Digest overnight.

In the morning, uncover the teflon cups, and leave on the steam bath (set on high) for about 5 hours. Transfer the cups to a pre-heated sand bath under a fume hood, and heat until perchloric acid fumes form. Heat for an additional five minutes, then remove the cups from the sand bath. Allow the cups to cool to room temperature. Add precisely 5 ml of distilled water (filling the teflon cups about half-way) and put the cups (sealed with caps) on the steam bath set on high. Allow to digest for approximately one hour, then leave the cups overnight on the steam bath set on low. The next morning, remove the cups from the bath and cool to room temperature. Transfer the contents to a 250 ml volumetric flask, and add distilled water to bring the liquid level to the 250 ml mark. Shake well, then transfer to 250 ml polyethylene bottles. 20 ml of 5% $La_2O_3$ solution was added in the subsequent dilutions to offset any chemical interference. Standard solutions (using rock standards NIM-G and SY-3) were used to determine chemical accuracy.

### II-2-2. Decomposition for Si

Weight accurately 0.1000g of rock powder onto weighing paper, and transfer into a polycarbonate bottle. Place bottle on boiling steam bath for 30 min. Remove from heat, and let cool for 10 min. Add 50 ml boric acid with a measuring cylinder. Replace cap, and return bottle to steam bath for an hour. Remove from steam bath, loosen cap, and allow to cool to room temperature. Transfer contents to clean 200 ml volumetric flasks, and add distilled water to bring to

the 200 ml mark. Transfer to 250 ml polyethylene bottles. A standard solution for Si was made by dissolving precisely 0.1020 g pure $SiO_2$ in 5 ml HF and adding 50 ml of saturated boric acid solution.

## II-3. Analytical techniques

### II-3-1. Al, Si, Fe3+, Mn, Mg, Ca, Na, K, Ti

These elements were analyzed at Dalhousie University using the Perkin Elmer (model 503) atomic absorption unit. An air-acetylene flame was used for all elements, except for Al and Ti which used a nitrous oxide acetylene flame.

### II-3-2. Phosphorus

Phosphorus was analyzed colorimetrically. 5 ml of sample solution was pipetted into a 50 ml volumetric flask which was specially prepared for P analysis. To this solution was added 20 ml of a combined reagent solution composed of 3N $H_2SO_4$, ammonium molybdate, ascorbic acid, and distilled water. This solution was further diluted with distilled water to 50 ml. The solution was then measured for phosphorus using a Bausch and Lomb Spectric 70 spectrophotometer at 827 nm using 4 cm cells. Blank solution readings were subtracted from each sample reading, and the results were averaged.

### II-3-3. Ferrous Iron

The ferrous iron content was determined using the method of Wilson, as cited in Johnson and Maxwell (1981). Weigh accurately approximately 0.2 g rock powder onto weighing paper and transfer to a small plastic flask. Add 5 ml 0.1N ammonium vanadate and 10 ml of HF. Place the flask on shaker overnight. In the morning, add 10 ml of a prepared solution composed of a 1:2:2 mixture of $H_3O_4$:$H_2SO_4$:$H_2O$. Transfer the contents of the flask to a beaker containing 100 ml of 5% boric acid solution. Add 10 ml of 0.05N ferrous ammonium sulphate solution with pipette. Add 16 drops of 0.2% barium diphenylamine sulphonate indicator. Stir, and titrate to a grey end-point with 0.05 N $K_2Cr_2O_7$ solution.

II-3-4. Water

The total water content ($H_2O^+$ and $H_2O^-$) was determined using the Penfield Method, as given in Johnson and Maxwell (1981). A small amount of sample (0.4 g) was mixed with 2.5 g of dry flux composed of a 2:1:1 mixture of $PbO_2$:$PbCrO_4$:$NaWO_4$). $H_2O^-$ was determined by drying 0.5 g of rock powder in an oven at 110°C for 4 hours. $H_2O^+$ was calculated by subtraction.

II-3-5. Ba, Rb, Sr, Zr, Y, Pb and Zn

These trace elements were analyzed by X-Ray Fluorescence at Saint Mary's University, Halifax. The analyses were determined in a Philips PW-1400 sequential wavelength dispersive X-ray fluorescence spectrometer using a Rh-anode x-ray tube with 2.4 kilowatts of applied power. Ten grams of samples were accurately weighed and homogenized with 1.5 g of binding agent (phenolic resin). This mixture was pelletized and subsequently analyzed on the spectrometer. Loss on ignition (LOI) was determined by heating the sample for 1.5 hours at 1050°C in an electric furnace.

The accuracy was assessed with 2 international standards and precision with 4 duplicates (see Table II-1).

II-3-6. Mo, Ag, Be, B, Sn

The samples were analyzed for these trace elements at Bondar-Clegg and Company Limited, Ottawa, Ontario. For Mo and Ag, the method involved atomic absorption using $HNO_3$-HCL hot extraction, and Be analyses involved Hf-$H_2O_4$ (total metal digestion method) followed by HCL dissolution.

Powders for B analyses were first fused with KOH in a Ni-crucible, the residue then dissolved in HCL, and the solution analyzed on a direct-current emission plasma spectrometer.

Sn analyses involved x-ray fluorescence. The samples were mixed with a binding agent, pelletized and analyzed on an x-ray spectrometer.

One internal standard and 6 duplicates were used with the samples to analyses accuracy and precision (see Table II-2).

**TABLE II-1**
**TRACE ELEMENT ERROR ANALYSES**

| Element (Method*) | (Standard) | Obtained Value | Accepted Value** | Deviation (%) | Deviation (Mean %) |
|---|---|---|---|---|---|
| Li | (BCR-1) | 14 | 13 | 7.7 | 6.4 |
| (AA) | (BM) | 75 | 70 | 7.1 | |
| | (SY-3) | 86 | 90 | 4.4 | |
| Ba | (AGX) | 1073 | N/A | - | |
| (XRF) | (AGX) | 1068 | N/A | - | |
| | (JG-1) | 433 | 460 | 5.9 | 8.2 |
| | (SY-3) | 347 | 440 | 21.1 | |
| | (GSP-1) | 1259 | 1300 | 3.2 | |
| | (GSP-1) | 1249 | 1300 | 3.9 | |
| | (G-2) | 1726 | 1850 | 6.7 | |
| Rb | (AGX) | 238 | 243 | 2.1 | 2.5 |
| (XRF) | (AGX) | 240 | 243 | 1.2 | |
| | (JG-1) | 175 | 185 | 5.4 | |
| | (SY-3) | 221 | 210 | 5.2 | |
| | (GSP-1) | 253 | 254.7 | 0.7 | |
| | (GSP-1) | 252 | 254.7 | 1.1 | |
| | (G-2) | 166 | 169.3 | 1.9 | |
| Sr | (AGX) | 172 | 175.2 | 1.8 | 2.1 |
| (XRF) | (AGX) | 172 | 175.2 | 1.8 | |
| | (JG-1) | 180 | 185 | 2.7 | |
| | (SY-3) | 306 | 300 | 2.0 | |
| | (GSP-1) | 229 | 233.1 | 1.8 | |
| | (GSP-1) | 231 | 233.1 | 0.9 | |
| | (G-2) | 460 | 476.3 | 3.4 | |
| Zr | (AGX) | 86 | N/A | - | |
| (XRF) | (AGX) | 86 | N/A | - | |
| | (JG-1) | 103 | 110? | 6.4 | 3.5 |
| | (SY-3) | 308 | 340 | 9.4 | |
| | (GSP-1) | 503 | 500 | 0.6 | |
| | (GSP-1) | 503 | 500 | 0.6 | |
| | (G-2) | 302 | 300 | 0.7 | |
| Pb | (AGX) | 41 | N/A | - | |
| (XRF) | (AGX) | 37 | N/A | - | |
| | (JG-1) | 27 | 26? | 26? | 4.5 |
| | (SY-3) | 120 | 130 | 7.7 | |
| | (GSP-1) | 51 | 53 | 3.8 | |
| | (GSP-1) | 51 | 53 | 3.8 | |
| | (G-2) | 28 | 29 | 3.4 | |

II-3-7. U, Th, W and Au

U, Th, W, and Au analyzed at Nova Track Analysts Limited, Vancouver, British Columbia, using neutron activation analyses (NAA). The samples were irradiated in a high density neutron flux, with the resultant activation of specific isotopes measured on a multi-channel gamma-spectrometer, then extrapolated to elemental concentrations.

One internal standard and 4 duplicates were included and the results tabulated (see Table II-2).

II-3-8. Rare Earth Element (REE) Analyses

Six representative samples from four of the HCQP phases were analysed for seven REE's (Ce, Nd, Sm, Eu, Tb, Yb and Lu). Lanthanum was not analysed. The samples were analysed by neutron activation (NAA) at Waterloo University in Kitchener, Ontario. Approximately 0.1-0.2 grams of rock powder were weighed accurately and sealed in clean plastic ampoules. The samples were then sent to the Waterloo Nuclear Reactor with two standards. The precision of these analyses is listed below, comparing the recommended results with those obtained by Waterloo University.

## TABLE II-3

## TRACE ELEMENT DUPLICATE ANALYSES

| Sample No. | AGX | | GSP-1 | | CG-1 | | F-G001 | | F-G004 | | F-G005 | | |
|---|---|---|---|---|---|---|---|---|---|---|---|---|---|
| Duplicate | I | II | I | II | I | II | I | II | I | II | I | II | III |
| Li | - | - | - | - | - | - | - | - | 256 | 248 | - | - | - |
| Ba | 1073 | 1068 | 1259 | 1249 | - | - | - | - | - | - | 19 | 21 | 23 |
| Rb | 238 | 240 | 253 | 252 | - | - | - | - | - | - | 374 | 375 | 377 |
| Sr | 172 | 172 | 229 | 231 | - | - | - | - | - | - | 29 | 30 | 29 |
| Zr | 86 | 86 | 503 | 503 | - | - | - | - | - | - | 48 | 47 | 48 |
| Pb | 41 | 37 | 51 | 51 | - | - | - | - | - | - | 17 | 16 | 18 |
| Zn | 27 | 28 | 101 | 103 | - | - | - | - | - | - | 56 | 57 | 58 |
| F | - | - | - | - | 900 | 690 | - | - | - | - | 660 | 640 | - |
| Cu | - | - | 33 | 35 | - | - | - | - | - | - | 2 | 2 | - |
| Mo | - | - | - | - | 1 | 1 | 1 | 2 | - | - | - | - | - |
| Ag | - | - | - | - | 1.3 | 1.1 | 0.2 | <0.1 | - | - | - | - | - |
| Be | - | - | - | - | 2.0 | 1.5 | 13.0 | 26.0 | - | - | - | - | - |
| B | - | - | - | - | 20 | 25 | 20 | 30 | - | - | - | - | - |
| Sn | - | - | - | - | 7 | 6 | 23 | 19 | - | - | - | - | - |
| U | - | - | - | - | 2.9 | 2.5 | 15.9 | 16.0 | - | - | - | - | - |
| Th | - | - | - | - | 13 | 13 | 3 | 3 | - | - | - | - | - |
| W | - | - | - | - | 4 | 3 | 6 | 4 | - | - | - | - | - |
| Au (ppb) | - | - | - | - | 16 | 14 | 1 | 2 | - | - | - | - | - |

| Sample No. | F-G022 | | F6-G004 | | F5-G004 | | | SL-12 | | LR-5 | | LR-G009 | |
|---|---|---|---|---|---|---|---|---|---|---|---|---|---|
| Duplicate | I[1] | II[2] | I[1] | II[2] | I | II | III | I | II | I | II | I | II |
| Li | - | - | - | - | - | - | - | - | - | - | - | 130 | 130 |
| Ba | - | - | - | - | 12 | 15 | 15 | - | - | - | - | - | - |
| Rb | - | - | - | - | 423 | 421 | 424 | - | - | - | - | - | - |
| Sr | - | - | - | - | 93 | 96 | 95 | - | - | - | - | - | - |
| Zr | - | - | - | - | 20 | 20 | 19 | - | - | - | - | - | - |
| Pb | - | - | - | - | 12 | 14 | 13 | - | - | - | - | - | - |
| Zn | - | - | - | - | 16 | 15 | 17 | - | - | - | - | - | - |
| F | - | - | - | - | 240 | 210 | 240 | - | - | - | - | - | - |
| Cu | - | - | - | - | 8 | 8 | 7 | - | - | - | - | - | - |
| Mo | 1 | 2 | 1 | 1 | - | - | - | <1 | 1 | <1 | 1 | - | - |
| Ag | 0.1 | 0.1 | 0.1 | 0.4 | - | - | - | <0.1 | 0.1 | 0.1 | 0.1 | - | - |
| Be | 5.0 | 5.5 | 4.5 | 5.0 | - | - | - | 4.5 | 5.0 | 5.0 | 5.5 | - | - |
| B | 20 | 20 | 25 | 25 | - | - | - | 30 | 25 | 35 | 30 | - | - |
| Sn | 24 | 30 | 4 | 7 | - | - | - | 20 | 14 | 3 | 6 | - | - |
| U | 10.1 | 9.7 | 4.5 | 4.2 | - | - | - | 17.8 | 17.3 | 3.3 | 3.5 | - | - |
| Th | <1 | <1 | 6 | 7 | - | - | - | 5 | 5 | 8 | 8 | - | - |
| W | 718 | 2 | 760 | 2 | - | - | - | 4 | 2 | 1 | 3 | - | - |
| Au (ppb) | 3 | 2 | <1 | 1 | - | - | - | 4 | 2 | 5 | 6 | - | - |

1 = Tungsten-carbide crushed.
2 = Ceramic crushed.

TABLE C-5 Waterloo University

Comparison of REE's + Ba + Th with International Standards

GSP-1 (granodiorite)

| | RECOMMENDED (1984) | OBTAINED WATERLOO | PERCENT DEVIATION |
|---|---|---|---|
| Ce | 400 | 508.28 | 27 |
| Nd | 190 | 260.17 | 36.9 |
| Sm | 26.8 | 32.96 | 22.9 |
| Eu | 2.4 | 2.72 | 13.3 |
| Tb | 1.36 | 0.81 | -40.4 |
| Yb | 1.7 | 2.19 | 28.8 |
| Th | 105 | 127.87 | 21.7 |
| Ba | 1310 | 970.87 | -25.88 |

TABLE C-6 Waterloo University

NIM-G granite

| | RECOMMENDED (1984) | OBTAINED WATERLOO | PERCENT DEVIATION |
|---|---|---|---|
| Ce | 195 | 204.26 | 4.7 |
| Nd | 72 | 80.40 | 11.2 |
| Sm | 15.8 | 15.07 | -4.6 |
| Eu | 0.35 | 0.34 | -2.8 |
| Tb | 3 | 4.60 | 53.3 |
| Yb | 14.2 | 14.46 | 1.8 |
| Lu | 2 | 1.98 | -1.0 |
| Th | 51 | 18.05 | -64.6 |
| Ta | 4.5 | 4.45 | -1.1 |
| Ba | 120 | 78.74 | -34.38 |

TABLE C-7 Waterloo University NAA repeatability
(After Douma, 1988)

NPM458 (sample of Douma, 1988)

| | NPM458 | REPEAT | % deviation |
|---|---|---|---|
| Ce | 56.80 | 55.56 | -2.1 |
| Nd | 29.23 | 29.24 | 0.03 |
| Sm | 6.39 | 6.33 | 0.93 |
| Eu | 0.83 | 0.84 | 1.2 |
| Tb | 0.67 | 0.72 | 7.4 |
| Yb | 2.03 | 2.16 | 6.4 |
| Lu | 0.27 | 0.28 | 3.7 |
| Th | 12.86 | 12.89 | 0.23 |
| Ta | 1.01 | 1.04 | 2.9 |
| Ba | 241.42 | 249.82 | 3.4 |

## APPENDIX III

Petrographic descriptions of samples (chemically analyzed with several miscellaneous samples)

### III-1. Definition of terms

#### III-3-1. Rock type

Rock type names used in the thesis are after Streckeisen (1976). The location of each rock sample is on map 2 in back pocket.

#### III-3-2. Grain size

The following grain size designations were used in the rock descriptions:

fine grain size: <0.1 cm.

medium grain size: 0.1-0.5 cm.

coarse grain size: >0.5 cm

III-2. Petrographic descriptions

Rock sample: QP1 Porphyritic biotite monzogranite

Rock phase: HCQP1A

Degree of alteration: moderate

This rock sample represents one of two that were taken of the "intensely porphyritic" phase of the Queensport pluton. It is coarse-grained, with alkali feldspar, plagioclase, quartz, biotite and muscovite. Alkali feldspar phenocrysts (3.5-4 cm long and 2 cm wide) average 10-20% of the matrix, but may vary to 30-40% in local areas. Smaller K-feldspars occur within the matrix as poorly developed concentrations. Biotite (1-2 mm) is most plentiful of the micas, and occurs rimming the feldspars. Small biotites and muscovites are included within the feldspars. There are small, localized altered spots within the matrix, which look to be pyrite or some other sulphide (possibly incorporated from remnant xenoliths ?). Muscovite occurs in trace amounts as a discrete mineral, but occurs as an alteration product of both biotite and the feldspars.

Rock sample: QP4 Biotite muscovite monzogranite

Rock phase: HCQP4

Degree of alteration: slight, very "fresh" and "clean"

This rock is fine- to medium-grained, and contains alkali-feldspar, plagioclase, quartz, biotite and muscovite. The feldspars (both plagioclase and K-feldspar) are generally larger than the groundmass (up to 8 mm), with the majority of the megacrysts being K-

feldspar. Minor albitization and saussuritization of the feldspars occurs. Quartz occurs as translucent, rounded, anhedral to subhedral grains. Both biotite and muscovite are abundant as are generally small grains (1-2 mm). Muscovite (3 mm) occurs as a discrete mineral, in addition to occurring as alteration products of the feldspars and biotite. Abundant inclusions (both muscovite and biotite) are found within the feldspars, with muscovite most abundant.

Rock sample: QP5 Biotite muscovite monzogranite

Rock phase: HCQP4

Degree of alteration: slight to moderate

This rock is fine- to medium-grained and generally equigranular with a few larger megacrysts of alkali-feldspar. Biotite and muscovite are both plentiful, occurring in approximately equal amounts (5-6%). Biotite occurs as small grains (average <1, with a range of up to 2 mm) within the groundmass and included within feldspars. Biotite clots also occur, and could represent schlieren or remnant xenoliths.

Rock sample: QP6 Biotite (muscovite) monzogranite

Rock phase: HCQP1

Degree of alteration: slight

This rock is coarse-grained and contains alkali-feldspar, plagioclase, quartz, biotite and muscovite. Both feldspars occur as subhedral grains to well-developed laths up to 1 cm. Quartz occurs both as individual small (<5 mm), rounded grains, and as grain aggregates, some of which are slightly elongate. Most quartz grains are clear and translucent, but some grains are darkened. Biotite is

plentiful (10%), and occurs predominantly as larger grains (2-5 mm), with some smaller (<1 mm and 1mm) grains which commonly occur rimming feldspars. It is moderately well preserved, although edges are rimmed by muscovite. There is a subtle but definite alignment of the biotites, and this alignment is reinforced by the slightly elongate quartzes. Muscovite occurs predominantly as pale brown, small (<1mm) grains in close association with biotite, and also occurs as alteration of the feldspars.

One interesting aspect of this rock is the presence of leucogranite developed along small fractures. The leucocratic portions do not have a sharp contact with the host rock. Garnets and apatite are found within the fractures, the garnet being reddish, euhedral to subhedral, and 1mm to 9 mm.

Rock sample: QP7 Biotite (muscovite) monzogranite

Rock phase: HCQP1

Degree of alteration: moderate to strong

This rock is coarse-grained, with overall grain size coarser than most of the other samples. The mineralogy includes feldspar (both K-feldspar and minor plagioclase), quartz, biotite and muscovite. Both feldspars occur both as smaller anhedral to subhedral grains within the groundmass (up to 1 cm) and larger subhedral to euhedral laths (up to 2 cm). Abundant inclusions (biotite and muscovite) occur within the feldspars. There is minor hematization and saussurization of the cores of K-feldspar and plagioclase, respectively. Quartz occurs as clear, subhedral grains (average size 2 mm) and grain aggregates. Biotite occurs as subhedral grains and minor aggregates (average size 1-2 mm,

up to 5 mm). Hematization of the biotites is moderate to strong. Muscovite occurs as secondary alteration products of other minerals (biotite and feldspars).

Rock sample: QP8 Biotite (muscovite) monzogranite

Rock phase: HCQP1

Degree of alteration: moderate to extensive

This rock is coarse-grained, with some large phenocrysts of K-spar (2-3 cm). Selective strong hematization occurs throughout the matrix. Average grain size of feldspars within the groundmass is 1 cm, and some of the potassium feldspars are well-developed grains with Carlsbad twinning. Other feldspar grains are anhedral to subhedral. All feldspars exhibit some saussurization. Quartz is clear to whitish, translucent, and occurs as individual grains (1 mm) and grain aggregates (<5 mm). Biotite is altered, with hematite rims and moderately well developed alteration to muscovite. Muscovite occurs predominantly as secondary alteration product of minerals (i.e. biotite, K-feldspar).

Rock sample: QP9 Biotite muscovite monzogranite

Rock phase: HCQP1

Degree of alteration: moderate and pervasive

This rock is medium-grained and contains alkali feldspar, plagioclase, quartz, biotite and muscovite. Feldspar grains are subhedral to euhedral (<5 mm), and are selectively hematized to reddish-pink. Minor inclusions (biotite and muscovite) occur within the feldspars. Biotite grains are generally small, with few grains

larger than 1 mm. Muscovite is common, occurring both as small (<1 mm) grains, which occur as obvious alteration products of other minerals, and as larger, discrete grains (1-5mm).

Rock sample: QP15 Biotite-muscovite monzogranite

Rock phase: HCQP4

Degree of alteration: slight

This rock is medium grained, slightly megacrystic, with alkali feldspar, plagioclase, quartz, biotite and muscovite. Feldspar grains predominantly subhedral, exhibit minor hematization, and K-feldspar grains contain well-developed Carlsbad twinning. Biotite grains are generally <1mm. Biotite and muscovite occur both within the feldspars and as rims. Muscovite occurs in similar associations to those documented previously.

Rock sample: QP17 Biotite muscovite monzogranite

Rock phase: HCQP4

Degree of alteration: slight

This rock is fine- (to medium-) grained and is generally equigranular, although some alkali feldspar phenocrysts (1-1.5 cm) are larger than the groundmass. Euhedral to anhedral K-feldspars exhibit good Carlsbad twinning, and are generally 5 mm in size. Minor hematization occurs within the feldspars. Biotite occurs as both small grains (<1mm), which occur predominantly within alkali feldspar, and as larger (1-2 mm) grains within the groundmass. Muscovite and biotite occur in approximately equal proportions (5-6%). Muscovite occurs as

large, euhedral grains (3-4 mm), in addition to occurring intergrown with biotite.

Rock sample: QP19 Biotite-muscovite monzogranite

Rock phase: HCQP4

Degree of alteration: slight

This rocks is medium grained and moderately equigranular. The feldspars occur as anhedral to subhedral grains (1 cm) with slightly reddened. Quartz grains are slightly darkened. Biotite exhibits minor alteration to muscovite and hematite, and is found in several modes of occurrence: within the groundmass; within K-spars; and close association with muscovite. Biotite and muscovite occur in approximately equal proportions (5-6%). Muscovite occurs as large grains (3-4 mm) within the groundmass, and also in other modes (growing with biotite, in the cores of feldspar).

Rock sample: QP22 Biotite (muscovite) monzogranite

Rock phase: HCQP1

Degree of alteration: moderate

This rock is coarse-grained and moderately megacrystic with large (3-4 cm), subhedral to euhedral, alkali-feldspars which comprise <10% of the matrix. Quartz occurs as small (1-2 mm), anhedral grains, which are commonly darkened. Both biotite and muscovite are present, but biotite is dominant (10% biotite compared with 1% muscovite), occurring both within the groundmass and included within feldspars. Muscovite occurs primarily as alteration products of other minerals, principally the biotites.

Rock sample: HC01 Biotite muscovite monzogranite

Rock phase: HCQP2

Degree of alteration: slight to moderate

This rock is coarse-grained and moderately equigranular, with minor feldspar megacrysts. The mineralogy includes two feldspars (alkali feldspar and plagioclase), quartz, biotite, muscovite and minor amounts of apatite and garnet. The feldspars occur as anhedral grains and exhibit minor saucceritization. A weak foliation occurs, outlined by elongation of quartz grains and alignment of the biotites. There are biotite concentrations (secondary ?) along parallel fracture surfaces. Muscovite occurs as both large (2-3 mm), discrete grains and as alteration products similar to the modes of occurrence previously documented. Reddish-pink garnet (average size .1-1 mm) occurs in trace amounts within the groundmass and within the cores of feldspars.

Rock sample: HC03 Biotite muscovite monzogranite

Rock phase: HCQP3

Degree of alteration: moderate

This rock is medium- (to coarse-) grained, with feldspars (both plagioclase and alkali feldspar), quartz, biotite and muscovite. There are relatively few phenocrysts of feldspar, and those that are found are generally euhedral (1-1.5mm) grains with hematized cores. Most feldspars occur within the groundmass as subhedral to anhedral grains. Quartz grains are rounded (average size 1-2 mm) with some grain aggregates of 5 mm. Biotite occurs in two modes of occurrence, one being small, individual grains (<1-1 mm), which are generally

hematized, and the other mode being larger grains (3-5 mm), which are less altered. Muscovite is abundant (modal content 6%) and occurs as both large discrete grains (1-3mm) and as alteration products of biotite and feldspars. Blue-green subhedral grains of apatite (1-2 mm) occur in trace amounts.

Rock sample: HC04 Biotite muscovite monzogranite

Rock phase: HCQP3

Degree of alteration: moderate to extensive

This rock is medium to coarse-grained, and contains alkali feldspar, plagioclase, quartz, biotite, muscovite and trace apatite. The feldspars occur both as anhedral grains and as euhedral, irregularly sized grains up to 1.5 cm long and 2-3 cm wide. The larger feldspars are generally not altered, but the majority of the smaller feldspar grains exhibit hematization and saussuritization in their cores. Quartz occurs as small (2-3 mm), slightly darkened, anhedral grains, both as single grains and grain aggregates. Biotite is the most plentiful of micas (7-8%, compared with 2-3% muscovite) and is generally unaltered. The biotite grain size averages 1 mm, with local grain concentrations up to 2 cm. Muscovite occurs principally as a secondary alteration products of the other minerals (biotite and both feldspars), but also occurs throughout the matrix as small (1mm) discrete grains.

Rock sample: HC05 Biotite-muscovite monzogranite

Rock phase: HCQP2

Degree of alteration: slight to moderate

This rock is medium to coarse-grained. Mineralogy consists of biotite, muscovite, plagioclase, alkali-feldspar, quartz and apatite. The feldspars form subhedral masses to euhedral laths (up to 1 cm) with localized hematization evident. Quartz grains occur both as aggregates and subhedral grains that are slightly translucent. The biotites appear to be most altered of the minerals, with minor hematization apparent. Most flakes do not have their glossy, shiny appearance that is most common in other rocks, but are dull. A very faint foliation is developed within the biotites. Muscovite is very common, occurring as euhedral grains 3-4 mm and occurring in close association with biotite. Apatite is evident (<1%) and occurs within the cores of feldspars.

Rock sample: HC06 Biotite muscovite monzogranite

Rock phase: HCQP2

Degree of alteration: slight to moderate

This rock is medium grained and moderately equigranular, with some euhedral feldspar grains (3-4 cm). Biotite is more predominant of the mica (6-7%, as compared with 3-4% muscovite). Both biotite and muscovite occur included within feldspars. Local spots of hematization occur within the groundmass, predominantly within cores of feldspars and surrounding some biotite grains. Small (<2mm) greenish apatite occurs in trace amounts within the groundmass.

Rock sample: HC07 Biotite muscovite monzogranite

Rock phase: HCQP2

Degree of alteration: moderate

This rock is coarse-grained, with mineralogy which includes alkali feldspar and plagioclase, quartz, biotite, muscovite, trace apatite and trace garnet. Feldspars grains are predominantly anhedral to euhedral. Quartz grains commonly occur as grain aggregates (<5 mm). Biotite is the most abundant mica (6-7%, compared with 3-4% muscovite). Small (<1mm) apatite and reddish garnet grains occur both within the groundmass and within the cores of feldspars.

Rock sample: HC-83-L025 Biotite muscovite monzogranite

Rock phase: HCQP2

Degree of alteration: Extensive

This rock is fine grained and pinkish, with abundant hematization and muscovite development on surfaces. The granite is highly foliated, compact, and silicifed. Quartz grains are commonly elongated with a ratio of 6:1 (6 cm long, 1 cm wide), but can be variable in size. Narrow (<1mm) quartz veins, randomly oriented, occur throughout the matrix. Pink feldspar grains, euhedral to subhedral, commonly have their cores replaced by hematite and muscovite. Small quartz grains (1-2 mm) often rim feldspar grains. Muscovite (6-7%) occurs generally as a secondary alteration product (sericite). Biotite is completely replaced by chlorite and muscovite.

Rock sample: HC-83-L026 Biotite muscovite monzogranite

Rock phase: HCQP2

Degree of alteration: moderate to extensive

This rock is coarse-grained and moderately equigranular with minor megacrysts of feldspar. It is pinkish-white to green, and is well

foliated. The mineralogy includes K-feldspar and plagioclase, with alkali feldspar dominant, quartz, muscovite, biotite and chlorite. A well-developed foliation is outlined by elongated quartz grains, aligned biotite and small, parallel hairline fractures (1 mm thick and 5 mm apart), which are filled with green to black chlorite. The small fractures are not continuous, but often break and branch. Stretched quartzes occur both parallel to the fractures and at angles (45-60°) to them. Small biotite (<1mm) exhibits foliation parallel both to the hairline fractures and to the direction outlined by the stretched quartzes. Feldspars are slightly pinkish and do not exhibit elongation or foliation. Muscovite is abundant (6-7%), and occurs principally as small (1mm) grains (sericite) between other minerals, although some larger grains (up to 4 mm) do occur.

Rock sample: HC-83-L030 Biotite muscovite monzogranite

Rock phase: HCQP2

Degree of alteration: moderate to extensive

This whitish to pink rock is medium to coarse-grained. Foliation is moderately well-developed, but not as extensive as that seen in L025 and L026. Quartzes are elongated generally 2:1 with maximum elongation 3:1, and the elongated and irregular shapes of the quartzes give the rock a "wispy" appearance. Feldspars occur as pinkish, anhedral grains with moderate hematization. Small quartz inclusions and flecks of biotite occur within the feldspars. Biotite exhibits minor and parallel foliation with quartz. Abundant blackish-green chlorite and biotite veins occur in random orientation. Small parallel fractures (<1 mm) filled with hematite are apparent throughout the matrix.

Muscovite occurs predominantly as small grains (1mm) with some larger grains (2-3 mm). It occurs primarily intergrown with biotite, in close association with chlorite (both replacing biotite ?) and some intergrown with feldspar.

## APPENDIX IV

### IV-1. Electron Microprobe Analysis

Mineral analyses were calculated by a computer program EDATA2 by Smith et al. (1980). This program corrects for background, instrument drift, fluorescence and adsorption. Precision is better than +1% for oxides in quantities of greater than 8%, but decreases to +2% or greater for oxides present in lower concentrations. Accurate and precise analyses are obtained by the electron microprobe, but it cannot provide quantitative data on different oxidation ratios, e.g., Fe, Mn and Ti. Additionally, the elemental weight of the hydrous minerals and the quantity of water cannot be measured and must be recalculated. In addition, for certain minerals (biotite, muscovite), the recalculation program involves calculations on the basis of 24 oxygen (as opposed to 22), which does not take into consideration additional elements (OH, F) that could be incorporated into the mineral structure. Recalculation for plagioclase and potassium feldspar involved a BASIC computer program (Richard, 1986, unpublished data), based on OH values suggested by Deer et al. (1966).

The standards used for mineral analyses were as follows:

1) Plagioclase and K-feldspar

Sanidine (for K), Kakanui Kersutite (Ca, Ti, Mg, Fe), Albite (Na, Al, Si).

2) Biotite and Chlorite

Ilm 96189 (Mn), Gnt 12442 (Fe), Bio LP6 (Si, Al, Mg, K), Kakanui Kersutite (Ti, Na, Ca).

3) White Mica Analysis

Musc-M (Si, Al, K), Sodalite (Cl), Bio LP6 (Si, Al, Mg, K), Gnt 12442 (Fe, Mn), Kakanui Kersutite (Ti, Na, Ca).

APPENDIX IV-2 Biotite analyses

| SAMPLE | NQP03 | NQP03 | NQP03 | NQP03 | NQP03 | NQP07 | NQP07 | NQP07 | NQP07 | NQP07 |
|---|---|---|---|---|---|---|---|---|---|---|
| ANALYSES | 5B | 1B | 2B | 6B | 7B | 3 | 1 | 2A | 5 | 4 |
| MINERAL | BI | BI | BI | BI | BI | BI | BI | BI | BI | BI |
| LOCATION | HCQP1 | HCQP1 | HCQP1 | HCQP1 | HCQP1 | HCQP1 | HCQP1 | HCQP1 | HCQP1 | HCQP1 |
| SIO2 | 36.25 | 36.32 | 36.26 | 36.60 | 36.26 | 37.99 | 38.39 | 38.15 | 38.29 | 38.40 |
| TIO2 | 3.30 | 3.11 | 3.41 | 3.00 | 3.04 | 2.86 | 3.60 | 3.50 | 3.41 | 3.26 |
| AL2O3 | 18.52 | 19.30 | 19.45 | 18.92 | 19.29 | 17.26 | 18.05 | 17.53 | 17.91 | 17.89 |
| CR2O3 | 0.00 | 0.00 | 0.00 | 0.00 | 0.00 | 0.00 | 0.00 | 0.00 | 0.00 | 0.00 |
| FEO | 20.85 | 20.30 | 21.63 | 21.34 | 21.72 | 20.31 | 20.24 | 19.57 | 19.91 | 19.93 |
| MNO | 0.44 | 0.30 | 0.33 | 0.48 | 0.52 | 0.75 | 0.72 | 0.83 | 0.79 | 0.79 |
| MGO | 6.67 | 6.54 | 6.67 | 7.03 | 6.84 | 5.87 | 6.13 | 5.98 | 6.02 | 6.09 |
| CAO | 0.00 | 0.00 | 0.00 | 0.00 | 0.00 | 0.14 | 0.13 | 0.11 | 0.06 | 0.14 |
| NA2O | 0.00 | 0.00 | 0.00 | 0.00 | 0.00 | 0.00 | 0.00 | 0.00 | 0.00 | 0.00 |
| K2O | 9.43 | 9.39 | 9.66 | 9.78 | 9.84 | 9.45 | 9.72 | 9.65 | 9.85 | 9.90 |
| P2O5 | 0.00 | 0.00 | 0.00 | 0.00 | 0.00 | 0.00 | 0.00 | 0.00 | 0.00 | 0.00 |
| H2O | 3.92 | 3.93 | 3.99 | 3.98 | 3.98 | 3.90 | 4.01 | 3.94 | 3.98 | 3.98 |
| TOTAL | 99.38 | 99.19 | 101.40 | 101.13 | 101.49 | 98.53 | 100.99 | 99.26 | 100.22 | 100.38 |
| CSI | 5.539 | 5.533 | 5.445 | 5.510 | 5.453 | 5.830 | 5.740 | 5.795 | 5.769 | 5.778 |
| CTI | 0.379 | 0.356 | 0.385 | 0.340 | 0.344 | 0.330 | 0.405 | 0.400 | 0.386 | 0.369 |
| CAL4 | 2.461 | 2.467 | 2.555 | 2.490 | 2.547 | 2.170 | 2.259 | 2.204 | 2.231 | 2.222 |
| CAL6 | 0.874 | 0.998 | 0.886 | 0.866 | 0.872 | 0.952 | 0.921 | 0.934 | 0.949 | 0.950 |
| CCR | 0.000 | 0.000 | 0.000 | 0.000 | 0.000 | 0.000 | 0.000 | 0.000 | 0.000 | 0.000 |
| CFE | 2.664 | 2.586 | 2.716 | 2.687 | 2.732 | 2.607 | 2.531 | 2.486 | 2.509 | 2.508 |
| CMN | 0.057 | 0.039 | 0.042 | 0.061 | 0.066 | 0.097 | 0.091 | 0.107 | 0.101 | 0.101 |
| CMG | 1.519 | 1.485 | 1.493 | 1.577 | 1.533 | 1.343 | 1.366 | 1.354 | 1.352 | 1.366 |
| CCA | 0.000 | 0.000 | 0.000 | 0.000 | 0.000 | 0.023 | 0.021 | 0.018 | 0.010 | 0.023 |
| CNA | 0.000 | 0.000 | 0.000 | 0.000 | 0.000 | 0.000 | 0.000 | 0.000 | 0.000 | 0.000 |
| CK | 1.838 | 1.825 | 1.851 | 1.878 | 1.888 | 1.850 | 1.854 | 1.870 | 1.893 | 1.900 |
| CP | 0.000 | 0.000 | 0.000 | 0.000 | 0.000 | 0.000 | 0.000 | 0.000 | 0.000 | 0.000 |
| COH | 4.000 | 4.000 | 4.000 | 4.000 | 4.000 | 4.000 | 4.000 | 4.000 | 4.000 | 4.000 |
| PHLO | 35.8 | 36.1 | 35.1 | 36.5 | 35.4 | 33.2 | 34.3 | 34.3 | 34.1 | 34.4 |
| ANN | 63.8 | 62.9 | 63.9 | 62.1 | 63.1 | 64.4 | 63.5 | 63.0 | 63.3 | 63.1 |
| MN | 1.3 | 0.9 | 1.0 | 1.4 | 1.5 | 2.4 | 2.3 | 2.7 | 2.5 | 2.5 |
| FE+MG | 4.18 | 4.07 | 4.21 | 4.26 | 4.27 | 3.95 | 3.90 | 3.84 | 3.86 | 3.87 |
| FE/FE+MG | 0.64 | 0.64 | 0.65 | 0.63 | 0.64 | 0.66 | 0.65 | 0.65 | 0.65 | 0.65 |

| SAMPLE | NQP07 | NQP08 | NQP08 | NQP08 | NQP08 | NQP08 | NQP08 | NQP10 | NQP10 | NQP10 |
|---|---|---|---|---|---|---|---|---|---|---|
| ANALYSES | 5-2 | 4 | 3 | 1 | 4 | 2 | 1 | 2-2 | 6 | 5 |
| MINERAL | BI | BI | BI | BI | BI | BI | BI | BI | BI | BI |
| LOCATION | HCQP1 | HCQP1 | HCQP1 | HCQP1 | HCQP1 | HCQP1 | HCQP1 | HCQP1 | HCQP1 | HCQP1 |
| SIO2 | 38.45 | 39.04 | 38.35 | 39.25 | 36.84 | 36.28 | 36.07 | 36.47 | 37.72 | 38.24 |
| TIO2 | 3.36 | 3.41 | 3.51 | 3.13 | 2.84 | 3.19 | 3.09 | 3.57 | 3.18 | 3.60 |
| AL2O3 | 17.96 | 17.76 | 17.57 | 17.94 | 18.64 | 18.84 | 19.24 | 19.22 | 18.41 | 18.18 |
| CR2O3 | 0.00 | 0.00 | 0.00 | 0.00 | 0.00 | 0.00 | 0.00 | 0.00 | 0.00 | 0.00 |
| FEO | 19.61 | 20.48 | 21.56 | 20.78 | 20.85 | 20.34 | 20.65 | 21.02 | 22.18 | 22.25 |
| MNO | 0.76 | 0.40 | 0.31 | 0.38 | 0.27 | 0.39 | 0.37 | 0.34 | 0.44 | 0.52 |
| MGO | 6.07 | 4.98 | 4.86 | 5.19 | 7.98 | 8.22 | 8.16 | 7.35 | 4.59 | 4.63 |
| CAO | 0.06 | 0.12 | 0.00 | 0.09 | 0.00 | 0.00 | 0.00 | 0.00 | 0.00 | 0.10 |
| NA2O | 0.00 | 0.00 | 0.00 | 0.00 | 0.00 | 0.00 | 0.00 | 0.00 | 0.00 | 0.00 |
| K2O | 9.98 | 9.90 | 9.86 | 10.08 | 9.58 | 9.76 | 9.55 | 9.44 | 9.82 | 9.76 |
| P2O5 | 0.00 | 0.00 | 0.00 | 0.00 | 0.00 | 0.00 | 0.00 | 0.00 | 0.00 | 0.00 |
| H2O | 3.98 | 3.97 | 3.95 | 4.00 | 3.99 | 3.99 | 3.99 | 4.01 | 3.94 | 3.98 |
| TOTAL | 100.23 | 100.06 | 99.97 | 100.84 | 100.99 | 101.01 | 101.12 | 101.42 | 100.28 | 101.26 |
| CSI | 5.785 | 5.885 | 5.824 | 5.878 | 5.529 | 5.448 | 5.411 | 5.453 | 5.731 | 5.749 |
| CTI | 0.380 | 0.387 | 0.401 | 0.353 | 0.321 | 0.360 | 0.349 | 0.401 | 0.363 | 0.407 |
| CAL4 | 2.215 | 2.115 | 2.176 | 2.122 | 2.471 | 2.551 | 2.589 | 2.547 | 2.269 | 2.251 |
| CAL6 | 0.968 | 1.040 | 0.968 | 1.044 | 0.826 | 0.783 | 0.812 | 0.839 | 1.027 | 0.970 |
| CCR | 0.000 | 0.000 | 0.000 | 0.000 | 0.000 | 0.000 | 0.000 | 0.000 | 0.000 | 0.000 |
| CFE | 2.467 | 2.582 | 2.738 | 2.603 | 2.617 | 2.555 | 2.591 | 2.628 | 2.818 | 2.798 |
| CMN | 0.097 | 0.051 | 0.040 | 0.048 | 0.034 | 0.050 | 0.047 | 0.043 | 0.057 | 0.066 |
| CMG | 1.361 | 1.119 | 1.100 | 1.158 | 1.785 | 1.840 | 1.824 | 1.638 | 1.039 | 1.037 |
| CCA | 0.010 | 0.019 | 0.000 | 0.014 | 0.000 | 0.000 | 0.000 | 0.000 | 0.000 | 0.016 |
| CNA | 0.000 | 0.000 | 0.000 | 0.000 | 0.000 | 0.000 | 0.000 | 0.000 | 0.000 | 0.000 |
| CK | 1.916 | 1.904 | 1.910 | 1.926 | 1.834 | 1.870 | 1.828 | 1.801 | 1.903 | 1.872 |
| CP | 0.000 | 0.000 | 0.000 | 0.000 | 0.000 | 0.000 | 0.000 | 0.000 | 0.000 | 0.000 |
| COH | 4.000 | 4.000 | 4.000 | 4.000 | 4.000 | 4.000 | 4.000 | 4.000 | 4.000 | 4.000 |
| PHLO | 34.7 | 29.8 | 29.4 | 30.1 | 40.2 | 41.4 | 40.9 | 38.0 | 26.6 | 26.6 |
| ANN | 62.9 | 68.8 | 70.6 | 68.3 | 59.0 | 57.5 | 58.1 | 61.0 | 72.0 | 71.7 |
| MN | 2.5 | 1.4 | 1.0 | 1.3 | 0.8 | 1.1 | 1.1 | 1.0 | 1.4 | 1.7 |
| FE+MG | 3.83 | 3.70 | 3.84 | 3.76 | 4.40 | 4.40 | 4.42 | 4.27 | 3.86 | 3.84 |
| FE/FE+MG | 0.64 | 0.70 | 0.71 | 0.69 | 0.59 | 0.58 | 0.59 | 0.62 | 0.73 | 0.73 |

| SAMPLE | NQP10 | NQP10 | NQP10 | NQP10 | NQP10 | NQP10 | NQP11 | NQP11 | NQP11 | NQP11 |
|---|---|---|---|---|---|---|---|---|---|---|
| ANALYSES | 4 | 3 | 2 | 1-2 | 3 | 1 | 2-2 | 3 | 2 | 5 |
| MINERAL | BI | BI | BI | BI | BI | BI | BI | BI | BI | BI |
| LOCATION | HCQP1 | HCQP1 | HCQP1 | HCQP1 | HCQP1 | HCQP1 | HCQP1 | HCQP1 | HCQP1 | HCQP1 |
| SIO2 | 38.29 | 37.69 | 37.71 | 38.17 | 35.59 | 36.31 | 38.68 | 38.75 | 35.73 | 38.88 |
| TIO2 | 3.70 | 3.51 | 3.34 | 3.18 | 2.98 | 2.85 | 3.47 | 3.46 | 2.93 | 2.87 |
| AL2O3 | 18.16 | 18.36 | 18.24 | 18.17 | 19.17 | 18.93 | 17.83 | 17.64 | 19.01 | 17.67 |
| CR2O3 | 0.00 | 0.00 | 0.00 | 0.00 | 0.00 | 0.00 | 0.00 | 0.00 | 0.00 | 0.00 |
| FEO | 21.93 | 21.96 | 21.52 | 22.17 | 20.95 | 21.19 | 20.17 | 20.47 | 20.46 | 20.92 |
| MNO | 0.55 | 0.50 | 0.55 | 0.43 | 0.51 | 0.41 | 0.69 | 0.73 | 0.42 | 0.73 |
| MGO | 4.56 | 4.62 | 4.54 | 4.75 | 7.29 | 7.62 | 5.84 | 5.85 | 7.27 | 5.98 |
| CAO | 0.13 | 0.13 | 0.06 | 0.16 | 0.00 | 0.00 | 0.08 | 0.00 | 0.39 | 0.00 |
| NA2O | 0.00 | 0.00 | 0.00 | 0.00 | 0.00 | 0.00 | 0.00 | 0.00 | 0.00 | 0.00 |
| K2O | 9.94 | 9.80 | 9.67 | 9.78 | 9.51 | 9.60 | 9.70 | 9.89 | 9.41 | 9.74 |
| P2O5 | 0.00 | 0.00 | 0.00 | 0.00 | 0.00 | 0.00 | 0.00 | 0.00 | 0.00 | 0.00 |
| H2O | 3.99 | 3.95 | 3.93 | 3.97 | 3.93 | 3.97 | 3.99 | 3.99 | 3.93 | 3.99 |
| TOTAL | 101.25 | 100.52 | 99.56 | 100.78 | 99.93 | 100.88 | 100.45 | 100.78 | 99.55 | 100.78 |
| CSI | 5.756 | 5.711 | 5.755 | 5.765 | 5.421 | 5.474 | 5.807 | 5.813 | 5.451 | 5.836 |
| CTI | 0.418 | 0.400 | 0.383 | 0.361 | 0.341 | 0.323 | 0.392 | 0.390 | 0.336 | 0.324 |
| CAL4 | 2.244 | 2.289 | 2.245 | 2.234 | 2.579 | 2.535 | 2.193 | 2.187 | 2.549 | 2.164 |
| CAL6 | 0.973 | 0.989 | 1.035 | 1.000 | 0.861 | 0.837 | 0.961 | 0.931 | 0.868 | 0.962 |
| CCR | 0.000 | 0.000 | 0.000 | 0.000 | 0.000 | 0.000 | 0.000 | 0.000 | 0.000 | 0.000 |
| CFE | 2.757 | 2.783 | 2.747 | 2.801 | 2.669 | 2.672 | 2.532 | 2.568 | 2.610 | 2.626 |
| CMN | 0.070 | 0.064 | 0.071 | 0.055 | 0.066 | 0.052 | 0.088 | 0.093 | 0.054 | 0.093 |
| CMG | 1.022 | 1.043 | 1.033 | 1.069 | 1.655 | 1.712 | 1.307 | 1.308 | 1.653 | 1.338 |
| CCA | 0.021 | 0.021 | 0.010 | 0.026 | 0.000 | 0.000 | 0.013 | 0.000 | 0.064 | 0.000 |
| CNA | 0.000 | 0.000 | 0.000 | 0.000 | 0.000 | 0.000 | 0.000 | 0.000 | 0.000 | 0.000 |
| CK | 1.906 | 1.894 | 1.883 | 1.885 | 1.848 | 1.846 | 1.858 | 1.893 | 1.832 | 1.865 |
| CP | 0.000 | 0.000 | 0.000 | 0.000 | 0.000 | 0.000 | 0.000 | 0.000 | 0.000 | 0.000 |
| COH | 4.000 | 4.000 | 4.000 | 4.000 | 4.000 | 4.000 | 4.000 | 4.000 | 4.000 | 4.000 |
| PHLO | 26.5 | 26.8 | 26.8 | 27.2 | 37.7 | 38.6 | 33.3 | 33.0 | 39.3 | 33.0 |
| ANN | 71.6 | 71.5 | 71.3 | 71.4 | 60.8 | 60.2 | 64.5 | 64.7 | 60.5 | 64.7 |
| MN | 1.8 | 1.7 | 1.8 | 1.4 | 1.5 | 1.2 | 2.2 | 2.3 | 1.3 | 2.3 |
| FE+MG | 3.78 | 3.83 | 3.78 | 3.87 | 4.32 | 4.38 | 3.84 | 3.88 | 4.26 | 3.96 |
| FE/FE+MG | 0.73 | 0.73 | 0.73 | 0.72 | 0.62 | 0.61 | 0.66 | 0.66 | 0.61 | 0.66 |

| SAMPLE | NQP12 | NQPL004 | NQPL004 | NQPL004 | NQPL038 | NQPL038 | NQPL038 | NQPL038 | NQPL038 | NQPL038 |
|---|---|---|---|---|---|---|---|---|---|---|
| ANALYSES | 3B-2 | 1B-1 | 1B-3 | 1B-2 | 2B-2 | 1B-1 | 1B-2 | 2B-1 | 3B-1 | 4B-1 |
| MINERAL | BI | BI | BI | BI | BI | BI | BI | BI | BI | BI |
| LOCATION | HCQP1 | HCQP1 | HCQP1 | HCQP1 | HCQP1 | HCQP1 | HCQP1 | HCQP1 | HCQP1 | HCQP1 |
| SIO2 | 36.41 | 36.41 | 36.94 | 36.73 | 35.97 | 36.10 | 36.12 | 35.91 | 35.93 | 35.92 |
| TIO2 | 3.44 | 2.62 | 3.05 | 2.73 | 3.25 | 3.07 | 3.30 | 3.31 | 2.89 | 3.17 |
| AL2O3 | 19.09 | 19.71 | 19.61 | 19.39 | 19.05 | 19.16 | 18.92 | 19.27 | 19.06 | 19.07 |
| CR2O3 | 0.00 | 0.00 | 0.00 | 0.00 | 0.00 | 0.00 | 0.00 | 0.00 | 0.00 | 0.00 |
| FEO | 19.96 | 22.64 | 21.61 | 22.74 | 20.96 | 20.90 | 21.49 | 21.36 | 21.06 | 21.23 |
| MNO | 0.64 | 0.47 | 0.41 | 0.55 | 0.50 | 0.56 | 0.66 | 0.63 | 0.52 | 0.50 |
| MGO | 7.80 | 5.11 | 4.55 | 4.97 | 6.92 | 7.07 | 7.17 | 7.07 | 7.25 | 6.78 |
| CAO | 0.00 | 0.00 | 0.00 | 0.00 | 0.00 | 0.00 | 0.00 | 0.00 | 0.00 | 0.13 |
| NA2O | 0.00 | 0.00 | 0.00 | 0.00 | 0.00 | 0.00 | 0.00 | 0.00 | 0.00 | 0.00 |
| K2O | 9.42 | 9.28 | 9.30 | 9.17 | 9.42 | 9.41 | 9.40 | 9.39 | 9.47 | 9.05 |
| P2O5 | 0.00 | 0.00 | 0.00 | 0.00 | 0.00 | 0.00 | 0.00 | 0.00 | 0.00 | 0.00 |
| H2O | 3.99 | 3.93 | 3.93 | 3.94 | 3.94 | 3.95 | 3.97 | 3.97 | 3.94 | 3.94 |
| TOTAL | 100.75 | 100.17 | 99.40 | 100.22 | 100.01 | 100.22 | 101.03 | 100.91 | 100.12 | 99.79 |
| CSI | 5.463 | 5.544 | 5.633 | 5.588 | 5.465 | 5.470 | 5.447 | 5.419 | 5.459 | 5.468 |
| CTI | 0.388 | 0.300 | 0.350 | 0.312 | 0.371 | 0.350 | 0.374 | 0.376 | 0.330 | 0.363 |
| CAL4 | 2.537 | 2.456 | 2.367 | 2.412 | 2.535 | 2.530 | 2.553 | 2.581 | 2.541 | 2.532 |
| CAL6 | 0.839 | 1.081 | 1.156 | 1.065 | 0.876 | 0.891 | 0.810 | 0.845 | 0.871 | 0.889 |
| CCR | 0.000 | 0.000 | 0.000 | 0.000 | 0.000 | 0.000 | 0.000 | 0.000 | 0.000 | 0.000 |
| CFE | 2.505 | 2.883 | 2.756 | 2.894 | 2.663 | 2.648 | 2.711 | 2.696 | 2.676 | 2.703 |
| CMN | 0.081 | 0.061 | 0.053 | 0.071 | 0.064 | 0.072 | 0.084 | 0.081 | 0.067 | 0.064 |
| CMG | 1.744 | 1.160 | 1.034 | 1.127 | 1.567 | 1.597 | 1.612 | 1.590 | 1.641 | 1.538 |
| CCA | 0.000 | 0.000 | 0.000 | 0.000 | 0.000 | 0.000 | 0.000 | 0.000 | 0.000 | 0.021 |
| CNA | 0.000 | 0.000 | 0.000 | 0.000 | 0.000 | 0.000 | 0.000 | 0.000 | 0.000 | 0.000 |
| CK | 1.803 | 1.803 | 1.809 | 1.780 | 1.826 | 1.819 | 1.809 | 1.808 | 1.835 | 1.758 |
| CP | 0.000 | 0.000 | 0.000 | 0.000 | 0.000 | 0.000 | 0.000 | 0.000 | 0.000 | 0.000 |
| COH | 4.000 | 4.000 | 4.000 | 4.000 | 4.000 | 4.000 | 4.000 | 4.000 | 4.000 | 4.000 |
| PHLO | 40.3 | 28.3 | 26.9 | 27.3 | 36.5 | 37.0 | 36.6 | 36.4 | 37.4 | 35.8 |
| ANN | 57.8 | 70.3 | 71.7 | 70.7 | 62.0 | 61.3 | 61.5 | 61.7 | 61.0 | 62.8 |
| MN | 1.9 | 1.5 | 1.4 | 1.7 | 1.5 | 1.7 | 1.9 | 1.8 | 1.5 | 1.5 |
| FE+MG | 4.25 | 4.04 | 3.79 | 4.02 | 4.23 | 4.25 | 4.32 | 4.29 | 4.32 | 4.24 |
| FE/FE+MG | 0.59 | 0.71 | 0.73 | 0.72 | 0.63 | 0.62 | 0.63 | 0.63 | 0.62 | 0.64 |

| SAMPLE | NQP12 | NQPL004 | NQPL004 | NQPL004 | NQPL038 | NQPL038 | NQPL038 | NQPL038 | NQPL038 | NQPL038 |
|---|---|---|---|---|---|---|---|---|---|---|
| ANALYSES | 3B-2 | 1B-1 | 1B-3 | 1B-2 | 2B-2 | 1B-1 | 1B-2 | 2B-1 | 3B-1 | 4B-1 |
| MINERAL | BI | BI | BI | BI | BI | BI | BI | BI | BI | BI |
| LOCATION | HCQP1 | HCQP1 | HCQP1 | HCQP1 | HCQP1 | HCQP1 | HCQP1 | HCQP1 | HCQP1 | HCQP1 |
| SIO2 | 36.41 | 36.41 | 36.94 | 36.73 | 35.97 | 36.10 | 36.12 | 35.91 | 35.93 | 35.92 |
| TIO2 | 3.44 | 2.62 | 3.05 | 2.73 | 3.25 | 3.07 | 3.30 | 3.31 | 2.89 | 3.17 |
| AL203 | 19.09 | 19.71 | 19.61 | 19.39 | 19.05 | 19.16 | 18.92 | 19.27 | 19.06 | 19.07 |
| CR203 | 0.00 | 0.00 | 0.00 | 0.00 | 0.00 | 0.00 | 0.00 | 0.00 | 0.00 | 0.00 |
| FEO | 19.96 | 22.64 | 21.61 | 22.74 | 20.96 | 20.90 | 21.49 | 21.36 | 21.06 | 21.23 |
| MNO | 0.64 | 0.47 | 0.41 | 0.55 | 0.50 | 0.56 | 0.66 | 0.63 | 0.52 | 0.50 |
| MGO | 7.80 | 5.11 | 4.55 | 4.97 | 6.92 | 7.07 | 7.17 | 7.07 | 7.25 | 6.78 |
| CAO | 0.00 | 0.00 | 0.00 | 0.00 | 0.00 | 0.00 | 0.00 | 0.00 | 0.00 | 0.13 |
| NA2O | 0.00 | 0.00 | 0.00 | 0.00 | 0.00 | 0.00 | 0.00 | 0.00 | 0.00 | 0.00 |
| K2O | 9.42 | 9.28 | 9.30 | 9.17 | 9.42 | 9.41 | 9.40 | 9.39 | 9.47 | 9.05 |
| P2O5 | 0.00 | 0.00 | 0.00 | 0.00 | 0.00 | 0.00 | 0.00 | 0.00 | 0.00 | 0.00 |
| H2O | 3.99 | 3.93 | 3.93 | 3.94 | 3.94 | 3.95 | 3.97 | 3.97 | 3.94 | 3.94 |
| TOTAL | 100.75 | 100.17 | 99.40 | 100.22 | 100.01 | 100.22 | 101.03 | 100.91 | 100.12 | 99.79 |
| CSI | 5.463 | 5.544 | 5.633 | 5.588 | 5.465 | 5.470 | 5.447 | 5.419 | 5.459 | 5.468 |
| CTI | 0.388 | 0.300 | 0.350 | 0.312 | 0.371 | 0.350 | 0.374 | 0.376 | 0.330 | 0.363 |
| CAL4 | 2.537 | 2.456 | 2.367 | 2.412 | 2.535 | 2.530 | 2.553 | 2.581 | 2.541 | 2.532 |
| CAL6 | 0.839 | 1.081 | 1.156 | 1.065 | 0.876 | 0.891 | 0.810 | 0.845 | 0.871 | 0.889 |
| CCR | 0.000 | 0.000 | 0.000 | 0.000 | 0.000 | 0.000 | 0.000 | 0.000 | 0.000 | 0.000 |
| CFE | 2.505 | 2.883 | 2.756 | 2.894 | 2.663 | 2.648 | 2.711 | 2.696 | 2.676 | 2.703 |
| CMN | 0.081 | 0.061 | 0.053 | 0.071 | 0.064 | 0.072 | 0.084 | 0.081 | 0.067 | 0.064 |
| CMG | 1.744 | 1.160 | 1.034 | 1.127 | 1.567 | 1.597 | 1.612 | 1.590 | 1.641 | 1.538 |
| CCA | 0.000 | 0.000 | 0.000 | 0.000 | 0.000 | 0.000 | 0.000 | 0.000 | 0.000 | 0.021 |
| CNA | 0.000 | 0.000 | 0.000 | 0.000 | 0.000 | 0.000 | 0.000 | 0.000 | 0.000 | 0.000 |
| CK | 1.803 | 1.803 | 1.809 | 1.780 | 1.826 | 1.819 | 1.809 | 1.808 | 1.835 | 1.758 |
| CP | 0.000 | 0.000 | 0.000 | 0.000 | 0.000 | 0.000 | 0.000 | 0.000 | 0.000 | 0.000 |
| COH | 4.000 | 4.000 | 4.000 | 4.000 | 4.000 | 4.000 | 4.000 | 4.000 | 4.000 | 4.000 |
| PHLO | 40.3 | 28.3 | 26.9 | 27.3 | 36.5 | 37.0 | 36.6 | 36.4 | 37.4 | 35.8 |
| ANN | 57.8 | 70.3 | 71.7 | 70.7 | 62.0 | 61.3 | 61.5 | 61.7 | 61.0 | 62.8 |
| MN | 1.9 | 1.5 | 1.4 | 1.7 | 1.5 | 1.7 | 1.9 | 1.8 | 1.5 | 1.5 |
| FE+MG | 4.25 | 4.04 | 3.79 | 4.02 | 4.23 | 4.25 | 4.32 | 4.29 | 4.32 | 4.24 |
| FE/FE+MG | 0.59 | 0.71 | 0.73 | 0.72 | 0.63 | 0.62 | 0.63 | 0.63 | 0.62 | 0.64 |

| SAMPLE | NQPL038 | NQPL038 | NQPL038 | NQP01 | NQP01 | NQP01 | NQP01 | NQP01 | NQP01 | NQP01 |
|---|---|---|---|---|---|---|---|---|---|---|
| ANALYSES | 4B-2 | 6B | 7B | 3 | 6 | 3 | 4 | 5 | 2 | 1 |
| MINERAL | BI | BI | BI | BI | BI | BI | BI | BI | BI | BI |
| LOCATION | HCQP1 | HCQP1 | HCQP1 | HCQP1A | HCQP1A | HCQP1A | HCQP1A | HCQP1A | HCQP1A | HCQP1A |
| SIO2 | 36.36 | 35.86 | 36.30 | 37.89 | 36.11 | 35.80 | 36.45 | 36.61 | 36.42 | 35.91 |
| TIO2 | 2.95 | 3.41 | 3.66 | 3.57 | 2.46 | 3.00 | 2.62 | 2.24 | 2.97 | 3.06 |
| AL2O3 | 19.09 | 18.67 | 19.02 | 17.73 | 18.78 | 18.88 | 18.48 | 18.73 | 19.38 | 18.91 |
| CR2O3 | 0.00 | 0.00 | 0.00 | 0.00 | 0.00 | 0.00 | 0.00 | 0.00 | 0.00 | 0.00 |
| FEO | 21.00 | 20.76 | 21.38 | 20.44 | 20.27 | 19.88 | 20.00 | 20.17 | 20.07 | 20.27 |
| MNO | 0.53 | 0.49 | 0.59 | 0.66 | 0.45 | 0.59 | 0.44 | 0.51 | 0.61 | 0.54 |
| MGO | 7.17 | 7.07 | 6.80 | 5.47 | 7.87 | 7.64 | 8.39 | 8.16 | 7.67 | 9.09 |
| CAO | 0.32 | 0.00 | 0.00 | 0.14 | 0.00 | 0.00 | 0.00 | 0.00 | 0.00 | 0.05 |
| NA2O | 0.00 | 0.00 | 0.00 | 0.00 | 0.00 | 0.00 | 0.00 | 0.00 | 0.00 | 0.00 |
| K2O | 8.73 | 9.34 | 9.31 | 9.51 | 9.66 | 9.40 | 9.54 | 9.60 | 9.50 | 9.57 |
| P2O5 | 0.00 | 0.00 | 0.00 | 0.00 | 0.00 | 0.00 | 0.00 | 0.00 | 0.00 | 0.00 |
| H2O | 3.96 | 3.93 | 3.98 | 3.94 | 3.93 | 3.92 | 3.95 | 3.96 | 3.99 | 4.00 |
| TOTAL | 100.11 | 99.53 | 101.04 | 99.35 | 99.53 | 99.11 | 99.87 | 99.98 | 100.61 | 101.40 |
| CSI | 5.497 | 5.473 | 5.463 | 5.768 | 5.503 | 5.469 | 5.522 | 5.543 | 5.474 | 5.375 |
| CTI | 0.335 | 0.391 | 0.414 | 0.409 | 0.282 | 0.345 | 0.299 | 0.255 | 0.336 | 0.344 |
| CAL4 | 2.503 | 2.527 | 2.537 | 2.232 | 2.497 | 2.531 | 2.478 | 2.457 | 2.526 | 2.625 |
| CAL6 | 0.898 | 0.831 | 0.835 | 0.948 | 0.876 | 0.868 | 0.822 | 0.885 | 0.907 | 0.711 |
| CCR | 0.000 | 0.000 | 0.000 | 0.000 | 0.000 | 0.000 | 0.000 | 0.000 | 0.000 | 0.000 |
| CFE | 2.655 | 2.650 | 2.691 | 2.602 | 2.584 | 2.540 | 2.534 | 2.554 | 2.523 | 2.537 |
| CMN | 0.068 | 0.063 | 0.075 | 0.085 | 0.058 | 0.076 | 0.056 | 0.065 | 0.078 | 0.068 |
| CMG | 1.615 | 1.608 | 1.525 | 1.241 | 1.788 | 1.739 | 1.894 | 1.841 | 1.718 | 2.028 |
| CCA | 0.052 | 0.000 | 0.000 | 0.023 | 0.000 | 0.000 | 0.000 | 0.000 | 0.000 | 0.008 |
| CNA | 0.000 | 0.000 | 0.000 | 0.000 | 0.000 | 0.000 | 0.000 | 0.000 | 0.000 | 0.000 |
| CK | 1.684 | 1.819 | 1.787 | 1.847 | 1.878 | 1.832 | 1.844 | 1.854 | 1.822 | 1.828 |
| CP | 0.000 | 0.000 | 0.000 | 0.000 | 0.000 | 0.000 | 0.000 | 0.000 | 0.000 | 0.000 |
| COH | 4.000 | 4.000 | 4.000 | 4.000 | 4.000 | 4.000 | 4.000 | 4.000 | 4.000 | 4.000 |
| PHLO | 37.2 | 37.2 | 35.5 | 31.6 | 40.4 | 39.9 | 42.2 | 41.3 | 39.8 | 43.8 |
| ANN | 61.2 | 61.3 | 62.7 | 66.2 | 58.3 | 58.3 | 56.5 | 57.3 | 58.4 | 54.8 |
| MN | 1.6 | 1.5 | 1.8 | 2.2 | 1.3 | 1.8 | 1.3 | 1.5 | 1.8 | 1.5 |
| FE+MG | 4.27 | 4.26 | 4.22 | 3.84 | 4.37 | 4.28 | 4.43 | 4.40 | 4.24 | 4.57 |
| FE/FE+MG | 0.62 | 0.62 | 0.64 | 0.68 | 0.59 | 0.59 | 0.57 | 0.58 | 0.59 | 0.56 |

| SAMPLE | NQP01 | NQP01 | NQP02 | NQP02 | NQP02 | NQP02 | NQP02 | NQP02 | NQP02 | NQP02 |
|---|---|---|---|---|---|---|---|---|---|---|
| ANALYSES | 1 | 4 | 7B-1 | 3B-1 | 5B-2 | 6B-1 | 6B-2 | 4B-1 | 7B-2 | 8B-1 |
| MINERAL | BI | BI | BI | BI | BI | BI | BI | BI | BI | BI |
| LOCATION | HCQP1A | HCQP1A | HCQP1A | HCQP1A | HCQP1A | HCQP1A | HCQP1A | HCQP1A | HCQP1A | HCQP1A |
| SIO2 | 38.49 | 38.69 | 35.72 | 36.45 | 37.11 | 35.99 | 36.19 | 36.42 | 36.20 | 36.30 |
| TIO2 | 3.39 | 3.40 | 3.23 | 3.14 | 3.10 | 2.84 | 3.22 | 3.55 | 3.30 | 3.16 |
| AL2O3 | 17.70 | 17.39 | 18.69 | 18.99 | 18.82 | 19.16 | 19.36 | 18.54 | 18.97 | 19.44 |
| CR2O3 | 0.00 | 0.00 | 0.00 | 0.00 | 0.00 | 0.00 | 0.00 | 0.00 | 0.00 | 0.00 |
| FEO | 20.87 | 20.29 | 20.18 | 20.34 | 19.80 | 20.74 | 20.17 | 20.09 | 20.72 | 20.18 |
| MNO | 0.69 | 0.54 | 0.62 | 0.43 | 0.53 | 0.55 | 0.57 | 0.47 | 0.64 | 0.62 |
| MGO | 5.61 | 5.82 | 7.59 | 7.76 | 8.29 | 7.76 | 7.73 | 7.94 | 7.90 | 8.18 |
| CAO | 0.08 | 0.11 | 0.00 | 0.00 | 0.05 | 0.00 | 0.00 | 0.00 | 0.00 | 0.00 |
| NA2O | 0.00 | 0.00 | 0.00 | 0.00 | 0.00 | 0.00 | 0.00 | 0.00 | 0.00 | 0.00 |
| K2O | 9.76 | 9.87 | 9.43 | 9.41 | 9.34 | 9.54 | 9.61 | 9.43 | 9.53 | 9.59 |
| P2O5 | 0.00 | 0.00 | 0.00 | 0.00 | 0.00 | 0.00 | 0.00 | 0.00 | 0.00 | 0.00 |
| H2O | 3.98 | 3.97 | 3.92 | 3.98 | 4.02 | 3.96 | 3.99 | 3.98 | 3.99 | 4.02 |
| TOTAL | 100.57 | 100.08 | 99.38 | 100.50 | 101.06 | 100.54 | 100.84 | 100.42 | 101.25 | 101.49 |
| CSI | 5.796 | 5.840 | 5.454 | 5.487 | 5.534 | 5.438 | 5.436 | 5.487 | 5.431 | 5.416 |
| CTI | 0.384 | 0.386 | 0.371 | 0.355 | 0.348 | 0.323 | 0.364 | 0.402 | 0.372 | 0.355 |
| CAL4 | 2.204 | 2.160 | 2.546 | 2.513 | 2.466 | 2.562 | 2.564 | 2.513 | 2.569 | 2.584 |
| CAL6 | 0.937 | 0.933 | 0.817 | 0.856 | 0.841 | 0.850 | 0.863 | 0.779 | 0.785 | 0.835 |
| CCR | 0.000 | 0.000 | 0.000 | 0.000 | 0.000 | 0.000 | 0.000 | 0.000 | 0.000 | 0.000 |
| CFE | 2.628 | 2.561 | 2.577 | 2.561 | 2.469 | 2.621 | 2.534 | 2.532 | 2.600 | 2.518 |
| CMN | 0.088 | 0.069 | 0.080 | 0.055 | 0.067 | 0.070 | 0.073 | 0.060 | 0.081 | 0.078 |
| CMG | 1.259 | 1.309 | 1.727 | 1.741 | 1.842 | 1.747 | 1.730 | 1.783 | 1.766 | 1.819 |
| CCA | 0.013 | 0.018 | 0.000 | 0.000 | 0.008 | 0.000 | 0.000 | 0.000 | 0.000 | 0.000 |
| CNA | 0.000 | 0.000 | 0.000 | 0.000 | 0.000 | 0.000 | 0.000 | 0.000 | 0.000 | 0.000 |
| CK | 1.875 | 1.901 | 1.837 | 1.807 | 1.777 | 1.839 | 1.842 | 1.813 | 1.824 | 1.826 |
| CP | 0.000 | 0.000 | 0.000 | 0.000 | 0.000 | 0.000 | 0.000 | 0.000 | 0.000 | 0.000 |
| COH | 4.000 | 4.000 | 4.000 | 4.000 | 4.000 | 4.000 | 4.000 | 4.000 | 4.000 | 4.000 |
| PHLO | 31.7 | 33.2 | 39.4 | 40.0 | 42.1 | 39.4 | 39.9 | 40.8 | 39.7 | 41.2 |
| ANN | 66.1 | 65.0 | 58.8 | 58.8 | 56.4 | 59.0 | 58.4 | 57.9 | 58.5 | 57.0 |
| MN | 2.2 | 1.8 | 1.8 | 1.3 | 1.5 | 1.6 | 1.7 | 1.4 | 1.8 | 1.8 |
| FE+MG | 3.89 | 3.87 | 4.30 | 4.30 | 4.31 | 4.37 | 4.26 | 4.32 | 4.37 | 4.34 |
| FE/FE+MG | 0.68 | 0.66 | 0.60 | 0.60 | 0.57 | 0.60 | 0.59 | 0.59 | 0.60 | 0.58 |

| SAMPLE | NQP02 | NQP02 | NQP02 | NQP02 | NHC01 | NHC01 | NHC01 | NHC02 | NHC02 | NHC02 |
|---|---|---|---|---|---|---|---|---|---|---|
| ANALYSES | 8B-2 | 2B-1 | 1B-1 | 2B-2 | 1 | 2 | 4 | 3B-1 | 7B-1 | 7B-2 |
| MINERAL | BI | BI | BI | BI | BI | BI | BI | BI | BI | BI |
| LOCATION | HCQP1A | HCQP1A | HCQP1A | HCQP1A | HCQP2 | HCQP2 | HCQP2 | HCQP2 | HCQP2 | HCQP2 |
| SIO2 | 36.72 | 36.28 | 35.97 | 36.01 | 38.23 | 37.93 | 38.12 | 35.59 | 35.80 | 36.07 |
| TIO2 | 3.32 | 3.70 | 2.98 | 2.87 | 2.39 | 2.81 | 2.96 | 3.18 | 3.51 | 3.01 |
| AL203 | 19.27 | 19.12 | 19.19 | 18.87 | 19.21 | 18.82 | 18.39 | 20.36 | 19.63 | 19.84 |
| CR203 | 0.00 | 0.00 | 0.00 | 0.00 | 0.00 | 0.00 | 0.00 | 0.00 | 0.00 | 0.00 |
| FEO | 19.44 | 19.87 | 20.53 | 19.95 | 22.35 | 21.79 | 22.31 | 22.26 | 22.50 | 22.89 |
| MNO | 0.48 | 0.62 | 0.55 | 0.45 | 0.87 | 0.68 | 0.78 | 0.49 | 0.35 | 0.37 |
| MGO | 7.92 | 7.72 | 7.65 | 7.88 | 4.05 | 4.01 | 4.20 | 5.67 | 5.08 | 5.44 |
| CAO | 0.00 | 0.00 | 0.00 | 0.00 | 0.11 | 0.08 | 0.05 | 0.00 | 0.00 | 0.08 |
| NA2O | 0.00 | 0.00 | 0.00 | 0.00 | 0.00 | 0.00 | 0.00 | 0.00 | 0.00 | 0.00 |
| K2O | 9.71 | 9.31 | 9.64 | 9.54 | 9.63 | 9.45 | 9.56 | 9.46 | 9.41 | 9.46 |
| P2O5 | 0.00 | 0.00 | 0.00 | 0.00 | 0.00 | 0.00 | 0.00 | 0.00 | 0.00 | 0.00 |
| H2O | 4.01 | 3.99 | 3.96 | 3.94 | 3.97 | 3.93 | 3.95 | 3.96 | 3.93 | 3.96 |
| TOTAL | 100.87 | 100.61 | 100.47 | 99.51 | 100.81 | 99.50 | 100.32 | 100.97 | 100.21 | 101.12 |
| CSI | 5.489 | 5.447 | 5.437 | 5.479 | 5.771 | 5.785 | 5.786 | 5.382 | 5.459 | 5.456 |
| CTI | 0.373 | 0.418 | 0.339 | 0.328 | 0.271 | 0.322 | 0.338 | 0.362 | 0.403 | 0.342 |
| CAL4 | 2.511 | 2.553 | 2.563 | 2.521 | 2.229 | 2.215 | 2.214 | 2.618 | 2.541 | 2.544 |
| CAL6 | 0.883 | 0.830 | 0.855 | 0.862 | 1.187 | 1.167 | 1.075 | 1.010 | 0.986 | 0.993 |
| CCR | 0.000 | 0.000 | 0.000 | 0.000 | 0.000 | 0.000 | 0.000 | 0.000 | 0.000 | 0.000 |
| CFE | 2.430 | 2.495 | 2.595 | 2.538 | 2.821 | 2.779 | 2.832 | 2.815 | 2.869 | 2.896 |
| CMN | 0.061 | 0.079 | 0.070 | 0.058 | 0.111 | 0.088 | 0.100 | 0.063 | 0.045 | 0.047 |
| CMG | 1.764 | 1.727 | 1.723 | 1.787 | 0.911 | 0.911 | 0.950 | 1.278 | 1.154 | 1.226 |
| CCA | 0.000 | 0.000 | 0.000 | 0.000 | 0.018 | 0.013 | 0.008 | 0.000 | 0.000 | 0.013 |
| CNA | 0.000 | 0.000 | 0.000 | 0.000 | 0.000 | 0.000 | 0.000 | 0.000 | 0.000 | 0.000 |
| CK | 1.852 | 1.783 | 1.859 | 1.852 | 1.854 | 1.839 | 1.851 | 1.825 | 1.831 | 1.826 |
| CP | 0.000 | 0.000 | 0.000 | 0.000 | 0.000 | 0.000 | 0.000 | 0.000 | 0.000 | 0.000 |
| COH | 4.000 | 4.000 | 4.000 | 4.000 | 4.000 | 4.000 | 4.000 | 4.000 | 4.000 | 4.000 |
| PHLO | 41.5 | 40.2 | 39.3 | 40.8 | 23.7 | 24.1 | 24.5 | 30.8 | 28.4 | 29.4 |
| ANN | 57.1 | 58.0 | 59.1 | 57.9 | 73.4 | 73.6 | 72.9 | 67.7 | 70.5 | 69.4 |
| MN | 1.4 | 1.8 | 1.6 | 1.3 | 2.9 | 2.3 | 2.6 | 1.5 | 1.1 | 1.1 |
| FE+MG | 4.19 | 4.22 | 4.32 | 4.33 | 3.73 | 3.69 | 3.78 | 4.09 | 4.02 | 4.12 |
| FE/FE+MG | 0.58 | 0.59 | 0.60 | 0.59 | 0.76 | 0.75 | 0.75 | 0.69 | 0.71 | 0.70 |

| SAMPLE | NHC02 | NHC02 | NHC02 | NHC06 | NHC06 | NHC06 | NHC06 | NHC06 | NHCL014 | NHCL014 |
|---|---|---|---|---|---|---|---|---|---|---|
| ANALYSES | 4B-2 | 4B-1 | 3B-2 | 4B | 3 | 1 | 2B | 2 | 1B-3 | 1B-5 |
| MINERAL | BI | BI | BI | BI | BI | BI | BI | BI | BI | BI |
| LOCATION | HCQP2 | HCQP2 | HCQP2 | HCQP2 | HCQP2 | HCQP2 | HCQP2 | HCQP2 | HCQP2 | HCQP2 |
| SIO2 | 35.90 | 35.89 | 36.36 | 35.82 | 38.24 | 37.69 | 35.98 | 38.16 | 35.62 | 35.64 |
| TIO2 | 3.37 | 3.35 | 3.19 | 3.08 | 3.50 | 3.67 | 3.10 | 3.26 | 1.22 | 1.42 |
| AL203 | 20.05 | 19.99 | 19.94 | 19.55 | 18.32 | 18.50 | 19.72 | 18.74 | 20.61 | 20.68 |
| CR203 | 0.00 | 0.00 | 0.00 | 0.00 | 0.00 | 0.00 | 0.00 | 0.00 | 0.00 | 0.00 |
| FEO | 22.36 | 22.57 | 22.03 | 20.78 | 21.53 | 22.11 | 21.27 | 22.27 | 24.79 | 24.51 |
| MNO | 0.44 | 0.38 | 0.40 | 0.24 | 0.28 | 0.30 | 0.22 | 0.37 | 0.66 | 0.64 |
| MGO | 5.74 | 5.57 | 5.76 | 6.07 | 4.46 | 4.41 | 6.01 | 4.58 | 3.84 | 3.68 |
| CAO | 0.15 | 0.00 | 0.00 | 0.13 | 0.09 | 0.19 | 0.00 | 0.12 | 0.00 | 0.00 |
| NA20 | 0.00 | 0.00 | 0.00 | 0.00 | 0.00 | 0.00 | 0.00 | 0.00 | 0.00 | 0.00 |
| K20 | 9.20 | 9.32 | 9.61 | 8.70 | 9.64 | 9.35 | 9.43 | 9.80 | 8.88 | 9.29 |
| P205 | 0.00 | 0.00 | 0.00 | 0.00 | 0.00 | 0.00 | 0.00 | 0.00 | 0.00 | 0.00 |
| H20 | 3.98 | 3.97 | 3.98 | 3.90 | 3.96 | 3.95 | 3.93 | 3.99 | 3.87 | 3.88 |
| TOTAL | 101.19 | 101.04 | 101.27 | 98.27 | 100.02 | 100.17 | 99.66 | 101.29 | 99.49 | 99.74 |
| CSI | 5.410 | 5.422 | 5.469 | 5.505 | 5.791 | 5.715 | 5.480 | 5.730 | 5.511 | 5.505 |
| CTI | 0.382 | 0.381 | 0.361 | 0.356 | 0.399 | 0.418 | 0.355 | 0.368 | 0.142 | 0.165 |
| CAL4 | 2.590 | 2.577 | 2.531 | 2.495 | 2.209 | 2.285 | 2.520 | 2.270 | 2.489 | 2.495 |
| CAL6 | 0.971 | 0.981 | 1.004 | 1.045 | 1.060 | 1.020 | 1.019 | 1.046 | 1.268 | 1.269 |
| CCR | 0.000 | 0.000 | 0.000 | 0.000 | 0.000 | 0.000 | 0.000 | 0.000 | 0.000 | 0.000 |
| CFE | 2.818 | 2.852 | 2.771 | 2.671 | 2.727 | 2.804 | 2.709 | 2.797 | 3.208 | 3.166 |
| CMN | 0.056 | 0.049 | 0.051 | 0.031 | 0.036 | 0.039 | 0.028 | 0.047 | 0.086 | 0.084 |
| CMG | 1.289 | 1.254 | 1.291 | 1.390 | 1.007 | 0.996 | 1.364 | 1.025 | 0.885 | 0.847 |
| CCA | 0.024 | 0.000 | 0.000 | 0.021 | 0.015 | 0.031 | 0.000 | 0.019 | 0.000 | 0.000 |
| CNA | 0.000 | 0.000 | 0.000 | 0.000 | 0.000 | 0.000 | 0.000 | 0.000 | 0.000 | 0.000 |
| CK | 1.769 | 1.796 | 1.844 | 1.706 | 1.862 | 1.809 | 1.832 | 1.877 | 1.753 | 1.831 |
| CP | 0.000 | 0.000 | 0.000 | 0.000 | 0.000 | 0.000 | 0.000 | 0.000 | 0.000 | 0.000 |
| COH | 4.000 | 4.000 | 4.000 | 4.000 | 4.000 | 4.000 | 4.000 | 4.000 | 4.000 | 4.000 |
| PHLO | 31.0 | 30.2 | 31.4 | 34.0 | 26.7 | 26.0 | 33.3 | 26.5 | 21.2 | 20.7 |
| ANN | 67.7 | 68.6 | 67.4 | 65.3 | 72.3 | 73.0 | 66.0 | 72.3 | 76.7 | 77.3 |
| MN | 1.3 | 1.2 | 1.2 | 0.8 | 1.0 | 1.0 | 0.7 | 1.2 | 2.1 | 2.0 |
| FE+MG | 4.11 | 4.11 | 4.06 | 4.06 | 3.73 | 3.80 | 4.07 | 3.82 | 4.09 | 4.01 |
| FE/FE+MG | 0.69 | 0.69 | 0.68 | 0.66 | 0.73 | 0.74 | 0.67 | 0.73 | 0.78 | 0.79 |

| SAMPLE | NHCL014 | NHCL014 | NHCL014 | NHCL036 | NHCL036 | NHCL036 | NHCL036 | NHCL036 | NHCL036 | NHCL036 |
|---|---|---|---|---|---|---|---|---|---|---|
| ANALYSES | 2B-1 | 2B-2 | 2B-3 | 1B-2 | 4B-2 | 1B-1 | 3B-2 | 3B-1 | 4B-1 | 2B-3 |
| MINERAL | BI | BI | BI | BI | BI | BI | BI | BI | BI | BI |
| LOCATION | HCQP2 | HCQP2 | HCQP2 | HCQP2 | HCQP2 | HCQP2 | HCQP2 | HCQP2 | HCQP2 | HCQP2 |
| SIO2 | 35.93 | 35.86 | 35.36 | 35.80 | 36.15 | 35.76 | 35.43 | 35.68 | 36.19 | 35.78 |
| TIO2 | 1.16 | 1.13 | 1.12 | 2.30 | 2.40 | 2.53 | 2.58 | 2.66 | 2.37 | 2.74 |
| AL2O3 | 20.48 | 20.85 | 20.51 | 19.58 | 19.63 | 19.80 | 19.66 | 19.13 | 19.74 | 19.29 |
| CR2O3 | 0.00 | 0.00 | 0.00 | 0.00 | 0.00 | 0.00 | 0.00 | 0.00 | 0.00 | 0.00 |
| FEO | 24.40 | 24.61 | 24.93 | 21.95 | 21.61 | 22.09 | 21.07 | 21.53 | 21.13 | 22.02 |
| MNO | 0.60 | 0.57 | 0.61 | 0.59 | 0.68 | 0.56 | 0.71 | 0.55 | 0.62 | 0.46 |
| MGO | 3.51 | 3.62 | 4.07 | 6.68 | 7.37 | 6.76 | 6.94 | 6.87 | 7.07 | 6.57 |
| CAO | 0.00 | 0.00 | 0.00 | 0.00 | 0.00 | 0.00 | 0.00 | 0.00 | 0.00 | 0.00 |
| NA2O | 0.00 | 0.00 | 0.00 | 0.00 | 0.00 | 0.00 | 0.00 | 0.00 | 0.00 | 0.00 |
| K2O | 9.44 | 9.41 | 8.21 | 9.35 | 9.54 | 9.43 | 9.36 | 9.41 | 9.52 | 9.26 |
| P2O5 | 0.00 | 0.00 | 0.00 | 0.00 | 0.00 | 0.00 | 0.00 | 0.00 | 0.00 | 0.00 |
| H2O | 3.87 | 3.89 | 3.85 | 3.93 | 3.99 | 3.96 | 3.92 | 3.92 | 3.97 | 3.93 |
| TOTAL | 99.39 | 99.94 | 98.66 | 100.18 | 101.37 | 100.89 | 99.67 | 99.75 | 100.61 | 100.05 |
| CSI | 5.567 | 5.526 | 5.504 | 5.452 | 5.435 | 5.412 | 5.411 | 5.455 | 5.466 | 5.455 |
| CTI | 0.135 | 0.131 | 0.131 | 0.263 | 0.271 | 0.288 | 0.296 | 0.306 | 0.269 | 0.314 |
| CAL4 | 2.433 | 2.473 | 2.496 | 2.548 | 2.565 | 2.588 | 2.589 | 2.545 | 2.534 | 2.545 |
| CAL6 | 1.306 | 1.313 | 1.266 | 0.966 | 0.912 | 0.942 | 0.950 | 0.901 | 0.979 | 0.921 |
| CCR | 0.000 | 0.000 | 0.000 | 0.000 | 0.000 | 0.000 | 0.000 | 0.000 | 0.000 | 0.000 |
| CFE | 3.162 | 3.172 | 3.245 | 2.796 | 2.717 | 2.796 | 2.691 | 2.753 | 2.669 | 2.808 |
| CMN | 0.079 | 0.074 | 0.080 | 0.076 | 0.087 | 0.072 | 0.092 | 0.071 | 0.079 | 0.059 |
| CMG | 0.811 | 0.831 | 0.944 | 1.516 | 1.651 | 1.525 | 1.580 | 1.565 | 1.591 | 1.493 |
| CCA | 0.000 | 0.000 | 0.000 | 0.000 | 0.000 | 0.000 | 0.000 | 0.000 | 0.000 | 0.000 |
| CNA | 0.000 | 0.000 | 0.000 | 0.000 | 0.000 | 0.000 | 0.000 | 0.000 | 0.000 | 0.000 |
| CK | 1.866 | 1.850 | 1.630 | 1.817 | 1.830 | 1.821 | 1.824 | 1.835 | 1.834 | 1.801 |
| CP | 0.000 | 0.000 | 0.000 | 0.000 | 0.000 | 0.000 | 0.000 | 0.000 | 0.000 | 0.000 |
| COH | 4.000 | 4.000 | 4.000 | 4.000 | 4.000 | 4.000 | 4.000 | 4.000 | 4.000 | 4.000 |
| PHLO | 20.0 | 20.4 | 22.1 | 34.6 | 37.1 | 34.7 | 36.2 | 35.7 | 36.7 | 34.2 |
| ANN | 78.0 | 77.8 | 76.0 | 63.7 | 61.0 | 63.7 | 61.7 | 62.7 | 61.5 | 64.4 |
| MN | 1.9 | 1.8 | 1.9 | 1.7 | 1.9 | 1.6 | 2.1 | 1.6 | 1.8 | 1.4 |
| FE+MG | 3.97 | 4.00 | 4.19 | 4.31 | 4.37 | 4.32 | 4.27 | 4.32 | 4.26 | 4.30 |
| FE/FE+MG | 0.80 | 0.79 | 0.77 | 0.65 | 0.62 | 0.65 | 0.63 | 0.64 | 0.63 | 0.65 |

| SAMPLE | NHCL036 | NHCL036 | NHC03 | NHC03 | NHC03 | NHC03 | NHC03 | NHC03 | NHC03 | NHC03 |
|---|---|---|---|---|---|---|---|---|---|---|
| ANALYSES | 2B-2 | 2B-1 | 6 | 3A | 5 | 1B | 2B | 4B | 6B | 5B |
| MINERAL | BI | BI | BI | BI | BI | BI | BI | BI | BI | BI |
| LOCATION | HCØP2 | HCØP2 | HCØP3 | HCØP3 | HCØP3 | HCØP3 | HCØP3 | HCØP3 | HCØP3 | HCØP3 |
| SIO2 | 35.70 | 36.14 | 36.06 | 36.18 | 36.57 | 35.80 | 35.52 | 35.43 | 35.45 | 36.13 |
| TIO2 | 2.96 | 3.22 | 3.02 | 2.93 | 2.98 | 2.59 | 3.66 | 2.69 | 3.23 | 3.23 |
| AL203 | 19.26 | 19.18 | 19.32 | 19.15 | 19.92 | 20.05 | 18.59 | 19.54 | 19.52 | 20.13 |
| CR203 | 0.00 | 0.00 | 0.00 | 0.00 | 0.00 | 0.00 | 0.00 | 0.00 | 0.00 | 0.00 |
| FEO | 22.48 | 21.04 | 21.35 | 21.26 | 20.53 | 22.36 | 21.92 | 22.32 | 21.78 | 21.10 |
| MNO | 0.57 | 0.54 | 0.34 | 0.29 | 0.30 | 0.26 | 0.21 | 0.24 | 0.29 | 0.29 |
| MGO | 6.52 | 6.64 | 7.67 | 7.93 | 7.30 | 6.63 | 6.18 | 6.22 | 6.09 | 6.44 |
| CAO | 0.06 | 0.00 | 0.00 | 0.00 | 0.00 | 0.00 | 0.00 | 0.00 | 0.00 | 0.00 |
| NA2O | 0.00 | 0.00 | 0.00 | 0.00 | 0.00 | 0.00 | 0.00 | 0.00 | 0.00 | 0.00 |
| K2O | 9.36 | 9.10 | 9.69 | 9.70 | 9.04 | 9.78 | 9.67 | 9.79 | 9.44 | 9.73 |
| P2O5 | 0.00 | 0.00 | 0.00 | 0.00 | 0.00 | 0.00 | 0.00 | 0.00 | 0.00 | 0.00 |
| H2O | 3.95 | 3.94 | 3.99 | 3.99 | 4.00 | 3.98 | 3.90 | 3.92 | 3.92 | 3.99 |
| TOTAL | 100.86 | 99.80 | 101.44 | 101.43 | 100.64 | 101.45 | 99.65 | 100.15 | 99.72 | 101.04 |
| CSI | 5.419 | 5.491 | 5.412 | 5.427 | 5.476 | 5.395 | 5.453 | 5.419 | 5.422 | 5.429 |
| CTI | 0.338 | 0.368 | 0.341 | 0.331 | 0.336 | 0.294 | 0.423 | 0.309 | 0.372 | 0.365 |
| CAL4 | 2.581 | 2.509 | 2.588 | 2.573 | 2.524 | 2.605 | 2.547 | 2.581 | 2.578 | 2.571 |
| CAL6 | 0.863 | 0.925 | 0.829 | 0.812 | 0.991 | 0.955 | 0.816 | 0.940 | 0.940 | 0.993 |
| CCR | 0.000 | 0.000 | 0.000 | 0.000 | 0.000 | 0.000 | 0.000 | 0.000 | 0.000 | 0.000 |
| CFE | 2.854 | 2.674 | 2.680 | 2.667 | 2.571 | 2.818 | 2.814 | 2.855 | 2.786 | 2.652 |
| CMN | 0.073 | 0.069 | 0.043 | 0.037 | 0.038 | 0.033 | 0.027 | 0.031 | 0.038 | 0.037 |
| CMG | 1.475 | 1.504 | 1.716 | 1.773 | 1.629 | 1.489 | 1.414 | 1.418 | 1.388 | 1.442 |
| CCA | 0.010 | 0.000 | 0.000 | 0.000 | 0.000 | 0.000 | 0.000 | 0.000 | 0.000 | 0.000 |
| CNA | 0.000 | 0.000 | 0.000 | 0.000 | 0.000 | 0.000 | 0.000 | 0.000 | 0.000 | 0.000 |
| CK | 1.812 | 1.764 | 1.855 | 1.856 | 1.727 | 1.880 | 1.894 | 1.910 | 1.842 | 1.865 |
| CP | 0.000 | 0.000 | 0.000 | 0.000 | 0.000 | 0.000 | 0.000 | 0.000 | 0.000 | 0.000 |
| COH | 4.000 | 4.000 | 4.000 | 4.000 | 4.000 | 4.000 | 4.000 | 4.000 | 4.000 | 4.000 |
| PHLO | 33.5 | 35.4 | 38.7 | 39.6 | 38.4 | 34.3 | 33.2 | 32.9 | 33.0 | 34.9 |
| ANN | 64.8 | 63.0 | 60.4 | 59.6 | 60.7 | 64.9 | 66.1 | 66.3 | 66.1 | 64.2 |
| MN | 1.7 | 1.6 | 1.0 | 0.8 | 0.9 | 0.8 | 0.6 | 0.7 | 0.9 | 0.9 |
| FE+MG | 4.33 | 4.18 | 4.40 | 4.44 | 4.20 | 4.31 | 4.23 | 4.27 | 4.17 | 4.09 |
| FE/FE+MG | 0.66 | 0.64 | 0.61 | 0.60 | 0.61 | 0.65 | 0.67 | 0.67 | 0.67 | 0.65 |

| SAMPLE | NHC04 | NHC04 | NHC04 | NHC04 | NHC04 | NHC04 | NQP13 | NQP13 | NQP13 | NQP13 |
|---|---|---|---|---|---|---|---|---|---|---|
| ANALYSES | 3B-1 | 5B-1 | B-1 | 2B-1 | 2B-2 | 3B-2 | 2 | 5 | 2B | 5-1 |
| MINERAL | BI | BI | BI | BI | BI | BI | BI | BI | BI | BI |
| LOCATION | HCQP3 | HCQP3 | HCQP3 | HCQP3 | HCQP3 | HCQP3 | HCQP4 | HCQP4 | HCQP4 | HCQP4 |
| SIO2 | 36.05 | 35.80 | 35.86 | 35.97 | 35.72 | 36.23 | 35.57 | 36.54 | 35.55 | 36.31 |
| TIO2 | 2.53 | 2.82 | 2.91 | 2.83 | 2.32 | 2.86 | 3.09 | 3.40 | 3.54 | 3.03 |
| AL2O3 | 18.76 | 19.24 | 19.17 | 19.34 | 19.54 | 18.89 | 18.84 | 18.69 | 18.70 | 19.36 |
| CR2O3 | 0.00 | 0.00 | 0.00 | 0.00 | 0.00 | 0.00 | 0.00 | 0.00 | 0.00 | 0.00 |
| FEO | 21.25 | 21.34 | 21.43 | 22.00 | 22.12 | 21.94 | 20.32 | 20.33 | 20.27 | 20.31 |
| MNO | 0.67 | 0.67 | 0.57 | 0.68 | 0.75 | 0.69 | 0.37 | 0.36 | 0.37 | 0.41 |
| MGO | 6.15 | 6.17 | 6.09 | 6.34 | 6.17 | 6.24 | 8.10 | 8.35 | 6.98 | 7.90 |
| CAO | 0.00 | 0.04 | 0.00 | 0.00 | 0.00 | 0.00 | 0.00 | 0.00 | 0.00 | 0.00 |
| NA2O | 0.00 | 0.00 | 0.00 | 0.00 | 0.00 | 0.00 | 0.00 | 0.00 | 0.00 | 0.00 |
| K2O | 9.42 | 9.32 | 9.41 | 9.57 | 9.33 | 9.42 | 9.29 | 9.69 | 9.29 | 9.96 |
| P2O5 | 0.00 | 0.00 | 0.00 | 0.00 | 0.00 | 0.00 | 0.00 | 0.00 | 0.00 | 0.00 |
| H2O | 3.88 | 3.91 | 3.91 | 3.95 | 3.92 | 3.93 | 3.93 | 4.01 | 3.90 | 4.00 |
| TOTAL | 98.71 | 99.31 | 99.35 | 100.68 | 99.87 | 100.20 | 99.51 | 101.37 | 98.60 | 101.28 |
| CSI | 5.562 | 5.490 | 5.498 | 5.460 | 5.466 | 5.519 | 5.419 | 5.462 | 5.466 | 5.439 |
| CTI | 0.294 | 0.325 | 0.336 | 0.323 | 0.267 | 0.328 | 0.354 | 0.382 | 0.409 | 0.341 |
| CAL4 | 2.438 | 2.510 | 2.502 | 2.540 | 2.534 | 2.480 | 2.581 | 2.538 | 2.534 | 2.561 |
| CAL6 | 0.973 | 0.967 | 0.962 | 0.920 | 0.990 | 0.911 | 0.801 | 0.754 | 0.854 | 0.856 |
| CCR | 0.000 | 0.000 | 0.000 | 0.000 | 0.000 | 0.000 | 0.000 | 0.000 | 0.000 | 0.000 |
| CFE | 2.742 | 2.737 | 2.748 | 2.793 | 2.831 | 2.795 | 2.589 | 2.542 | 2.606 | 2.544 |
| CMN | 0.088 | 0.087 | 0.074 | 0.087 | 0.097 | 0.089 | 0.048 | 0.046 | 0.048 | 0.052 |
| CMG | 1.414 | 1.410 | 1.392 | 1.434 | 1.407 | 1.417 | 1.839 | 1.860 | 1.599 | 1.764 |
| CCA | 0.000 | 0.007 | 0.000 | 0.000 | 0.000 | 0.000 | 0.000 | 0.000 | 0.000 | 0.000 |
| CNA | 0.000 | 0.000 | 0.000 | 0.000 | 0.000 | 0.000 | 0.000 | 0.000 | 0.000 | 0.000 |
| CK | 1.854 | 1.823 | 1.841 | 1.853 | 1.822 | 1.831 | 1.806 | 1.848 | 1.822 | 1.903 |
| CP | 0.000 | 0.000 | 0.000 | 0.000 | 0.000 | 0.000 | 0.000 | 0.000 | 0.000 | 0.000 |
| COH | 4.000 | 4.000 | 4.000 | 4.000 | 4.000 | 4.000 | 4.000 | 4.000 | 4.000 | 4.000 |
| PHLO | 33.3 | 33.3 | 33.0 | 33.2 | 32.5 | 32.9 | 41.1 | 41.8 | 37.6 | 40.5 |
| ANN | 64.6 | 64.6 | 65.2 | 64.7 | 65.3 | 65.0 | 57.8 | 57.1 | 61.3 | 58.4 |
| MN | 2.1 | 2.1 | 1.8 | 2.0 | 2.2 | 2.1 | 1.1 | 1.0 | 1.1 | 1.2 |
| FE+MG | 4.16 | 4.15 | 4.14 | 4.23 | 4.24 | 4.21 | 4.43 | 4.40 | 4.21 | 4.31 |
| FE/FE+MG | 0.66 | 0.66 | 0.66 | 0.66 | 0.67 | 0.66 | 0.58 | 0.58 | 0.62 | 0.59 |

| SAMPLE | NQP13 | NQP13 | NQP13 | NQP13 | NQP13 | NQP13 | NQP14 | NQP14 | NQP14 | NQP14 |
|---|---|---|---|---|---|---|---|---|---|---|
| ANALYSES | 4B | 6 | 1B | 3B | 6B | 6-1 | 4 | 3 | 5 | 1 |
| MINERAL | BI | BI | BI | BI | BI | BI | BI | BI | BI | BI |
| LOCATION | HCQP4 | HCQP4 | HCQP4 | HCQP4 | HCQP4 | HCQP4 | HCQP4 | HCQP4 | HCQP4 | HCQP4 |
| SIO2 | 36.81 | 36.00 | 35.97 | 36.32 | 36.01 | 36.12 | 38.20 | 38.58 | 37.93 | 38.34 |
| TIO2 | 3.35 | 3.17 | 3.10 | 2.45 | 3.07 | 2.86 | 3.00 | 2.77 | 4.30 | 3.13 |
| AL2O3 | 18.60 | 18.66 | 18.63 | 19.06 | 19.29 | 18.76 | 17.92 | 17.63 | 17.96 | 18.10 |
| CR2O3 | 0.00 | 0.00 | 0.00 | 0.00 | 0.00 | 0.00 | 0.00 | 0.00 | 0.00 | 0.00 |
| FEO | 20.56 | 19.02 | 20.95 | 21.15 | 21.07 | 20.48 | 21.94 | 21.50 | 21.58 | 21.55 |
| MNO | 0.46 | 0.37 | 0.47 | 0.54 | 0.44 | 0.25 | 0.47 | 0.39 | 0.49 | 0.41 |
| MGO | 7.46 | 8.97 | 7.04 | 7.17 | 7.22 | 7.69 | 4.99 | 5.05 | 4.75 | 4.77 |
| CAO | 0.00 | 0.00 | 0.00 | 0.00 | 0.05 | 0.00 | 0.16 | 0.05 | 0.08 | 0.00 |
| NA2O | 0.00 | 0.00 | 0.00 | 0.00 | 0.00 | 0.00 | 0.00 | 0.00 | 0.00 | 0.00 |
| K2O | 9.49 | 9.58 | 9.87 | 9.95 | 9.01 | 9.62 | 9.76 | 9.78 | 9.56 | 9.75 |
| P2O5 | 0.00 | 0.00 | 0.00 | 0.00 | 0.00 | 0.00 | 0.00 | 0.00 | 0.00 | 0.00 |
| H2O | 3.98 | 3.96 | 3.93 | 3.95 | 3.96 | 3.94 | 3.95 | 3.94 | 3.97 | 3.95 |
| TOTAL | 100.71 | 99.73 | 99.96 | 100.59 | 100.12 | 99.72 | 100.39 | 99.69 | 100.62 | 100.00 |
| CSI | 5.535 | 5.445 | 5.486 | 5.503 | 5.452 | 5.493 | 5.789 | 5.868 | 5.723 | 5.813 |
| CTI | 0.379 | 0.361 | 0.356 | 0.279 | 0.350 | 0.327 | 0.342 | 0.317 | 0.488 | 0.357 |
| CAL4 | 2.465 | 2.555 | 2.514 | 2.497 | 2.548 | 2.507 | 2.211 | 2.132 | 2.277 | 2.187 |
| CAL6 | 0.831 | 0.770 | 0.834 | 0.906 | 0.894 | 0.856 | 0.988 | 1.028 | 0.916 | 1.047 |
| CCR | 0.000 | 0.000 | 0.000 | 0.000 | 0.000 | 0.000 | 0.000 | 0.000 | 0.000 | 0.000 |
| CFE | 2.586 | 2.406 | 2.672 | 2.680 | 2.668 | 2.605 | 2.780 | 2.735 | 2.723 | 2.733 |
| CMN | 0.059 | 0.047 | 0.061 | 0.069 | 0.056 | 0.032 | 0.060 | 0.050 | 0.063 | 0.053 |
| CMG | 1.672 | 2.022 | 1.600 | 1.619 | 1.629 | 1.743 | 1.127 | 1.145 | 1.068 | 1.078 |
| CCA | 0.000 | 0.000 | 0.000 | 0.000 | 0.008 | 0.000 | 0.026 | 0.008 | 0.013 | 0.000 |
| CNA | 0.000 | 0.000 | 0.000 | 0.000 | 0.000 | 0.000 | 0.000 | 0.000 | 0.000 | 0.000 |
| CK | 1.821 | 1.848 | 1.920 | 1.923 | 1.740 | 1.867 | 1.887 | 1.898 | 1.840 | 1.886 |
| CP | 0.000 | 0.000 | 0.000 | 0.000 | 0.000 | 0.000 | 0.000 | 0.000 | 0.000 | 0.000 |
| COH | 4.000 | 4.000 | 4.000 | 4.000 | 4.000 | 4.000 | 4.000 | 4.000 | 4.000 | 4.000 |
| PHLO | 38.7 | 45.2 | 36.9 | 37.6 | 37.4 | 39.8 | 27.4 | 29.1 | 27.7 | 27.9 |
| ANN | 59.9 | 53.8 | 61.7 | 61.3 | 61.3 | 59.5 | 70.1 | 69.6 | 70.7 | 70.7 |
| MN | 1.4 | 1.1 | 1.4 | 1.6 | 1.3 | 0.7 | 1.5 | 1.3 | 1.6 | 1.4 |
| FE+MG | 4.26 | 4.43 | 4.27 | 4.30 | 4.30 | 4.35 | 3.91 | 3.88 | 3.79 | 3.81 |
| FE/FE+MG | 0.61 | 0.54 | 0.63 | 0.62 | 0.62 | 0.60 | 0.71 | 0.70 | 0.72 | 0.72 |

| SAMPLE | NQP14 | NQP15 | NQP15 | NQP15 | NQP15 | NQP15 | NQP15 | NQP16 | NQP16 | NQP16 |
|---|---|---|---|---|---|---|---|---|---|---|
| ANALYSES | 6 | 1 | 4 | 3 | 1B | 3B | 4B | 1B | 2B | 4B |
| MINERAL | BI | BI | BI | BI | BI | BI | BI | BI | BI | BI |
| LOCATION | HCQP4 | HCQP4 | HCQP4 | HCQP4 | HCQP4 | HCQP4 | HCQP4 | HCQP4 | HCQP4 | HCQP4 |
| SIO2 | 39.07 | 37.75 | 38.01 | 37.89 | 36.00 | 35.80 | 35.86 | 36.37 | 35.93 | 35.80 |
| TIO2 | 3.18 | 2.98 | 2.76 | 3.04 | 2.89 | 2.61 | 2.57 | 2.67 | 2.47 | 2.88 |
| AL2O3 | 17.75 | 18.93 | 19.24 | 19.24 | 20.25 | 20.34 | 20.72 | 18.78 | 18.86 | 19.16 |
| CR2O3 | 0.00 | 0.00 | 0.00 | 0.00 | 0.00 | 0.00 | 0.00 | 0.00 | 0.00 | 0.00 |
| FEO | 21.31 | 24.19 | 23.83 | 24.13 | 23.44 | 23.59 | 23.41 | 20.94 | 20.40 | 20.79 |
| MNO | 0.41 | 0.70 | 0.80 | 0.90 | 0.55 | 0.67 | 0.76 | 0.51 | 0.38 | 0.33 |
| MGO | 5.06 | 2.17 | 2.27 | 2.32 | 2.92 | 3.14 | 3.26 | 6.89 | 7.24 | 6.74 |
| CAO | 0.13 | 0.04 | 0.11 | 0.15 | 0.00 | 0.06 | 0.00 | 0.05 | 0.00 | 0.00 |
| NA2O | 0.00 | 0.00 | 0.00 | 0.00 | 0.00 | 0.00 | 0.00 | 0.00 | 0.00 | 0.00 |
| K2O | 9.94 | 9.49 | 9.42 | 9.39 | 9.07 | 9.05 | 9.18 | 9.62 | 9.39 | 9.41 |
| P2O5 | 0.00 | 0.00 | 0.00 | 0.00 | 0.00 | 0.00 | 0.00 | 0.00 | 0.00 | 0.00 |
| H2O | 3.99 | 3.91 | 3.93 | 3.95 | 3.88 | 3.88 | 3.90 | 3.93 | 3.90 | 3.91 |
| TOTAL | 100.84 | 100.16 | 100.37 | 101.01 | 99.00 | 99.14 | 99.66 | 99.76 | 98.57 | 99.02 |
| CSI | 5.867 | 5.783 | 5.795 | 5.752 | 5.563 | 5.534 | 5.511 | 5.542 | 5.524 | 5.487 |
| CTI | 0.359 | 0.343 | 0.316 | 0.347 | 0.336 | 0.303 | 0.297 | 0.306 | 0.286 | 0.332 |
| CAL4 | 2.133 | 2.217 | 2.205 | 2.248 | 2.437 | 2.465 | 2.489 | 2.458 | 2.476 | 2.513 |
| CAL6 | 1.008 | 1.200 | 1.251 | 1.193 | 1.251 | 1.240 | 1.263 | 0.915 | 0.941 | 0.948 |
| CCR | 0.000 | 0.000 | 0.000 | 0.000 | 0.000 | 0.000 | 0.000 | 0.000 | 0.000 | 0.000 |
| CFE | 2.676 | 3.099 | 3.038 | 3.063 | 3.029 | 3.050 | 3.009 | 2.669 | 2.623 | 2.665 |
| CMN | 0.052 | 0.091 | 0.103 | 0.116 | 0.072 | 0.088 | 0.099 | 0.066 | 0.049 | 0.043 |
| CMG | 1.132 | 0.495 | 0.516 | 0.525 | 0.672 | 0.723 | 0.747 | 1.565 | 1.659 | 1.540 |
| CCA | 0.021 | 0.007 | 0.018 | 0.024 | 0.000 | 0.010 | 0.000 | 0.008 | 0.000 | 0.000 |
| CNA | 0.000 | 0.000 | 0.000 | 0.000 | 0.000 | 0.000 | 0.000 | 0.000 | 0.000 | 0.000 |
| CK | 1.904 | 1.855 | 1.832 | 1.819 | 1.788 | 1.785 | 1.800 | 1.870 | 1.842 | 1.840 |
| CP | 0.000 | 0.000 | 0.000 | 0.000 | 0.000 | 0.000 | 0.000 | 0.000 | 0.000 | 0.000 |
| COH | 4.000 | 4.000 | 4.000 | 4.000 | 4.000 | 4.000 | 4.000 | 4.000 | 4.000 | 4.000 |
| PHLO | 29.3 | 13.4 | 14.1 | 14.2 | 17.8 | 18.7 | 19.4 | 36.4 | 38.3 | 36.3 |
| ANN | 69.3 | 84.1 | 83.1 | 82.7 | 80.3 | 79.0 | 78.1 | 62.1 | 60.6 | 62.7 |
| MN | 1.4 | 2.5 | 2.8 | 3.1 | 1.9 | 2.3 | 2.6 | 1.5 | 1.1 | 1.0 |
| FE+MG | 3.81 | 3.59 | 3.55 | 3.59 | 3.70 | 3.77 | 3.76 | 4.23 | 4.28 | 4.20 |
| FE/FE+MG | 0.70 | 0.86 | 0.85 | 0.85 | 0.82 | 0.81 | 0.80 | 0.63 | 0.61 | 0.63 |

| SAMPLE | NQP16 | NQP18 | NQP18 | NQP18 | NQP18 | NQP18 | NQP18 | NQP18 | NQP18 | NQP18 |
|---|---|---|---|---|---|---|---|---|---|---|
| ANALYSES | 7 | 1B-1 | 1B-2 | 2B-1 | 2B-2 | 5B-2 | 3B-2 | 4B-2 | 5B-1 | 3B-1 |
| MINERAL | BI | BI | BI | BI | BI | BI | BI | BI | BI | BI |
| LOCATION | HCQP4 | HCQP4 | HCQP4 | HCQP4 | HCQP4 | HCQP4 | HCQP4 | HCQP4 | HCQP4 | HCQP4 |
| SIO2 | 37.79 | 36.88 | 36.97 | 36.41 | 36.52 | 36.68 | 37.35 | 36.82 | 36.57 | 36.97 |
| TIO2 | 3.06 | 3.34 | 3.29 | 2.87 | 2.83 | 3.11 | 2.91 | 2.91 | 3.11 | 2.66 |
| AL2O3 | 19.94 | 18.88 | 18.98 | 18.72 | 18.10 | 18.78 | 18.66 | 18.39 | 19.04 | 18.77 |
| CR2O3 | 0.00 | 0.00 | 0.00 | 0.00 | 0.00 | 0.00 | 0.00 | 0.00 | 0.00 | 0.00 |
| FEO | 18.67 | 20.48 | 20.33 | 20.25 | 20.99 | 20.41 | 20.03 | 20.11 | 19.84 | 21.16 |
| MNO | 0.28 | 0.39 | 0.39 | 0.35 | 0.11 | 0.33 | 0.36 | 0.14 | 0.27 | 0.46 |
| MGO | 6.69 | 6.89 | 7.32 | 6.76 | 6.84 | 7.05 | 7.50 | 6.96 | 7.02 | 7.36 |
| CAO | 0.00 | 0.00 | 0.00 | 0.00 | 0.00 | 0.00 | 0.00 | 0.00 | 0.00 | 0.00 |
| NA2O | 0.00 | 0.00 | 0.00 | 0.00 | 0.00 | 0.00 | 0.00 | 0.00 | 0.00 | 0.00 |
| K2O | 9.23 | 9.70 | 9.99 | 9.81 | 9.56 | 9.68 | 9.70 | 9.68 | 9.56 | 9.69 |
| P2O5 | 0.00 | 0.00 | 0.00 | 0.00 | 0.00 | 0.00 | 0.00 | 0.00 | 0.00 | 0.00 |
| H2O | 4.01 | 3.98 | 4.00 | 3.92 | 3.90 | 3.96 | 3.99 | 3.92 | 3.95 | 3.99 |
| TOTAL | 99.67 | 100.54 | 101.27 | 99.09 | 98.85 | 100.00 | 100.50 | 98.93 | 99.36 | 101.06 |
| CSI | 5.650 | 5.554 | 5.530 | 5.570 | 5.609 | 5.555 | 5.609 | 5.624 | 5.554 | 5.557 |
| CTI | 0.344 | 0.378 | 0.370 | 0.330 | 0.327 | 0.354 | 0.329 | 0.334 | 0.355 | 0.301 |
| CAL4 | 2.350 | 2.446 | 2.470 | 2.430 | 2.391 | 2.445 | 2.391 | 2.376 | 2.446 | 2.443 |
| CAL6 | 1.163 | 0.905 | 0.876 | 0.945 | 0.885 | 0.906 | 0.911 | 0.935 | 0.961 | 0.881 |
| CCR | 0.000 | 0.000 | 0.000 | 0.000 | 0.000 | 0.000 | 0.000 | 0.000 | 0.000 | 0.000 |
| CFE | 2.334 | 2.579 | 2.543 | 2.591 | 2.696 | 2.585 | 2.516 | 2.569 | 2.520 | 2.660 |
| CMN | 0.035 | 0.050 | 0.049 | 0.045 | 0.014 | 0.042 | 0.046 | 0.018 | 0.035 | 0.059 |
| CMG | 1.491 | 1.546 | 1.632 | 1.541 | 1.566 | 1.591 | 1.679 | 1.584 | 1.589 | 1.649 |
| CCA | 0.000 | 0.000 | 0.000 | 0.000 | 0.000 | 0.000 | 0.000 | 0.000 | 0.000 | 0.000 |
| CNA | 0.000 | 0.000 | 0.000 | 0.000 | 0.000 | 0.000 | 0.000 | 0.000 | 0.000 | 0.000 |
| CK | 1.760 | 1.864 | 1.907 | 1.915 | 1.873 | 1.870 | 1.858 | 1.886 | 1.852 | 1.858 |
| CP | 0.000 | 0.000 | 0.000 | 0.000 | 0.000 | 0.000 | 0.000 | 0.000 | 0.000 | 0.000 |
| COH | 4.000 | 4.000 | 4.000 | 4.000 | 4.000 | 4.000 | 4.000 | 4.000 | 4.000 | 4.000 |
| PHLO | 38.6 | 37.0 | 38.6 | 36.9 | 36.6 | 37.7 | 39.6 | 38.0 | 38.4 | 37.8 |
| ANN | 60.5 | 61.8 | 60.2 | 62.0 | 63.0 | 61.3 | 59.3 | 61.6 | 60.8 | 60.9 |
| MN | 0.9 | 1.2 | 1.2 | 1.1 | 0.3 | 1.0 | 1.1 | 0.4 | 0.8 | 1.3 |
| FE+MG | 3.83 | 4.13 | 4.18 | 4.13 | 4.26 | 4.18 | 4.19 | 4.15 | 4.11 | 4.31 |
| FE/FE+MG | 0.61 | 0.63 | 0.61 | 0.63 | 0.63 | 0.62 | 0.60 | 0.62 | 0.61 | 0.62 |

| SAMPLE | NQP18 | NQP18 | NQP18 | NQP18 | NQP18 | NQP18 | NQP20 | NQP20 | NQP20 | NQP20 |
|---|---|---|---|---|---|---|---|---|---|---|
| ANALYSES | 6B-1 | 6B-2 | 7B-1 | 7B-2 | 8B-1 | 8B-2 | 5 | 2 | 2 | 1 |
| MINERAL | BI | BI | BI | BI | BI | BI | BI | BI | BI | BI |
| LOCATION | HCQP4 | HCQP4 | HCQP4 | HCQP4 | HCQP4 | HCQP4 | HCQP4 | HCQP4 | HCQP4 | HCQP4 |
| SIO2 | 36.82 | 36.85 | 36.97 | 36.54 | 36.31 | 36.54 | 34.64 | 36.25 | 38.64 | 38.12 |
| TIO2 | 3.45 | 3.11 | 2.89 | 2.88 | 3.22 | 3.30 | 2.21 | 2.90 | 3.45 | 3.31 |
| AL2O3 | 18.72 | 18.62 | 19.36 | 19.05 | 18.71 | 18.19 | 18.71 | 19.08 | 17.66 | 17.82 |
| CR2O3 | 0.00 | 0.00 | 0.00 | 0.00 | 0.00 | 0.00 | 0.00 | 0.00 | 0.00 | 0.00 |
| FEO | 20.40 | 20.61 | 20.09 | 20.00 | 19.96 | 20.31 | 24.08 | 20.58 | 21.98 | 21.14 |
| MNO | 0.27 | 0.13 | 0.34 | 0.34 | 0.45 | 0.57 | 0.42 | 0.40 | 0.39 | 0.57 |
| MGO | 7.22 | 7.04 | 7.15 | 7.06 | 6.80 | 7.03 | 9.42 | 8.08 | 4.91 | 5.07 |
| CAO | 0.00 | 0.00 | 0.00 | 0.00 | 0.07 | 0.00 | 0.05 | 0.00 | 0.00 | 0.19 |
| NA2O | 0.00 | 0.00 | 0.00 | 0.00 | 0.00 | 0.00 | 0.00 | 0.00 | 0.00 | 0.00 |
| K2O | 9.99 | 9.96 | 9.89 | 9.61 | 9.41 | 9.61 | 5.96 | 9.71 | 9.93 | 9.62 |
| P2O5 | 0.00 | 0.00 | 0.00 | 0.00 | 0.00 | 0.00 | 0.00 | 0.00 | 0.00 | 0.00 |
| H2O | 3.99 | 3.96 | 3.99 | 3.94 | 3.92 | 3.93 | 3.92 | 3.99 | 3.98 | 3.94 |
| TOTAL | 100.86 | 100.28 | 100.68 | 99.42 | 98.85 | 99.48 | 99.41 | 100.99 | 100.94 | 99.78 |
| CSI | 5.535 | 5.572 | 5.549 | 5.553 | 5.554 | 5.571 | 5.289 | 5.448 | 5.820 | 5.792 |
| CTI | 0.390 | 0.354 | 0.326 | 0.329 | 0.370 | 0.378 | 0.254 | 0.328 | 0.391 | 0.378 |
| CAL4 | 2.465 | 2.428 | 2.451 | 2.447 | 2.446 | 2.429 | 2.771 | 2.552 | 2.180 | 2.208 |
| CAL6 | 0.851 | 0.890 | 0.973 | 0.964 | 0.926 | 0.840 | 0.656 | 0.827 | 0.954 | 0.983 |
| CCR | 0.000 | 0.000 | 0.000 | 0.000 | 0.000 | 0.000 | 0.000 | 0.000 | 0.000 | 0.000 |
| CFE | 2.565 | 2.606 | 2.522 | 2.542 | 2.553 | 2.590 | 3.075 | 2.587 | 2.769 | 2.686 |
| CMN | 0.034 | 0.017 | 0.043 | 0.044 | 0.058 | 0.074 | 0.054 | 0.051 | 0.050 | 0.073 |
| CMG | 1.617 | 1.586 | 1.599 | 1.599 | 1.550 | 1.597 | 2.144 | 1.810 | 1.102 | 1.148 |
| CCA | 0.000 | 0.000 | 0.000 | 0.000 | 0.011 | 0.000 | 0.008 | 0.000 | 0.000 | 0.031 |
| CNA | 0.000 | 0.000 | 0.000 | 0.000 | 0.000 | 0.000 | 0.000 | 0.000 | 0.000 | 0.000 |
| CK | 1.916 | 1.921 | 1.894 | 1.863 | 1.836 | 1.869 | 1.161 | 1.862 | 1.908 | 1.865 |
| CP | 0.000 | 0.000 | 0.000 | 0.000 | 0.000 | 0.000 | 0.000 | 0.000 | 0.000 | 0.000 |
| COH | 4.000 | 4.000 | 4.000 | 4.000 | 4.000 | 4.000 | 4.000 | 4.000 | 4.000 | 4.000 |
| PHLO | 38.4 | 37.7 | 38.4 | 38.2 | 37.3 | 37.5 | 40.7 | 40.7 | 28.1 | 29.4 |
| ANN | 60.8 | 61.9 | 60.6 | 60.7 | 61.3 | 60.8 | 58.3 | 58.2 | 70.6 | 68.7 |
| MN | 0.8 | 0.4 | 1.0 | 1.0 | 1.4 | 1.7 | 1.0 | 1.1 | 1.3 | 1.9 |
| FE+MG | 4.18 | 4.19 | 4.12 | 4.14 | 4.10 | 4.19 | 5.22 | 4.40 | 3.87 | 3.83 |
| FE/FE+MG | 0.61 | 0.62 | 0.61 | 0.61 | 0.62 | 0.62 | 0.59 | 0.59 | 0.72 | 0.70 |

| SAMPLE | NQP20 | NQP20 | NQP20 | NQP20 |
|---|---|---|---|---|
| ANALYSES | 3 | 4 | 5 | 6 |
| MINERAL | BI | BI | BI | BI |
| LOCATION | HCQP4 | HCQP4 | HCQP4 | HCQP4 |
| SIO2 | 38.87 | 38.42 | 38.75 | 38.57 |
| TIO2 | 3.35 | 3.45 | 3.66 | 3.06 |
| AL2O3 | 17.68 | 18.02 | 17.76 | 18.31 |
| CR2O3 | 0.00 | 0.00 | 0.00 | 0.00 |
| FEO | 21.16 | 21.44 | 21.35 | 20.98 |
| MNO | 0.44 | 0.50 | 0.39 | 0.45 |
| MGO | 5.16 | 4.94 | 5.09 | 4.92 |
| CAO | 0.12 | 0.11 | 0.14 | 0.00 |
| NA2O | 0.00 | 0.00 | 0.00 | 0.00 |
| K2O | 9.75 | 9.78 | 9.75 | 10.05 |
| P2O5 | 0.00 | 0.00 | 0.00 | 0.00 |
| H2O | 3.98 | 3.98 | 3.99 | 3.97 |
| TOTAL | 100.51 | 100.64 | 100.88 | 100.31 |
| CSI | 5.851 | 5.791 | 5.817 | 5.820 |
| CTI | 0.379 | 0.391 | 0.413 | 0.347 |
| CAL4 | 2.149 | 2.209 | 2.183 | 2.180 |
| CAL6 | 0.987 | 0.991 | 0.959 | 1.076 |
| CCR | 0.000 | 0.000 | 0.000 | 0.000 |
| CFE | 2.664 | 2.702 | 2.680 | 2.648 |
| CMN | 0.056 | 0.064 | 0.050 | 0.058 |
| CMG | 1.158 | 1.110 | 1.139 | 1.106 |
| CCA | 0.019 | 0.018 | 0.023 | 0.000 |
| CNA | 0.000 | 0.000 | 0.000 | 0.000 |
| CK | 1.872 | 1.881 | 1.867 | 1.935 |
| CP | 0.000 | 0.000 | 0.000 | 0.000 |
| COH | 4.000 | 4.000 | 4.000 | 4.000 |
| PHLO | 29.9 | 29.6 | 29.4 | 29.0 |
| ANN | 68.7 | 69.7 | 69.3 | 69.5 |
| MN | 1.4 | 1.6 | 1.3 | 1.5 |
| FE+MG | 3.82 | 3.81 | 3.82 | 3.75 |
| FE/FE+MG | 0.70 | 0.71 | 0.70 | 0.71 |

APPENDIX IV-3 Muscovite analyses

| SAMPLE | NQP07 | NQP07 | NQP08 | NQP08 | NQP08 | NQP08 | NQP08 | NQP08 | NQP10 | NQP10 |
|---|---|---|---|---|---|---|---|---|---|---|
| ANALYSES | 3M | 4M | 4M-2 | 5M-2 | 2M-1 | 2M-2 | 3M-2A | 1M-2 | 2M | 3M |
| MINERAL | PL | BIO | WM | PR | PL | PR | BIO | BIO | PR | WM |
| PHASE | HCQP1 | HCQP1 | HCQP1 | HCQP1 | HCQP1 | HCQP1 | HCQP1 | HCQP1 | HCQP1 | HCQP1 |
| SIO2 | 46.77 | 47.14 | 47.06 | 47.09 | 47.66 | 46.97 | 47.81 | 47.19 | 47.07 | 46.69 |
| TIO2 | 0.48 | 0.76 | 1.03 | 1.02 | 1.03 | 0.22 | 0.78 | 0.97 | 0.74 | 1.05 |
| AL2O3 | 36.58 | 35.36 | 35.23 | 35.43 | 33.87 | 35.45 | 33.77 | 34.32 | 36.14 | 36.04 |
| CR2O3 | 0.00 | 0.00 | 0.00 | 0.05 | 0.00 | 0.05 | 0.00 | 0.00 | 0.00 | 0.00 |
| FEO | 1.12 | 1.39 | 1.38 | 1.21 | 1.85 | 1.50 | 1.83 | 1.68 | 1.20 | 1.03 |
| MNO | 0.00 | 0.06 | 0.00 | 0.00 | 0.00 | 0.00 | 0.00 | 0.00 | 0.00 | 0.00 |
| MGO | 0.43 | 0.75 | 0.62 | 0.57 | 0.97 | 0.60 | 1.05 | 0.84 | 0.40 | 0.59 |
| CAO | 0.00 | 0.00 | 0.00 | 0.00 | 0.00 | 0.06 | 0.05 | 0.00 | 0.00 | 0.00 |
| NA2O | 0.00 | 0.12 | 0.19 | 0.48 | 0.12 | 0.00 | 0.07 | 0.04 | 0.56 | 0.62 |
| K2O | 11.47 | 11.18 | 11.02 | 10.52 | 10.95 | 10.28 | 10.92 | 10.95 | 10.74 | 10.82 |
| P2O5 | 0.00 | 0.00 | 0.00 | 0.00 | 0.00 | 0.00 | 0.00 | 0.00 | 0.00 | 0.00 |
| H2O | 4.57 | 4.56 | 4.55 | 4.56 | 4.54 | 4.52 | 4.54 | 4.53 | 4.58 | 4.57 |
| TOTAL | 101.42 | 101.32 | 101.08 | 100.93 | 100.99 | 99.65 | 100.82 | 100.52 | 101.43 | 101.41 |
| CSI | 6.130 | 6.190 | 6.190 | 6.184 | 6.284 | 6.230 | 6.310 | 6.246 | 6.158 | 6.116 |
| CTI | 0.047 | 0.075 | 0.102 | 0.101 | 0.102 | 0.022 | 0.077 | 0.097 | 0.073 | 0.103 |
| CALTOTAL | 5.653 | 5.474 | 5.463 | 5.485 | 5.265 | 5.543 | 5.254 | 5.355 | 5.574 | 5.566 |
| CALIV | 1.87 | 1.81 | 1.81 | 1.816 | 1.716 | 1.77 | 1.69 | 1.754 | 1.842 | 1.884 |
| CALVI | 3.783 | 3.664 | 3.653 | 3.669 | 3.549 | 3.773 | 3.564 | 3.601 | 3.732 | 3.682 |
| CCR | 0.000 | 0.000 | 0.000 | 0.012 | 0.000 | 0.012 | 0.000 | 0.000 | 0.000 | 0.000 |
| CFE | 0.123 | 0.153 | 0.152 | 0.133 | 0.204 | 0.166 | 0.202 | 0.186 | 0.131 | 0.113 |
| CMN | 0.000 | 0.007 | 0.000 | 0.000 | 0.000 | 0.000 | 0.000 | 0.000 | 0.000 | 0.000 |
| CMG | 0.084 | 0.147 | 0.122 | 0.112 | 0.191 | 0.119 | 0.207 | 0.166 | 0.078 | 0.115 |
| CCA | 0.000 | 0.000 | 0.000 | 0.000 | 0.000 | 0.009 | 0.007 | 0.000 | 0.000 | 0.000 |
| CNA | 0.000 | 0.031 | 0.048 | 0.122 | 0.031 | 0.000 | 0.018 | 0.010 | 0.142 | 0.157 |
| CK | 1.918 | 1.873 | 1.849 | 1.762 | 1.842 | 1.740 | 1.839 | 1.849 | 1.793 | 1.808 |
| CP | 0.000 | 0.000 | 0.000 | 0.000 | 0.000 | 0.000 | 0.000 | 0.000 | 0.000 | 0.000 |
| COH | 4.000 | 4.000 | 4.000 | 4.000 | 4.000 | 4.000 | 4.000 | 4.000 | 4.000 | 4.000 |

PL = alteration product of plagioclase
BIO = alteration product of biotite
WM = secondary white mica
PR = primary white mica
SE = sericite alteration of plagioclase (included in PL or KS category)
KS = alteration product of potassium feldspar
BIO DIFF = primary white mica intergrown with biotite at different angle

| SAMPLE | NQP10 | NQP11 | NQP11 | NQP12 | NQP12 | NQP12 | NQP12 | NQP12 | NQP12 | NQP12 |
|---|---|---|---|---|---|---|---|---|---|---|
| ANALYSES | 4M | 2M | 1M | 1M-1 | 5M-1 | 6M-1 | 5M-2 | 4M-2 | 3M-1 | 3M-2 |
| MINERAL | SE - PL | SE | KS | BIO | BIO | SE - KS | BIO | PL | PR | WM |
| PHASE | HCQP1 | HCQP1 | HCQP1 | HCQP1 | HCQP1 | HCQP1 | HCQP1 | HCQP1 | HCQP1 | HCQP1 |
| SIO2 | 46.67 | 46.84 | 45.96 | 47.08 | 46.76 | 46.82 | 47.11 | 47.15 | 46.59 | 46.12 |
| TIO2 | 0.46 | 0.38 | 0.16 | 0.79 | 1.01 | 0.63 | 0.54 | 0.34 | 1.08 | 0.64 |
| AL2O3 | 35.52 | 36.44 | 35.01 | 35.96 | 35.78 | 36.11 | 36.31 | 35.95 | 36.31 | 35.58 |
| CR2O3 | 0.00 | 0.00 | 0.00 | 0.00 | 0.00 | 0.00 | 0.00 | 0.00 | 0.07 | 0.00 |
| FEO | 1.34 | 1.09 | 1.00 | 1.12 | 1.43 | 1.16 | 1.13 | 1.18 | 0.96 | 1.08 |
| MNO | 0.06 | 0.00 | 0.07 | 0.00 | 0.00 | 0.00 | 0.00 | 0.00 | 0.00 | 0.00 |
| MGO | 0.66 | 0.51 | 1.29 | 0.50 | 0.52 | 0.64 | 0.62 | 0.60 | 0.54 | 0.58 |
| CAO | 0.00 | 0.00 | 1.71 | 0.00 | 0.00 | 0.00 | 0.12 | 0.00 | 0.05 | 0.11 |
| NA2O | 0.12 | 0.21 | 0.13 | 0.25 | 0.14 | 0.16 | 0.15 | 0.17 | 0.26 | 0.27 |
| K2O | 11.31 | 11.28 | 10.27 | 10.74 | 11.01 | 11.05 | 10.88 | 10.88 | 10.77 | 10.50 |
| P2O5 | 0.00 | 0.00 | 0.00 | 0.00 | 0.00 | 0.00 | 0.00 | 0.00 | 0.00 | 0.00 |
| H2O | 4.53 | 4.57 | 4.50 | 4.57 | 4.56 | 4.56 | 4.58 | 4.56 | 4.57 | 4.49 |
| TOTAL | 100.67 | 101.32 | 100.10 | 101.01 | 101.21 | 101.13 | 101.44 | 100.83 | 101.20 | 99.37 |
| CSI | 6.173 | 6.142 | 6.113 | 6.176 | 6.144 | 6.147 | 6.157 | 6.198 | 6.102 | 6.151 |
| CTI | 0.046 | 0.037 | 0.016 | 0.078 | 0.100 | 0.062 | 0.053 | 0.034 | 0.106 | 0.064 |
| CALTOTAL | 5.539 | 5.634 | 5.490 | 5.561 | 5.542 | 5.589 | 5.595 | 5.571 | 5.606 | 5.594 |
| CALIV | 1.827 | 1.858 | 1.887 | 1.824 | 1.856 | 1.853 | 1.843 | 1.802 | 1.898 | 1.849 |
| CALVI | 3.712 | 3.776 | 3.603 | 3.737 | 3.686 | 3.736 | 3.752 | 3.769 | 3.708 | 3.745 |
| CCR | 0.000 | 0.000 | 0.000 | 0.000 | 0.000 | 0.000 | 0.000 | 0.000 | 0.016 | 0.000 |
| CFE | 0.148 | 0.120 | 0.111 | 0.123 | 0.157 | 0.127 | 0.124 | 0.130 | 0.105 | 0.120 |
| CMN | 0.007 | 0.000 | 0.008 | 0.000 | 0.000 | 0.000 | 0.000 | 0.000 | 0.000 | 0.000 |
| CMG | 0.130 | 0.100 | 0.256 | 0.098 | 0.102 | 0.125 | 0.121 | 0.118 | 0.105 | 0.115 |
| CCA | 0.000 | 0.000 | 0.244 | 0.000 | 0.000 | 0.000 | 0.017 | 0.000 | 0.007 | 0.016 |
| CNA | 0.031 | 0.053 | 0.034 | 0.064 | 0.036 | 0.041 | 0.038 | 0.043 | 0.066 | 0.070 |
| CK | 1.909 | 1.887 | 1.743 | 1.797 | 1.846 | 1.851 | 1.814 | 1.825 | 1.800 | 1.786 |
| CP | 0.000 | 0.000 | 0.000 | 0.000 | 0.000 | 0.000 | 0.000 | 0.000 | 0.000 | 0.000 |
| COH | 4.000 | 4.000 | 4.000 | 4.000 | 4.000 | 4.000 | 4.000 | 4.000 | 4.000 | 4.000 |

| SAMPLE | NQP12 | NQP12 | NQP12 | NQPL028 | NQPL028 | NQPL028 | NQPL028 | NQPL028 | NQPL038 | NQPL038 |
|---|---|---|---|---|---|---|---|---|---|---|
| ANALYSES | 6M-2 | 4M-1 | 2M-2 | 1MA | 6M | 3M | 4M | 1M | 3M-1 | 3M-2 |
| MINERAL | SE - KS | PL | PL | SE | SE - KS | PL | PL | WM | BIO DIFF | BIO |
| PHASE | HCQP1 | HCQP1 | HCQP1 | HCQP1 | HCQP1 | HCQP1 | HCQP1 | HCQP1 | HCQP1 | HCQP1 |
| SIO2 | 47.18 | 46.57 | 47.43 | 47.63 | 48.56 | 47.24 | 47.66 | 46.70 | 47.20 | 47.14 |
| TIO2 | 1.13 | 0.58 | 0.65 | 0.25 | 0.12 | 0.00 | 0.10 | 0.35 | 1.20 | 0.42 |
| AL2O3 | 35.22 | 36.15 | 34.48 | 33.67 | 32.77 | 36.84 | 35.28 | 36.26 | 34.36 | 34.16 |
| CR2O3 | 0.00 | 0.00 | 0.00 | 0.00 | 0.00 | 0.00 | 0.00 | 0.00 | 0.00 | 0.00 |
| FEO | 1.09 | 1.16 | 2.03 | 1.78 | 2.33 | 1.30 | 1.68 | 1.27 | 1.43 | 1.41 |
| MNO | 0.00 | 0.00 | 0.00 | 0.00 | 0.00 | 0.00 | 0.00 | 0.00 | 0.00 | 0.00 |
| MGO | 0.64 | 0.51 | 0.85 | 0.88 | 1.52 | 0.33 | 0.72 | 0.43 | 0.80 | 0.77 |
| CAO | 0.00 | 0.08 | 0.05 | 0.17 | 0.00 | 0.08 | 0.00 | 0.00 | 0.00 | 0.00 |
| NA2O | 0.00 | 0.20 | 0.05 | 0.00 | 0.00 | 0.25 | 0.17 | 0.28 | 0.00 | 0.00 |
| K2O | 11.06 | 10.81 | 10.60 | 10.38 | 11.08 | 10.61 | 10.90 | 10.82 | 10.92 | 10.64 |
| P2O5 | 0.00 | 0.00 | 0.00 | 0.00 | 0.00 | 0.00 | 0.00 | 0.00 | 0.00 | 0.00 |
| H2O | 4.55 | 4.54 | 4.54 | 4.49 | 4.53 | 4.58 | 4.56 | 4.55 | 4.53 | 4.48 |
| TOTAL | 100.87 | 100.60 | 100.68 | 99.25 | 100.91 | 101.23 | 101.07 | 100.66 | 100.44 | 99.02 |
| CSI | 6.206 | 6.141 | 6.262 | 6.359 | 6.415 | 6.175 | 6.261 | 6.155 | 6.243 | 6.307 |
| CTI | 0.112 | 0.058 | 0.065 | 0.025 | 0.012 | 0.000 | 0.010 | 0.035 | 0.119 | 0.042 |
| CALTOTAL | 5.461 | 5.620 | 5.367 | 5.300 | 5.104 | 5.677 | 5.464 | 5.634 | 5.358 | 5.388 |
| CALIV | 1.794 | 1.859 | 1.738 | 1.641 | 1.585 | 1.825 | 1.739 | 1.845 | 1.757 | 1.693 |
| CALVI | 3.667 | 3.761 | 3.629 | 3.659 | 3.519 | 3.852 | 3.725 | 3.789 | 3.601 | 3.695 |
| CCR | 0.000 | 0.000 | 0.000 | 0.000 | 0.000 | 0.000 | 0.000 | 0.000 | 0.000 | 0.000 |
| CFE | 0.120 | 0.128 | 0.224 | 0.199 | 0.257 | 0.142 | 0.185 | 0.140 | 0.158 | 0.158 |
| CMN | 0.000 | 0.000 | 0.000 | 0.000 | 0.000 | 0.000 | 0.000 | 0.000 | 0.000 | 0.000 |
| CMG | 0.125 | 0.100 | 0.167 | 0.175 | 0.299 | 0.064 | 0.141 | 0.084 | 0.158 | 0.154 |
| CCA | 0.000 | 0.011 | 0.007 | 0.024 | 0.000 | 0.011 | 0.000 | 0.000 | 0.000 | 0.000 |
| CNA | 0.000 | 0.051 | 0.013 | 0.000 | 0.000 | 0.063 | 0.043 | 0.072 | 0.000 | 0.000 |
| CK | 1.856 | 1.819 | 1.785 | 1.768 | 1.867 | 1.769 | 1.827 | 1.819 | 1.843 | 1.816 |
| CP | 0.000 | 0.000 | 0.000 | 0.000 | 0.000 | 0.000 | 0.000 | 0.000 | 0.000 | 0.000 |
| COH | 4.000 | 4.000 | 4.000 | 4.000 | 4.000 | 4.000 | 4.000 | 4.000 | 4.000 | 4.000 |

| SAMPLE | NQPL038 | NQPL038 | NQPL038 | NQPL038 | NQPL038 | NQPL038 | NQPL038 | NQP01 | NQP01 | NQP01 |
|---|---|---|---|---|---|---|---|---|---|---|
| ANALYSES | 5M | 4M | 6M | 2M-2 | 1M-2 | 2M-1 | 1M-1 | 6M | 3M | 2M |
| MINERAL | WM | PL | PR | BIO | BIO DIFF | BIO DIFF | BIO DIFF | BIO | BIO | BIO |
| PHASE | HCQP1 | HCQP1 | HCQP1 | HCQP1 | HCQP1 | HCQP1 | HCQP1 | HCQP1A | HCQP1A | HCQP1A |
| SIO2 | 46.60 | 46.62 | 46.69 | 46.65 | 46.39 | 46.95 | 46.36 | 47.13 | 46.98 | 47.16 |
| TIO2 | 0.32 | 0.88 | 0.87 | 0.48 | 1.32 | 0.89 | 0.64 | 0.74 | 1.69 | 1.55 |
| AL2O3 | 36.73 | 36.36 | 36.22 | 35.16 | 34.62 | 35.91 | 36.23 | 36.05 | 34.36 | 33.87 |
| CR2O3 | 0.00 | 0.00 | 0.00 | 0.00 | 0.00 | 0.00 | 0.00 | 0.00 | 0.00 | 0.00 |
| FEO | 1.00 | 1.22 | 1.14 | 1.13 | 1.50 | 1.22 | 1.08 | 1.00 | 1.36 | 1.45 |
| MNO | 0.00 | 0.00 | 0.00 | 0.00 | 0.00 | 0.00 | 0.00 | 0.00 | 0.00 | 0.00 |
| MGO | 0.26 | 0.43 | 0.33 | 0.30 | 0.54 | 0.53 | 0.44 | 0.57 | 0.79 | 0.85 |
| CAO | 0.00 | 0.00 | 0.00 | 0.00 | 0.00 | 0.06 | 0.00 | 0.00 | 0.00 | 0.00 |
| NA2O | 0.00 | 0.30 | 0.28 | 0.00 | 0.00 | 0.14 | 0.35 | 0.13 | 0.00 | 0.00 |
| K2O | 10.92 | 10.74 | 10.82 | 10.97 | 10.78 | 10.92 | 10.36 | 11.26 | 11.08 | 11.23 |
| P2O5 | 0.00 | 0.00 | 0.00 | 0.00 | 0.00 | 0.00 | 0.00 | 0.00 | 0.00 | 0.00 |
| H2O | 4.54 | 4.57 | 4.56 | 4.48 | 4.49 | 4.57 | 4.53 | 4.58 | 4.54 | 4.53 |
| TOTAL | 100.37 | 101.12 | 100.91 | 99.17 | 99.64 | 101.19 | 99.99 | 101.46 | 100.80 | 100.64 |
| CSI | 6.145 | 6.117 | 6.138 | 6.236 | 6.188 | 6.159 | 6.135 | 6.167 | 6.202 | 6.243 |
| CTI | 0.032 | 0.087 | 0.086 | 0.048 | 0.132 | 0.088 | 0.064 | 0.073 | 0.168 | 0.154 |
| CALTOTAL | 5.710 | 5.625 | 5.613 | 5.541 | 5.444 | 5.553 | 5.652 | 5.562 | 5.348 | 5.286 |
| CALIV | 1.855 | 1.883 | 1.862 | 1.764 | 1.812 | 1.841 | 1.865 | 1.833 | 1.798 | 1.757 |
| CALVI | 3.855 | 3.742 | 3.751 | 3.777 | 3.632 | 3.712 | 3.787 | 3.729 | 3.550 | 3.529 |
| CCR | 0.000 | 0.000 | 0.000 | 0.000 | 0.000 | 0.000 | 0.000 | 0.000 | 0.000 | 0.000 |
| CFE | 0.110 | 0.134 | 0.125 | 0.126 | 0.167 | 0.134 | 0.120 | 0.109 | 0.150 | 0.161 |
| CMN | 0.000 | 0.000 | 0.000 | 0.000 | 0.000 | 0.000 | 0.000 | 0.000 | 0.000 | 0.000 |
| CMG | 0.051 | 0.084 | 0.065 | 0.060 | 0.107 | 0.104 | 0.087 | 0.111 | 0.155 | 0.168 |
| CCA | 0.000 | 0.000 | 0.000 | 0.000 | 0.000 | 0.008 | 0.000 | 0.000 | 0.000 | 0.000 |
| CNA | 0.000 | 0.076 | 0.071 | 0.000 | 0.000 | 0.036 | 0.090 | 0.033 | 0.000 | 0.000 |
| CK | 1.837 | 1.798 | 1.815 | 1.871 | 1.835 | 1.827 | 1.749 | 1.880 | 1.866 | 1.897 |
| CP | 0.000 | 0.000 | 0.000 | 0.000 | 0.000 | 0.000 | 0.000 | 0.000 | 0.000 | 0.000 |
| COH | 4.000 | 4.000 | 4.000 | 4.000 | 4.000 | 4.000 | 4.000 | 4.000 | 4.000 | 4.000 |

| SAMPLE | NHC01 | NHC01 | NHC01 | NHC01 | NHC02 | NHC02 | NHC02 | NHC02 | NHC02 | NHC02 |
|---|---|---|---|---|---|---|---|---|---|---|
| ANALYSES | 4M | 2M | 3M | 1M | 4M-2 | 2M-1 | 7M-1 | 4M-1 | 5M-2 | 2M-2 |
| MINERAL | BIO | BIO | KS | WM | PR | BIO DIFF | BIO | PR | SE-PLAG | BIO |
| PHASE | HCQP2 | HCQP2 | HCQP2 | HCQP2 | HCQP2 | HCQP2 | HCQP2 | HCQP2 | HCQP2 | HCQP2 |
| SIO2 | 47.22 | 46.94 | 48.78 | 46.55 | 46.78 | 46.99 | 47.07 | 46.92 | 47.33 | 47.31 |
| TIO2 | 0.26 | 0.26 | 0.00 | 0.60 | 0.73 | 0.88 | 0.51 | 0.71 | 0.00 | 0.54 |
| AL2O3 | 36.60 | 35.84 | 33.97 | 36.14 | 36.06 | 36.09 | 36.58 | 36.35 | 36.63 | 36.78 |
| CR2O3 | 0.00 | 0.00 | 0.00 | 0.00 | 0.00 | 0.00 | 0.00 | 0.00 | 0.00 | 0.00 |
| FEO | 0.94 | 1.16 | 1.15 | 1.12 | 0.97 | 1.08 | 1.24 | 0.94 | 1.34 | 1.01 |
| MNO | 0.00 | 0.00 | 0.00 | 0.00 | 0.00 | 0.00 | 0.00 | 0.00 | 0.00 | 0.00 |
| MGO | 0.34 | 0.47 | 0.53 | 0.53 | 0.18 | 0.52 | 0.34 | 0.28 | 0.47 | 0.22 |
| CAO | 0.00 | 0.00 | 0.15 | 0.00 | 0.00 | 0.07 | 0.05 | 0.00 | 0.00 | 0.00 |
| NA2O | 0.38 | 0.09 | 1.29 | 0.72 | 0.22 | 0.60 | 0.42 | 0.12 | 0.14 | 0.23 |
| K2O | 10.95 | 11.11 | 9.92 | 10.58 | 10.31 | 10.49 | 10.54 | 10.71 | 10.93 | 10.78 |
| P2O5 | 0.00 | 0.00 | 0.00 | 0.00 | 0.00 | 0.00 | 0.00 | 0.00 | 0.00 | 0.00 |
| H2O | 4.58 | 4.53 | 4.55 | 4.55 | 4.53 | 4.58 | 4.58 | 4.56 | 4.58 | 4.60 |
| TOTAL | 101.27 | 100.40 | 100.34 | 100.79 | 99.78 | 101.30 | 101.33 | 100.59 | 101.42 | 101.47 |
| CSI | 6.176 | 6.202 | 6.421 | 6.129 | 6.189 | 6.148 | 6.152 | 6.168 | 6.185 | 6.168 |
| CTI | 0.026 | 0.026 | 0.000 | 0.059 | 0.073 | 0.087 | 0.050 | 0.070 | 0.000 | 0.053 |
| CALTOTAL | 5.644 | 5.583 | 5.272 | 5.610 | 5.624 | 5.567 | 5.637 | 5.634 | 5.643 | 5.653 |
| CALIV | 1.824 | 1.798 | 1.579 | 1.871 | 1.811 | 1.852 | 1.848 | 1.832 | 1.815 | 1.832 |
| CALVI | 3.820 | 3.785 | 3.693 | 3.739 | 3.813 | 3.715 | 3.789 | 3.802 | 3.828 | 3.821 |
| CCR | 0.000 | 0.000 | 0.000 | 0.000 | 0.000 | 0.000 | 0.000 | 0.000 | 0.000 | 0.000 |
| CFE | 0.103 | 0.128 | 0.127 | 0.123 | 0.107 | 0.118 | 0.136 | 0.103 | 0.146 | 0.110 |
| CMN | 0.000 | 0.000 | 0.000 | 0.000 | 0.000 | 0.000 | 0.000 | 0.000 | 0.000 | 0.000 |
| CMG | 0.066 | 0.093 | 0.104 | 0.104 | 0.035 | 0.101 | 0.066 | 0.055 | 0.092 | 0.043 |
| CCA | 0.000 | 0.000 | 0.021 | 0.000 | 0.000 | 0.010 | 0.007 | 0.000 | 0.000 | 0.000 |
| CNA | 0.096 | 0.023 | 0.329 | 0.184 | 0.056 | 0.152 | 0.106 | 0.031 | 0.035 | 0.058 |
| CK | 1.827 | 1.873 | 1.666 | 1.777 | 1.740 | 1.751 | 1.758 | 1.796 | 1.822 | 1.793 |
| CP | 0.000 | 0.000 | 0.000 | 0.000 | 0.000 | 0.000 | 0.000 | 0.000 | 0.000 | 0.000 |
| COH | 4.000 | 4.000 | 4.000 | 4.000 | 4.000 | 4.000 | 4.000 | 4.000 | 4.000 | 4.000 |

| SAMPLE | NHC02 | NHC02 | NHC02 | NHC02 | NHC06 | NHC06 | NHC06 | NHC06 | NHC06 | NHCL034 |
|---|---|---|---|---|---|---|---|---|---|---|
| ANALYSES | 3M-2 | 6M-2 | 5M-1 | 7M-2 | 4M | 6M | 1M | 3M | 5M | 6M |
| MINERAL | KS | PL | SE | BIO | KS | PL | PL | KS | SE-KS | KS |
| PHASE | HCQP2 | HCQP2 | HCQP2 | HCQP2 | HCQP2 | HCQP2 | HCQP2 | HCQP2 | HCQP2 | HCQP2 |
| SIO2 | 46.73 | 47.79 | 47.03 | 47.03 | 47.18 | 46.70 | 47.47 | 46.89 | 46.13 | 47.38 |
| TIO2 | 0.44 | 0.38 | 0.10 | 0.51 | 0.07 | 0.50 | 0.00 | 0.06 | 0.07 | 0.48 |
| AL2O3 | 35.92 | 35.26 | 36.13 | 36.78 | 36.19 | 36.17 | 36.17 | 37.14 | 36.31 | 35.18 |
| CR2O3 | 0.00 | 0.00 | 0.00 | 0.00 | 0.00 | 0.00 | 0.00 | 0.00 | 0.00 | 0.00 |
| FEO | 1.26 | 1.53 | 1.03 | 1.13 | 1.30 | 1.19 | 1.10 | 1.07 | 1.12 | 1.62 |
| MNO | 0.00 | 0.00 | 0.00 | 0.00 | 0.00 | 0.00 | 0.00 | 0.00 | 0.00 | 0.00 |
| MGO | 0.33 | 0.72 | 0.42 | 0.31 | 0.41 | 0.26 | 0.45 | 0.26 | 0.35 | 0.66 |
| CAO | 0.08 | 0.07 | 0.00 | 0.00 | 0.06 | 0.00 | 0.00 | 0.00 | 0.00 | 0.00 |
| NA2O | 0.00 | 0.15 | 0.18 | 0.35 | 0.19 | 0.32 | 0.33 | 0.26 | 0.20 | 0.12 |
| K2O | 11.03 | 10.87 | 10.79 | 10.63 | 10.89 | 10.88 | 11.21 | 10.98 | 10.86 | 11.10 |
| P2O5 | 0.00 | 0.00 | 0.00 | 0.00 | 0.00 | 0.00 | 0.00 | 0.00 | 0.00 | 0.00 |
| H2O | 4.53 | 4.58 | 4.54 | 4.59 | 4.56 | 4.54 | 4.57 | 4.58 | 4.50 | 4.55 |
| TOTAL | 100.32 | 101.35 | 100.22 | 101.33 | 100.85 | 100.56 | 101.30 | 101.24 | 99.54 | 101.09 |
| CSI | 6.182 | 6.258 | 6.209 | 6.144 | 6.202 | 6.161 | 6.218 | 6.137 | 6.145 | 6.233 |
| CTI | 0.044 | 0.037 | 0.010 | 0.050 | 0.007 | 0.050 | 0.000 | 0.006 | 0.007 | 0.047 |
| CALTOTAL | 5.602 | 5.443 | 5.623 | 5.665 | 5.609 | 5.626 | 5.585 | 5.731 | 5.702 | 5.456 |
| CALIV | 1.818 | 1.742 | 1.791 | 1.856 | 1.798 | 1.839 | 1.782 | 1.863 | 1.855 | 1.767 |
| CALVI | 3.784 | 3.701 | 3.832 | 3.809 | 3.811 | 3.787 | 3.803 | 3.868 | 3.847 | 3.689 |
| CCR | 0.000 | 0.000 | 0.000 | 0.000 | 0.000 | 0.000 | 0.000 | 0.000 | 0.000 | 0.000 |
| CFE | 0.139 | 0.168 | 0.114 | 0.123 | 0.143 | 0.131 | 0.120 | 0.117 | 0.125 | 0.178 |
| CMN | 0.000 | 0.000 | 0.000 | 0.000 | 0.000 | 0.000 | 0.000 | 0.000 | 0.000 | 0.000 |
| CMG | 0.065 | 0.141 | 0.083 | 0.060 | 0.080 | 0.051 | 0.088 | 0.051 | 0.069 | 0.129 |
| CCA | 0.011 | 0.010 | 0.000 | 0.000 | 0.008 | 0.000 | 0.000 | 0.000 | 0.000 | 0.000 |
| CNA | 0.000 | 0.038 | 0.046 | 0.089 | 0.048 | 0.082 | 0.084 | 0.066 | 0.052 | 0.031 |
| CK | 1.861 | 1.816 | 1.817 | 1.772 | 1.826 | 1.831 | 1.873 | 1.833 | 1.846 | 1.863 |
| CP | 0.000 | 0.000 | 0.000 | 0.000 | 0.000 | 0.000 | 0.000 | 0.000 | 0.000 | 0.000 |
| COH | 4.000 | 4.000 | 4.000 | 4.000 | 4.000 | 4.000 | 4.000 | 4.000 | 4.000 | 4.000 |

| SAMPLE | NHCL034 | NHCL034 | NHCL034 | NHCL034 | NHCL034 | NHCL034 | NHCL036 | NHCL036 | NHCL036 | NHCL036 |
|---|---|---|---|---|---|---|---|---|---|---|
| ANALYSES | 1M | 7M | 2M-2 | 3M | 1M | 4M | 4M-1 | 6M-1 | 1M-1 | 5M-2 |
| MINERAL | PR | BIO | SE-KS | SE-KS | KS | WM | KS | WM | PR | WM |
| PHASE | HCQP2 | HCQP2 | HCQP2 | HCQP2 | HCQP2 | HCQP2 | HCQP2 | HCQP2 | HCQP2 | HCQP2 |
| SIO2 | 47.23 | 47.36 | 47.43 | 46.75 | 46.96 | 46.92 | 46.69 | 46.72 | 46.32 | 45.75 |
| TIO2 | 0.45 | 0.55 | 0.43 | 0.75 | 0.46 | 0.60 | 0.27 | 0.26 | 0.54 | 0.32 |
| AL2O3 | 34.98 | 36.36 | 34.84 | 36.21 | 36.22 | 36.38 | 35.35 | 36.31 | 35.95 | 35.48 |
| CR2O3 | 0.00 | 0.00 | 0.00 | 0.00 | 0.00 | 0.00 | 0.00 | 0.00 | 0.00 | 0.00 |
| FEO | 1.79 | 1.13 | 1.48 | 1.03 | 1.14 | 1.09 | 1.21 | 1.26 | 1.15 | 1.24 |
| MNO | 0.00 | 0.00 | 0.00 | 0.00 | 0.00 | 0.00 | 0.00 | 0.05 | 0.00 | 0.00 |
| MGO | 0.76 | 0.50 | 0.75 | 0.38 | 0.39 | 0.36 | 0.53 | 0.56 | 0.45 | 0.60 |
| CAO | 0.00 | 0.00 | 0.00 | 0.00 | 0.00 | 0.00 | 0.00 | 0.08 | 0.07 | 0.00 |
| NA2O | 0.26 | 0.45 | 0.14 | 0.32 | 0.57 | 0.46 | 0.00 | 0.41 | 0.69 | 0.17 |
| K2O | 10.85 | 10.45 | 11.07 | 10.88 | 10.84 | 10.64 | 10.89 | 10.57 | 10.87 | 10.58 |
| P2O5 | 0.00 | 0.00 | 0.00 | 0.00 | 0.00 | 0.00 | 0.00 | 0.00 | 0.00 | 0.00 |
| H2O | 4.54 | 4.59 | 4.54 | 4.56 | 4.57 | 4.57 | 4.49 | 4.55 | 4.53 | 4.45 |
| TOTAL | 100.86 | 101.39 | 100.68 | 100.88 | 101.15 | 101.02 | 99.43 | 100.77 | 100.57 | 98.59 |
| CSI | 6.229 | 6.178 | 6.261 | 6.146 | 6.162 | 6.153 | 6.224 | 6.147 | 6.126 | 6.153 |
| CTI | 0.045 | 0.054 | 0.043 | 0.074 | 0.045 | 0.059 | 0.027 | 0.026 | 0.054 | 0.032 |
| CALTOTAL | 5.439 | 5.592 | 5.422 | 5.612 | 5.603 | 5.625 | 5.555 | 5.633 | 5.606 | 5.626 |
| CALIV | 1.771 | 1.822 | 1.739 | 1.854 | 1.838 | 1.847 | 1.776 | 1.853 | 1.874 | 1.847 |
| CALVI | 3.668 | 3.770 | 3.683 | 3.758 | 3.765 | 3.778 | 3.779 | 3.780 | 3.732 | 3.779 |
| CCR | 0.000 | 0.000 | 0.000 | 0.000 | 0.000 | 0.000 | 0.000 | 0.000 | 0.000 | 0.000 |
| CFE | 0.197 | 0.123 | 0.163 | 0.113 | 0.125 | 0.120 | 0.135 | 0.139 | 0.127 | 0.139 |
| CMN | 0.000 | 0.000 | 0.000 | 0.000 | 0.000 | 0.000 | 0.000 | 0.006 | 0.000 | 0.000 |
| CMG | 0.149 | 0.097 | 0.148 | 0.074 | 0.076 | 0.070 | 0.105 | 0.110 | 0.089 | 0.120 |
| CCA | 0.000 | 0.000 | 0.000 | 0.000 | 0.000 | 0.000 | 0.000 | 0.011 | 0.010 | 0.000 |
| CNA | 0.066 | 0.114 | 0.036 | 0.082 | 0.145 | 0.117 | 0.000 | 0.105 | 0.177 | 0.044 |
| CK | 1.826 | 1.739 | 1.864 | 1.825 | 1.815 | 1.780 | 1.852 | 1.774 | 1.834 | 1.815 |
| CP | 0.000 | 0.000 | 0.000 | 0.000 | 0.000 | 0.000 | 0.000 | 0.000 | 0.000 | 0.000 |
| COH | 4.000 | 4.000 | 4.000 | 4.000 | 4.000 | 4.000 | 4.000 | 4.000 | 4.000 | 4.000 |

| SAMPLE | NHCL036 | NHCL036 | NHCL036 | NHC03 | NHC03 | NHC03 | NHC03 | NHC03 | NHC04 | NHC04 |
|---|---|---|---|---|---|---|---|---|---|---|
| ANALYSES | 1M-2 | 2M-2 | 4M-2 | 2M | 4M | 3M | 1M | 6M | 5M-1 | 3M-1 |
| MINERAL | PR | BIO | KS | BIO | BIO | KS | KS-PL | PL | BIO DIFF | BIO DIFF |
| PHASE | HCQP2 | HCQP2 | HCQP2 | HCQP3 | HCQP3 | HCQP3 | HCQP3 | HCQP3 | HCQP3 | HCQP3 |
| SIO2 | 47.12 | 46.86 | 46.47 | 46.72 | 46.88 | 46.81 | 46.57 | 46.56 | 47.22 | 46.49 |
| TIO2 | 0.44 | 0.38 | 0.25 | 0.91 | 1.00 | 0.83 | 0.52 | 0.91 | 0.61 | 0.90 |
| AL2O3 | 36.32 | 36.51 | 36.10 | 34.46 | 35.83 | 35.88 | 36.11 | 36.40 | 35.84 | 35.26 |
| CR2O3 | 0.00 | 0.00 | 0.00 | 0.00 | 0.00 | 0.00 | 0.00 | 0.00 | 0.07 | 0.00 |
| FEO | 1.07 | 1.16 | 1.21 | 1.04 | 1.30 | 1.11 | 1.09 | 1.09 | 1.05 | 1.03 |
| MNO | 0.00 | 0.00 | 0.00 | 0.00 | 0.00 | 0.00 | 0.00 | 0.00 | 0.00 | 0.00 |
| MGO | 0.47 | 0.44 | 0.45 | 0.28 | 0.49 | 0.46 | 0.45 | 0.40 | 0.36 | 0.38 |
| CAO | 0.00 | 0.05 | 0.00 | 0.00 | 0.08 | 0.00 | 0.00 | 0.06 | 0.00 | 0.00 |
| NA2O | 0.62 | 0.49 | 0.10 | 0.56 | 0.38 | 0.58 | 0.10 | 0.51 | 0.43 | 0.00 |
| K2O | 10.48 | 10.42 | 10.89 | 10.44 | 10.77 | 10.38 | 11.58 | 10.94 | 10.75 | 11.06 |
| P2O5 | 0.00 | 0.00 | 0.00 | 0.00 | 0.00 | 0.00 | 0.00 | 0.00 | 0.00 | 0.00 |
| H2O | 4.58 | 4.57 | 4.52 | 4.47 | 4.57 | 4.55 | 4.54 | 4.57 | 4.56 | 4.50 |
| TOTAL | 101.10 | 100.88 | 99.99 | 98.88 | 101.30 | 100.60 | 100.96 | 101.44 | 100.89 | 99.62 |
| CSI | 6.170 | 6.149 | 6.163 | 6.258 | 6.148 | 6.162 | 6.141 | 6.101 | 6.198 | 6.192 |
| CTI | 0.043 | 0.038 | 0.025 | 0.092 | 0.099 | 0.082 | 0.052 | 0.090 | 0.060 | 0.090 |
| CALTOTAL | 5.607 | 5.648 | 5.644 | 5.442 | 5.539 | 5.569 | 5.613 | 5.623 | 5.546 | 5.537 |
| CALIV | 1.83 | 1.851 | 1.837 | 1.742 | 1.852 | 1.838 | 1.859 | 1.899 | 1.802 | 1.808 |
| CALVI | 3.777 | 3.797 | 3.807 | 3.700 | 3.687 | 3.731 | 3.754 | 3.724 | 3.744 | 3.729 |
| CCR | 0.000 | 0.000 | 0.000 | 0.000 | 0.000 | 0.000 | 0.000 | 0.000 | 0.016 | 0.000 |
| CFE | 0.117 | 0.127 | 0.134 | 0.117 | 0.143 | 0.122 | 0.120 | 0.119 | 0.115 | 0.115 |
| CMN | 0.000 | 0.000 | 0.000 | 0.000 | 0.000 | 0.000 | 0.000 | 0.000 | 0.000 | 0.000 |
| CMG | 0.092 | 0.086 | 0.089 | 0.056 | 0.096 | 0.090 | 0.088 | 0.078 | 0.070 | 0.075 |
| CCA | 0.000 | 0.007 | 0.000 | 0.000 | 0.011 | 0.000 | 0.000 | 0.008 | 0.000 | 0.000 |
| CNA | 0.157 | 0.125 | 0.026 | 0.145 | 0.097 | 0.148 | 0.026 | 0.130 | 0.109 | 0.000 |
| CK | 1.751 | 1.744 | 1.843 | 1.784 | 1.802 | 1.743 | 1.948 | 1.829 | 1.800 | 1.879 |
| CP | 0.000 | 0.000 | 0.000 | 0.000 | 0.000 | 0.000 | 0.000 | 0.000 | 0.000 | 0.000 |
| COH | 4.000 | 4.000 | 4.000 | 4.000 | 4.000 | 4.000 | 4.000 | 4.000 | 4.000 | 4.000 |

| SAMPLE | NHC04 | NHC04 | NHC04 | NHC04 | NHC04 | NHC04 | NHC04 | NQP13 | NQP13 | NQP13 |
|---|---|---|---|---|---|---|---|---|---|---|
| ANALYSES | 1M-1 | 3M-2 | 6M-1 | 4M-1 | 2M-2 | 4M-2 | 5M-2 | 1M | 2M | 3M |
| MINERAL | SE - PLK | BIO DIFF | BIO | KS | PR | KS | BIO DIFF | KS | KS | BIO |
| PHASE | HCQP3 | HCQP3 | HCQP3 | HCQP3 | HCQP3 | HCQP3 | HCQP3 | HCQP4 | HCQP4 | HCQP4 |
| SIO2 | 47.42 | 46.97 | 47.24 | 45.92 | 46.85 | 46.99 | 47.12 | 47.75 | 46.80 | 46.84 |
| TIO2 | 0.45 | 0.45 | 0.34 | 0.20 | 0.64 | 0.16 | 0.42 | 0.58 | 1.06 | 0.94 |
| AL203 | 34.61 | 35.98 | 35.81 | 35.99 | 36.09 | 35.50 | 35.92 | 33.59 | 35.86 | 35.71 |
| CR203 | 0.00 | 0.00 | 0.00 | 0.00 | 0.00 | 0.00 | 0.00 | 0.05 | 0.00 | 0.00 |
| FEO | 1.44 | 1.20 | 0.94 | 1.00 | 1.12 | 0.89 | 1.01 | 1.81 | 1.10 | 1.17 |
| MNO | 0.00 | 0.00 | 0.00 | 0.00 | 0.00 | 0.00 | 0.00 | 0.00 | 0.00 | 0.00 |
| MGO | 0.56 | 0.54 | 0.43 | 0.21 | 0.43 | 0.27 | 0.35 | 1.28 | 0.59 | 0.75 |
| CAO | 0.00 | 0.08 | 0.07 | 0.00 | 0.00 | 0.00 | 0.00 | 0.00 | 0.00 | 0.00 |
| NA20 | 0.00 | 0.62 | 0.52 | 0.00 | 0.21 | 0.15 | 0.33 | 0.26 | 0.40 | 0.65 |
| K20 | 10.99 | 10.81 | 10.75 | 11.25 | 11.15 | 10.93 | 10.58 | 11.23 | 11.00 | 10.80 |
| P205 | 0.00 | 0.00 | 0.00 | 0.00 | 0.00 | 0.00 | 0.00 | 0.00 | 0.00 | 0.00 |
| H20 | 4.51 | 4.57 | 4.55 | 4.47 | 4.56 | 4.50 | 4.54 | 4.54 | 4.57 | 4.57 |
| TOTAL | 99.98 | 101.22 | 100.65 | 99.04 | 101.05 | 99.39 | 100.27 | 101.09 | 101.38 | 101.43 |
| CSI | 6.293 | 6.164 | 6.216 | 6.156 | 6.158 | 6.255 | 6.214 | 6.300 | 6.135 | 6.139 |
| CTI | 0.045 | 0.044 | 0.034 | 0.020 | 0.063 | 0.016 | 0.042 | 0.058 | 0.105 | 0.093 |
| CALTOTAL | 5.415 | 5.567 | 5.556 | 5.688 | 5.592 | 5.571 | 5.584 | 5.225 | 5.542 | 5.518 |
| CALIV | 1.707 | 1.836 | 1.784 | 1.844 | 1.842 | 1.745 | 1.786 | 1.7 | 1.865 | 1.861 |
| CALVI | 3.708 | 3.731 | 3.772 | 3.844 | 3.750 | 3.826 | 3.798 | 3.525 | 3.677 | 3.657 |
| CCR | 0.000 | 0.000 | 0.000 | 0.000 | 0.000 | 0.000 | 0.000 | 0.012 | 0.000 | 0.000 |
| CFE | 0.160 | 0.132 | 0.103 | 0.112 | 0.123 | 0.099 | 0.111 | 0.200 | 0.121 | 0.128 |
| CMN | 0.000 | 0.000 | 0.000 | 0.000 | 0.000 | 0.000 | 0.000 | 0.000 | 0.000 | 0.000 |
| CMG | 0.111 | 0.106 | 0.084 | 0.042 | 0.084 | 0.054 | 0.069 | 0.252 | 0.115 | 0.146 |
| CCA | 0.000 | 0.011 | 0.010 | 0.000 | 0.000 | 0.000 | 0.000 | 0.000 | 0.000 | 0.000 |
| CNA | 0.000 | 0.158 | 0.133 | 0.000 | 0.054 | 0.039 | 0.084 | 0.067 | 0.102 | 0.165 |
| CK | 1.861 | 1.810 | 1.805 | 1.924 | 1.870 | 1.856 | 1.780 | 1.890 | 1.840 | 1.806 |
| CP | 0.000 | 0.000 | 0.000 | 0.000 | 0.000 | 0.000 | 0.000 | 0.000 | 0.000 | 0.000 |
| COH | 4.000 | 4.000 | 4.000 | 4.000 | 4.000 | 4.000 | 4.000 | 4.000 | 4.000 | 4.000 |

| SAMPLE | NQP14 | NQP14 | NQP14 | NQP15 | NQP15 | NQP15 | NQP15 | NQP15 | NQP16 | NQP16 |
|---|---|---|---|---|---|---|---|---|---|---|
| ANALYSES | 5M | 1M | 3M | 5M | 1MA | 1M | 4M | 3M | 6M | 4M |
| MINERAL | PL | BIO | WM | SE | SE | WM | KS | WM | SE | BIO |
| PHASE | HCQP4 | HCQP4 | HCQP4 | HCQP4 | HCQP4 | HCQP4 | HCQP4 | HCQP4 | HCQP4 | HCQP4 |
| SIO2 | 46.46 | 47.18 | 46.89 | 47.05 | 49.67 | 46.38 | 47.17 | 46.55 | 47.14 | 46.92 |
| TIO2 | 0.00 | 0.89 | 1.06 | 0.22 | 0.15 | 0.38 | 0.42 | 0.34 | 0.80 | 1.02 |
| AL2O3 | 34.57 | 35.13 | 35.39 | 34.46 | 32.54 | 35.44 | 35.26 | 35.37 | 35.81 | 35.80 |
| CR2O3 | 0.00 | 0.00 | 0.00 | 0.00 | 0.00 | 0.00 | 0.00 | 0.00 | 0.00 | 0.00 |
| FEO | 1.31 | 1.35 | 1.33 | 2.51 | 2.44 | 1.53 | 1.91 | 1.57 | 1.17 | 1.20 |
| MNO | 0.00 | 0.00 | 0.00 | 0.00 | 0.00 | 0.00 | 0.00 | 0.00 | 0.00 | 0.00 |
| MGO | 0.67 | 0.64 | 0.64 | 0.84 | 0.56 | 0.45 | 0.45 | 0.36 | 0.59 | 0.63 |
| CAO | 0.00 | 0.00 | 0.00 | 0.06 | 0.00 | 0.00 | 0.06 | 0.13 | 0.10 | 0.00 |
| NA2O | 0.00 | 0.10 | 0.41 | 0.11 | 0.00 | 0.20 | 0.00 | 0.29 | 0.59 | 0.62 |
| K2O | 11.06 | 11.19 | 11.00 | 10.89 | 10.54 | 10.75 | 10.87 | 10.48 | 10.54 | 10.39 |
| P2O5 | 0.00 | 0.00 | 0.00 | 0.00 | 0.00 | 0.00 | 0.00 | 0.00 | 0.00 | 0.00 |
| H2O | 4.44 | 4.55 | 4.56 | 4.52 | 4.54 | 4.49 | 4.54 | 4.50 | 4.58 | 4.57 |
| TOTAL | 98.51 | 101.03 | 101.28 | 100.66 | 100.44 | 99.62 | 100.68 | 99.59 | 101.32 | 101.15 |
| CSI | 6.263 | 6.210 | 6.161 | 6.242 | 6.555 | 6.184 | 6.229 | 6.202 | 6.171 | 6.150 |
| CTI | 0.000 | 0.088 | 0.105 | 0.022 | 0.015 | 0.038 | 0.042 | 0.034 | 0.079 | 0.101 |
| CALTOTAL | 5.494 | 5.451 | 5.482 | 5.389 | 5.063 | 5.571 | 5.490 | 5.556 | 5.526 | 5.532 |
| CALIV | 1.737 | 1.79 | 1.839 | 1.758 | 1.445 | 1.816 | 1.771 | 1.798 | 1.829 | 1.85 |
| CALVI | 3.757 | 3.661 | 3.643 | 3.631 | 3.618 | 3.755 | 3.719 | 3.758 | 3.697 | 3.682 |
| CCR | 0.000 | 0.000 | 0.000 | 0.000 | 0.000 | 0.000 | 0.000 | 0.000 | 0.000 | 0.000 |
| CFE | 0.148 | 0.149 | 0.146 | 0.278 | 0.269 | 0.171 | 0.211 | 0.175 | 0.128 | 0.132 |
| CMN | 0.000 | 0.000 | 0.000 | 0.000 | 0.000 | 0.000 | 0.000 | 0.000 | 0.000 | 0.000 |
| CMG | 0.135 | 0.126 | 0.125 | 0.166 | 0.110 | 0.089 | 0.089 | 0.071 | 0.115 | 0.123 |
| CCA | 0.000 | 0.000 | 0.000 | 0.009 | 0.000 | 0.000 | 0.008 | 0.019 | 0.014 | 0.000 |
| CNA | 0.000 | 0.026 | 0.104 | 0.028 | 0.000 | 0.052 | 0.000 | 0.075 | 0.150 | 0.158 |
| CK | 1.902 | 1.879 | 1.844 | 1.843 | 1.775 | 1.829 | 1.831 | 1.781 | 1.760 | 1.737 |
| CP | 0.000 | 0.000 | 0.000 | 0.000 | 0.000 | 0.000 | 0.000 | 0.000 | 0.000 | 0.000 |
| COH | 4.000 | 4.000 | 4.000 | 4.000 | 4.000 | 4.000 | 4.000 | 4.000 | 4.000 | 4.000 |

| SAMPLE | NQP16 | NQP16 | NQP16 | NQP16 | NQP18 | NQP18 | NQP18 | NQP18 | NQP18 | NQP18 |
|---|---|---|---|---|---|---|---|---|---|---|
| ANALYSES | 1M | 3M | 6M-2 | 5M | 2M-1 | 8M-2 | 3M-1 | 7M-1 | 5M-1 | 4M-1 |
| MINERAL | PL | BIO | WM | KS | KS | PR | PR | PR | KS | PL |
| PHASE | HCQP4 | HCQP4 | HCQP4 | HCQP4 | HCQP4 | HCQP4 | HCQP4 | HCQP4 | HCQP4 | HCQP4 |
| SIO2 | 47.25 | 46.94 | 46.79 | 46.80 | 47.83 | 47.50 | 47.76 | 47.07 | 47.34 | 47.84 |
| TIO2 | 0.28 | 1.07 | 0.71 | 0.35 | 0.83 | 1.24 | 0.85 | 1.42 | 1.02 | 0.46 |
| AL2O3 | 31.61 | 35.48 | 35.67 | 34.34 | 34.19 | 34.91 | 34.32 | 35.16 | 35.31 | 35.06 |
| CR2O3 | 0.00 | 0.00 | 0.00 | 0.00 | 0.00 | 0.00 | 0.00 | 0.00 | 0.00 | 0.00 |
| FEO | 3.54 | 1.30 | 1.12 | 1.66 | 1.66 | 1.05 | 1.35 | 1.04 | 1.11 | 1.23 |
| MNO | 0.00 | 0.00 | 0.00 | 0.00 | 0.00 | 0.00 | 0.00 | 0.00 | 0.00 | 0.00 |
| MGO | 1.87 | 0.80 | 0.74 | 0.94 | 0.86 | 0.53 | 0.76 | 0.42 | 0.58 | 0.60 |
| CAO | 0.00 | 0.09 | 0.00 | 0.00 | 0.00 | 0.00 | 0.00 | 0.00 | 0.05 | 0.00 |
| NA2O | 0.00 | 0.49 | 0.57 | 0.00 | 0.10 | 0.54 | 0.00 | 0.53 | 0.54 | 0.00 |
| K2O | 10.69 | 10.54 | 10.54 | 10.78 | 11.11 | 10.63 | 10.96 | 10.69 | 10.73 | 11.25 |
| P2O5 | 0.00 | 0.00 | 0.00 | 0.00 | 0.00 | 0.00 | 0.00 | 0.00 | 0.00 | 0.00 |
| H2O | 4.45 | 4.57 | 4.55 | 4.48 | 4.55 | 4.56 | 4.54 | 4.56 | 4.57 | 4.56 |
| TOTAL | 99.69 | 101.28 | 100.69 | 99.35 | 101.13 | 100.96 | 100.54 | 100.89 | 101.25 | 101.00 |
| CSI | 6.362 | 6.154 | 6.162 | 6.258 | 6.293 | 6.236 | 6.301 | 6.190 | 6.204 | 6.285 |
| CTI | 0.028 | 0.106 | 0.070 | 0.035 | 0.082 | 0.122 | 0.084 | 0.140 | 0.101 | 0.045 |
| CALTOTAL | 5.018 | 5.484 | 5.538 | 5.414 | 5.303 | 5.403 | 5.338 | 5.451 | 5.455 | 5.430 |
| CALIV | 1.638 | 1.846 | 1.838 | 1.742 | 1.707 | 1.764 | 1.699 | 1.81 | 1.796 | 1.715 |
| CALVI | 3.380 | 3.638 | 3.700 | 3.672 | 3.596 | 3.639 | 3.639 | 3.641 | 3.659 | 3.715 |
| CCR | 0.000 | 0.000 | 0.000 | 0.000 | 0.000 | 0.000 | 0.000 | 0.000 | 0.000 | 0.000 |
| CFE | 0.399 | 0.143 | 0.123 | 0.186 | 0.183 | 0.115 | 0.149 | 0.114 | 0.122 | 0.135 |
| CMN | 0.000 | 0.000 | 0.000 | 0.000 | 0.000 | 0.000 | 0.000 | 0.000 | 0.000 | 0.000 |
| CMG | 0.375 | 0.156 | 0.145 | 0.187 | 0.169 | 0.104 | 0.149 | 0.082 | 0.113 | 0.117 |
| CCA | 0.000 | 0.013 | 0.000 | 0.000 | 0.000 | 0.000 | 0.000 | 0.000 | 0.007 | 0.000 |
| CNA | 0.000 | 0.125 | 0.146 | 0.000 | 0.026 | 0.137 | 0.000 | 0.135 | 0.137 | 0.000 |
| CK | 1.836 | 1.763 | 1.771 | 1.839 | 1.865 | 1.780 | 1.845 | 1.794 | 1.794 | 1.885 |
| CP | 0.000 | 0.000 | 0.000 | 0.000 | 0.000 | 0.000 | 0.000 | 0.000 | 0.000 | 0.000 |
| COH | 4.000 | 4.000 | 4.000 | 4.000 | 4.000 | 4.000 | 4.000 | 4.000 | 4.000 | 4.000 |

| SAMPLE | NQP18 | NQP18 | NQP18 | NQP18 |
|---|---|---|---|---|
| ANALYSES | 6M-1A | 6M-1 | 2M-2 | 6M-2A |
| MINERAL | PR | PR | KS | PR |
| PHASE | HCQP4 | HCQP4 | HCQP4 | HCQP4 |
| SIO2 | 46.95 | 47.87 | 47.64 | 47.02 |
| TIO2 | 1.17 | 0.79 | 1.07 | 1.47 |
| AL2O3 | 35.31 | 34.13 | 34.23 | 35.05 |
| CR2O3 | 0.00 | 0.00 | 0.00 | 0.00 |
| FEO | 1.15 | 1.60 | 1.53 | 0.98 |
| MNO | 0.00 | 0.00 | 0.00 | 0.00 |
| MGO | 0.45 | 0.91 | 0.89 | 0.29 |
| CAO | 0.00 | 0.00 | 0.00 | 0.00 |
| NA2O | 0.41 | 0.00 | 0.00 | 0.43 |
| K2O | 10.59 | 11.22 | 11.06 | 10.45 |
| P2O5 | 0.00 | 0.00 | 0.00 | 0.00 |
| H2O | 4.54 | 4.55 | 4.55 | 4.54 |
| TOTAL | 100.57 | 101.07 | 100.97 | 100.23 |
| CSI | 6.189 | 6.301 | 6.273 | 6.210 |
| CTI | 0.116 | 0.078 | 0.106 | 0.146 |
| CALTOTAL | 5.488 | 5.296 | 5.314 | 5.458 |
| CALIV | 1.811 | 1.699 | 1.727 | 1.79 |
| CALVI | 3.677 | 3.597 | 3.587 | 3.668 |
| CCR | 0.000 | 0.000 | 0.000 | 0.000 |
| CFE | 0.127 | 0.176 | 0.168 | 0.108 |
| CMN | 0.000 | 0.000 | 0.000 | 0.000 |
| CMG | 0.088 | 0.179 | 0.175 | 0.057 |
| CCA | 0.000 | 0.000 | 0.000 | 0.000 |
| CNA | 0.105 | 0.000 | 0.000 | 0.110 |
| CK | 1.781 | 1.884 | 1.858 | 1.761 |
| CP | 0.000 | 0.000 | 0.000 | 0.000 |
| COH | 4.000 | 4.000 | 4.000 | 4.000 |

APPENDIX IV-4 Plagioclase analyses

| SAMPLE | NQP03 | NQP03 | NQP03 | NQP03 | NQP03 | NQP03 | NQP03 | NQP03 | NQP03 | NQP03 |
|---|---|---|---|---|---|---|---|---|---|---|
| ANALYSES | 3C | 5D | 3A | 2A | 4C | 3B | 4A | 7A | 4B | 5B |
| MINERAL | PL | PL | PL | PL | PL | PL | PL | PL | PL | PL |
| LOCATION | HCQP1 | HCQP1 | HCQP1 | HCQP1 | HCQP1 | HCQP1 | HCQP1 | HCQP1 | HCQP1 | HCQP1 |
| SIO2 | 63.29 | 67.31 | 66.68 | 64.40 | 65.34 | 65.77 | 64.52 | 65.00 | 65.17 | 67.17 |
| TIO2 | 0.00 | 0.00 | 0.00 | 0.00 | 0.00 | 0.00 | 0.00 | 0.00 | 0.06 | 0.00 |
| AL203 | 22.87 | 20.42 | 20.67 | 22.13 | 22.34 | 21.85 | 22.12 | 22.14 | 22.61 | 20.36 |
| FEO | 0.00 | 0.00 | 0.00 | 0.00 | 0.00 | 0.06 | 0.00 | 0.00 | 0.00 | 0.00 |
| MNO | 0.00 | 0.00 | 0.00 | 0.00 | 0.00 | 0.00 | 0.00 | 0.00 | 0.00 | 0.00 |
| MGO | 0.00 | 0.00 | 0.00 | 0.00 | 0.00 | 0.00 | 0.00 | 0.00 | 0.00 | 0.00 |
| CAO | 1.75 | 0.88 | 1.12 | 2.66 | 2.66 | 1.87 | 2.66 | 2.80 | 2.90 | 0.63 |
| NA2O | 9.67 | 11.69 | 11.48 | 10.31 | 10.61 | 10.89 | 10.71 | 10.12 | 10.31 | 11.50 |
| K2O | 0.99 | 0.23 | 0.06 | 0.31 | 0.12 | 0.25 | 0.22 | 0.30 | 0.31 | 0.14 |
| TOTAL | 98.57 | 100.62 | 100.01 | 99.81 | 101.07 | 100.69 | 100.23 | 100.36 | 101.36 | 99.80 |
| CSI | 11.320 | 11.745 | 11.706 | 11.387 | 11.401 | 11.504 | 11.374 | 11.419 | 11.352 | 11.793 |
| CTI | 0.000 | 0.000 | 0.000 | 0.000 | 0.000 | 0.000 | 0.000 | 0.000 | 0.008 | 0.000 |
| CAL | 4.823 | 4.201 | 4.278 | 4.613 | 4.595 | 4.506 | 4.597 | 4.585 | 4.643 | 4.214 |
| CFE | 0.000 | 0.000 | 0.000 | 0.000 | 0.000 | 0.009 | 0.000 | 0.000 | 0.000 | 0.000 |
| CMN | 0.000 | 0.000 | 0.000 | 0.000 | 0.000 | 0.000 | 0.000 | 0.000 | 0.000 | 0.000 |
| CMG | 0.000 | 0.000 | 0.000 | 0.000 | 0.000 | 0.000 | 0.000 | 0.000 | 0.000 | 0.000 |
| CCA | 0.335 | 0.165 | 0.211 | 0.504 | 0.497 | 0.350 | 0.502 | 0.527 | 0.541 | 0.119 |
| CNA | 3.354 | 3.955 | 3.908 | 3.535 | 3.590 | 3.693 | 3.661 | 3.447 | 3.482 | 3.915 |
| CK | 0.226 | 0.051 | 0.013 | 0.070 | 0.027 | 0.056 | 0.049 | 0.067 | 0.069 | 0.031 |
| OR | 5.8 | 1.2 | 0.3 | 1.7 | 0.7 | 1.4 | 1.2 | 1.7 | 1.7 | 0.8 |
| AB | 85.7 | 94.8 | 94.6 | 86.0 | 87.3 | 90.1 | 86.9 | 85.3 | 85.1 | 96.3 |
| AN | 8.6 | 4.0 | 5.1 | 12.3 | 12.1 | 8.5 | 11.9 | 13.0 | 13.2 | 2.9 |

| SAMPLE | NQP03 | NQP03 | NQP03 | NQP03 | NQP03 | NQP12 | NQP12 | NQP12 | NQP12 | NQP12 |
|---|---|---|---|---|---|---|---|---|---|---|
| ANALYSES | 6D | 2B | 8A | 7B | 6A | 5A | 5C | 4C | 5D | 4A |
| MINERAL | PL | PL | PL | PL | PL | PL | PL | PL | PL | PL |
| LOCATION | HCQP1 | HCQP1 | HCQP1 | HCQP1 | HCQP1 | HCQP1 | HCQP1 | HCQP1 | HCQP1 | HCQP1 |
| SIO2 | 67.71 | 67.98 | 65.53 | 65.31 | 67.50 | 63.51 | 59.63 | 61.08 | 60.61 | 65.43 |
| TIO2 | 0.00 | 0.06 | 0.00 | 0.00 | 0.00 | 0.00 | 0.00 | 0.00 | 0.00 | 0.06 |
| AL2O3 | 20.32 | 20.54 | 20.95 | 22.14 | 20.78 | 21.43 | 24.64 | 24.22 | 24.56 | 21.65 |
| FEO | 0.00 | 0.05 | 0.00 | 0.00 | 0.06 | 0.05 | 0.00 | 0.00 | 0.00 | 0.00 |
| MNO | 0.00 | 0.00 | 0.00 | 0.00 | 0.00 | 0.00 | 0.00 | 0.00 | 0.00 | 0.00 |
| MGO | 0.00 | 0.00 | 0.00 | 0.00 | 0.00 | 0.00 | 0.00 | 0.00 | 0.00 | 0.00 |
| CAO | 0.64 | 0.81 | 1.95 | 2.65 | 1.17 | 2.73 | 6.31 | 5.72 | 6.22 | 2.31 |
| NA2O | 11.65 | 11.72 | 10.57 | 10.71 | 11.53 | 9.34 | 7.72 | 8.21 | 8.06 | 10.27 |
| K2O | 0.14 | 0.11 | 0.10 | 0.26 | 0.30 | 1.19 | 0.22 | 0.28 | 0.18 | 0.30 |
| TOTAL | 100.46 | 101.27 | 99.10 | 101.17 | 101.39 | 98.25 | 98.52 | 99.51 | 99.68 | 100.12 |
| CSI | 11.813 | 11.777 | 11.617 | 11.395 | 11.704 | 11.437 | 10.767 | 10.904 | 10.812 | 11.496 |
| CTI | 0.000 | 0.008 | 0.000 | 0.000 | 0.000 | 0.000 | 0.000 | 0.000 | 0.000 | 0.008 |
| CAL | 4.179 | 4.195 | 4.378 | 4.554 | 4.248 | 4.550 | 5.245 | 5.097 | 5.165 | 4.485 |
| CFE | 0.000 | 0.007 | 0.000 | 0.000 | 0.009 | 0.008 | 0.000 | 0.000 | 0.000 | 0.000 |
| CMN | 0.000 | 0.000 | 0.000 | 0.000 | 0.000 | 0.000 | 0.000 | 0.000 | 0.000 | 0.000 |
| CMG | 0.000 | 0.000 | 0.000 | 0.000 | 0.000 | 0.000 | 0.000 | 0.000 | 0.000 | 0.000 |
| CCA | 0.120 | 0.150 | 0.370 | 0.495 | 0.217 | 0.527 | 1.221 | 1.094 | 1.189 | 0.435 |
| CNA | 3.941 | 3.937 | 3.633 | 3.627 | 3.876 | 3.261 | 2.703 | 2.842 | 2.788 | 3.499 |
| CK | 0.031 | 0.024 | 0.023 | 0.058 | 0.066 | 0.273 | 0.051 | 0.064 | 0.041 | 0.067 |
| OR | 0.8 | 0.6 | 0.6 | 1.4 | 1.6 | 6.7 | 1.3 | 1.6 | 1.0 | 1.7 |
| AB | 96.3 | 95.8 | 90.2 | 86.8 | 93.2 | 80.3 | 68.0 | 71.1 | 69.4 | 87.5 |
| AN | 2.9 | 3.6 | 9.2 | 11.8 | 5.2 | 13.0 | 30.7 | 27.4 | 29.6 | 10.9 |

| SAMPLE | NQP12 | NQP12 | NQP12 | NQP12 | NQP12 | NQP01 | NQP01 | NQP01 | NQP01 | NQP01 |
|---|---|---|---|---|---|---|---|---|---|---|
| ANALYSES | 5E | 5B | 4E | 4B | 4D | 2C | 2A | 5D | 6A | 6C |
| MINERAL | PL | PL | PL | PL | PL | PL | PL | PL | PL | PL |
| LOCATION | HCQP1 | HCQP1 | HCQP1 | HCQP1 | HCQP1 | HCQP1A | HCQP1A | HCQP1A | HCQP1A | HCQP1A |
| SIO2 | 63.77 | 60.54 | 60.34 | 64.19 | 59.55 | 63.25 | 62.93 | 65.00 | 64.57 | 62.78 |
| TIO2 | 0.00 | 0.14 | 0.00 | 0.08 | 0.00 | 0.07 | 0.00 | 0.00 | 0.10 | 0.00 |
| AL2O3 | 22.80 | 25.28 | 24.27 | 22.78 | 25.81 | 23.31 | 23.63 | 21.85 | 22.50 | 23.36 |
| FEO | 0.05 | 0.00 | 0.00 | 0.00 | 0.00 | 0.00 | 0.00 | 0.00 | 0.07 | 0.00 |
| MNO | 0.00 | 0.00 | 0.00 | 0.00 | 0.00 | 0.00 | 0.00 | 0.00 | 0.00 | 0.00 |
| MGO | 0.00 | 0.00 | 0.00 | 0.00 | 0.00 | 0.00 | 0.00 | 0.00 | 0.00 | 0.00 |
| CAO | 3.86 | 6.67 | 6.03 | 3.65 | 7.39 | 4.39 | 4.22 | 2.62 | 3.34 | 4.46 |
| NA2O | 9.19 | 7.92 | 7.68 | 9.65 | 7.32 | 9.52 | 9.68 | 10.16 | 9.97 | 9.29 |
| K2O | 0.27 | 0.28 | 0.08 | 0.34 | 0.22 | 0.17 | 0.14 | 0.13 | 0.30 | 0.11 |
| TOTAL | 99.94 | 100.83 | 98.40 | 100.69 | 100.37 | 100.71 | 100.60 | 99.76 | 100.94 | 100.00 |
| CSI | 11.267 | 10.703 | 10.875 | 11.270 | 10.580 | 11.129 | 11.086 | 11.468 | 11.303 | 11.116 |
| CTI | 0.000 | 0.019 | 0.000 | 0.011 | 0.000 | 0.009 | 0.000 | 0.000 | 0.013 | 0.000 |
| CAL | 4.749 | 5.269 | 5.157 | 4.715 | 5.406 | 4.835 | 4.908 | 4.545 | 4.643 | 4.876 |
| CFE | 0.007 | 0.000 | 0.000 | 0.000 | 0.000 | 0.000 | 0.000 | 0.000 | 0.010 | 0.000 |
| CMN | 0.000 | 0.000 | 0.000 | 0.000 | 0.000 | 0.000 | 0.000 | 0.000 | 0.000 | 0.000 |
| CMG | 0.000 | 0.000 | 0.000 | 0.000 | 0.000 | 0.000 | 0.000 | 0.000 | 0.000 | 0.000 |
| CCA | 0.731 | 1.264 | 1.164 | 0.687 | 1.407 | 0.828 | 0.797 | 0.495 | 0.626 | 0.846 |
| CNA | 3.148 | 2.715 | 2.684 | 3.285 | 2.522 | 3.248 | 3.307 | 3.476 | 3.384 | 3.189 |
| CK | 0.061 | 0.063 | 0.018 | 0.076 | 0.050 | 0.038 | 0.031 | 0.029 | 0.067 | 0.025 |
| OR | 1.5 | 1.6 | 0.5 | 1.9 | 1.3 | 0.9 | 0.7 | 0.7 | 1.6 | 0.6 |
| AB | 79.9 | 67.2 | 69.4 | 81.2 | 63.4 | 78.9 | 80.0 | 86.9 | 83.0 | 78.5 |
| AN | 18.6 | 31.3 | 30.1 | 17.0 | 35.4 | 20.1 | 19.3 | 12.4 | 15.4 | 20.8 |

| SAMPLE | NQP01 | NQP01 | NQP01 | NQP01 | NQP01 | NQP01 | NQP01 | NQP01 | NQP01 | NQP01 |
|---|---|---|---|---|---|---|---|---|---|---|
| ANALYSES | 6D | 5F | 2D | 3A | 3B | 5C | 2G | 5B | 5E | 5G |
| MINERAL | PL | PL | PL | PL | PL | PL | PL | PL | PL | PL |
| LOCATION | HCQP1A | HCQP1A | HCQP1A | HCQP1A | HCQP1A | HCQP1A | HCQP1A | HCQP1A | HCQP1A | HCQP1A |
| SIO2 | 64.39 | 58.95 | 63.33 | 63.60 | 61.78 | 62.77 | 62.69 | 65.61 | 61.00 | 58.00 |
| TIO2 | 0.00 | 0.00 | 0.00 | 0.00 | 0.00 | 0.21 | 0.00 | 0.00 | 0.00 | 0.00 |
| AL2O3 | 22.44 | 26.70 | 23.54 | 22.96 | 24.10 | 23.90 | 23.13 | 21.70 | 24.54 | 26.22 |
| FEO | 0.00 | 0.00 | 0.05 | 0.00 | 0.00 | 0.11 | 0.00 | 0.00 | 0.00 | 0.00 |
| MNO | 0.00 | 0.04 | 0.00 | 0.00 | 0.00 | 0.06 | 0.00 | 0.00 | 0.00 | 0.00 |
| MGO | 0.00 | 0.00 | 0.00 | 0.00 | 0.00 | 0.00 | 0.00 | 0.00 | 0.00 | 0.00 |
| CAO | 3.38 | 7.87 | 4.43 | 3.68 | 5.11 | 4.60 | 4.21 | 2.24 | 5.73 | 7.89 |
| NA2O | 9.96 | 7.45 | 9.41 | 9.72 | 9.02 | 9.38 | 9.20 | 10.38 | 8.38 | 7.06 |
| K2O | 0.22 | 0.18 | 0.23 | 0.25 | 0.33 | 0.37 | 0.04 | 0.09 | 0.17 | 0.07 |
| TOTAL | 100.44 | 101.28 | 101.08 | 100.21 | 100.34 | 101.55 | 99.27 | 100.02 | 99.82 | 99.24 |
| CSI | 11.320 | 10.413 | 11.099 | 11.224 | 10.946 | 10.981 | 11.161 | 11.529 | 10.858 | 10.444 |
| CTI | 0.000 | 0.000 | 0.000 | 0.000 | 0.000 | 0.028 | 0.000 | 0.000 | 0.000 | 0.000 |
| CAL | 4.651 | 5.560 | 4.864 | 4.777 | 5.034 | 4.929 | 4.855 | 4.495 | 5.150 | 5.566 |
| CFE | 0.000 | 0.000 | 0.007 | 0.000 | 0.000 | 0.016 | 0.000 | 0.000 | 0.000 | 0.000 |
| CMN | 0.000 | 0.006 | 0.000 | 0.000 | 0.000 | 0.009 | 0.000 | 0.000 | 0.000 | 0.000 |
| CMG | 0.000 | 0.000 | 0.000 | 0.000 | 0.000 | 0.000 | 0.000 | 0.000 | 0.000 | 0.000 |
| CCA | 0.637 | 1.490 | 0.832 | 0.696 | 0.970 | 0.862 | 0.803 | 0.422 | 1.093 | 1.522 |
| CNA | 3.395 | 2.552 | 3.198 | 3.326 | 3.099 | 3.182 | 3.176 | 3.536 | 2.892 | 2.465 |
| CK | 0.049 | 0.041 | 0.051 | 0.056 | 0.075 | 0.083 | 0.009 | 0.020 | 0.039 | 0.016 |
| OR | 1.2 | 1.0 | 1.2 | 1.4 | 1.8 | 2.0 | 0.2 | 0.5 | 1.0 | 0.4 |
| AB | 83.2 | 62.5 | 78.4 | 81.6 | 74.8 | 77.1 | 79.6 | 88.9 | 71.9 | 61.6 |
| AN | 15.6 | 36.5 | 20.4 | 17.1 | 23.4 | 20.9 | 20.1 | 10.6 | 27.2 | 38.0 |

| SAMPLE | NQP01 | NQP01 | NQP01 | NQP01 | NQP01 | NQP01 | NHC01 | NHC01 | NHC01 | NHC01 |
|---|---|---|---|---|---|---|---|---|---|---|
| ANALYSES | 6B | 2F | 2E | 3C | 5 | 2B | 6C | 3A | 1F | 4B |
| MINERAL | PL | PL | PL | PL | PL | PL | PL | PL | PL | PL |
| LOCATION | HCQP1A | HCQP1A | HCQP1A | HCQP1A | HCQP1A | HCQP1A | HCQP2 | HCQP2 | HCQP2 | HCQP2 |
| SIO2 | 62.38 | 63.23 | 63.15 | 62.65 | 64.28 | 62.50 | 67.57 | 67.42 | 68.58 | 67.11 |
| TIO2 | 0.00 | 0.06 | 0.00 | 0.11 | 0.00 | 0.08 | 0.00 | 0.00 | 0.10 | 0.00 |
| AL2O3 | 23.77 | 23.84 | 23.28 | 23.55 | 22.38 | 23.87 | 20.49 | 20.21 | 20.28 | 20.87 |
| FEO | 0.00 | 0.00 | 0.00 | 0.08 | 0.00 | 0.00 | 0.00 | 0.00 | 0.08 | 0.00 |
| MNO | 0.00 | 0.00 | 0.00 | 0.08 | 0.00 | 0.00 | 0.00 | 0.00 | 0.00 | 0.00 |
| MGO | 0.00 | 0.00 | 0.00 | 0.00 | 0.00 | 0.00 | 0.00 | 0.00 | 0.00 | 0.00 |
| CAO | 4.39 | 4.45 | 4.29 | 4.47 | 2.98 | 4.61 | 0.74 | 0.38 | 0.34 | 1.11 |
| NA2O | 9.05 | 9.52 | 9.26 | 9.42 | 9.93 | 9.26 | 11.69 | 11.73 | 11.76 | 11.45 |
| K2O | 0.19 | 0.23 | 0.16 | 0.33 | 0.14 | 0.24 | 0.19 | 0.06 | 0.23 | 0.12 |
| TOTAL | 99.78 | 101.45 | 100.14 | 100.69 | 35.43 | 100.56 | 100.68 | 99.80 | 101.42 | 100.66 |
| CSI | 11.066 | 11.046 | 11.156 | 11.053 | 12.418 | 11.025 | 11.776 | 11.828 | 11.844 | 11.704 |
| CTI | 0.000 | 0.008 | 0.000 | 0.015 | 0.000 | 0.011 | 0.000 | 0.000 | 0.013 | 0.000 |
| CAL | 4.971 | 4.910 | 4.848 | 4.898 | 0.000 | 4.964 | 4.210 | 4.180 | 4.129 | 4.291 |
| CFE | 0.000 | 0.000 | 0.000 | 0.012 | 0.000 | 0.000 | 0.000 | 0.000 | 0.012 | 0.000 |
| CMN | 0.000 | 0.000 | 0.000 | 0.012 | 0.000 | 0.000 | 0.000 | 0.000 | 0.000 | 0.000 |
| CMG | 0.000 | 0.000 | 0.000 | 0.000 | 0.000 | 0.000 | 0.000 | 0.000 | 0.000 | 0.000 |
| CCA | 0.834 | 0.833 | 0.812 | 0.845 | 1.772 | 0.871 | 0.138 | 0.071 | 0.063 | 0.207 |
| CNA | 3.113 | 3.225 | 3.172 | 3.222 | 10.684 | 3.167 | 3.950 | 3.990 | 3.938 | 3.872 |
| CK | 0.043 | 0.051 | 0.036 | 0.074 | 0.099 | 0.054 | 0.042 | 0.013 | 0.051 | 0.027 |
| OR | 1.1 | 1.2 | 0.9 | 1.8 | 0.8 | 1.3 | 1.0 | 0.3 | 1.3 | 0.7 |
| AB | 78.0 | 78.5 | 78.9 | 77.8 | 85.1 | 77.4 | 95.6 | 97.9 | 97.2 | 94.3 |
| AN | 20.9 | 20.3 | 20.2 | 20.4 | 14.1 | 21.3 | 3.3 | 1.7 | 1.6 | 5.0 |

| SAMPLE | NHC01 | NHC01 | NHC01 | NHC06 | NHC06 | NHC06 | NHC06 | NHC06 | NHC06 | NHC06 |
|---|---|---|---|---|---|---|---|---|---|---|
| ANALYSES | 3B | 4A | 1B | 3A | 1E | 3C | 1C | 2B | 1B | 1F |
| MINERAL | PL | PL | PL | PL | PL | PL | PL | PL | PL | PL |
| LOCATION | HCQP2 | HCQP2 | HCQP2 | HCQP2 | HCQP2 | HCQP2 | HCQP2 | HCQP2 | HCQP2 | HCQP2 |
| SIO2 | 67.65 | 66.16 | 67.05 | 68.00 | 63.34 | 65.81 | 63.37 | 66.09 | 66.45 | 64.37 |
| TIO2 | 0.11 | 0.00 | 0.00 | 0.00 | 0.00 | 0.00 | 0.00 | 0.00 | 0.00 | 0.00 |
| AL2O3 | 20.58 | 21.82 | 20.78 | 19.90 | 22.80 | 20.29 | 22.39 | 20.32 | 20.60 | 22.01 |
| FEO | 0.11 | 0.00 | 0.00 | 0.00 | 0.00 | 0.05 | 0.00 | 0.00 | 0.00 | 0.04 |
| MNO | 0.00 | 0.00 | 0.00 | 0.00 | 0.00 | 0.00 | 0.00 | 0.00 | 0.00 | 0.00 |
| MGO | 0.00 | 0.00 | 0.00 | 0.00 | 0.00 | 0.00 | 0.00 | 0.00 | 0.00 | 0.00 |
| CAO | 0.70 | 2.08 | 1.09 | 0.55 | 3.75 | 1.23 | 3.13 | 1.37 | 1.40 | 2.94 |
| NA2O | 11.57 | 11.03 | 11.46 | 11.42 | 9.41 | 11.25 | 9.49 | 10.68 | 10.98 | 10.00 |
| K2O | 0.17 | 0.24 | 0.29 | 0.18 | 0.30 | 0.30 | 0.27 | 0.15 | 0.18 | 0.32 |
| TOTAL | 100.96 | 101.33 | 100.73 | 100.05 | 99.60 | 98.93 | 98.65 | 98.61 | 99.61 | 99.68 |
| CSI | 11.752 | 11.507 | 11.695 | 11.893 | 11.240 | 11.702 | 11.325 | 11.747 | 11.710 | 11.396 |
| CTI | 0.014 | 0.000 | 0.000 | 0.000 | 0.000 | 0.000 | 0.000 | 0.000 | 0.000 | 0.000 |
| CAL | 4.215 | 4.474 | 4.273 | 4.103 | 4.770 | 4.254 | 4.717 | 4.258 | 4.280 | 4.594 |
| CFE | 0.016 | 0.000 | 0.000 | 0.000 | 0.000 | 0.007 | 0.000 | 0.000 | 0.000 | 0.006 |
| CMN | 0.000 | 0.000 | 0.000 | 0.000 | 0.000 | 0.000 | 0.000 | 0.000 | 0.000 | 0.000 |
| CMG | 0.000 | 0.000 | 0.000 | 0.000 | 0.000 | 0.000 | 0.000 | 0.000 | 0.000 | 0.000 |
| CCA | 0.130 | 0.388 | 0.204 | 0.103 | 0.713 | 0.234 | 0.599 | 0.261 | 0.264 | 0.558 |
| CNA | 3.897 | 3.720 | 3.876 | 3.873 | 3.238 | 3.879 | 3.288 | 3.681 | 3.752 | 3.433 |
| CK | 0.038 | 0.053 | 0.065 | 0.040 | 0.068 | 0.068 | 0.062 | 0.034 | 0.040 | 0.072 |
| OR | 0.9 | 1.3 | 1.6 | 1.0 | 1.7 | 1.6 | 1.6 | 0.9 | 1.0 | 1.8 |
| AB | 95.9 | 89.4 | 93.5 | 96.4 | 80.6 | 92.8 | 83.3 | 92.6 | 92.5 | 84.5 |
| AN | 3.2 | 9.3 | 4.9 | 2.6 | 17.7 | 5.6 | 15.2 | 6.6 | 6.5 | 13.7 |

| SAMPLE | NHC06 | NHC06 | NHC06 | NHCL028 | NHCL028 | NHCL028 | NHCL028 | NHCL028 | NHCL028 | NHCL028 |
|---|---|---|---|---|---|---|---|---|---|---|
| ANALYSES | 2A | 5A | 1A | 2B | 2A | 1B | 4B | 5A | 2C | 1A |
| MINERAL | PL | PL | PL | PL | PL | PL | PL | PL | PL | PL |
| LOCATION | HCQP2 | HCQP2 | HCQP2 | HCQP2 | HCQP2 | HCQP2 | HCQP2 | HCQP2 | HCQP2 | HCQP2 |
| SIO2 | 67.08 | 64.67 | 63.98 | 67.45 | 67.66 | 66.81 | 67.42 | 68.98 | 67.49 | 68.09 |
| TIO2 | 0.00 | 0.06 | 0.00 | 0.00 | 0.00 | 0.00 | 0.00 | 0.00 | 0.07 | 0.00 |
| AL2O3 | 20.01 | 21.25 | 22.29 | 19.60 | 20.63 | 20.34 | 20.24 | 19.90 | 20.40 | 20.29 |
| FEO | 0.00 | 0.04 | 0.00 | 0.00 | 0.07 | 0.25 | 0.05 | 0.00 | 0.11 | 0.08 |
| MNO | 0.00 | 0.00 | 0.00 | 0.00 | 0.00 | 0.00 | 0.00 | 0.00 | 0.00 | 0.00 |
| MGO | 0.00 | 0.00 | 0.00 | 0.00 | 0.00 | 0.00 | 0.00 | 0.00 | 0.00 | 0.00 |
| CAO | 0.69 | 2.25 | 3.23 | 0.39 | 1.06 | 1.07 | 0.96 | 0.38 | 1.13 | 0.79 |
| NA2O | 11.35 | 10.32 | 9.65 | 11.29 | 11.37 | 10.98 | 11.25 | 11.60 | 11.33 | 11.66 |
| K2O | 0.28 | 0.24 | 0.18 | 0.09 | 0.19 | 0.15 | 0.20 | 0.09 | 0.20 | 0.11 |
| TOTAL | 99.41 | 98.83 | 99.33 | 98.82 | 100.98 | 99.60 | 100.12 | 100.95 | 100.73 | 101.15 |
| CSI | 11.829 | 11.522 | 11.355 | 11.926 | 11.758 | 11.767 | 11.806 | 11.941 | 11.765 | 11.807 |
| CTI | 0.000 | 0.008 | 0.000 | 0.000 | 0.000 | 0.000 | 0.000 | 0.000 | 0.009 | 0.000 |
| CAL | 4.160 | 4.463 | 4.664 | 4.086 | 4.227 | 4.223 | 4.179 | 4.061 | 4.192 | 4.148 |
| CFE | 0.000 | 0.006 | 0.000 | 0.000 | 0.010 | 0.037 | 0.007 | 0.000 | 0.016 | 0.012 |
| CMN | 0.000 | 0.000 | 0.000 | 0.000 | 0.000 | 0.000 | 0.000 | 0.000 | 0.000 | 0.012 |
| CMG | 0.000 | 0.000 | 0.000 | 0.000 | 0.000 | 0.000 | 0.000 | 0.000 | 0.000 | 0.000 |
| CCA | 0.130 | 0.430 | 0.614 | 0.074 | 0.197 | 0.202 | 0.180 | 0.070 | 0.211 | 0.147 |
| CNA | 3.881 | 3.565 | 3.321 | 3.871 | 3.831 | 3.750 | 3.820 | 3.893 | 3.829 | 3.920 |
| CK | 0.063 | 0.055 | 0.041 | 0.020 | 0.042 | 0.034 | 0.045 | 0.020 | 0.044 | 0.024 |
| OR | 1.5 | 1.4 | 1.0 | 0.5 | 1.0 | 0.9 | 1.1 | 0.5 | 1.1 | 0.6 |
| AB | 95.3 | 88.0 | 83.5 | 97.6 | 94.1 | 94.1 | 94.4 | 97.7 | 93.8 | 95.8 |
| AN | 3.2 | 10.6 | 15.4 | 1.9 | 4.8 | 5.1 | 4.4 | 1.8 | 5.2 | 3.6 |

| SAMPLE | NHC03 | NHC03 | NHC03 | NHC03 | NHC03 | NQP13 | NQP13 | NQP13 | NQP13 | NQP13 |
|---|---|---|---|---|---|---|---|---|---|---|
| ANALYSES | 4C | 2A | 2B | 4B | 1B | 3D | 2E | 3B | 4B | 2A |
| MINERAL | PL | PL | PL | PL | PL | PL | PL | PL | PL | PL |
| LOCATION | HCQP3 | HCQP3 | HCQP3 | HCQP3 | HCQP3 | HCQP4 | HCQP4 | HCQP4 | HCQP4 | HCQP4 |
| SIO2 | 65.97 | 66.12 | 66.68 | 65.73 | 65.53 | 61.19 | 66.58 | 65.45 | 65.77 | 65.02 |
| TIO2 | 0.00 | 0.00 | 0.00 | 0.00 | 0.00 | 0.00 | 0.00 | 0.00 | 0.00 | 0.00 |
| AL2O3 | 20.43 | 20.92 | 21.23 | 20.69 | 21.67 | 24.08 | 21.28 | 20.68 | 21.53 | 22.56 |
| FEO | 0.00 | 0.00 | 0.15 | 0.10 | 0.00 | 0.63 | 0.09 | 0.00 | 0.00 | 0.12 |
| MNO | 0.00 | 0.00 | 0.05 | 0.00 | 0.00 | 0.00 | 0.00 | 0.00 | 0.00 | 0.00 |
| MGO | 0.00 | 0.00 | 0.00 | 0.00 | 0.00 | 0.08 | 0.00 | 0.00 | 0.00 | 0.00 |
| CAO | 1.42 | 1.64 | 1.69 | 1.57 | 2.50 | 1.04 | 1.81 | 1.71 | 2.31 | 3.38 |
| NA2O | 10.83 | 10.65 | 11.04 | 10.65 | 10.15 | 8.09 | 10.60 | 10.35 | 10.12 | 10.04 |
| K2O | 0.16 | 0.23 | 0.31 | 0.22 | 0.34 | 3.10 | 0.30 | 0.00 | 0.27 | 0.28 |
| TOTAL | 98.81 | 99.56 | 101.20 | 98.96 | 100.19 | 98.21 | 100.66 | 98.19 | 100.00 | 101.40 |
| CSI | 11.716 | 11.660 | 11.602 | 11.667 | 11.514 | 11.091 | 11.625 | 11.679 | 11.559 | 11.334 |
| CTI | 0.000 | 0.000 | 0.000 | 0.000 | 0.000 | 0.000 | 0.000 | 0.000 | 0.000 | 0.000 |
| CAL | 4.277 | 4.349 | 4.355 | 4.330 | 4.489 | 5.146 | 4.380 | 4.350 | 4.461 | 4.636 |
| CFE | 0.000 | 0.000 | 0.022 | 0.015 | 0.000 | 0.096 | 0.013 | 0.000 | 0.000 | 0.017 |
| CMN | 0.000 | 0.000 | 0.007 | 0.000 | 0.000 | 0.000 | 0.000 | 0.000 | 0.000 | 0.000 |
| CMG | 0.000 | 0.000 | 0.000 | 0.000 | 0.000 | 0.022 | 0.000 | 0.000 | 0.000 | 0.000 |
| CCA | 0.270 | 0.310 | 0.315 | 0.299 | 0.471 | 0.202 | 0.339 | 0.327 | 0.435 | 0.631 |
| CNA | 3.729 | 3.641 | 3.725 | 3.665 | 3.458 | 2.843 | 3.589 | 3.581 | 3.449 | 3.394 |
| CK | 0.036 | 0.052 | 0.069 | 0.050 | 0.076 | 0.717 | 0.067 | 0.000 | 0.061 | 0.062 |
| OR | 0.9 | 1.3 | 1.7 | 1.2 | 1.9 | 19.1 | 1.7 | 0.0 | 1.5 | 1.5 |
| AB | 92.4 | 91.0 | 90.7 | 91.3 | 86.3 | 75.6 | 89.8 | 91.6 | 87.4 | 83.0 |
| AN | 6.7 | 7.7 | 7.7 | 7.4 | 11.8 | 5.4 | 8.5 | 8.4 | 11.0 | 15.4 |

| SAMPLE | NQP13 | NQP13 | NQP13 | NQP13 | NQP13 | NQP13 | NQP13 | NQP13 | NQP13 | NQP13 |
|---|---|---|---|---|---|---|---|---|---|---|
| ANALYSES | 7B | 2D | 3A | 3E | 7A | 3C | 7C | 2B | 2C | 7C-1 |
| MINERAL | PL | PL | PL | PL | PL | PL | PL | PL | PL | PL |
| LOCATION | HCQP4 | HCQP4 | HCQP4 | HCQP4 | HCQP4 | HCQP4 | HCQP4 | HCQP4 | HCQP4 | HCQP4 |
| SIO2 | 65.57 | 64.19 | 66.92 | 66.95 | 65.98 | 66.35 | 64.41 | 64.57 | 64.55 | 64.85 |
| TIO2 | 0.11 | 0.00 | 0.00 | 0.00 | 0.00 | 0.00 | 0.00 | 0.00 | 0.00 | 0.00 |
| AL2O3 | 21.38 | 22.32 | 20.56 | 21.04 | 21.32 | 21.54 | 21.72 | 22.28 | 22.21 | 21.11 |
| FEO | 0.06 | 0.05 | 0.00 | 0.00 | 0.00 | 0.13 | 0.00 | 0.00 | 0.00 | 0.05 |
| MNO | 0.00 | 0.00 | 0.00 | 0.00 | 0.00 | 0.00 | 0.00 | 0.00 | 0.00 | 0.00 |
| MGO | 0.00 | 0.00 | 0.00 | 0.00 | 0.00 | 0.00 | 0.00 | 0.00 | 0.00 | 0.00 |
| CAO | 1.85 | 3.71 | 1.29 | 1.55 | 2.09 | 1.99 | 2.52 | 3.47 | 3.42 | 2.05 |
| NA2O | 10.17 | 9.67 | 10.73 | 10.93 | 10.51 | 10.66 | 9.54 | 9.68 | 9.64 | 10.47 |
| K2O | 0.42 | 0.22 | 0.08 | 0.20 | 0.17 | 0.33 | 0.28 | 0.19 | 0.32 | 0.16 |
| TOTAL | 99.56 | 100.21 | 99.58 | 100.67 | 100.07 | 101.05 | 98.47 | 100.19 | 100.19 | 98.69 |
| CSI | 11.575 | 11.316 | 11.764 | 11.676 | 11.588 | 11.557 | 11.492 | 11.368 | 11.367 | 11.560 |
| CTI | 0.015 | 0.000 | 0.000 | 0.000 | 0.000 | 0.000 | 0.000 | 0.000 | 0.000 | 0.000 |
| CAL | 4.449 | 4.639 | 4.261 | 4.326 | 4.414 | 4.423 | 4.569 | 4.624 | 4.611 | 4.436 |
| CFE | 0.009 | 0.007 | 0.000 | 0.000 | 0.000 | 0.019 | 0.000 | 0.000 | 0.000 | 0.007 |
| CMN | 0.000 | 0.000 | 0.000 | 0.000 | 0.000 | 0.000 | 0.000 | 0.000 | 0.000 | 0.000 |
| CMG | 0.000 | 0.000 | 0.000 | 0.000 | 0.000 | 0.000 | 0.000 | 0.000 | 0.000 | 0.000 |
| CCA | 0.350 | 0.701 | 0.243 | 0.290 | 0.393 | 0.371 | 0.482 | 0.655 | 0.645 | 0.392 |
| CNA | 3.481 | 3.305 | 3.657 | 3.696 | 3.579 | 3.600 | 3.300 | 3.304 | 3.291 | 3.619 |
| CK | 0.095 | 0.049 | 0.018 | 0.044 | 0.038 | 0.073 | 0.064 | 0.043 | 0.072 | 0.036 |
| OR | 2.4 | 1.2 | 0.5 | 1.1 | 0.9 | 1.8 | 1.7 | 1.1 | 1.8 | 0.9 |
| AB | 88.7 | 81.5 | 93.3 | 91.7 | 89.3 | 89.0 | 85.8 | 82.6 | 82.1 | 89.4 |
| AN | 8.9 | 17.3 | 6.2 | 7.2 | 9.8 | 9.2 | 12.5 | 16.4 | 16.1 | 9.7 |

| SAMPLE | NQP13 | NQP14 | NQP14 | NQP14 | NQP14 | NQP14 | NQP14 | NQP14 | NQP14 | NQP14 |
|---|---|---|---|---|---|---|---|---|---|---|
| ANALYSES | 4A | 1A | 7A | 7C | 2A | 1C | 9C | 3A | 1K | 1B |
| MINERAL | PL | PL | PL | PL | PL | PL | PL | PL | PL | PL |
| LOCATION | HCQP4 | HCQP4 | HCQP4 | HCQP4 | HCQP4 | HCQP4 | HCQP4 | HCQP4 | HCQP4 | HCQP4 |
| SIO2 | 66.08 | 66.10 | 66.16 | 65.94 | 63.86 | 66.80 | 66.40 | 65.60 | 65.85 | 68.02 |
| TIO2 | 0.00 | 0.00 | 0.00 | 0.00 | 0.00 | 0.00 | 0.00 | 0.00 | 0.00 | 0.00 |
| AL2O3 | 21.05 | 21.58 | 21.22 | 21.32 | 21.43 | 20.87 | 20.83 | 21.81 | 21.68 | 20.38 |
| FEO | 0.00 | 0.00 | 0.00 | 0.00 | 0.08 | 0.10 | 0.00 | 0.00 | 0.00 | 0.07 |
| MNO | 0.00 | 0.00 | 0.00 | 0.00 | 0.00 | 0.00 | 0.00 | 0.00 | 0.00 | 0.00 |
| MGO | 0.00 | 0.00 | 0.00 | 0.00 | 0.00 | 0.00 | 0.00 | 0.00 | 0.00 | 0.00 |
| CAO | 1.81 | 1.88 | 1.62 | 1.87 | 2.41 | 1.34 | 1.63 | 2.33 | 2.16 | 0.75 |
| NA2O | 10.61 | 11.20 | 10.97 | 10.67 | 10.19 | 11.49 | 10.85 | 10.76 | 10.93 | 11.92 |
| K2O | 0.34 | 0.25 | 0.30 | 0.23 | 1.08 | 0.12 | 0.05 | 0.27 | 0.33 | 0.11 |
| TOTAL | 99.89 | 101.01 | 100.27 | 100.03 | 99.10 | 100.72 | 99.78 | 100.77 | 100.95 | 101.25 |
| CSI | 11.630 | 11.534 | 11.607 | 11.589 | 11.418 | 11.665 | 11.680 | 11.479 | 11.505 | 11.793 |
| CTI | 0.000 | 0.000 | 0.000 | 0.000 | 0.000 | 0.000 | 0.000 | 0.000 | 0.000 | 0.000 |
| CAL | 4.367 | 4.439 | 4.389 | 4.417 | 4.517 | 4.297 | 4.318 | 4.499 | 4.465 | 4.166 |
| CFE | 0.000 | 0.000 | 0.000 | 0.000 | 0.012 | 0.015 | 0.000 | 0.000 | 0.000 | 0.010 |
| CMN | 0.000 | 0.000 | 0.000 | 0.000 | 0.000 | 0.000 | 0.000 | 0.000 | 0.000 | 0.000 |
| CMG | 0.000 | 0.000 | 0.000 | 0.000 | 0.000 | 0.000 | 0.000 | 0.000 | 0.000 | 0.000 |
| CCA | 0.341 | 0.351 | 0.305 | 0.352 | 0.462 | 0.251 | 0.307 | 0.437 | 0.404 | 0.139 |
| CNA | 3.621 | 3.789 | 3.731 | 3.636 | 3.533 | 3.891 | 3.699 | 3.651 | 3.703 | 4.007 |
| CK | 0.076 | 0.056 | 0.067 | 0.052 | 0.246 | 0.027 | 0.011 | 0.060 | 0.074 | 0.024 |
| OR | 1.9 | 1.3 | 1.6 | 1.3 | 5.8 | 0.6 | 0.3 | 1.4 | 1.8 | 0.6 |
| AB | 89.7 | 90.3 | 90.9 | 90.0 | 83.3 | 93.3 | 92.1 | 88.0 | 88.6 | 96.1 |
| AN | 8.4 | 8.4 | 7.4 | 8.7 | 10.9 | 6.0 | 7.6 | 10.5 | 9.7 | 3.3 |

| SAMPLE | NQP14 | NQP14 | NQP14 | NQP14 | NQP14 | NQP16 | NQP16 | NQP16 | NQP16 | NQP16 |
|---|---|---|---|---|---|---|---|---|---|---|
| ANALYSES | 1J | 8A | 8B | 2B | 7B | 5C | 1D | 5D | 5B | 3B |
| MINERAL | PL | PL | PL | PL | PL | PL | PL | PL | PL | PL |
| LOCATION | HCQP4 | HCQP4 | HCQP4 | HCQP4 | HCQP4 | HCQP4 | HCQP4 | HCQP4 | HCQP4 | HCQP4 |
| SIO2 | 66.68 | 66.92 | 66.03 | 64.58 | 65.64 | 65.43 | 63.75 | 65.69 | 65.67 | 64.92 |
| TIO2 | 0.07 | 0.00 | 0.00 | 0.00 | 0.00 | 0.00 | 0.06 | 0.07 | 0.00 | 0.00 |
| AL203 | 20.94 | 20.60 | 21.31 | 22.53 | 21.76 | 21.21 | 22.44 | 21.31 | 21.02 | 21.99 |
| FEO | 0.00 | 0.00 | 0.00 | 0.12 | 0.00 | 0.00 | 0.00 | 0.00 | 0.00 | 0.00 |
| MNO | 0.00 | 0.00 | 0.00 | 0.00 | 0.00 | 0.00 | 0.00 | 0.00 | 0.00 | 0.00 |
| MGO | 0.00 | 0.00 | 0.00 | 0.00 | 0.00 | 0.00 | 0.00 | 0.00 | 0.00 | 0.00 |
| CAO | 1.24 | 1.30 | 1.94 | 0.46 | 2.05 | 1.95 | 3.28 | 2.23 | 1.93 | 2.74 |
| NA2O | 11.34 | 10.84 | 10.71 | 10.00 | 10.98 | 10.53 | 9.38 | 10.66 | 10.60 | 10.14 |
| K2O | 0.31 | 0.00 | 0.24 | 1.69 | 0.22 | 0.15 | 0.58 | 0.26 | 0.04 | 0.25 |
| TOTAL | 100.58 | 99.66 | 100.23 | 99.38 | 100.65 | 99.27 | 99.49 | 100.22 | 99.32 | 100.12 |
| CSI | 11.659 | 11.755 | 11.587 | 11.457 | 11.494 | 11.583 | 11.318 | 11.546 | 11.608 | 11.423 |
| CTI | 0.009 | 0.000 | 0.000 | 0.000 | 0.000 | 0.000 | 0.008 | 0.009 | 0.000 | 0.000 |
| CAL | 4.316 | 4.266 | 4.409 | 4.712 | 4.492 | 4.427 | 4.697 | 4.416 | 4.380 | 4.562 |
| CFE | 0.000 | 0.000 | 0.000 | 0.018 | 0.000 | 0.000 | 0.000 | 0.000 | 0.000 | 0.000 |
| CMN | 0.000 | 0.000 | 0.000 | 0.000 | 0.000 | 0.000 | 0.000 | 0.000 | 0.000 | 0.000 |
| CMG | 0.000 | 0.000 | 0.000 | 0.000 | 0.000 | 0.000 | 0.000 | 0.000 | 0.000 | 0.000 |
| CCA | 0.232 | 0.245 | 0.365 | 0.087 | 0.385 | 0.370 | 0.624 | 0.420 | 0.366 | 0.517 |
| CNA | 3.845 | 3.692 | 3.644 | 3.440 | 3.728 | 3.614 | 3.229 | 3.633 | 3.633 | 3.459 |
| CK | 0.069 | 0.000 | 0.054 | 0.383 | 0.049 | 0.034 | 0.131 | 0.058 | 0.009 | 0.056 |
| OR | 1.7 | 0.0 | 1.3 | 9.8 | 1.2 | 0.8 | 3.3 | 1.4 | 0.2 | 1.4 |
| AB | 92.7 | 93.8 | 89.7 | 88.0 | 89.6 | 89.9 | 81.0 | 88.4 | 90.6 | 85.8 |
| AN | 5.6 | 6.2 | 9.0 | 2.2 | 9.3 | 9.2 | 15.7 | 10.2 | 9.1 | 12.8 |

APPENDIX IV-5 Potassium feldspar analyses

| SAMPLE | NQP03 | NQP03 | NQP03 | NQP03 | NQP12 | NQP12 | NQP12 | NQP12 | NQP12 | NQP01 |
|---|---|---|---|---|---|---|---|---|---|---|
| ANALYSES | 1A | 1B | 5C | 8B | 3B | 1A | 3A | 2 | 2B | 1E |
| MINERAL | KS | KS | KS | KS | KS | KS | KS | KS | KS | KS |
| PHASE | HCQP1 | HCQP1 | HCQP1 | HCQP1 | HCQP1 | HCQP1 | HCQP1 | HCQP1 | HCQP1 | HCQP1A |
| SIO2 | 64.36 | 64.03 | 64.38 | 63.76 | 64.88 | 64.54 | 64.28 | 64.48 | 64.06 | 64.34 |
| TIO2 | 0.17 | 0.00 | 0.09 | 0.09 | 0.00 | 0.00 | 0.12 | 0.00 | 0.00 | 0.00 |
| AL2O3 | 18.97 | 18.96 | 19.13 | 18.76 | 18.67 | 18.85 | 18.63 | 18.65 | 18.52 | 19.09 |
| FEO | 0.00 | 0.05 | 0.00 | 0.00 | 0.00 | 0.04 | 0.00 | 0.00 | 0.00 | 0.08 |
| MNO | 0.00 | 0.00 | 0.00 | 0.00 | 0.00 | 0.00 | 0.00 | 0.00 | 0.00 | 0.00 |
| MGO | 0.00 | 0.00 | 0.00 | 0.00 | 0.00 | 0.00 | 0.00 | 0.00 | 0.00 | 0.00 |
| CAO | 0.08 | 0.13 | 0.00 | 0.00 | 0.07 | 0.18 | 0.00 | 0.16 | 0.15 | 0.13 |
| NA2O | 0.86 | 0.37 | 1.88 | 0.00 | 0.98 | 0.92 | 0.55 | 0.63 | 0.24 | 0.69 |
| K2O | 15.14 | 15.61 | 13.98 | 16.15 | 14.75 | 14.85 | 15.05 | 15.31 | 15.69 | 15.23 |
| TOTAL | 99.58 | 99.15 | 99.46 | 98.81 | 99.35 | 99.38 | 98.63 | 99.23 | 98.66 | 99.61 |
| CSI | 11.898 | 11.907 | 11.877 | 11.913 | 11.986 | 11.938 | 11.972 | 11.962 | 11.969 | 11.890 |
| CTI | 0.024 | 0.000 | 0.012 | 0.013 | 0.000 | 0.000 | 0.017 | 0.000 | 0.000 | 0.000 |
| CAL | 4.134 | 4.157 | 4.160 | 4.132 | 4.066 | 4.110 | 4.091 | 4.079 | 4.079 | 4.159 |
| CFE | 0.000 | 0.008 | 0.000 | 0.000 | 0.000 | 0.006 | 0.000 | 0.000 | 0.000 | 0.012 |
| CMN | 0.000 | 0.000 | 0.000 | 0.000 | 0.000 | 0.000 | 0.000 | 0.000 | 0.000 | 0.000 |
| CMG | 0.000 | 0.000 | 0.000 | 0.000 | 0.000 | 0.000 | 0.000 | 0.000 | 0.000 | 0.000 |
| CCA | 0.016 | 0.026 | 0.000 | 0.000 | 0.014 | 0.036 | 0.000 | 0.032 | 0.030 | 0.026 |
| CNA | 0.308 | 0.133 | 0.672 | 0.000 | 0.351 | 0.330 | 0.199 | 0.227 | 0.087 | 0.247 |
| CK | 3.571 | 3.703 | 3.290 | 3.850 | 3.477 | 3.504 | 3.576 | 3.624 | 3.740 | 3.591 |
| OR | 91.7 | 95.9 | 83.0 | 100.0 | 90.5 | 90.6 | 94.7 | 93.3 | 97.0 | 92.9 |
| AB | 7.9 | 3.5 | 17.0 | 0.0 | 9.1 | 8.5 | 5.3 | 5.8 | 2.3 | 6.4 |
| AN | 4.1 | 0.7 | 0.0 | 0.0 | 0.4 | 0.9 | 0.0 | 0.8 | 0.8 | 0.7 |

| SAMPLE | NQP01 | NQP01 | NQP01 | NQP01 | NHC01 | NHC01 | NHC01 | NHC01 | NHC01 | NHC06 |
|---|---|---|---|---|---|---|---|---|---|---|
| ANALYSES | 1D | 1A | 1B | 1C | 6D | 1A | 1D | 1E | 5A | 6B |
| MINERAL | KS | KS | KS | KS | KS | KS | KS | KS | KS | KS |
| PHASE | HCQP1A | HCQP1A | HCQP1A | HCQP1A | HCQP2 | HCQP2 | HCQP2 | HCQP2 | HCQP2 | HCQP2 |
| SIO2 | 64.71 | 64.03 | 63.89 | 64.31 | 64.20 | 63.08 | 64.22 | 64.32 | 63.88 | 63.59 |
| TIO2 | 0.00 | 0.00 | 0.00 | 0.00 | 0.07 | 0.00 | 0.00 | 0.00 | 0.00 | 0.00 |
| AL2O3 | 18.93 | 19.04 | 19.17 | 19.17 | 19.24 | 19.40 | 18.98 | 19.24 | 18.49 | 18.76 |
| FEO | 0.00 | 0.00 | 0.00 | 0.08 | 0.00 | 0.08 | 0.00 | 0.00 | 0.04 | 0.00 |
| MNO | 0.00 | 0.00 | 0.00 | 0.00 | 0.00 | 0.05 | 0.00 | 0.00 | 0.00 | 0.00 |
| MGO | 0.00 | 0.00 | 0.00 | 0.00 | 0.00 | 0.00 | 0.00 | 0.00 | 0.00 | 0.00 |
| CAO | 0.00 | 0.10 | 0.10 | 0.09 | 0.00 | 0.06 | 0.00 | 0.00 | 0.08 | 0.08 |
| NA2O | 1.11 | 1.05 | 1.01 | 0.97 | 0.96 | 0.84 | 0.63 | 0.96 | 0.10 | 1.07 |
| K2O | 14.83 | 14.99 | 15.07 | 14.94 | 15.00 | 15.07 | 15.09 | 15.01 | 16.16 | 14.67 |
| TOTAL | 99.58 | 99.21 | 99.24 | 99.61 | 99.47 | 98.58 | 98.92 | 99.53 | 98.75 | 98.17 |
| CSI | 11.940 | 11.884 | 11.860 | 11.876 | 11.873 | 11.800 | 11.931 | 11.886 | 11.955 | 11.911 |
| CTI | 0.000 | 0.000 | 0.000 | 0.000 | 0.010 | 0.000 | 0.000 | 0.000 | 0.000 | 0.000 |
| CAL | 4.118 | 4.166 | 4.195 | 4.173 | 4.195 | 4.278 | 4.157 | 4.192 | 4.080 | 4.143 |
| CFE | 0.000 | 0.000 | 0.000 | 0.012 | 0.000 | 0.013 | 0.000 | 0.000 | 0.006 | 0.000 |
| CMN | 0.000 | 0.000 | 0.000 | 0.000 | 0.000 | 0.008 | 0.000 | 0.000 | 0.000 | 0.000 |
| CMG | 0.000 | 0.000 | 0.000 | 0.000 | 0.000 | 0.000 | 0.000 | 0.000 | 0.000 | 0.000 |
| CCA | 0.000 | 0.020 | 0.020 | 0.018 | 0.000 | 0.012 | 0.000 | 0.000 | 0.016 | 0.016 |
| CNA | 0.397 | 0.378 | 0.364 | 0.347 | 0.344 | 0.305 | 0.227 | 0.344 | 0.036 | 0.389 |
| CK | 3.491 | 3.549 | 3.569 | 3.520 | 3.539 | 3.596 | 3.577 | 3.539 | 3.859 | 3.506 |
| OR | 89.8 | 89.9 | 90.3 | 90.6 | 91.1 | 91.9 | 94.0 | 91.1 | 98.7 | 89.7 |
| AB | 10.2 | 9.6 | 9.2 | 8.9 | 8.9 | 7.8 | 6.0 | 8.9 | 0.9 | 9.9 |
| AN | 0.0 | 0.5 | 0.5 | 0.5 | 0.0 | 0.3 | 0.0 | 0.0 | 0.4 | 0.4 |

| SAMPLE | NHC06 | NHC06 | NHC06 | NHC06 | NHC06 | NHCL028 | NHCL028 | NHCL028 | NHCL028 | NHCL028 |
|---|---|---|---|---|---|---|---|---|---|---|
| ANALYSES | 8A | 8B | 4A | 6A | 4B | 4A | 4C | 3C | 3B | 3A |
| MINERAL | KS | KS | KS | KS | KS | KS | KS | KS | KS | KS |
| PHASE | HCQP2 | HCQP2 | HCQP2 | HCQP2 | HCQP2 | HCQP2 | HCQP2 | HCQP2 | HCQP2 | HCQP2 |
| SIO2 | 63.75 | 63.49 | 63.86 | 63.23 | 63.08 | 64.45 | 64.47 | 64.24 | 64.14 | 64.53 |
| TIO2 | 0.00 | 0.00 | 0.00 | 0.00 | 0.20 | 0.11 | 0.00 | 0.14 | 0.00 | 0.00 |
| AL2O3 | 18.66 | 18.91 | 18.76 | 18.66 | 18.66 | 18.26 | 18.27 | 18.57 | 18.59 | 18.72 |
| FEO | 0.00 | 0.00 | 0.09 | 0.00 | 0.00 | 0.00 | 0.00 | 0.00 | 0.00 | 0.00 |
| MNO | 0.00 | 0.00 | 0.00 | 0.00 | 0.00 | 0.00 | 0.00 | 0.00 | 0.00 | 0.00 |
| MGO | 0.00 | 0.00 | 0.00 | 0.00 | 0.00 | 0.00 | 0.00 | 0.00 | 0.00 | 0.00 |
| CAO | 0.14 | 0.08 | 0.15 | 0.00 | 0.09 | 0.07 | 0.00 | 0.07 | 0.00 | 0.13 |
| NA2O | 1.35 | 0.91 | 0.65 | 1.04 | 0.82 | 0.00 | 0.00 | 0.00 | 0.00 | 0.00 |
| K2O | 14.16 | 15.07 | 15.30 | 14.78 | 14.79 | 15.89 | 16.01 | 15.87 | 16.10 | 15.91 |
| TOTAL | 98.11 | 98.46 | 98.81 | 97.71 | 97.64 | 98.78 | 98.75 | 98.89 | 98.83 | 99.29 |
| CSI | 11.921 | 11.881 | 11.914 | 11.910 | 11.889 | 12.021 | 12.032 | 11.971 | 11.973 | 11.974 |
| CTI | 0.000 | 0.000 | 0.000 | 0.000 | 0.028 | 0.015 | 0.000 | 0.020 | 0.000 | 0.000 |
| CAL | 4.114 | 4.172 | 4.126 | 4.144 | 4.146 | 4.015 | 4.020 | 4.080 | 4.091 | 4.095 |
| CFE | 0.000 | 0.000 | 0.014 | 0.000 | 0.000 | 0.000 | 0.000 | 0.000 | 0.000 | 0.000 |
| CMN | 0.000 | 0.000 | 0.000 | 0.000 | 0.000 | 0.000 | 0.000 | 0.000 | 0.000 | 0.000 |
| CMG | 0.000 | 0.000 | 0.000 | 0.000 | 0.000 | 0.000 | 0.000 | 0.000 | 0.000 | 0.000 |
| CCA | 0.028 | 0.016 | 0.030 | 0.000 | 0.018 | 0.014 | 0.000 | 0.014 | 0.000 | 0.026 |
| CNA | 0.489 | 0.330 | 0.235 | 0.380 | 0.300 | 0.000 | 0.000 | 0.000 | 0.000 | 0.000 |
| CK | 3.378 | 3.598 | 3.642 | 3.552 | 3.556 | 3.781 | 3.812 | 3.773 | 3.834 | 3.766 |
| OR | 86.7 | 91.2 | 93.2 | 90.3 | 91.8 | 99.6 | 100.0 | 99.6 | 100.0 | 99.3 |
| AB | 12.6 | 8.4 | 6.0 | 9.7 | 7.7 | 0.0 | 0.0 | 0.0 | 0.0 | 0.0 |
| AN | 0.7 | 0.4 | 0.8 | 0.0 | 0.5 | 0.4 | 0.0 | 0.4 | 0.0 | 0.7 |

| SAMPLE | NHCL028 | NHC03 | NHC03 | NHC03 | NHC03 | NHC03 | NHC03 | NHC03 | NQP13 | NQP13 |
|---|---|---|---|---|---|---|---|---|---|---|
| ANALYSES | 1C | 3B | 5B | 5A | 3A | 1A | 1C | 3C | 1A | 6B |
| MINERAL | KS | KS | KS | KS | KS | KS | KS | KS | KS | KS |
| PHASE | HCQP2 | HCQP3 | HCQP3 | HCQP3 | HCQP3 | HCQP3 | HCQP3 | HCQP3 | HCQP4 | HCQP4 |
| SI02 | 63.77 | 63.64 | 63.69 | 63.87 | 63.17 | 63.92 | 63.64 | 63.23 | 64.12 | 64.06 |
| TI02 | 0.00 | 0.00 | 0.00 | 0.00 | 0.11 | 0.00 | 0.21 | 0.00 | 0.00 | 0.00 |
| AL203 | 18.50 | 18.78 | 18.57 | 18.54 | 18.65 | 18.89 | 18.56 | 18.56 | 18.78 | 18.76 |
| FE0 | 0.07 | 0.00 | 0.00 | 0.00 | 0.00 | 0.05 | 0.00 | 0.00 | 0.00 | 0.04 |
| MN0 | 0.00 | 0.00 | 0.00 | 0.00 | 0.00 | 0.00 | 0.00 | 0.00 | 0.00 | 0.00 |
| MG0 | 0.00 | 0.00 | 0.00 | 0.00 | 0.00 | 0.00 | 0.00 | 0.00 | 0.00 | 0.00 |
| CA0 | 0.21 | 0.08 | 0.06 | 0.10 | 0.13 | 0.09 | 0.07 | 0.15 | 0.05 | 0.11 |
| NA20 | 0.00 | 1.23 | 0.37 | 0.28 | 0.97 | 0.72 | 0.77 | 1.43 | 0.37 | 0.72 |
| K20 | 15.95 | 14.40 | 15.54 | 15.41 | 14.45 | 14.80 | 14.87 | 13.85 | 15.61 | 14.95 |
| TOTAL | 98.50 | 98.13 | 98.23 | 98.20 | 97.48 | 98.52 | 98.12 | 97.22 | 98.93 | 98.64 |
| CSI | 11.954 | 11.912 | 11.950 | 11.971 | 11.906 | 11.916 | 11.928 | 11.926 | 11.942 | 11.940 |
| CTI | 0.000 | 0.000 | 0.000 | 0.000 | 0.016 | 0.000 | 0.030 | 0.000 | 0.000 | 0.000 |
| CAL | 4.088 | 4.144 | 4.108 | 4.097 | 4.144 | 4.152 | 4.101 | 4.127 | 4.123 | 4.122 |
| CFE | 0.011 | 0.000 | 0.000 | 0.000 | 0.000 | 0.008 | 0.000 | 0.000 | 0.000 | 0.006 |
| CMN | 0.000 | 0.000 | 0.000 | 0.000 | 0.000 | 0.000 | 0.000 | 0.000 | 0.000 | 0.000 |
| CMG | 0.000 | 0.000 | 0.000 | 0.000 | 0.000 | 0.000 | 0.000 | 0.000 | 0.000 | 0.000 |
| CCA | 0.042 | 0.016 | 0.012 | 0.020 | 0.026 | 0.018 | 0.014 | 0.030 | 0.010 | 0.022 |
| CNA | 0.000 | 0.446 | 0.135 | 0.102 | 0.354 | 0.260 | 0.280 | 0.523 | 0.134 | 0.260 |
| CK | 3.814 | 3.439 | 3.720 | 3.685 | 3.475 | 3.520 | 3.556 | 3.333 | 3.709 | 3.555 |
| OR | 98.9 | 88.1 | 96.2 | 96.8 | 90.1 | 92.7 | 92.4 | 85.8 | 96.3 | 92.6 |
| AB | 0.0 | 11.4 | 3.5 | 2.7 | 9.2 | 6.9 | 7.3 | 13.5 | 3.5 | 6.8 |
| AN | 1.1 | 0.4 | 0.3 | 0.5 | 0.7 | 0.5 | 0.4 | 0.8 | 0.3 | 0.6 |

| SAMPLE | NQP13 | NQP13 | NQP13 | NQP13 | NQP14 | NQP14 | NQP14 | NQP14 | NQP14 | NQP14 |
|---|---|---|---|---|---|---|---|---|---|---|
| ANALYSES | 1B | 5B | 6A | 5A | 1H | 1G | 4A | 4B | 1D | 1E |
| MINERAL | KS | KS | KS | KS | KS | KS | KS | KS | KS | KS |
| PHASE | HCQP4 | HCQP4 | HCQP4 | HCQP4 | HCQP4 | HCQP4 | HCQP4 | HCQP4 | HCQP4 | HCQP4 |
| SIO2 | 63.70 | 63.77 | 63.69 | 64.41 | 64.49 | 64.30 | 64.13 | 64.32 | 64.40 | 64.18 |
| TIO2 | 0.17 | 0.00 | 0.26 | 0.00 | 0.00 | 0.00 | 0.16 | 0.00 | 0.00 | 0.00 |
| AL2O3 | 18.45 | 18.76 | 18.96 | 18.67 | 18.95 | 19.03 | 19.25 | 19.11 | 19.26 | 19.05 |
| FEO | 0.00 | 0.00 | 0.00 | 0.00 | 0.04 | 0.00 | 0.06 | 0.00 | 0.00 | 0.00 |
| MNO | 0.00 | 0.00 | 0.00 | 0.00 | 0.00 | 0.00 | 0.00 | 0.00 | 0.00 | 0.00 |
| MGO | 0.00 | 0.00 | 0.00 | 0.00 | 0.00 | 0.00 | 0.00 | 0.00 | 0.00 | 0.00 |
| CAO | 0.00 | 0.09 | 0.21 | 0.14 | 0.09 | 0.00 | 0.13 | 0.07 | 0.15 | 0.13 |
| NA2O | 0.00 | 0.94 | 0.99 | 1.04 | 0.30 | 0.81 | 0.91 | 0.75 | 1.23 | 0.43 |
| K2O | 15.77 | 14.48 | 14.34 | 14.66 | 16.01 | 15.35 | 15.02 | 14.88 | 14.91 | 15.55 |
| TOTAL | 98.09 | 98.04 | 98.45 | 98.92 | 99.88 | 99.49 | 99.66 | 99.13 | 99.95 | 99.34 |
| CSI | 11.966 | 11.936 | 11.875 | 11.959 | 11.920 | 11.905 | 11.849 | 11.916 | 11.863 | 11.904 |
| CTI | 0.024 | 0.000 | 0.036 | 0.000 | 0.000 | 0.000 | 0.022 | 0.000 | 0.000 | 0.000 |
| CAL | 4.086 | 4.140 | 4.168 | 4.087 | 4.129 | 4.154 | 4.193 | 4.174 | 4.182 | 4.166 |
| CFE | 0.000 | 0.000 | 0.000 | 0.000 | 0.006 | 0.000 | 0.009 | 0.000 | 0.000 | 0.000 |
| CMN | 0.000 | 0.000 | 0.000 | 0.000 | 0.000 | 0.000 | 0.000 | 0.000 | 0.000 | 0.000 |
| CMG | 0.000 | 0.000 | 0.000 | 0.000 | 0.000 | 0.000 | 0.000 | 0.000 | 0.000 | 0.000 |
| CCA | 0.000 | 0.018 | 0.042 | 0.028 | 0.018 | 0.000 | 0.026 | 0.014 | 0.030 | 0.026 |
| CNA | 0.000 | 0.341 | 0.358 | 0.374 | 0.108 | 0.291 | 0.326 | 0.269 | 0.439 | 0.155 |
| CK | 3.780 | 3.458 | 3.411 | 3.473 | 3.775 | 3.626 | 3.541 | 3.517 | 3.504 | 3.680 |
| OR | 100.0 | 90.6 | 89.5 | 89.6 | 96.8 | 92.6 | 91.0 | 92.5 | 88.2 | 95.3 |
| AB | 0.0 | 8.9 | 9.4 | 9.7 | 2.8 | 7.4 | 8.4 | 7.1 | 11.1 | 4.0 |
| AN | 0.0 | 0.5 | 1.1 | 0.7 | 0.5 | 0.0 | 0.7 | 0.4 | 0.7 | 0.7 |

| SAMPLE | NQP16 | NQP16 | NQP16 | NQP16 | NQP16 | NQP16 | NQP16 | NQP16 | NQP16 | NQP18 |
|---|---|---|---|---|---|---|---|---|---|---|
| ANALYSES | 2D | 2E | 2C | 2A | 4D | 4A | 4C | 4B | 2B | 4C |
| MINERAL | KS | KS | KS | KS | KS | KS | KS | KS | KS | KS |
| PHASE | HCQP4 | HCQP4 | HCQP4 | HCQP4 | HCQP4 | HCQP4 | HCQP4 | HCQP4 | HCQP4 | HCQP4 |
| SIO2 | 63.81 | 63.76 | 63.41 | 64.42 | 63.97 | 64.37 | 63.71 | 64.26 | 63.53 | 64.03 |
| TIO2 | 0.00 | 0.07 | 0.42 | 0.00 | 0.10 | 0.09 | 0.00 | 0.15 | 0.00 | 0.00 |
| AL2O3 | 18.63 | 18.79 | 18.66 | 18.80 | 18.70 | 18.78 | 18.74 | 18.66 | 18.46 | 18.72 |
| FEO | 0.00 | 0.00 | 0.00 | 0.00 | 0.00 | 0.00 | 0.00 | 0.00 | 0.00 | 0.05 |
| MNO | 0.00 | 0.00 | 0.00 | 0.00 | 0.00 | 0.00 | 0.00 | 0.00 | 0.00 | 0.00 |
| MGO | 0.00 | 0.00 | 0.00 | 0.00 | 0.00 | 0.00 | 0.00 | 0.00 | 0.00 | 0.00 |
| CAO | 0.00 | 0.00 | 0.07 | 0.12 | 0.17 | 0.05 | 0.05 | 0.06 | 0.07 | 0.13 |
| NA2O | 0.80 | 0.48 | 0.78 | 0.89 | 0.62 | 0.61 | 0.99 | 0.41 | 0.27 | 0.62 |
| K2O | 14.59 | 15.01 | 14.55 | 14.99 | 14.89 | 15.43 | 14.68 | 15.37 | 15.29 | 15.29 |
| TOTAL | 97.83 | 98.11 | 97.89 | 99.22 | 98.45 | 99.33 | 98.17 | 98.91 | 97.62 | 98.84 |
| CSI | 11.966 | 11.939 | 11.897 | 11.941 | 11.940 | 11.936 | 11.927 | 11.955 | 11.973 | 11.933 |
| CTI | 0.000 | 0.010 | 0.059 | 0.000 | 0.014 | 0.013 | 0.000 | 0.021 | 0.000 | 0.000 |
| CAL | 4.119 | 4.148 | 4.127 | 4.108 | 4.115 | 4.105 | 4.136 | 4.093 | 4.102 | 4.113 |
| CFE | 0.000 | 0.000 | 0.000 | 0.000 | 0.000 | 0.000 | 0.000 | 0.000 | 0.000 | 0.008 |
| CMN | 0.000 | 0.000 | 0.000 | 0.000 | 0.000 | 0.000 | 0.000 | 0.000 | 0.000 | 0.000 |
| CMG | 0.000 | 0.000 | 0.000 | 0.000 | 0.000 | 0.000 | 0.000 | 0.000 | 0.000 | 0.000 |
| CCA | 0.000 | 0.000 | 0.014 | 0.024 | 0.034 | 0.010 | 0.010 | 0.012 | 0.014 | 0.026 |
| CNA | 0.291 | 0.174 | 0.284 | 0.320 | 0.224 | 0.219 | 0.359 | 0.148 | 0.099 | 0.224 |
| CK | 3.490 | 3.586 | 3.483 | 3.545 | 3.546 | 3.650 | 3.506 | 3.648 | 3.676 | 3.636 |
| OR | 92.3 | 95.4 | 92.1 | 91.2 | 93.2 | 94.1 | 90.5 | 95.8 | 97.0 | 93.6 |
| AB | 7.7 | 4.6 | 7.5 | 8.2 | 5.9 | 5.7 | 9.3 | 3.9 | 2.6 | 5.8 |
| AN | 0.0 | 0.0 | 0.4 | 0.6 | 0.9 | 0.3 | 0.3 | 0.3 | 0.4 | 0.7 |

| SAMPLE | NQP18 | NQP18 | NQP18 | NQP18 | NQP18 | NQP18 | NQP18 | NQP18 | NQP18 | NQP18 |
|---|---|---|---|---|---|---|---|---|---|---|
| ANALYSES | 6C | 6A | 5B | 4D | 6B | 4A | 3C | 3B | 3A | 1A |
| MINERAL | KS | KS | KS | KS | KS | KS | KS | KS | KS | KS |
| PHASE | HCQP4 | HCQP4 | HCQP4 | HCQP4 | HCQP4 | HCQP4 | HCQP4 | HCQP4 | HCQP4 | HCQP4 |
| SIO2 | 63.65 | 64.62 | 60.34 | 64.45 | 63.90 | 64.58 | 64.50 | 63.76 | 63.51 | 63.69 |
| TIO2 | 0.00 | 0.00 | 0.39 | 0.00 | 0.15 | 0.00 | 0.21 | 0.00 | 0.00 | 0.00 |
| AL2O3 | 18.71 | 19.00 | 23.22 | 18.64 | 18.68 | 18.51 | 18.90 | 18.80 | 18.88 | 18.86 |
| FEO | 0.00 | 0.00 | 0.71 | 0.00 | 0.00 | 0.00 | 0.00 | 0.00 | 0.00 | 0.00 |
| MNO | 0.00 | 0.00 | 0.00 | 0.00 | 0.00 | 0.00 | 0.00 | 0.00 | 0.00 | 0.00 |
| MGO | 0.00 | 0.00 | 0.51 | 0.00 | 0.00 | 0.00 | 0.00 | 0.00 | 0.00 | 0.00 |
| CAO | 0.16 | 0.14 | 0.70 | 0.00 | 0.16 | 0.05 | 0.12 | 0.15 | 0.11 | 0.12 |
| NA2O | 0.31 | 0.82 | 5.05 | 0.25 | 0.30 | 0.21 | 0.83 | 0.99 | 1.01 | 0.82 |
| K2O | 15.62 | 15.09 | 6.97 | 15.67 | 15.55 | 15.41 | 14.65 | 14.66 | 14.41 | 14.89 |
| TOTAL | 98.45 | 99.67 | 98.01 | 99.01 | 98.80 | 98.76 | 99.21 | 98.36 | 97.92 | 98.38 |
| CSI | 11.923 | 11.925 | 11.091 | 11.984 | 11.916 | 12.016 | 11.929 | 11.915 | 11.906 | 11.908 |
| CTI | 0.000 | 0.000 | 0.054 | 0.000 | 0.021 | 0.000 | 0.029 | 0.000 | 0.000 | 0.000 |
| CAL | 4.132 | 4.133 | 5.032 | 4.086 | 4.107 | 4.060 | 4.121 | 4.142 | 4.173 | 4.157 |
| CFE | 0.000 | 0.000 | 0.109 | 0.000 | 0.000 | 0.000 | 0.000 | 0.000 | 0.000 | 0.000 |
| CMN | 0.000 | 0.000 | 0.000 | 0.000 | 0.000 | 0.000 | 0.000 | 0.000 | 0.000 | 0.000 |
| CMG | 0.000 | 0.000 | 0.140 | 0.000 | 0.000 | 0.000 | 0.000 | 0.000 | 0.000 | 0.000 |
| CCA | 0.032 | 0.028 | 0.138 | 0.000 | 0.032 | 0.010 | 0.024 | 0.030 | 0.022 | 0.024 |
| CNA | 0.113 | 0.293 | 1.800 | 0.090 | 0.108 | 0.076 | 0.298 | 0.359 | 0.367 | 0.297 |
| CK | 3.733 | 3.553 | 1.634 | 3.717 | 3.700 | 3.658 | 3.457 | 3.495 | 3.446 | 3.552 |
| OR | 96.3 | 91.7 | 45.8 | 97.6 | 96.3 | 97.7 | 91.5 | 90.0 | 89.9 | 91.7 |
| AB | 2.9 | 7.6 | 50.4 | 2.4 | 2.8 | 2.0 | 7.9 | 9.2 | 9.6 | 7.7 |
| AN | 0.8 | 0.7 | 3.9 | 0.0 | 0.8 | 0.3 | 0.6 | 0.8 | 0.6 | 0.6 |

| SAMPLE | NQP18 | NQP18 |
|---|---|---|
| ANALYSES | 1B | 1C |
| MINERAL | KS | KS |
| PHASE | HCQP4 | HCQP4 |
| SIO2 | 63.93 | 63.77 |
| TIO2 | 0.00 | 0.11 |
| AL2O3 | 18.87 | 18.63 |
| FEO | 0.00 | 0.00 |
| MNO | 0.00 | 0.00 |
| MGO | 0.00 | 0.00 |
| CAO | 0.00 | 0.11 |
| NA2O | 0.85 | 0.91 |
| K2O | 14.69 | 14.47 |
| TOTAL | 98.34 | 98.00 |
| CSI | 11.934 | 11.942 |
| CTI | 0.000 | 0.015 |
| CAL | 4.153 | 4.113 |
| CFE | 0.000 | 0.000 |
| CMN | 0.000 | 0.000 |
| CMG | 0.000 | 0.000 |
| CCA | 0.000 | 0.022 |
| CNA | 0.308 | 0.330 |
| CK | 3.498 | 3.457 |
| OR | 91.9 | 90.7 |
| AB | 8.1 | 8.7 |
| AN | 0.0 | 0.6 |

APPENDIX IV-6 Garnet analyses

| SAMPLE | GRANITE1 | GRANITE1 | GRANITE1 | GRANITE1 | GRANITE1 | GRANITE1 | GRANITE1 | GRANITE1 | GRANITE1 | GRANITE1 |
|---|---|---|---|---|---|---|---|---|---|---|
| ANALYSES | 1 | 1 | 2 | 2 | 3 | 3 | 3 | 4 | 4 | 5 |
| LOCATION | CORE | RIM | RIM | CORE | RIM | CORE | CORE | RIM | CORE | RIM |
| SIO2 | 35.98 | 36.40 | 36.14 | 36.21 | 36.32 | 35.91 | 36.13 | 36.31 | 36.33 | 36.06 |
| AL2O3 | 20.87 | 20.84 | 20.90 | 20.81 | 21.15 | 21.12 | 20.94 | 21.12 | 21.24 | 20.44 |
| FEO | 25.66 | 23.96 | 23.70 | 25.25 | 23.83 | 24.82 | 24.03 | 24.48 | 25.81 | 24.35 |
| MNO | 16.60 | 17.14 | 17.25 | 15.63 | 17.40 | 16.70 | 17.46 | 16.96 | 15.10 | 16.88 |
| MGO | 1.47 | 1.28 | 1.30 | 1.60 | 1.28 | 1.44 | 1.26 | 1.39 | 1.79 | 1.21 |
| CAO | 0.34 | 0.51 | 0.50 | 0.42 | 0.49 | 0.39 | 0.36 | 0.52 | 0.48 | 0.51 |
| NA2O | 0.00 | 0.00 | 0.00 | 0.00 | 0.00 | 0.00 | 0.00 | 0.00 | 0.00 | 0.00 |
| TOTAL | 100.92 | 100.13 | 99.79 | 100.03 | 100.47 | 100.38 | 100.18 | 100.78 | 100.75 | 99.45 |
| CSI | 5.877 | 5.956 | 5.935 | 5.929 | 5.924 | 5.877 | 5.921 | 5.911 | 5.900 | 5.957 |
| CAL | 4.019 | 4.020 | 4.046 | 4.017 | 4.067 | 4.075 | 4.046 | 4.053 | 4.067 | 3.981 |
| CFE | 3.505 | 3.279 | 3.255 | 3.458 | 3.251 | 3.397 | 3.294 | 3.333 | 3.506 | 3.364 |
| CMN | 2.297 | 2.376 | 2.400 | 2.168 | 2.404 | 2.315 | 2.424 | 2.339 | 2.077 | 2.362 |
| CMG | 0.358 | 0.312 | 0.318 | 0.390 | 0.311 | 0.351 | 0.308 | 0.337 | 0.433 | 0.298 |
| CCA | 0.060 | 0.089 | 0.088 | 0.074 | 0.086 | 0.068 | 0.063 | 0.091 | 0.084 | 0.090 |
| CNA | 0.000 | 0.000 | 0.000 | 0.000 | 0.000 | 0.000 | 0.000 | 0.000 | 0.000 | 0.000 |
| SPESS | 36.9 | 39.2 | 39.6 | 35.6 | 39.7 | 37.8 | 39.8 | 38.3 | 34.0 | 38.6 |
| ALMAN | 56.4 | 54.1 | 53.7 | 56.8 | 53.7 | 55.4 | 54.1 | 54.6 | 57.5 | 55.0 |
| PYROPE | 5.8 | 5.2 | 5.2 | 6.4 | 5.1 | 5.7 | 5.1 | 5.5 | 7.1 | 4.9 |
| GROSS | 1.0 | 1.5 | 1.5 | 1.2 | 1.4 | 1.1 | 1.0 | 1.5 | 1.4 | 1.5 |

GRANITE 1 = HC-83-L037
GRANITE 2 = HC-83-L014
HFX = metasedimentary rock 11F6-83-L002

| SAMPLE | GRANITE1 | HFX | HFX | HFX | HFX | HFX | HFX | HFX | HFX | HFX |
|---|---|---|---|---|---|---|---|---|---|---|
| ANALYSES | 5 | 1 | 1 | 2 | 2 | 3 | 3 | 4 | 4 | 5 |
| LOCATION | CORE | RIM | CORE | RIM | CORE | RIM | CORE | CORE | RIM | CORE |
| SIO2 | 35.80 | 36.16 | 36.22 | 36.00 | 36.09 | 36.07 | 36.01 | 36.19 | 36.19 | 36.05 |
| AL2O3 | 20.77 | 21.14 | 20.96 | 21.12 | 20.73 | 20.85 | 20.95 | 20.81 | 20.88 | 20.89 |
| FEO | 23.09 | 32.92 | 31.41 | 31.96 | 29.45 | 32.63 | 29.13 | 31.14 | 32.75 | 32.12 |
| MNO | 18.64 | 7.19 | 8.81 | 8.16 | 10.66 | 7.69 | 11.32 | 8.28 | 7.44 | 8.29 |
| MGO | 1.18 | 1.45 | 1.33 | 1.40 | 1.52 | 1.40 | 1.52 | 1.54 | 1.52 | 1.42 |
| CAO | 0.41 | 0.81 | 0.98 | 0.93 | 0.81 | 0.84 | 0.83 | 1.02 | 0.86 | 0.92 |
| NA2O | 0.00 | 0.00 | 0.00 | 0.00 | 0.00 | 0.00 | 0.00 | 0.00 | 0.00 | 0.00 |
| TOTAL | 99.89 | 99.67 | 99.71 | 99.57 | 99.26 | 99.48 | 99.82 | 98.98 | 99.64 | 99.69 |
| CSI | 5.900 | 5.930 | 5.943 | 5.915 | 5.948 | 5.937 | 5.909 | 5.964 | 5.942 | 5.925 |
| CAL | 4.035 | 4.087 | 4.054 | 4.091 | 4.028 | 4.046 | 4.053 | 4.043 | 4.041 | 4.048 |
| CFE | 3.182 | 4.515 | 4.310 | 4.392 | 4.059 | 4.492 | 3.998 | 4.292 | 4.497 | 4.415 |
| CMN | 2.602 | 0.999 | 1.224 | 1.136 | 1.488 | 1.072 | 1.573 | 1.156 | 1.035 | 1.154 |
| CMG | 0.290 | 0.354 | 0.325 | 0.343 | 0.373 | 0.343 | 0.372 | 0.378 | 0.372 | 0.348 |
| CCA | 0.072 | 0.142 | 0.172 | 0.164 | 0.143 | 0.148 | 0.146 | 0.180 | 0.151 | 0.162 |
| CNA | 0.000 | 0.000 | 0.000 | 0.000 | 0.000 | 0.000 | 0.000 | 0.000 | 0.000 | 0.000 |
| SPESS | 42.3 | 16.6 | 20.3 | 18.8 | 24.5 | 17.7 | 25.8 | 19.2 | 17.1 | 19.0 |
| ALMAN | 51.8 | 75.1 | 71.5 | 72.8 | 66.9 | 74.2 | 65.7 | 71.5 | 74.3 | 72.6 |
| PYROPE | 4.7 | 5.9 | 5.4 | 5.7 | 6.2 | 5.7 | 6.1 | 6.3 | 6.1 | 5.7 |
| GROSS | 1.2 | 2.4 | 2.9 | 2.7 | 2.4 | 2.4 | 2.4 | 3.0 | 2.5 | 2.7 |

| SAMPLE | HFX | HFX | HFX | GRANITE2 | GRANITE2 | GRANITE2 | GRANITE2 |
|---|---|---|---|---|---|---|---|
| ANALYSES | 5 | 6 | 6 | 1 | 1 | 2 | 3 |
| LOCATION | RIM | CORE | CORE | RIM | CORE | CORE | RIM |
| SIO2 | 36.08 | 35.85 | 36.35 | 35.57 | 35.35 | 35.35 | 35.90 |
| AL2O3 | 20.92 | 20.97 | 20.91 | 20.89 | 20.89 | 20.66 | 20.87 |
| FEO | 31.35 | 28.96 | 32.52 | 25.50 | 25.60 | 24.13 | 25.43 |
| MNO | 9.26 | 10.99 | 7.42 | 16.91 | 17.15 | 18.97 | 17.03 |
| MGO | 1.52 | 1.35 | 1.38 | 0.36 | 0.40 | 0.34 | 0.39 |
| CAO | 0.87 | 0.81 | 0.89 | 0.14 | 0.12 | 0.13 | 0.19 |
| NA2O | 0.00 | 0.00 | 0.00 | 0.00 | 0.00 | 0.00 | 0.00 |
| TOTAL | 100.00 | 98.93 | 99.47 | 100.41 | 99.51 | 99.58 | 99.81 |
| CSI | 5.914 | 5.926 | 5.968 | 5.848 | 5.879 | 5.886 | 5.935 |
| CAL | 4.043 | 4.087 | 4.048 | 4.049 | 4.096 | 4.056 | 4.067 |
| CFE | 4.298 | 4.004 | 4.466 | 3.506 | 3.561 | 3.360 | 3.516 |
| CMN | 1.286 | 1.539 | 1.032 | 2.355 | 2.416 | 2.676 | 2.385 |
| CMG | 0.371 | 0.333 | 0.338 | 0.088 | 0.099 | 0.084 | 0.096 |
| CCA | 0.153 | 0.143 | 0.157 | 0.025 | 0.021 | 0.023 | 0.034 |
| CNA | 0.000 | 0.000 | 0.000 | 0.000 | 0.000 | 0.000 | 0.000 |
| SPESS | 21.1 | 25.6 | 17.2 | 39.4 | 39.6 | 43.6 | 39.5 |
| ALMAN | 70.4 | 66.5 | 74.5 | 58.7 | 58.4 | 54.7 | 58.3 |
| PYROPE | 6.1 | 5.5 | 5.6 | 1.5 | 1.6 | 1.4 | 1.6 |
| GROSS | 2.5 | 2.4 | 2.6 | 0.4 | 0.3 | 0.4 | 0.6 |

## REFERENCES


Abbott, R. N., Jr., 1978. Peritectic reactions in the system An-Ab-Or-Qz-$H_2O$; Canadian Mineralogist, v. 16, p. 245-256.

_____, 1985. Muscovite-bearing granites in the AFM liquidus projections; Canadian Mineralogist, v. 23, p. 553-561.

_____ and Clarke, D. B., 1979. Hypothetical liquidus relationships in the subsystem $Al_2O_3$-FeO-MgO projected from quartz, alkali feldspar and plagioclase, $a(H_2O) \leq 1$; Canadian Mineralogist, v. 17, p. 549-560.

Adams, J. A. S., Osmond, K. J. and Rogers, J. J. W., 1959. The geochemistry of thorium and uranium; Physics and Chemistry of the Earth, v. 3. p.298.

Akhavi, M. S., 1985. Application of a geocoded database for geological investigation and exploration; in Proceedings of the International symposium on remote sensing of environment; Remote sensing for exploration geology, p. 271-277

de Albuquerque, C. A. R., 1973. Geochemistry of biotites from granitic rocks, Northern Portugal; Geochimica et Cosmochimica Acta, v. 37. p. 1779-1802.

_____, 1977. Geochemistry of the tonalitic and granitic rocks of the Nova Scotia southern plutons; Geochimica et Cosmochimica Acta, v. 41, p. 1-13.

Alderton, D. H. M., Pearce, J. A. and Potts, P. J., 1980. REE mobility during granite alteration: evidence from southwest England; Earth and Planetary Science Letters, v. 49, p. 149-165.

Allan, B. D. and Clarke, D. B., 1981. Occurrence and origin of garnet in the South Mountain Batholith, Nova Scotia; Canadian Mineralogist, v. 19, p. 19-24.

Allen, R. G. H., 1963. Granitic rocks of the Halifax Harbour - St. Margaret's Bay area; unpublished M.Sc. thesis, Dalhousie University, 37 p.

Allen, P. L. and Barr, S. M., 1983. The Ellison Lake Pluton: a cordierite-bearing monzogranitic intrusive body in southwestern Nova Scotia; Canadian Mineralogist, v. 21, p. 583-590.

Alizay, K. M., 1981. Zur Geologie und Geochemie des Sherbroke-Plutons (Nova Scotia, Kanada); post-graduate thesis, Department of Geological Sciences, University of Hamburg, Germany.

Althaus, E., Karotke, E., Nitsch, K. H. and Winkler, H. G. F., 1970. An experimental re-examination of the upper stability limit of muscovite plus quartz; Neues Jahrb. Mineral. Monatsh, v. , 325-336.

Anderson, J. L. and Rowley, M. C., 1981. Synkinematic intrusion of peraluminous and associated metaluminous granitic magmas, Whipple Mountains, California; Canadian Mineralogist, v. 19, p. 83-101.

Backlund, H. G., 1938. The problem of the rapakivi granites; Journal of Geology, v. 46, p. 339-396.

Baker, J. H., 1985. Rare earth and other trace element mobility accompanying albitization in a Proterozoic granite, W. Bergslagen, Sweden; Mineralogical Magazine, v. 49, p. 107-115.

Balk, R., 1937. Structural Behaviour of Igneous Rocks, Geological Society of America, Memoir 5, 177 p.

Bateman, P. C., Huber, N. K., Moore, J. G. and Rinehart, C. D., 1963. The Sierra Nevada batholith - a synthesis or recent work across the central part; Professional Paper, U. S. Geological Survey, 414D, 46 p.

le Bel, L., 1979. Micas magmatiques et hydrothermaux dans l'environnement du porphyre cuprifere de Cerro Verde-Santa Rose, Perou; Bulletin Mineralogique, v. 102, p. 35-41.

Benson, D. G., 1967. Geology of Hopewell map-area, Nova Scotia; Geological Survey of Canada, Memoir 343, 58 p.

Berger, A. R. and Pitcher, W. S., 1970. Structures in granitic rocks: a commentary and a critique on granite tectonics; Proceedings of the Geological Society of London, v. 81, p. 441-461.

Berthe, D., Choukroune, P. and Jegouzo, P., 1979. Orthogneiss, mylonite and non-coaxial deformation of granites: the example of the South Amorican shear zone; Journal of Structural Geology, v. 1, p. 31-42.

Bingley, J. M. and Richardson, K. A., 1978. Regional lake sediment geochemical surveys for Eastern Mainland Nova Scotia; Nova Scotia Department of Mines and Energy, Open File 371.

Bizouard, H., Capdevila, R. and Gaven, C., 1970. Microanalysis of aplite garnets and granites of eastern Galicia, Spain; Spain Inst. Geol. Minero, Bol. Geol Minero, v. 81, no. 2-3, p. 299-304.

Boone, G. M., 1969. Origin of clouded red feldspars: petrologic contrast in a granitic porphyry intrusion; American Journal of Science, v. 267, p. 633-668.

Buddington, A. F., 1959. Granite emplacement with special reference to North America; Bulletin of the Geological Society of America, v.

70, p. 671-747.

Buma, G., Frey, F. A. and Wones, D. R., 1971. New England granites: trace element evidence regarding their origin and differentiation; Contributions to Mineralogy and Petrology, v. 31. p. 300-320.

Burnham, C. W., 1979. The importance of volatile constituents; in The Evolution of Igneous Rocks (Fiftieth Anniversary Perspectives), H. S. Yoder, ed., Princeton University Press, Princeton, N.J., p. 439-482.

Burnham, C. W. and Ohmoto, H., 1980. Late-stage processes of felsic magmatism; Mining Geology Special Issue, eds. S. Ishihara and S. Takenouchi, v. 8, p. 1-11.

Butler, J. R., Bowden, P. and Smith, A. Z., 1962. K/Rb ratios in the evolution of the Younger Granites of Northern Nigeria; Geochimica et Cosmochimica Acta, v. 26, p. 89-100.

Chappell, B. W., 1978. Granitoids from the Moonbi District, New England Batholith, Eastern Australia; Journal of the Geological Society of Australia, v. 25, p. 267-283.

Chappell, B. W. and White, A. J. R., 1974. Two contrasting granitic types; Pacific Geology, v. 8, p. 173-174.

Charest, M. H., 1976. Petrology, geochemistry and mineralization of the New Ross area, Lunenburg County, Nova Scotia; unpublished M.Sc. thesis, Dalhousie University, Halifax.

Chatterjee, A. K. and Muecke, G. K., 1982. Geochemistry and the distribution of uranium and thorium in the granitic rocks of the South Mountain Batholith, Nova Scotia: some genetic and exploration implications; in Uranium in Granites, ed. Y. T. Maurice; Geological Survey of Canada, Paper 81-23, p. 11-17.

Chatterjee, A. K., Strong, D. F. and Muecke, G. K., 1983. A multivariate approach to geochemical distinction between tin-specialized and uranium granites of southern Nova Scotia; Canadian Journal of Earth Sciences, v. 20, p. 420-430.

_____, Robertson, J., and Pollock, D., 1982. A summary of the petrometallogenesis of the uranium mineralization at Millet Brook, South Mountain Batholith, Nova Scotia; Nova Scotia Department of Mines and Energy, Report 82-1, p. 57-66.

_____ and Strong, D. F., 1984. Discriminant and factor analysis of geochemical data from granitoid rocks hosting the Millet Brook uranium mineralization, South Mountain Batholith, Nova Scotia; Uranium 1(4), p. 289-305.

Chevalier, B. M., 1983. Petrography and geochemistry of the Bull Ridge pluton, Guysborough County, Nova Scotia; unpublished B. Sc. honours thesis, Acadia University, Wolfville, Nova Scotia.

Clark, A. M., 1984. Mineralogy of the Rare Earth Elements; in Rare Earth Element Geochemistry, ed. P. Henderson, Elsevier Science Publishing Company Limited, New York, p. 33-61.

Clarke, D. B., 1981. The mineralogy of peraluminous granites: a review; Canadian Mineralogist, v. 19, p. 3-17.

_____ and Chatterjee, A. K., 1985. Physical and Chemical Processes in the South Mountain batholith; in Granite-related mineral deposits: geology, petrogenesis and tectonic setting, R. P. Taylor and D. F. Strong (Eds.), CIM conference, Halifax, p. 58-62.

_____ and Chatterjee, A. K., 1988. Meguma Zone basement I: Sr-Nd isotopic study of the Liscomb complex and the origin of peraluminous granites in the Meguma Zone (abst); in Geological Association of Canada, Program with Abstracts, v. 13, A21.

_____ and Halliday, A. N., 1980. Strontium isotope geology of the South Mountain batholith, Nova Scotia; Geochimica et Cosmochimica Acta, v. 44, p. 1045-58.

_____ and Halliday, A. N., 1985. Sm/Nd isotopic investigation of the age and origin of the Meguma Zone metasedimentary rocks; Canadian Journal of Earth Sciences, v. 22, p. 102-107.

_____, Halliday, A. N. and Hamilton, P. J., 1988. Neodymium and strontium isotopic constraints on the origin of the peraluminous granitoids of the South Mountain Batholith, Nova Scotia, Canada; Chemical Geology, Isotope Geoscience Section, v. 73, p. 15-24.

_____, McKenzie, C. B., Muecke, G. K. and Richardson, S. W., 1976. Magmatic andalusite from the South Mountain Batholith, Nova Scotia; Contributions to Mineralogy and Petrology, v. 56, p. 279-287.

_____ and Muecke, G. K., 1980. Igneous and metamorphic geology of southern Nova Scotia, Field trip guide (No. 21), Geological Association of Canada and Mineralogical Association of Canada, 101 p.

_____ and Muecke, G. K., 1985. Review of the petrochemistry and origin of the South Mountain Batholith and associated plutons, Nova Scotia, Canada; in High Heat Production (HHP) Granites, Hydrothermal Circulation and Ore Genesis; St. Austell, Cornwall, England, September 22-25, 1985, p. 41-54.

Clemens, J. D. and Wall, V. J., 1981. Origin and crystallization of some peraluminous (S-type) granitic magmas; Canadian Mineralogist, v. 19, p. 111-132.

_____, Holloway, J. R. and White, A. J. R., 1986. Origin of an A-type granite: experimental constraints; American

Mineralogist, v. 71, p. 317-324.

Corey, M. C., 1988. An occurrence of metasomatic aluminosilicates related to high alumina hydrothermal alteration within the South Mountain Batholith, Nova Scotia; Maritime Sediments and Atlantic Geology, v. 24, p. 83-95.

Crosby, D. G., 1962. Wolfville map-area, Nova Scotia; Geological Survey of Canada Memoir, 325, 67 p.

Cullers, R. L. and Graf, J. L., 1984. Rare earth elements in igneous rocks of the continental crust: intermediate and silicic rocks - ore petrogenesis; in Rare Earth Element Geochemistry, ed. P. Henderson, Elsevier Science Publishing Company Limited, New York, p. 275-316.

Dallmeyer, R. D. and Keppie, J. D., 1985. Geochronological constraints on the accretion of the Meguma Terrane with North America (abst); in Mines and Minerals Branch, Report of Activities, 1985, eds. K. L. Mills and J. L. Bates, Nova Scotia Department of Mines and Energy, Report 85-1, p. 167.

Deer, W. A., Howie, R. A. and Zussman, J., 1966. An Introduction to the Rock Forming Minerals; Longman Group Ltd: London, 528 p.

Dickie, J. R., 1978. Geological, mineralogical and fluid-inclusion studies at the Dunbrack lead-silver deposit, Musquodoboit Harbour, Halifax County, Nova Scotia; unpublished B.Sc. (Honours) thesis, Dalhousie University, Halifax.

Dickie, G. B., 1986. Building stone project; in Mines and Minerals Branch, Report of Activities, 1985, eds. J. L. Bates, Nova Scotia Department of Mines and Energy, Report 86-1, p. 45-50.

_____, 1987. Building stone project; in Mines and Minerals Branch, Report of Activities, 1986, eds. J. L. Bates and D. R. MacDonald, Nova Scotia Department of Mines and Energy, Report 87-1, p. 47-53.

Didier, J., 1973. Granites and their enclaves: The bearing of enclaves on the origin of granites; Elsevier, Amsterdam, 393 p.

Dodge, F. C. W. and Moore, J. G., 1968. Occurrence and composition of biotites from the Cartridge Pass pluton of the Sierra Nevada batholith; U.S. Geol. Surv. Prof. Paper 600-B, B6-B10.

Doman, R. C., 1972. 'Tantalum', in the Encyclopedia of Geochemistry and Environmental Sciences, ed. R. W. Fairbridge, p. 1162-1163. Van Nostrand Reinhold Co., New York.

(Woodend) Douma, S. L., 1988. The Mineralogy, Petrology and Geochemistry of the Port Mouton Pluton, Nova Scotia, Canada; unpublished M.Sc. thesis, Dalhousie University, Halifax, Nova Scotia.

Eddy, B. G., 1987. Deformation and metamorphism of the Whitehead Harbour area, Guysborough County, Nova Scotia; unpublished B.Sc. (Honours) thesis, Acadia University, Wolfville.

Elders, W. A., 1966. Mantled feldspars from the granites of Wisconsin; Journal of Geology, v. 76, p. 37-49.

Elias, P., 1986. Thermal History of the Meguma Terrane: A Study based on $^{40}Ar/^{39}Ar$ and Fission Track Dating; unpublished Ph.D thesis, Dalhousie University, Halifax, Nova Scotia.

Elliston, J. N., 1985. Rapakivi texture: an indication of the crystallization of hydrosilicates, II; Earth Science Reviews, v. 22, p. 1-92.

Emmermann, R., Daieva, L. and Schneider, J., 1975. Petrologic significance of rare earths distribution in granites; Contributions to Mineralogy and Petrology, v. 52, p. 267-283.

Eugster, H. P., 1985. Granites and hydrothermal ore deposits: a geochemical framework; Mineralogical Magazine, v. 49, p. 7-23.

Fairbairn, H. W., Hurley, P. M., Pinson, W. H. and Cormier, R. F., 1960. Age of the granitic rocks of Nova Scotia; Geological Society of America Bulletin, V. 71, p. 399-419.

Fairbairn, H. W., Hurley, P. M. and Pinson, W. H., 1964. Preliminary age study and initial $Sr^{87}/Sr^{86}$ of Nova Scotia granitic rocks by the Rb-Sr whole rock method; Bulletin of the Geological Society of America, v. 75, p. 253-258.

Faribault, E. R., 1908a. City of Halifax Sheet, Map No. 68; Geological Survey of Canada, Publication No. 1019.

_____, 1908b. Aspotogan Sheet, Map No. 70; Geological Survey of Canada, Publication No. 1043.

_____, 1908c. St. Margaret's Bay Sheet, Map No. 71; Geological Survey of Canada, Publication No. 1036.

_____, 1916. Ponhook Lake Sheet, Map No. 72; Geological Survey of Canada, Publication No. 1539.

_____, 1931. New Ross Sheet, Map No. 86; Geological Survey of Canada, Publication No. 2259.

Farley, E. J., 1979. Mineralization at the Turner and Walker Deposits, South Mountain Batholith, unpublished M.Sc. thesis, Dalhousie University, Halifax, Nova Scotia.

Fletcher, H. and Faribault, E. R., 1887. Geological map of the Chedabucto Bay area; Geological Survey of Canada Annual Report 1886, v. 2.

Ford, K. L. and Ballantyne, S. B., 1983. Uranium and thorium distribution patterns and lithogeochemistry of Devonian granites in the Chedabucto Bay area, Nova Scotia; in Current Research, Part A, Geological Survey of Canada, Paper 83-1A, p. 109-119.

_____ and O'Reilly, G. A., 1985. Airborne gamma ray spectrometric surveys as an indicator of granophile element specialization and associated mineral deposits in the granitic rocks of the Meguma Zone of Nova Scotia; in High Heat Production (HHP) Granites, Hydrothermal Circulation and Ore Genesis; Meeting of Institution of Mining and Metallurgy, St. Austell, Cornwall, England, 1985, p. 113-133.

Foster, M. D., 1960. Interpretation of the composition of trioctahedral micas; U. S. Geological Survey Professional Paper 354-B, p. 1-49.

Fourcade, S. and Allegre. C. J., 1981. Trace element behaviour in granite genesis: a case study - the calc-alkaline plutonic association from the Querigut complex (Pyrenees, France); Contributions to Mineralogy and Petrology, v. 76, p. 177-195.

Fyson, W. K., 1966. Structures in the Lower Paleozoic Meguma Group, Nova Scotia; Bulletin of the Geological Society of America, v. 77, p. 931-944

Gates, R. M., 1953. Petrogenetic significance of perthite; Geological Society of America, v. 52, p. 55-69.

Geological Survey of Canada, 1978. Geophysical Series Maps 35411G, 35511G, 35611G and 35821G.

_____, 1982. Airborne radioactivity maps and profiles, Nova Scotia; Geophysical Series Maps 35611(3)G, 35611(4)G, 35611(5)G and 35611(6)G).

Giles, P. S. and Chatterjee, A. K., 1987. Peraluminous granites of the Liscomb Complex; in Mines and Minerals Branch, Report of Activities, 1986, eds. J. L. Bates and D. R. MacDonald, Nova Scotia Department of Mines and Energy, Report 87-1, p. 95-98.

Giuliani, G., Cheilletz, A. and Mechiche, M., 1987. Behaviour of REE during thermal metamorphism and hydrothermal infiltration associated with skarn and vein-type tungsten ore bodies in Central Morocco; Chemical Geology, v. , p. 279-294.

Grasty, R. L. and Charbonneau, B. W., 1973. Uranium enrichment associated with the Deloro Stock, southern Ontario; in Report of Activities, Part B., Geological Survey of Canada, Paper No. 75-1, p. 49-52.

Green, T. H., 1977. Garnet in silicic liquids and its possible use as a P-T indicator; Contributions to Mineralogy and Petrology; v. 65, p. 56-67.

Gromet, L. P. and Silver, L. T., 1983. Rare-earth element distributions among minerals in a granodiorite and their petrogenetic implications; Geochimica et Cosmochimica Acta, v. 47, p. 925-939.

_____, 1986. REE variations across the Peninsular Ranges Batholith: Implications for batholithic petrogenesis and crustal growth in magmatic arcs; Journal of Petrology, v. 28, p. 72-125.

Guidotti, C. V., Cheney, J. T. and Conatore, P. D., 1975. Interrelationship between Mg/Fe ratio and octahedral Al content in

biotite; American Mineralogist, v. 60, p. 849-853.

Gulson, B. L. and Krogh, T. E., 1975. Evidence of multiple intrusion, possible resetting of U-Pb ages, and new crystallization of zircons in the post-tectonic intrusions ('Rapakivi granites') and gneisses from South Greenland; Geochimica et Cosmochimica Acta, v. 39, p. 65-82.

Gunow, A. J., Ludington, S. and Munoz, J. L., 1980. Fluorine in micas from the Henderson molybdenite deposit, Colorado; Economic Geology, v. 75, 1127-1131.

Haglund, D. S., 1972. 'Uranium', in Encyclopedia of Geochemistry and Environmental Sciences; R. W. Fairbridge (Ed.), Van Nostrand Reinhold Co: New York.

Hall, A., 1965. The origin of accessory garnet in the Donegal granite; Mineralogical Magazine, v. 35, p. 628-633.

Ham, L. J., 1987. South Mountain Batholith Project: Composition of muscovite within the SMB, in Mines and Minerals Branch, Report of Activities 1987, Part A, Nova Scotia Department of Mines and Energy, Report 87-5, eds. J. L. Bates and D. R. MacDonald, p. 115-119.

Ham, L. J. and Kontak, D. J., 1988. A Textural and Chemical study of white mica in the South Mountain Batholith, Nova Scotia: Primary versus secondary origin; Maritime Sediments and Atlantic Geology, v. 24, special issue, Granitoid and associated rocks of the Meguma Terrane, Nova Scotia, eds. D.J. Kontak and S.M. Barr, p. 111-121.

Ham, L. J. and O'Reilly, G. A., 1984. Geology of the granitoid rocks of the eastern Meguma Terrane of Nova Scotia (abst.); in The Geological Society of America, Northeastern section, 19th Annual

Meeting, Abstracts with Programs - Geological Society of America, 16(1), p. 21-22.

Hanson, G. N., 1978. The application of trace elements to the petrogenesis of igneous rocks of granitic composition; Earth and Planetary Science Letters, v. 38, p. 26-43.

Harris, J. M. and Schenk, P. E., 1976. The Meguma Group; Maritime Sediments, v. 11, p. 25-46.

Haskin, L. A., Haskin, M. A., Frey, F. A. and Wildeman, T. R., 1968. Relative and absolute terrestrial abundances of the rare earths; in L. H. Ahrens (Ed.), Origin and Distribution of the Elements, International Series Monograph, Earth Sciences, v. 30, p. 889-912.

Hawkes, J., 1967. Rapakivi texture in the Dartmoor granite; Ussher Society Proceedings, v. 1, p. 270-271.

Heinrich, E. W., 1946. Studies in the mica group; Journal of Science, v. 244, p. 836-848.

Henderson, P., 1984. General geochemical properties and abundances of the rare earth elements; in Rare Earth Element Geochemistry, ed. P. Henderson, Elsevier Science Publishing Company Limited, New York, p. 1-32.

Hibbard, M. J., 1980. Indigenous source of late-stage dikes and veins in granitic plutons; Economic Geology, v. 75, p. 410-423.

_____, 1981. The magma-mixing origin of mantled feldspars; Contributions to Mineralogy and Petrology, v. 76, p. 158-170.

Hildreth, W., 1981. Gradients in Silicic Magma Chambers: Implications for Lithospheric Magmatism; Journal of Geophysical Research, v. 86, no. B11, p. 10153-10192.

Hill, J. D., 1986. Granitoid plutons in the Canso area, Nova Scotia; in Current Research, Part A, Geological Survey of Canada, Paper 86-1A, p. 185-192.

_____, 1988. Late Devonian peraluminous granitic plutons in the Canso area, Eastern Meguma Terrane, Nova Scotia; Maritime Sediments and Atlantic Geology, v. 24, p. 11-19.

_____ and Raeside, R. P., 1987. Discussion of "Structural study of highly deformed Meguma phyllite and granite, vicinity of White Head village, S.E. Nova Scotia" by C. K. Mawer and P. F. Williams; Maritime Sediments and Atlantic Geology, v. 23, p. 151-154.

Hofmeister, A. M. and Rossman, G. R., 1983. Color in feldspars; in Feldspar Mineralogy, Reviews in Mineralogy, Volume 2, second edition, ed. P. H. Ribbe; Mineralogical Society of America, p. 271-280.

Holdaway, M. J., 1971. Stability of andalusite and the aluminum silicate phase diagram; American Journal of Science, v. 271,p. 97-131.

_____ and Lee, S. M., 1977. Fe:Mg cordierite stability in high grade pelitic rocks based on experimental, theoretical and natural observations; Contributions to Mineralogy and Petrology, v. 63, p. 175-198.

Hutchison, C. S., 1974. Laboratory handbook of petrographic techniques; John Wiley and Sons, New York, 527 p.

Ishihara, S., 1977. The magnetite-series and ilmenite-series granitic rocks; Mining Geology, v. 27, p. 293-305.

_____, 1981. The granitoid series and mineralization; Economic Geology, 75th Anniversary Volume, p. 458-484.

James, R. S. and Hamilton, D. L., 1969. Phase relations in the system $NaAlSi_3O_8$-$KAlSi_3O_8$-$CaAl_2Si_2O_8$-$SiO_2$ at 1 kilobar water vapour pressure; Contributions to Mineralogy and Petrology, v. 21, p. 111-141.

Johnson, W. M. and Maxwell, J. A., 1981. Rock and Mineral Analyses (Second Edition). John Wiley and Sons: New York, 489 p.

Kamineni, D. C., 1986. Distribution of uranium, thorium and rare-earth elements in the Eye-Dashwa Lakes pluton - a study of some analogue elements; Chemical Geology, v. 55, p. 361-373.

Kay, R. W., 1984. Elemental abundances relevant to identification of magma sources; Phil. Transactions of the Royal Society of London, A310, p. 535-547.

Keppie, J. D., 1977. Tectonics of Southern Nova Scotia; Nova Scotia Department of Mines and Energy, paper 77-1.

_____, 1982. The Minas Geofracture; in Major Structural Zones and Faults of the Northern Appalachians, eds. P. St. Julien and J. Beland; Geological Association of Canada, Special Paper 24, p. 263-280.

_____, 1983. Geological history of the Isaacs Harbour area, parts of 11F/03 and 11F/04, Guysborough County, Nova Scotia; in Mines and Minerals Branch, Report of Activities, 1982; Nova Scotia Department of Mines and Energy, Report 83-1, p. 109-144.

_____, 1985. Geology and tectonics of Nova Scotia; in Appalachians Geotraverse (Canadian Mainland); Geological and Mineralogical Association of Canada annual meeting, guidebook to excursion 1, p. 23-108.

_____ and Muecke, G. K. (compilers), 1979. Metamorphic Map of Nova Scotia, Nova Scotia Department of Mines and Energy, Halifax, Nova Scotia.

Killeen, P. G., 1979. Gamma ray spectrometric methods in uranium exploration - application and interpretation; in Geophysics and Geochemistry in the Search for Metallic Ores; ed. Peter J. Hood, Geological Survey of Canada, Economic Geology Report 31, p.163-229.

Kimberly, M. M., 1978. Short course in uranium deposits: their mineralogy and origin, University of Toronto Press, 521 p.

Kistler, R. W., Ghent, E. O. and O'Neil, J. R., 1981. Petrogenesis of garnet two-mica granites in the Ruby Mountains, Neveda; in Granites and rhyolites; Journal of Geophysical Research B, v. 86, p. 10591-10606.

Koljonen, T. and Rosenberg, R. J., 1974. Rare earth elements in granitic rocks; Lithos, v. 7, p. 249-261.

Komar, P. D., 1972. Flow differentiation in igneous dikes and sills: Profiles of velocity and phenocryst concentration; Bulletin of the Geological Society of America, v. 83, p. 760-768.

Kontak, D. J., 1987. The East Kemptville Leucogranite: a possible mid-Carboniferous topaz granite; in Mines and Minerals Branch, Report of Activities, 1986, eds. J. L. Bates and D. R. MacDonald, Nova Scotia Department of Mines and Energy, Report 87-1, p. 81-94.

Kontak, D. J. and Corey, M. C., 1988. Metasomatic origin of spessartine-rich garnet in the South Mountain Batholith, Nova Scotia; Canadian Mineralogist, v. 26, p. 315-334.

Krogh, T. E. and Keppie, J. D., 1985. U-Pb zircon geochronology in the eastern Meguma Terrane of Nova Scotia (abst); in Mines and Minerals Branch, Report of Activities, 1984, eds. K.A. Mills and J.L. Bates, Nova Scotia Department of Mines and Energy, Report 85-1, p. 168.

_____, 1988. U-Pb ages of single zircon cores imply a Pan African source for two Meguma granites; in Geological Association of Canada and Mineralogical Association of Canada Joint Annual Meeting, Program with Abstracts, St. John's, Newfoundland, v. 13, p. A89.

Lane, T. E., 1976. Stratigraphy of the White Rock Formation; Maritime Sediments, v. 12, p. 87-106.

_____, 1980. Stratigraphy and sedimentology of the White Rock Formation (Silurian), Nova Scotia, Canada; unpublished M.Sc. thesis, Dalhousie University, Halifax, Nova Scotia.

Leake, B. E., 1967. Zoned garnets from the Galway granite and its aplites, Earth and Planetary Science Letters, v. 3, p. 311-316.

Leech, G. F., Lowden, J. A., Stockwell, C. H. and Wanless, R. K., 1963. Age determinations and geological studies; Geological Survey of Canada Paper, 63-17, 140 p.

Logothetis, J., 1985. Mineralogy and geochemistry of metasomatized granitoid rocks from occurrences in the South Mountain Batholith, New Ross area, southwestern Nova Scotia; unpublished M.Sc. thesis, Dalhousie University, Halifax, Nova Scotia.

Loiselle, M. C. and Wones, D. R., 1979. Characteristics and origin of anorogenic granites; Geological Society of America, Program with Abstracts, v. 11, p. 468.

Longstaffe, F. J., Smith, T.E. and Muehlenbachs, K., 1980. Oxygen isotope evidence for the genesis of Upper Paleozoic granitoids from southwestern Nova Scotia; Canadian Journal of Earth Sciences, v. 17, p. 132-141.

Luth, W. C., Jahns, R. H. and Tuttle, O. F., 1964. The granite system at pressures of 4 to 10 kilobars; Journal of Geophysical Research, v. 69, p. 759-773.

Lyons, P. C., 1971. Staining of feldspars on rock-slab surfaces for modal analysis; Mineralogical Magazine, v. 38, p. 518-519.

MacDonald, M. A., 1981. The Mineralogy, Petrology, and Geochemistry of the Musquodoboit Batholith; unpublished M.Sc. thesis, Dalhousie University, Halifax, Nova Scotia.

_____ and Clarke, D. B., 1985. The petrology, geochemistry and economic potential of the Musquodoboit batholith, Nova Scotia; Canadian Journal of Earth Sciences, v. 22, p. 1633-1642.

_____, Corey, M. C., Ham, L. J. and Horne, R. J., 1986. The geology of the South Mountain Batholith: NTS sheets 21A/09, 21A/10, 21A/15 and 21A/16 (west); in Mines and Minerals Branch, Report of Activities 1986, eds. J. L. Bates and D. R. MacDonald, Nova Scotia Department of Mines and Energy, Report 87-1, p. 107-122.

_____, 1987. South Mountain Batholith Project: Progress report; in Mines and Minerals Branch, Report of Activities 1987, Part A, eds. J. L. Bates and D. R. MacDonald, Nova Scotia Department of Mines and Energy, Report 87-5, p. 99-103.

MacMichael, T. P., 1975. The origin of the lead-zinc-silver ores and the alteration of the surrounding granites at the Dunbrack Mine, Musquodoboit Harbour, Nova Scotia; unpublished B.Sc. thesis, Dalhousie University, Halifax, Nova Scotia.

Maillet, L. A., 1984. The origin and occurrence of cordierite in the South Mountain Batholith; unpublished B.Sc thesis, Dalhousie University, Halifax, Nova Scotia.

_____ and Clarke, D. B., 1985. Cordierite in the peraluminous granites of the Meguma Zone, Nova Scotia, Canada; Mineralogical Magazine, v. 49, p. 695-702.

Manning, D. A. C., 1983. Chemical variation in garnets from aplites and pegmatites, peninsular Thailand; Mineralogical Magazine, v. 47, p. 353-358.

Manning, D. A. C. and Pichavant, M., 1985. Volatiles and their bearing on the behaviour of metals in granitic systems; in Granite-related mineral deposits: geology, petrogenesis and tectonic setting, R. P. Taylor and D. F. Strong (Eds.), CIM conference, Halifax, p. 184-187.

Marsh, B. D., 1982. On the mechanisms of igneous diapirism, stoping and zone melting; American Journal of Science, v. 282, p. 808-853.

Mawer, C. K. and White, J. C., 1987. Sense of displacement on the Cobequid-Chedabucto fault system, Nova Scotia, Canada; Canadian Journal of Earth Sciences, v. 24, p. 217-223.

_____ and Williams, P. F., 1986. Structural study of highly deformed Meguma phyllite and granite, vicinity of White Head village, S.E. Nova Scotia; Maritime Sediments and Atlantic Geology, v. 22, p. 51-64.

_____, 1987. Structural study of highly deformed Meguma phyllite and granite vicinity of White Head village, S.E. Nova Scotia: a reply to Hill and Raeside; Maritime Sediments and Atlantic Geology, v. 23, p. 155-157.

McBirney, A. R., 1980. Mixing and unmixing of magmas; Journal of Volcanology and Geothermal Research, v. 7, p. 357-371.

McCarthy, T. S. and Fripp, R. E. P., 1979. The crystallization history of a granitic magma, as revealed by trace element abundances; Journal of Geology, v. 88, p. 211-224.

McKenzie, C. B., 1974. Petrology of the South Mountain Batholith, Western Nova Scotia, unpublished M.Sc. thesis, Dalhousie University, Halifax, Nova Scotia.

_____ and Clarke, D. B., 1975. Petrology of the South Mountain Batholith, Nova Scotia; Canadian Journal of Earth Sciences, v. 12, p. 1209-1218.

_____ and MacGillivray, J., 1974. Eastern Nova Scotia granites project, Dalhousie University, Geology Department, Internal Report.

McNally, R. N., 1972. 'Zirconium', in The Encyclopedia of Geochemistry and Environmental Sciences, R. W. Fairbridge (Ed.), Van Nostrand Reinhold Co: New York.

Mendenhall, W. and Ott, L., 1972. Understanding Statistics, Duxbury Press, California, 310 p.

Metcalf, R. V. and Blackburn, W. H., 1981. Variation of uranium and thorium in the Old Rag Granite, Madison County, Virginia; Geological Society of America, Abstracts with programs, southeastern section, p. 30.

Miller, C. F. and Mittlefehldt, D. W., 1982. Depletion of light rare-earth elements during partial melting of granitic rocks; Geology, v. 10, p. 129-133.

_____ and Stoddard, E. F., 1981. Origin of garnet in granitic rocks; an example of the role of Mn from the Old Woman-Piute range, California; Journal of Geology, v. 89, p. 233-246.

_____, Stoddard, E. F., Bradfish, L. J. and Dollase, W. A., 1981. Composition of plutonic muscovite: genetic implications; Canadian Mineralogist, v. 19, p. 25-34.

Mittlefehldt, D. W. and Miller, C. F., 1983. Geochemistry of the Sweetwater Wash Pluton, California: implications for "anomalous" trace element behaviour during differentiation of felsic magmas; Geochimica et Cosmochimica Acta, v. 47; p. 109-124.

Monier, G., Mergoil-Daniel, J. and Labernardiere, H., 1984. Generations successives de muscovites et feldspaths potassiques dans les leucogranite du massif de Millevaches (Massif Central francais); Bulletin Mineralogique 107, p. 55-68.

Moore, W. S. and Swami, S. K., 1972. 'Thorium', in Encyclopedia of Geochemistry and Environmental Sciences; R. W. Fairbridge (Ed.), Van Nostrand Reinhold Co: New York.

Muecke, G. K. and Clarke, D. B., 1981. Geochemical evolution of the South Mountain Batholith, Nova Scotia: rare-earth-element evidence; Canadian Mineralogist, v. 19; p. 133-146.

_____, Elias, P. and Reynolds, P. H., 1988. Hercynian/Alleghanian overprinting of an Acadian Terrane: $^{40}Ar/^{39}Ar$ studies in the Meguma Zone, Nova Scotia; Isotope Geoscience (in press).

_____ and Moller, P., 1988. The not-so-rare earths; Scientific American, January, p. 72-77.

Neilson, M. J. and Haynes, S. J., 1973. Biotites in calc-alkaline intrusive rocks; Mineralogical Magazine, v. 39, 251-253.

Nichols, D., 1976. The metamorphic and structural evolution of the metasediments and granites in the Whitehaven area, Guysborough County, Nova Scotia; B.Sc. thesis, Dalhousie University, Halifax, Nova Scotia.

O'Brien, B. H., 1983. The structure of the Meguma Group between Gegogan Harbour and Country Harbour, Guysborough County; Nova Scotia Department of Mines and Energy; Report 83-1, p. 145-181.

_____, 1986. Preliminary report on the geology of the Mahone Bay area, Nova Scotia; in Current Research, Part A, Geological Survey of Canada, Paper 86-1A, p. 439-444.

O'Reilly, G. A., 1976. The Petrology of the Brenton pluton, Yarmouth County, Nova Scotia; unpublished B.Sc. (Honours) thesis, Dalhousie University, Halifax.

_____, 1984. Geology of the Sangster Lake and Larrys River plutons; in Mines and Minerals Branch, Report of Activities 1983, eds. K. A. Mills, Nova Scotia Department of Mines and Energy, Report 84-1, p. 231-235.

_____, 1985. Geochemical Variation within a granitic terrane displaying anomalous airborne radiometric signature from Eastern Nova Scotia; in Mines and Minerals Branch, Report of Activities 1984, eds. K. A. Mills and J. L. Bates, Nova Scotia Department of Mines and Energy, Report 85-1, p. 135-142.

_____, Farley, E. J. and Charest, M. H., 1982. Metasomatic-hydrothermal mineral deposits of the New Ross-Mahone Bay area, Nova Scotia; Nova Scotia Department of Mines and Energy Paper 82-2, 96 p.

Pabst, A., 1928. Observations on inclusions in the granitic rocks of the Sierra Nevada; University of California, Publication of the Geological Science; v. 17, p. 325-386.

Pagel, M., 1982. The mineralogy and geochemistry of uranium, thorium, and rare-earth elements in two radioactive granites of the Vosges, France; Mineralogical Magazine, v. 46, p. 149-161.

Parsons, I., 1978. Feldspars and fluids in cooling plutons; Mineralogical Magazine, v. 42, p. 1-17.

_____ and Brown, W. L., 1984. Feldspars and the thermal history of igneous rocks; in Feldspars and Feldspathoids: Structures, Properties and Occurrences, ed. W. L. Brown; NATO ASE Series, D. Reidel Publishing Company, Dordrecht, Holland, p. 318-361.

Pattison, D. R. M., Carmichael, D. M. and St.-Onge, M. R., 1982. Geothermometry and geobarometry applied to Early Proterozoic "S-type" granitoid plutons, Wopmay Orogeny, Northwest Territories; Contributions to Mineralogy and Petrology, v. 79, 394-404.

Phillips, G. N., Wall, V. J. and Clemens, J. D., 1981. Petrology of the Strathbogie batholith: a cordierite-bearing granite; Canadian Mineralogist, v. 19, p. 47-64.

Pilkey, O., 1972. 'Barium', in Encyclopedia of Geochemistry and Environmental Sciences; R. W. Fairbridge (Ed.), Van Nostrand Reinhold Co: New York.

Pitcher, W. S., 1979. The nature, ascent and emplacement of granitic magmas; Journal of the Geological Society, London, v. 136. p. 627-662.

_____, 1983. Granite type and tectonic environment; in K. Hsu (ed), Mountain Building Processes; Academic Press, London, p. 19-40.

Poldervaart, A. and Gilkey, A., 1954. On clouded plagioclase; American Mineralogist, v. 36, p. 25.

Pollard, P. J., 1983. Magmatic and postmagmatic process in the formation of rocks associated with rare-element deposits; Trans. Instn. Min. Metall. (Sect. B: Applied earth sciences), 92.

Ponce de Leon, M. I. and Choukrone, P., 1980. Shear zones in the Iberian Arc; Journal of Structural Geology, v. 2, p. 63-68.

Price, N. J. 1978. Fracture patterns and stresses in granites; Geoscience Canada.

Raeside, R. P., Hill, J. D. and Eddy, B. G., 1988. Metamorphism of Meguma Group metasedimentary rocks, Whitehead Harbour, Guysborough County, Nova Scotia; Maritime Sediments and Atlantic Geology, v. 24, p. 1-9.

Rankama, K. and Sahmam, T. G., 1950. "Geochemistry", University of Chicago, Chicago, 912 p.

Rapp, R. P. and Watson, E. B., 1986. Monazite solubility and dissolution kinetics: implications for the thorium and light rare earth chemistry of felsic magmas; Contributions to Mineralogy and Petrology, v. 94, p. 304-316.

Reynolds, R. C., 1972. 'Rubidium', in Encyclopedia of Geochemistry and Environmental Sciences, ed. R. W. Fairbridge.

Reynolds, P. H. and Muecke, G. K., 1978. Age studies on slates: applicability of the $^{40}Ar/^{39}Ar$ stepwise outgassing method; Earth and Planetary Science Letters, v. 40, p. 111-118.

Ribbe, P. H., 1983. Chemistry, structure and nomenclature of feldspars; in Feldspar Mineralogy, Volume 2, second edition, ed. P. H. Ribbe; Mineralogical Society of America, p. 1-19.

_____, 1984. Average structures of alkali and plagioclase feldspars: systematics and applications; in Feldspars and Feldspathoids: Structures, Properties and Occurrences, ed. W. L. Brown; NATO ASE Series, D. Reidel Publishing Company, Dordrecht, Holland, p. 1-54.

Richard, L. R., 1988. Geochemical Discrimination of the peraluminous Devono-Carboniferous granitoids of Nova Scotia and Morocco; unpublished M.Sc. thesis, Dalhousie University, Halifax, Nova Scotia.

Richardson, J. M., Spooner, E. T. C. and McAuslan, D. A., 1982. The East Kemptville tin deposit, Nova Scotia: an example of a large tonnage, low grade, greisen-hosted deposit in the endocontact zone of a granite batholith; in Current Research, Part B, Geological Survey of Canada, Paper 82-1B, p. 27-32.

Rogers, H. D., 1985. Granitoid rocks of Shelburne County and eastern Yarmouth County, Nova Scotia; in Guide to granites and mineral deposits of southwestern Nova Scotia, eds. A. K. Chatterjee and D. B. Clarke; Nova Scotia Department of Mines and Energy, preprint of paper 85-3.

Rogers, J. J. W. and Adams, J. A. S., 1969. 'Thorium', Chapter 90, in Handbook of Geochemistry, ed. K. H. Wedephol.

_____, 1970. 'Uranium', Chapter 92, in Handbook of Geochemistry, ed. K. H. Wedephol.

_____ and Ragland, P. C., 1961. Variation of thorium and uranium in selected granitic rocks; Geochimica et Cosmochimica Acta, v. 25, p. 99-109.

Saavedra, J., 1978. Geochemical and petrological characteristics of mineralised granites of the west centre of Spain; in Metallization Associated with Acid Magmatism 3; eds. M. Stemprok, L. Burnol and G. Tischendorf; Geol. Surz. Czech, p. 279-291.

Sarkar, P. K., 1978. Petrology and geochemistry of the White Rock meta-volcanic suite, Yarmouth, Nova Scotia; unpublished Ph.D. thesis, Dalhousie University, Halifax, Nova Scotia, 350 p.

Schenk, P. E., 1970. Regional variations of the flysch-like Meguma Group (Lower Paleozoic) of Nova Scotia compared to recent sedimentation off the Scotian Shelf; Geological Association of Canada, Special Paper 7, ed. J. Lajoie, p. 127-153.

_____, 1982. Stratigraphy and sedimentology of the Meguma Zone and part of the Avalon Zone; in The Caledonide Orogen, Nato Advanced Study Institute, Atlantic Canada, August, 1982. Compiled by A. F. King, Department of Earth Sciences, Memorial University of Newfoundland, St. John's, Newfoundland, IGCP project 17, report 9, p. 189-307.

_____ and Lane, T. E., 1982. Pre-Acadian sedimentary rocks of the Meguma Zone, Nova Scotia - passive continental margin justaposed against a volcanic arc; International Association of

sedimentologists, Excursion 5B Guidebook, 85 p.

Schiller, E. A., 1963. Mineralogy and geology of the Guysborough area, Nova Scotia, Canada; unpublished Ph.D. thesis, University of Utah, USA, 162 p.

Shand, S. J., 1927. Eruptive Rocks (1st ed.); J. Wiley & Sons, New York.

Simpson, C. and Schmid, S. M., 1983. An evaluation of criteria to deduce the sense of movement in sheared rocks; Geological Society of America Bulletin, v. 94, p. 1281-1288.

Smith, D. G. W., Gold, C. M., Tomlinson, D. A. and Wynne, D. A., 1980. A Fortran IV system for processing energy/wavelength dispersive microprobe data; Datum Geo-Services.

Smith, J. V., 1974. Feldspar minerals, vols. 1 and 2; Springer Verlag, Berlin.

Smith, P. K., 1981. Geology of the Sherbrooke area, Guysborough County, Nova Scotia; in Mineral Resources Division, Report of Activities, 1980, Nova Scotia Department of Mines and Energy, Report 81-1, p. 77-94.

_____, 1983. Geology of the Cochrane Hill Gold Deposit, Guysborough County, Nova Scotia; in Mines and Minerals Branch, Report of Activities, 1982, Nova Scotia Department of Mines and Energy, Report 83-1, p. 225-256.

_____, 1984. Geology and lithogeochemistry of the Cochrane Hill gold deposit - an indication of metalliferous source beds; in Mines and Minerals Branch, Report of Activities, 1983, Nova Scotia Department of Mines and Energy, Report 84-1, p. 203-214.

Smith, T. E., 1974. The geochemistry of the granitic rocks of Halifax Co., Nova Scotia; Canadian Journal of Earth Sciences, v. 11, p. 650.

_____, 1975. Layered Granitic Rocks at Chebucto Head, Halifax County, Nova Scotia; Canadian Journal of Earth Science, v. 12, p 456-463.

_____, 1979. The geochemistry and origin of the Devonian granitic rocks of southwest Nova Scotia: summary; Geological Society of America Bulletin, v. 90, p. 424-426.

Smitheringale, W. G., 1960. Geology of Nictaux-Torbrook map area, Annapolis and Kings Counties, Nova Scotia; Geological Survey of Canada, Paper 60-13, 32 p.

_____, 1973. Geology of parts of Digby, Bridgetown, and Gaspereau Lake map areas; Geological Survey of Canada, Memoir 374, 78 p.

Speer, J. A., 1984. Micas in Igneous Rocks; in Micas, Reviews in Mineralogy, Volume 13, ed. S. W. Bailey; Mineralogical Society of America, p. 299-356.

Stallard, V., 1975. Geochemistry of biotites as a guide to the evolution of the South Mountain Batholith; unpublished B.Sc. (Honours) thesis, Dalhousie University, Halifax.

Stea, R. R. and Fowler, J. H., 1979. Minor and trace element variations in Wisconsinan tills, Eastern Shore region, Nova Scotia; Nova Scotia Department of Mines and Energy, paper 79-4, 30 p.

Stevenson, I. M., 1964. Chedabucto Bay map area, Nova Scotia; Geological Survey of Canada, Map 1156A.

Streckeisen, A. L., 1976. To each plutonic rock its proper name; Earth Science Reviews, v. 12, p. 1-33.

Strong, D. F. and Chatterjee, A. K., 1985. Review of some chemical and mineralogical characteristics of granitoid rocks hosting Sn, W, U, Mo deposits in Newfoundland and Nova Scotia; in High heat production (HHP) granites, hydrothermal circulation and ore genesis; papers presented at the High heat production (HHP) granites, hydrothermal circulation and ore genesis conference, St. Austell, Cornwall, England, September 22-25, 1985, p. 489-516.

Stull, R. J., 1978. Mantled feldspars from the Golden Horn batholith, Washington; Lithos, v. 11, p. 243-249.

Takahasi, M., Aramaki, S. and Ishihara, S., 1980. Magnetite-series/Ilmenite-series vs. I-type/S-type granitoids; in Mining Geology Special Issue, no. 8, p. 13-28.

Taylor, F. C., 1967. Reconnaissance geology of Shelburne map-area, Nova Scotia; Geological Survey of Canada Memoir 349.

_____, 1969. Geology of the Annapolis-St. Mary's Bay map area, Nova Scotia (21A, 21B, east half); Geological Survey of Canada Memoir 358, 65 p.

_____ and Schiller, E. A., 1966. Metamorphism of the Meguma Group of Nova Scotia; Canadian Journal of Earth Sciences, v. 3, p. 959-974.

Taylor, R. G., 1979. Geology of Tin Deposits; Elsevier, Amsterdam, 543 p.

_____ and Pollard, P. J., 1985. Pervasive hydrothermal alteration in tin-bearing granites and its implication for the evolution of ore-bearing magmatic fluids; in Granite-related

mineral deposits: geology, petrogenesis and tectonic setting, R. P. Taylor and D. F. Strong (Eds.), CIM conference, Halifax, p. 263-264.

Taylor, S. R., 1965. The application of trace element data to problems in petrology; Physics and Chemistry of the Earth, v. 6, p. 133-213.

_____, 1972. Rare earths (Lanthanide Series); in The Encyclopedia of geochemistry and environmental sciences, R. W. Fairbridge (Ed.), Van Nostrand Reinhold Co.: New York, p. 1020-1029.

Taylor, W. P., 1976. Intrusion and differentiation of magma at a high level in the crust: the Puscao Pluton, Lima Province, Peru; Journal of Petrology, v. 17, 194-218.

Telford, W. M., Geldart, L. P., Sheriff, R. E. and Keys, D. A., 1976. Applied Geophysics, Cambridge University Press, New York, 860 p.

Thompson, A. B., 1982. Dehydration melting of pelitic rocks and the generation of $H_2O$-undersaturated granitic liquids; American Journal of Science, v. 282, p. 1567-1595.

Thornton, G. P. and Tuttle, O. F. 1960. Chemistry of igneous rocks 1. Differentiation Index; American Journal of Science, v. 258, p. 664-684.

Tischendorf, G., 1977. Geochemical and petrographic characteristics of silicic magmatic rocks associated with rare element mineralization; in Metallization Associated with Acid Magmatism, v. 2, edited by M. Stemprok, Geological Survey, Prague, p. 41-96.

Tuttle, O. F. and Bowen, N. L., 1958. Origin of granite in the light of experimental studies in the system $NaAlSi_3O_8$-$KAlSi_3O_8$-$SiO_2$-$H_2O$; Geological Society of America, Memoir 74, 153 p.

Vennum, W. R. and Meyer, C. E., 1979. Plutonic garnets from the Werner batholith, Lassiter Coast, Antarctica Peninsula; American Mineralogist, v. 64, p. 268-273.

Vernon, R. H., 1983. Restite, xenoliths and microgranitoid enclaves in granites; Journal and Proceedings, Royal Society of New South Wales, V. 116, p. 77-103.

Vorma, A., 1971. On the petrochemistry of rapakivi granites with special reference to the Laitila massif, southwestern Finland; Geological Survey of Finland, Bulletin 285, 98 p.

_____ and Flood, R. H., 1982. Some problems in the interpretation of microstructures in granitoid rocks, in New England Geology, eds. B. Runnegar and P. Flood, p. 201-210.

Wall, V. J., Clemens, J. D. and Clarke, D. B., 1987. Models for granitoid evolution and source compositions; The Journal of Geology, v. 95, p. 731-749.

_____ and Capobianco, C. J., 1981. Phosphorous and the rare earth elements in felsic magmas: an assessment of the role of apatite; Geochimica et Cosmochimica Acta, v. 45, p. 2349-2358.

Weber, C, Barbery, P., Cuney, M. and Martin, H., 1985. Trace element behaviour during migmatization: evidence for a complex melt residuum-fluid interaction in the St. Malo migmatitic dome (France); Contributions to Mineralogy and Petrology, v. 90, p. 52-62.

Wedepohl, K. H., 1970. 'Tantalum', Chapter 73, in Handbook of Geochemistry; K. H. Wedepohl, ed., p. 373-D-1 to 73-F-2.

Wehmiller, J., 1972. 'Strontium', in Encyclopedia of Geochemistry and Environmental Sciences; R. W. Fairbridge (Ed.), Van Nostrand

Reinhold Co: New York, p. 1121-1122.

Whalen, J. B., Currie, K. L. and Chappell, B. W., 1987. A-type granites: geochemical characteristics, discrimination and petrogenesis; Contributions to Mineralogy and Petrology, v. 95, p. 407-419.

White, A. J. R. and Chappell, B. W., 1977. Ultrametamorphism and granitoid genesis; Tectonophysics, v. 43, p. 7-22.

Whitfield, J. M., Rogers, J. J. W. and Adams, J. A. S., 1959. The relationship between the petrology and the thorium and uranium contents of some granitic rocks; Geochimica et Cosmochimica Acta, v. 17, p. 248-271.

Woodsworth, G. J., 1977. Homogenization of zoned garnets from pelitic schists; Canadian Mineralogist, v. 15, p. 230-242.

Wones, D. R. and Eugster, H. P., 1965. Stability of biotite: experimental, theory, and application; American Mineralogist, v. 50, p. 1228-1272.

Yoder, H. S. and Eugster, H. P., 1954. Phlogopite synthesis and stability range; Geochimica et Cosmochimica Acta, V. 6, p. 157-185.

Zen, E.-A., 1988. Phase relations of peraluminous granitic rocks and their petrogenetic implications; Annual Review of Earth and Planetary Sciences, v.16, p.21-51.

CHEDABUCTO BAY

Salmon River

Halfway Cove

Queensport

Lundy

Halfway Cove lobe

Queensport lobe

Larrys River

TOR BAY

HCQP1

HCQP1A

HCQP2

HCQP3

HCQP4

Donahue Lake

Halfway Cove Lake

Bonnet Lake

Jamieson Brook

€OG

€OH

extensive outcrop

aplite

quartz

abundant boulders

abundant outcrop

pegmatite

boulders

miles 0 2 3 4 miles

kilometres 0 1 2 3 4 kilometres

SCALE

N.T.S. Sheet 11 F/06C

## OUTCROP LOCATION MAP

| | | |
|---|---|---|
| Devono-Carboniferous | HCQP4 | fine- to medium-grained, equigranular muscovite-biotite monzogranite |
| | HCQP3 | medium- to coarse-grained, moderately equigranular, muscovite-biotite monzogranite |
| | HCQP2 | coarse grained, muscovite-biotite monzogranite |
| | HCQP1A | intensely porphyritic (megacrysts of potassium feldspar) biotite dominant, minor muscovite, coarse-grained monzogranite |
| | HCQP1 | biotite dominant, minor muscovite, coarse-grained monzogranite |
| Cambro-Ordovician | €OH | Halifax Formation |
| | €OG | Goldenville Formation |

### SYMBOLS

- Rock outcrop, area of outcrop, probable outcrop, float
- Geological boundary (defined, approximate, assumed)
- Bedding (horizontal, inclined, vertical)
- Shearing and intense fracturing, fracture cleavage (horizontal, inclined, vertical, dip unknown)
- Joint (horizontal, inclined, vertical, dip unknown)
- Fault (defined, approximate, assumed)
- Schistosity, gneissosity, cleavage, foliation (horizontal, inclined, vertical, dip unknown)

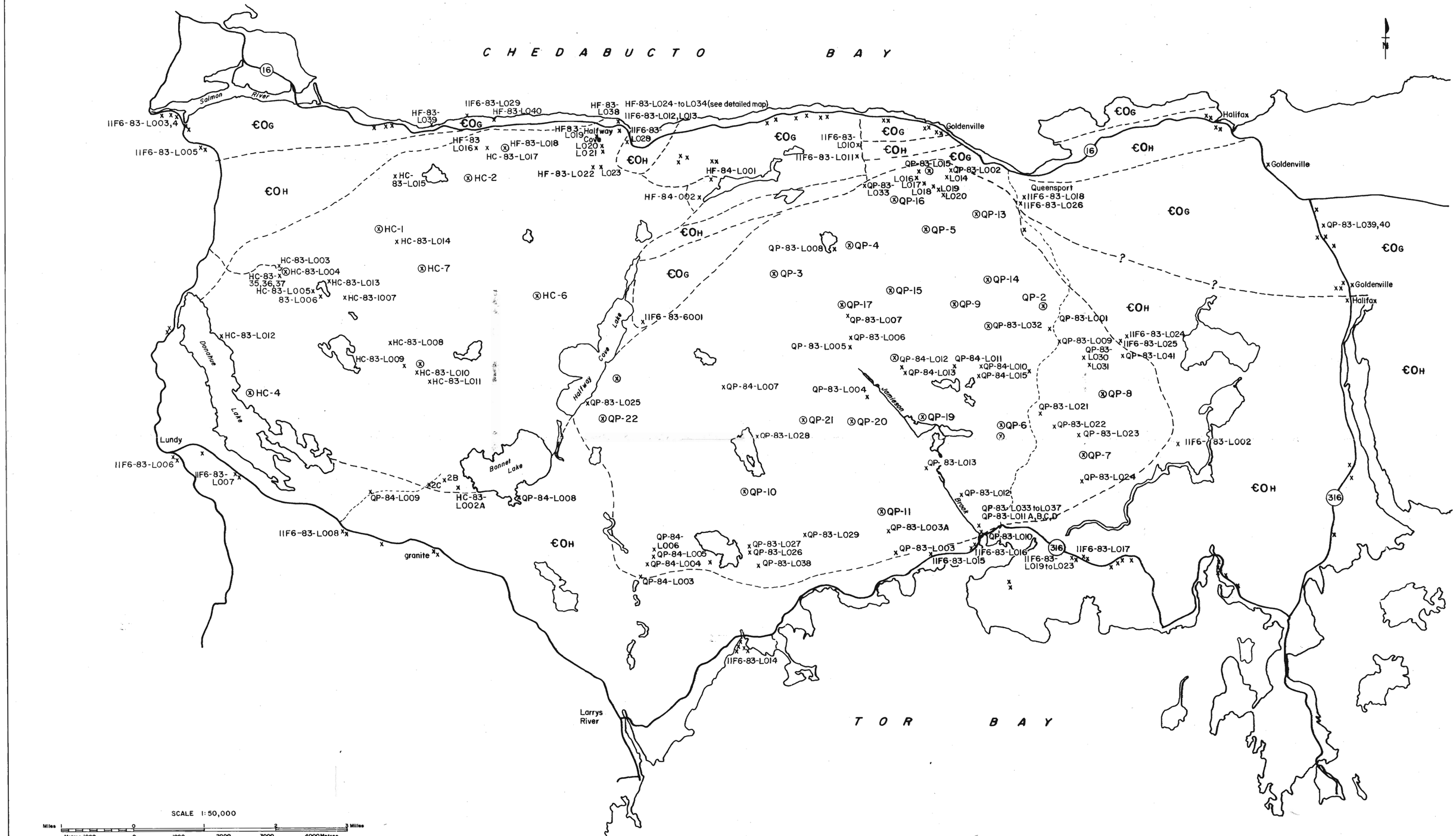


SAMPLE LOCATION MAP